

# Modeling of Hydrodynamics and Mass Transfer In Cocurrent Packed Columns

by

Mohammad Salman Mahmoud Naqvi

A Thesis Presented to the

FACULTY OF THE COLLEGE OF GRADUATE STUDIES

KING FAHD UNIVERSITY OF PETROLEUM & MINERALS

DHAHRAN, SAUDI ARABIA

In Partial Fulfillment of the  
Requirements for the Degree of

**MASTER OF SCIENCE**

In

**CHEMICAL ENGINEERING**

November, 1995

## INFORMATION TO USERS

This manuscript has been reproduced from the microfilm master. UMI films the text directly from the original or copy submitted. Thus, some thesis and dissertation copies are in typewriter face, while others may be from any type of computer printer.

**The quality of this reproduction is dependent upon the quality of the copy submitted.** Broken or indistinct print, colored or poor quality illustrations and photographs, print bleedthrough, substandard margins, and improper alignment can adversely affect reproduction.

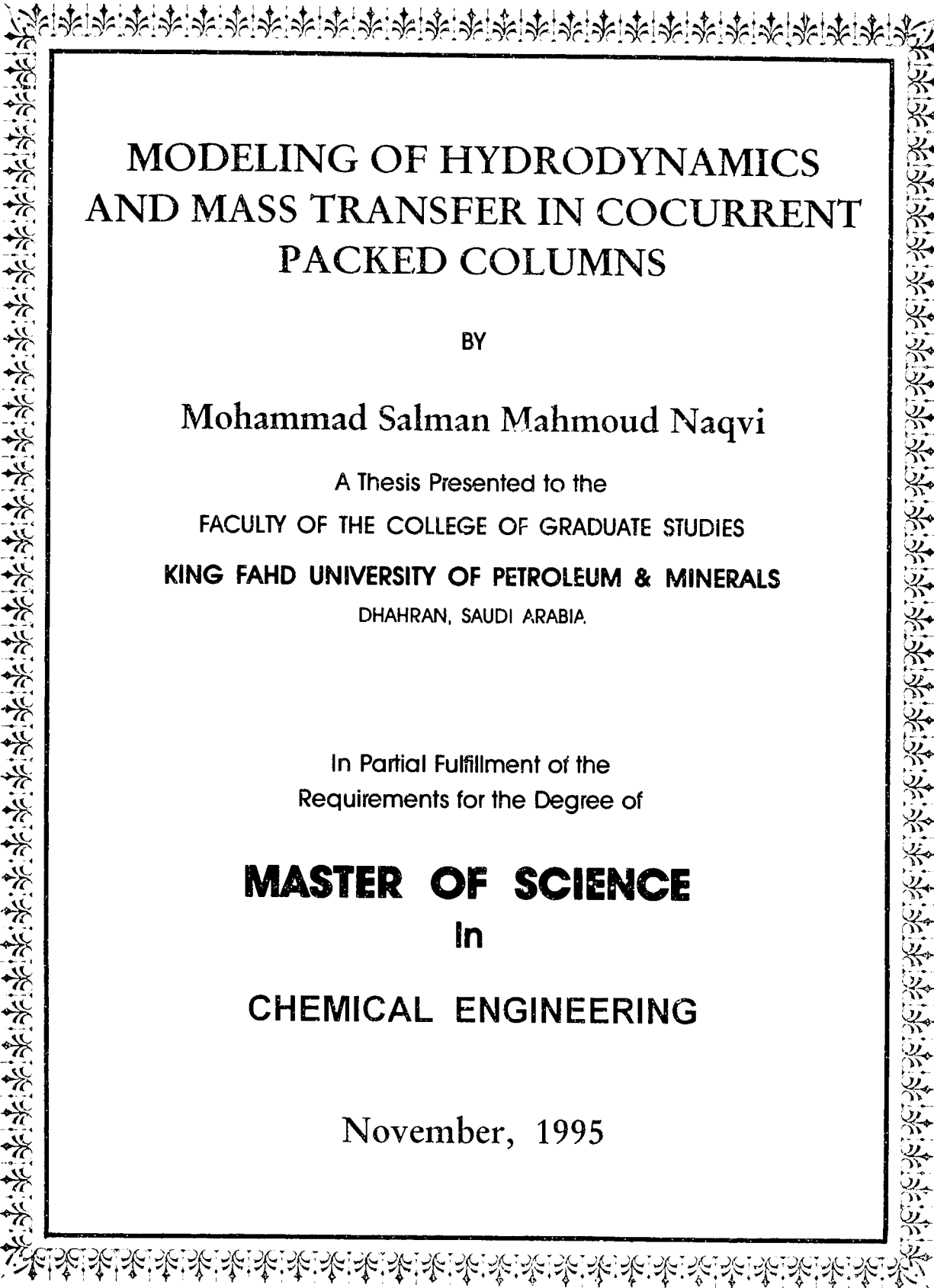
In the unlikely event that the author did not send UMI a complete manuscript and there are missing pages, these will be noted. Also, if unauthorized copyright material had to be removed, a note will indicate the deletion.

Oversize materials (e.g., maps, drawings, charts) are reproduced by sectioning the original, beginning at the upper left-hand corner and continuing from left to right in equal sections with small overlaps. Each original is also photographed in one exposure and is included in reduced form at the back of the book.

Photographs included in the original manuscript have been reproduced xerographically in this copy. Higher quality 6" x 9" black and white photographic prints are available for any photographs or illustrations appearing in this copy for an additional charge. Contact UMI directly to order.

# UMI

A Bell & Howell Information Company  
300 North Zeeb Road, Ann Arbor, MI 48106-1346 USA  
313/761-4700 800/521-0600



**MODELING OF HYDRODYNAMICS  
AND MASS TRANSFER IN COCURRENT  
PACKED COLUMNS**

BY

**Mohammad Salman Mahmoud Naqvi**

A Thesis Presented to the  
FACULTY OF THE COLLEGE OF GRADUATE STUDIES  
**KING FAHD UNIVERSITY OF PETROLEUM & MINERALS**  
DHAHRAN, SAUDI ARABIA.

In Partial Fulfillment of the  
Requirements for the Degree of

**MASTER OF SCIENCE**  
In  
**CHEMICAL ENGINEERING**

November, 1995

UMI Number: 1377136

---

UMI Microform 1377136

Copyright 1996, by UMI Company. All rights reserved.

This microform edition is protected against unauthorized  
copying under Title 17, United States Code.

---

UMI

300 North Zeeb Road  
Ann Arbor, MI 48103

**KING FAHD UNIVERSITY OF PETROLEUM & MINERALS**

**DHAHRAN, SAUDI ARABIA**

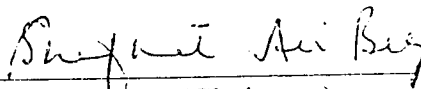
*This Thesis written by*

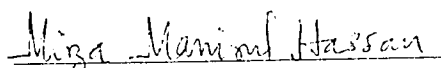
**Mohammad Salman Mahmoud Naqvi**

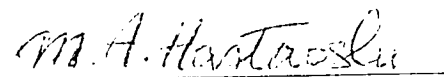
*under the direction of his Thesis Advisor, and approved by his Thesis Committee,  
has been presented to and accepted by the Dean, College of Graduate Studies, in  
partial fulfillment of the requirements for the degree of*

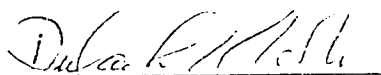
**MASTER OF SCIENCE IN CHEMICAL ENGINEERING**


*Thesis Committee:*

  
Dr. S. A. Beg (Chairman)

  
Dr. M. M. Hassan (Member)

  
Dr. M. A. Hastaoglu (Member)

  
Dr. Dulaihan K. Al-Harbi  
Department Chairman

  
Dr. Ala H. Al-Rabeh  
Dean, College of Graduate Studies

Date: 27. 11. 92



*Dedicated to*

*my beloved father,  
mother, brother and sisters*

*whose  
love, prayers and inspirations*

*led to this accomplishment*

## ACKNOWLEDGMENTS

*In the name of Allah, Most Gracious, Most Merciful. Read in the name of thy Lord and Cherisher, Who Created man from a {leech-like} clot. Read and thy Lord is Most Bountiful. He Who taught {the use of} the pen. Taught man that which he knew not. Nay, but man doth transgress all bounds. In that he looketh upon himself as self-sufficient. Verily, to thy Lord is the return {of all}.*

*(The Holy Quran, Surah Al-A'alaq, No. 96)*

First and foremost, all praise to Allah, *subhanahu-wa-ta'ala*, the Almighty, Who gave me an opportunity, courage and patience to carry out this work. I seek His mercy, favor and forgiveness. I feel privileged to glorify His name in the sincerest way through this small accomplishment. May He, *subhanahu-wa-ta'ala*, guide me and the whole humanity to the right path (*Aameen*).

Acknowledgment is due to King Fahd University of Petroleum & Minerals for extending all facilities to support this research work.

I am greatly indebted to my thesis advisor, Dr. Shafkat A. Beg, for his support, guidance and continuous encouragement throughout the course of this work. He was always kind, patient and sympathetic towards me. Working with him was indeed a productive and learning experience which I thoroughly enjoyed.

I wish to express my deepest gratitude to my thesis co-advisor, Dr. Mirza M. Hassan, for his professional help, invaluable suggestions and countless hours of attention he devoted during various stages of this work. My sincere appreciation goes to my committee member, Dr. Mehmet A. Hastaoglu for his interest, cooperation and constructive criticism.

I am also thankful to the department chairman, Dr. Dulaihan K. Al-Harbi and other faculty members for their help and cooperation.

Special thanks are due to Mr. Arshad S. Chaudhry, who was always by my side for the much needed support and encouragement, and provided help in innumerable number of ways.

Notable mentions go to all of my friends on the campus especially Zaka, Asim, Asif, Amir, Rashid, Abba, Qureshi and Ashraf who provided a wonderful company and support.

Last but not the least, thanks are due to the members of my family for their emotional and moral support throughout my academic career. This work is dedicated to my family for taking pains to fulfill my personal and academic pursuits and shaping my personality.



# Table of Contents

	Page
<b>Acknowledgment</b>	iii
<b>Table of Contents</b>	v
<b>List of Figures</b>	viii
<b>List of Tables</b>	xv
<b>Nomenclature</b>	xvi
<b>Thesis Abstract (English)</b>	xix
<b>Thesis Abstract (Arabic)</b>	xx
<b>Chapter 1. Introduction</b>	1
1.0 General	1
1.1 Packed columns with co-current downflow operation	4
1.2 Packed columns with co-current upflow operation	5
1.3 Hydrodynamics of packed columns	6
1.3.1 Hydrodynamic regimes in co-current downflow operation	8
1.3.2 Hydrodynamic regimes in co-current upflow operation	9
1.4 Mass transfer in co-current packed columns	9
1.5 Theoretical modeling of co-current packed columns	12
1.6 Important design parameters for a co-current packed column	15
1.6.1 Knowledge of flow regimes and flow uniformity	15
1.6.2 Pressure drop	16
1.6.3 Holdup of various phases	16

1.6.4	Residence time distribution and axial mixing	18
1.6.5	Gas-liquid mass transfer	19
1.6.6	Intrinsic kinetics	19
1.7	Objectives	20
<b>Chapter 2. Literature Review</b>		<b>21</b>
2.1	Hydrodynamics of co-current packed columns	22
2.2	Mass transfer studies for co-current packed columns	25
2.3	Theoretical modeling of co-current packed columns	31
2.4	Liquid holdup correlations	35
2.4.1	Dynamic liquid holdup	35
2.4.2	Stagnant liquid holdup	37
2.5	Analysis of the published work	38
<b>Chapter 3. Mathematical Model Formulation</b>		<b>39</b>
3.1	Development of a basic model	39
3.2	Model equations for gas absorption	44
3.3	Model equations for stripping	48
3.4	Model equations for gas absorption with chemical reaction	51
3.5	Solution of the model equations	57
<b>Chapter 4. Hydrodynamic Model: Validation and Parametric Study</b>		<b>59</b>
4.1	Introduction	59
4.2	Results and Discussion	60
4.2.1	Evaluation of model parameters	62
4.2.2	Results of numerical simulation	64
4.2.3	Comparison of Theoretical Predictions with Experimental Data	84
<b>Chapter 5. Modeling of Gas Absorption in Co-Current Packed Column</b>		<b>88</b>
5.1	Introduction	88

5.2.2 Results of numerical simulation	96
<b>Chapter 6. Modeling of Air Stripping in Co-Current Packed Column</b>	122
6.1 Introduction	122
6.2 Results and Discussion	125
<b>Chapter 7. Modeling of Gas Absorption with Chemical Reaction</b>	155
7.1 Introduction	155
7.2 Chemistry of the process modeled	157
7.3 Results and Discussion	159
<b>Chapter 8. Conclusions and Recommendations</b>	174
8.1 Conclusions	174
8.2 Recommendation for future work	179
<b>Bibliography</b>	181
<b>Appendix A The orthogonal Collocation Formulation of Model Equations</b>	190

## LIST OF FIGURES

Figure		Page
1.1a	Concentration profile for solute component when fed to the gas phase.	10
1.1b	Concentration profile for solute component when fed to the liquid phase.	10
2.1a	Hydrodynamic flow map for the downflow systems.	24
2.1b	Hydrodynamic flow map for the upflow systems.	24
3.1	Schematic diagram of a representative element of the bed.	40
3.2	Nodal representation of the numerical scheme employed for solving the model equations.	58
4.1a	The effect of $k_{SD}$ on the RTD of co-current upflow packed column for a step decrease in tracer concentration.	65
4.1b	The effect of $k_{SD}$ on the RTD of co-current downflow packed column for a step input in tracer concentration.	67
4.2	Concentration profiles in 3-dimensions for a co-current upflow packed column showing the effect of $k_{SD}$ when the column is subjected to a step decrease in tracer concentration, (a) $k_{SD} = 1.0 \times 10^{-7} \text{ m sec}^{-1}$ (b) $k_{SD} = 5.0 \times 10^{-7} \text{ m sec}^{-1}$	68
4.3a	The effect of $L_G$ on the RTD of co-current upflow packed column for a step decrease in tracer concentration.	69
4.3b	The effect of $L_G$ on the RTD of co-current downflow packed column for a step input in tracer concentration.	71

Figure		Page
4.4	Concentration profiles in 3-dimensions for a co-current upflow packed column showing the effect of $L_S$ when the column is subjected to a step decrease in tracer concentration, (a) $L_S = 7.0 \times 10^{-5}$ m    (b) $L_S = 2.0 \times 10^{-4}$ m	72
4.5	The effect of $D_S$ on the RTD of co-current upflow packed column for a step decrease in tracer concentration.	73
4.6a	Dynamic concentration profiles in the stagnant phase, for a co-current upflow packed column showing the effect of $D_S$ when the column is subjected to a step decrease in tracer concentration for, $D_S = 1.0 \times 10^{-10}$ m <sup>2</sup> sec <sup>-1</sup>	74
4.6b	Dynamic concentration profiles in the stagnant phase, for a co-current upflow packed column showing the effect of $D_S$ when the column is subjected to a step decrease in tracer concentration for, $D_S = 1.0 \times 10^{-11}$ m <sup>2</sup> sec <sup>-1</sup>	75
4.7a	The effect of $\phi$ on the RTD of co-current upflow packed column for a step decrease in tracer concentration.	76
4.7b	The effect of $\phi$ on the RTD of co-current downflow packed column for a step input in tracer concentration.	77
4.8a	The effect of $h_i$ on the RTD of co-current upflow packed column for a step decrease in tracer concentration.	79
4.8b	The effect of $h_i$ on the RTD of co-current downflow packed column for a step input in tracer concentration.	80
4.9a	The effect of $Pe_L$ on the RTD of co-current upflow packed column for a step decrease in tracer concentration.	81
4.9b	The effect of $Pe_L$ on the RTD of co-current downflow packed column for a step input in tracer concentration.	82

<b>Figure</b>	<b>Page</b>
4.10 The effect of $Re_L$ on the RTD for $Re_G = 12.2$ when a co-current downflow packed column is subjected to a step input in tracer concentration.	83
4.11 The effect of $Re_G$ on the RTD for $Re_L = 1.0$ when a co-current downflow packed column is subjected to a step input in tracer concentration.	84
4.12 Comparison of experimental data and model predictions for a step input in tracer concentration in a co-current downflow packed column (Data of Kan and Greenfield, 1983).	86
4.13 Comparison of experimental data with predictions of both the P-D-E and the present model when subjected to base parameters for a step decrease in tracer concentration in a co-current upflow packed column (Data of Skomorokov and Kirillov, 1986).	87
5.1a The effect of $Pe_L$ on the dynamics of gas and liquid phase exit concentrations for absorption of $NH_3$ .	97
5.1b The effect of $Pe_L$ on the dynamics of gas and liquid phase exit concentrations for absorption of HF .	98
5.1c The effect of $Pe_L$ on the dynamics of gas and liquid phase exit concentrations for absorption of $SO_2$ .	99
5.2a The effect of $Pe_L$ on steady state gas and liquid phase concentration profiles for absorption of $NH_3$ .	101
5.2b The effect of $Pe_L$ on steady state gas and liquid phase concentration profiles for absorption of HF .	102
5.2c The effect of $Pe_L$ on steady state gas and liquid phase concentration profiles for absorption of $SO_2$ .	103
5.3a The effect of $Pe_G$ on steady state gas and liquid phase concentration profiles for absorption of $NH_3$ .	105

Figure	Page
5.3b	The effect of $Pe_G$ on steady state gas and liquid phase concentration profiles for absorption of HF. 106
5.3c	The effect of $Pe_G$ on steady state gas and liquid phase concentration profiles for absorption of $SO_2$ . 107
5.4a	The effect of $St$ on steady state gas and liquid phase concentration profiles for absorption of $NH_3$ . 108
5.4b	The effect of $St$ on steady state gas and liquid phase concentration profiles for absorption of HF. 109
5.4c	The effect of $St$ on steady state gas and liquid phase concentration profiles for absorption of $SO_2$ . 110
5.5a	The effect of $St$ on the dynamics of gas and liquid phase exit concentrations for absorption of $NH_3$ . 112
5.5b	The effect of $St$ on the dynamics of gas and liquid phase exit concentrations for absorption of HF. 113
5.5c	The effect of $St$ on the dynamics of gas and liquid phase exit concentrations for absorption of $SO_2$ . 114
5.6	The effect of $\beta$ on the dynamics of liquid phase exit concentrations for absorption of $NH_3$ . 115
5.7	Stagnant phase concentration profiles in 3-D for absorption of $NH_3$ , illustrating the effect of, $\beta$ , (a) $\beta = 20.0$ (b) $\beta = 0.8577$ 116
5.8	The effect of $K_{SD}^*$ on the dynamics of liquid phase exit concentrations for absorption of $NH_3$ . 117
5.9	Stagnant phase concentration profiles in 3-D for absorption of $NH_3$ , illustrating the effect of $K_{SD}^*$ , (a) $K_{SD}^* = 1.0$ (b) $K_{SD}^* = 0.266$ 118

<b>Figure</b>	<b>Page</b>
5.10	Comparison of experimental data with model predictions for absorption of $\text{NH}_3$ in water (Data of Reiss, 1967). 120
6.1a	The effect of $Pe_L$ on the dynamics of gas and liquid phase exit concentrations for stripping of chloroform . 129
6.1b	The effect of $Pe_L$ on the dynamics of gas and liquid phase exit concentrations for stripping of dibromochloromethane. 130
6.1c	The effect of $Pe_L$ on the dynamics of gas and liquid phase exit concentrations for stripping of bromoform. 131
6.2a	The effect of $Pe_L$ on steady state gas and liquid phase concentration profiles for stripping of chloroform . 133
6.2b	The effect of $Pe_L$ on steady state gas and liquid phase concentration profiles for stripping of dibromochloromethane. 134
6.2c	The effect of $Pe_L$ on steady state gas and liquid phase concentration profiles for stripping of bromoform. 135
6.3a	The effect of $Pe_G$ on steady state gas and liquid phase concentration profiles for stripping of chloroform . 136
6.3b	The effect of $Pe_G$ on steady state gas and liquid phase concentration profiles for stripping of dibromochloromethane. 137
6.3c	The effect of $Pe_G$ on steady state gas and liquid phase concentration profiles for stripping of bromoform. 138
6.4a	The effect of $St$ on steady state gas and liquid phase concentration profiles for stripping of chloroform . 140
6.4b	The effect of $St$ on steady state gas and liquid phase concentration profiles for stripping of dibromochloromethane. 141
6.4c	The effect of $St$ on steady state gas and liquid phase concentration profiles for stripping of bromoform. 142



<b>Figure</b>	<b>Page</b>	
6.5	Dynamic liquid phase concentration profiles in 3-D for stripping of chloroform illustrating the effect of $St$ , (a) $St = 2.0$ (b) $St = 0.8577$	143
6.6a	The effect of $Re_L$ on steady state gas and liquid phase concentration profiles for stripping of chloroform.	144
6.6b	The effect of $Re_L$ on steady state gas and liquid phase concentration profiles for stripping of dibromochloromethane.	145
6.6c	The effect of $Re_L$ on steady state gas and liquid phase concentration profiles for stripping of bromoform.	146
6.7	Dynamic liquid phase concentration profiles in 3-D for stripping of chloroform, illustrating the effect of $Re_L$ , (a) $Re_L = 7.0$ (b) $Re_L = 5.0$ .	148
6.8a	The effect of $Re_G$ on steady state gas and liquid phase concentration profiles for stripping of chloroform.	149
6.8b	The effect of $Re_G$ on steady state gas and liquid phase concentration profiles for stripping of dibromochloromethane.	150
6.8c	The effect of $Re_G$ on steady state gas and liquid phase concentration profiles for stripping of bromoform.	151
6.9	Comparison of experimental data with model predictions for desorption of oxygen from water (Data of Reiss, 1967).	152
7.1	Effect of $Pe_L$ on steady state concentration profiles along the length of the column for $CO_2$ in the gas phase and NaOH in the liquid phase.	162
7.2	Effect of $Pe_L$ on transient exit concentrations for $CO_2$ in the gas phase and NaOH in the liquid phase.	163

<b>Figure</b>	<b>Page</b>
7.3	Effect of $Pe_G$ on steady state concentration profiles along the length of the column for $CO_2$ in the gas phase and NaOH in the liquid phase. 164
7.4	Effect of $Re_L$ on steady state concentration profiles along the length of the column for $CO_2$ in the gas phase and NaOH in the liquid phase. 166
7.5	Effect of $Re_G$ on steady state concentration profiles along the length of the column for $CO_2$ in the gas phase and NaOH in the liquid phase. 167
7.6	Effect of $St$ on steady state concentration profiles along the length of the column for $CO_2$ in the gas phase and NaOH in the liquid phase. 169
7.7	3-D concentration profiles for $CO_2$ in the dynamic liquid phase, illustrating the effect of $K_R^*$ , (a) $K_R^* = 1303.8$ (b) $K_R^* = 0.83$ 170
7.8	Effect of $K_R^*$ on steady state concentration profiles along the length of the column for $CO_2$ in the gas phase and NaOH in the liquid phase. 171
7.9	Comparison of experimental data with model predictions for absorption of $CO_2$ in aqueous solution of NaOH (Data of Morsi et al., 1984), for constant liquid mass velocity = $4.0 \text{ ( kg m}^{-2} \text{ s}^{-1} )$ 173

## LIST OF TABLES

Table		Page
2.1	Reported values of coefficients used in correlations for calculating $k_{GL}$ , $a_{GL}$ , for various packings.	27
2.2	Experimental studies of gas absorption with chemical reaction in downflow and upflow cocurrent packed columns.	30
4.1	Base values of parameters used in the hydrodynamic model computations for the liquid phase.	61
5.1	Diffusion coefficients and Henry's Law constants for the gas absorption systems.	92
5.2	Base values of parameters used for the parametric study of the model for gas absorption.	93
5.3	Base values of parameters for comparison of theoretical predictions with experimental data for absorption of ammonia in water.	121
6.1	Diffusion coefficients and Henry's Law constants for the air stripping systems.	126
6.2	Base values of parameters used for the parametric study of the model for air stripping.	128
6.3	Base values of parameters for comparison of theoretical predictions with experimental data for oxygen desorption from water.	153
7.1	Base values of parameters for comparison of theoretical predictions with experimental data for absorption of carbon dioxide in sodium hydroxide solution.	160

## Nomenclature

$a$	Interfacial area per unit volume of bed, $\text{m}^2 \text{m}^{-3}$
$a_C$	Packing external surface area, $\text{m}^2 \text{m}^{-3}$
$a_p$	Specific area of particle ( $= a_C/V_p$ ), $\text{m}^2 \text{m}^{-3}$
$Bi$	Biot number between the stagnant and dynamic liquid. defined in Eq. (3.30)
$c$	Concentration, $\text{kmol m}^{-3}$
$c^o$	Initial concentration, $\text{kmol m}^{-3}$
$c_{d_0}$	Maximum concentration in the liquid phase. $\text{kmol m}^{-3}$
$c_{g_0}$	Maximum concentration in the gas phase, $\text{kmol m}^{-3}$
$C$	Dimensionless concentration
$C^o$	Dimensionless initial concentration
$C \Big _{x=0^-}$	Dimensionless concentration immediately before the inlet
$C \Big _{x=0^+}$	Dimensionless concentration immediately after the inlet
$d_h$	Hydraulic diameter as defined by Krisher and Kast (1978). given in Eq. (5.2), m
$d_p$	Diameter of sphere with equivalent surface area as the particle ( $= 6/a_p$ ), m
$D$	Axial dispersion coefficient, $\text{m}^2 \text{s}^{-1}$
$D_C$	Diffusivity of the component to be absorbed in water, $\text{m}^2 \text{s}^{-1}$
$D_S$	Dispersion coefficient in the stagnant phase. $\text{m}^2 \text{s}^{-1}$
$E\ddot{o}^*$	Eotvos number, defined in Eq. (5.7)
$g$	Acceleration due to gravity, $\text{m s}^{-2}$
$G$	Superficial mass flux of the gas, $\text{kg m}^{-2} \text{s}^{-1}$
$h$	Holdup / unit volume of bed
$h_t$	Total liquid hold up ( $h_t = h_s + h_d$ )

$H$	Henry's constant (= Conc. in the liquid phase /Conc. in the gas phase)
$K$	Overall mass transfer coefficient, $\text{m s}^{-1}$
$k$	Mass transfer coefficient, $\text{m s}^{-1}$
$k_R$	Reaction rate constant, $\text{m}^3 \text{ kmol}^{-1} \text{ s}^{-1}$
$K_R^*$	Dimensionless reaction rate constant defined in Eq. (3.86)
$K_{SD}^*$	Dimensionless mass transfer coefficient between stagnant and dynamic liquid phases, defined in Eq. (3.9)
$L$	Superficial mass flux of the liquid, $\text{kg m}^{-2} \text{ s}^{-1}$
$L_C$	Length of the column, m
$L_S$	Thickness of the stagnant region, m
$Pe$	Peclet Number, defined in Eq. (3.9)
$\langle r \rangle$	Rate expression defined in Eq. (3.84), $\text{kmol m}^{-3} \text{ s}^{-1}$
$\langle R \rangle$	Dimensionless rate expression defined in Eq. (3.85)
$Re$	Reynolds number, defined in Eq. (5.2)
$Re'$	Reynolds number, defined in Eq. (5.11)
$Sc_L$	Schmidt number for the liquid phase
$Sh_{LG}^*$	Sherwood number between liquid and gas, as defined in Eq. (5.2)
$St$	Stanton number, defined in eq. (3.30)
$t$	Time, s
$U$	Superficial velocity, $\text{m s}^{-1}$
$We$	Weber number, defined in Eq. (5.2)
$x$	Dimensionless axial distance along the column, defined in Eq. (3.9), m
$y$	Depth in the stagnant film, m
$z$	Axial distance along the column, m

### ***Greek Symbols***

$\beta$	Dimensionless parameter, defined in Eq. (3.9)
$\varepsilon$	Bed void fraction
$\zeta$	Parameter defined in Eq. (5.5)
$\eta$	Dimensionless depth in the stagnant film, defined in Eq. (3.9)
$\theta$	Dimensionless time, defined in Eq. (3.9)
$\bar{\theta}$	Parameter defined in Eq. (5.2)
$\kappa$	Parameter defined in Eq. (5.4)
$\mu$	Viscosity, Pa s
$\xi$	Dimensionless parameter, defined in Eq. (3.30)
$\rho$	Density, kg m <sup>-3</sup>
$\sigma_L$	Surface tension of the liquid, N m <sup>-1</sup>
$\phi$	Ratio of dynamic to total liquid holdup, defined in Eq. (3.9)
$\psi$	Dimensionless parameter, defined in Eq. (3.30)
$\chi$	Lockhart-Martinelli parameter, defined in Eq. (5.2)

### ***Subscript***

1	Solute component
2	Reactant
$d$	Dynamic liquid phase
$g, G$	Gas phase
$L$	Liquid phase
$LG$	Between gas and dynamic liquid phase
$S$	Stagnant liquid phase
$SD$	Between stagnant liquid and dynamic liquid phase

# THESIS ABSTRACT

<b>NAME OF STUDENT</b>	Mohammad Salman Mahmoud Naqvi
<b>TITLE OF STUDY</b>	Modeling of Hydrodynamics and Mass Transfer in Cocurrent Packed Columns
<b>MAJOR FIELD</b>	Chemical Engineering
<b>DATE OF DEGREE</b>	November, 1995

A comprehensive mathematical model which considers the liquid phase to be divided into two zones ( dynamic and stagnant ), is developed for cocurrent packed columns to analyze the prevailing hydrodynamics and mass transport phenomena. The model predictions are shown to provide a good representation of the experimental data for both upflow and downflow operations. The model is also extended to simulate gas absorption and stripping operations. Parametric studies are carried out for absorption of ammonia, hydrogen fluoride and sulfur dioxide from air into water; and for stripping of bromoform, dibromochloromethane and chloroform from water into air. The model predictions are successfully tested against the available experimental data for absorption of ammonia and for desorption of oxygen in an air-water system. The model is extended to systems involving gas absorption accompanied by chemical reaction. Theoretical predictions are found to agree well with the experimental data for carbon dioxide absorption in aqueous sodium hydroxide.

*MASTER OF SCIENCE DEGREE*

**KING FAHD UNIVERSITY OF PETROLEUM & MINERALS  
Dhahran, Saudi Arabia**

**November, 1995**

## خلاصة الرسالة

اسم الطالب : محمد سلمان محمود نقوي  
عنوان الرسالة : نمذجة الهيدروديناميكيات وانتقال المادة في الأعمدة المخشوة ذات المسار الواحد  
التخصص : الهندسة الكيميائية  
تاريخ الشهادة : نوفمبر ١٩٩٥م

في هذه الدراسة تطوير نموذج رياضي شامل يقسم الجانب السائل في الأعمدة المخشوة إلى منطقتين (متحركة وراكدة) وذلك لكي يسهل تحليل الظواهر السائدة سواء الهيدروديناميكية أو ظواهر انتقال المادة. و نتائج استخدام هذا النموذج أثبتت أنه يمثل جيد للنتائج والمعلومات التي حُصلت باستخدام التجارب المعملية سواء لعمليات التدفق السفلي أو العلوي و بالإضافة إلى هذا فإن هذا النموذج يمتلك القدرة على محاكاة عمليات إمتصاص وانتزاع الغاز. وقد اجريت عدة دراسات بتغير بعض قيم هذا النموذج على إمتصاص الأمونيا وفلوريد الهيدروجين وثاني أكسيد الكبريت من الهواء إلى الماء وعلى إنتزاع نيتروموفورم ودايبروموكلوروميثان والكلوروفورم من الماء إلى الهواء و إختبار هذا النموذج بنجاح وذلك بالمقارنة مع نتائج التجارب المخبرية الموجودة لإمتصاص الأمونيا وانتزاع الأكسجين في نظام مائي هوائي أيضاً. استخدام هذا النموذج إلى العمليات التي تحتوي على إمتصاص الهواء المترافقة مع تفاعلات كيميائية. النتائج النظرية لإستخدام هذا النموذج إتفقت جيداً مع النتائج الموجودة من التجارب المخبرية لإمتصاص ثاني أكسيد انكربون في محلول هيدروكسيد الصوديوم.

درجة الماجستير في العلوم

جامعة الملك فهد للبترول والمعادن

الظهران - المملكة العربية السعودية

رجب ١٤١٦هـ

نوفمبر ١٩٩٥م



# CHAPTER 1

## INTRODUCTION

---

### 1.0 GENERAL

Packed columns are heavily used in process industries for gas-liquid contacting. The vast majority of these are operated counter-currently. The liquid phase falls downwards because of gravity, while the gas phase moves upwards through the column because of an imposed pressure gradient. The gas throughput in this type of operation is limited. Above a certain critical gas velocity, the gravity forces on the down flowing liquid are exceeded by the drag forces imposed on the liquid by the up flowing gas. This unstable condition is known as flooding and is the characteristics of all the counter-current gas-liquid contacting operations.

One means of overcoming this throughput limitation of counter-current operation is to operate the column cocurrently. However, cocurrent packed columns have a definite limitation from mass transfer point of view as it results in only one equilibrium stage and offers a relatively low overall concentration driving force. There are, however, a number of gas-liquid contacting operations where only one equilibrium stage is required. For example, as pointed out by Wen

et al. (1963), if component is transferred from one fluid phase and is consumed by chemical reaction in the other phase, only one equilibrium stage is required. For a conventional (physical) absorption at large liquid to gas ratios, the concentration of the transferring component in the liquid phase is low because of the excess of liquid. As this shifts the equilibrium, only one equilibrium stage may be required to reduce the concentration of the transferring component in the gas phase to the desired level. The same applies to stripping operations at low liquid to gas ratios. With an excess of gas, the gas phase concentration of the transferring component may be so low that the equilibrium is shifted. Hence, a stripping operation could also conceivably be carried out in one equilibrium stage. Operation at high liquid to gas or low liquid to gas ratios in the cocurrent mode does not present the flooding operation that these extreme liquid to gas ratios might present in counter current operation.

Therefore, cocurrent gas-liquid contacting is generally applicable for operations involving only one equilibrium stage. These include, absorption with chemical reaction in one phase, i.e. gas-liquid chemical reactors, physical absorption at high liquid to gas ratios, such as, absorption of lean pollutants from the exhaust gases, and desorption or stripping at low liquid to gas ratios, such as air stripping of pollutants from industrial waste water.

Some of the major advantages which make the use of cocurrent operation highly attractive are,

- i) Its capacity is not limited by the flooding of the column employing it can be operated at very wide ranges of gas and liquid flow rates.
- ii) At any specified value of superficial gas and liquid velocities, the pressure drop in a cocurrently operated column is about half of that in the case of a counter-currently operated column (Turpin and Huntington, 1967).
- iii) It offers a relatively much higher effective interfacial area between gas and liquid.
- iv) Packing imparts better contact and better mass transfer between gas and liquid.
- v) It can be operated at high pressures.
- vi) Liquid flow in such type of operation approaches piston flow leading to higher conversions for most reactions.
- vii) Liquid to solid ratio is small, minimizing the homogeneous side reactions if possible.
- viii) For catalytic systems, there is low catalyst loss, permitting the use of expensive catalysts.

Due to the advantages as highlighted above, packed columns with cocurrent flow of gas and liquid are widely used in chemical, petrochemical, biological and waste water treatment processes for many contacting purposes such as gas absorption, air stripping, gas absorption accompanied by a chemical reaction, and heterogeneous catalytic reactions.

Two modes of operation are possible in a cocurrent packed column, cocurrent upward flow, and cocurrent downward flow. The mode of cocurrent operation strongly affects the overall performance of the system and is defined completely by different set of hydrodynamic parameters.

## **1.1 PACKED COLUMNS WITH COCURRENT DOWNFLOW OPERATION**

Cocurrent packed columns are usually operated in downflow where both gas and liquid enter the column from the top, and the liquid trickles down the packing along with gas, and hence are generally called trickle beds. These trickle beds find applications in waste water treatment where they are heavily used for the oxidation of organic matter in waste water with fixed micro organisms or Pd catalysts. They are also utilized for gas stripping of lean pollutants from waste water, denitrification, pollutant removal from air streams by absorption in water

and for many other oxidation purposes like oxidation of formic acid in water. They further find usage in hydrodesulfurization, production of calcium sulphite, synthesis of 1-4 butynediol, demetallization, catalytic hydrocracking, catalytic hydrofinishing, and in many other catalytic hydrogenation processes as listed by Shah (1979), Gianetto and Silveston (1986) and Gianetto and Specchia (1992).

The characteristics of such mode of operation are:

- i) They offer low pressure drop as opposed to upflow operation.
- ii) Flooding is never a problem in such operations.
- iii) Liquid flows as a film, thus offering very small resistance to the diffusion of gaseous reactants.
- iv) It offers poor radial mixing of heat as compared to upflow operation.
- v) Flow is closer to plug flow, allowing higher conversions.
- vi) Liquid to solid ratio is small.

## **1.2 PACKED COLUMNS WITH COCURRENT UPFLOW OPERATION**

In the upflow mode of operation, gas and liquid phases enter the column from the bottom and flow cocurrently upwards. Although this operation implies

higher pressure drop and hence larger variation in the partial pressures of the gaseous reactants, it has several advantages to offer, such as.

- i) Better liquid-solid contacting.
- ii) Better mixing and temperature distribution.
- iii) Higher gas/liquid mass transfer coefficients.
- iv) Higher liquid holdups.
- v) Better heat transfer performance.

Due to these facts, this type of reactor has attracted much attention in recent years and is widely used in fermentation, alcohol amination, aromatic alkylation, hydration of olefins and nitrocompounds, coal liquefaction (synthiol reactor), Fischer-Tropsch synthesis, catalytic hydrodesulfurization and in many other hydrogenation reactions (Shah, 1979; Gianetto and Silveston, 1986; Gianetto and Specchia, 1992).

### **1.3 HYDRODYNAMICS OF PACKED COLUMNS**

In a fixed bed column with a single fluid phase, only two modes of operation are possible, either downflow (which is used in most cases) or upflow. Furthermore, only two different flow regimes of laminar or turbulent flow can be

observed. These regimes are characterized by Reynolds number as the single relevant dimensionless group.

In multiphase cocurrent fixed bed columns, the hydrodynamics is much more complex. Because there are now two flowing phases, it is possible to feed them either cocurrently in up- or downflow, or countercurrently. Whether cocurrent or countercurrent flow is used depends on throughput, heat recovery requirements and availability of driving forces for mass transfer and chemical reaction. The phenomenon of flooding known from countercurrent flow does not arise in cocurrent flow. The flow rates, therefore, can be much higher in this mode. Furthermore, not only do regimes of low interaction and strong interaction of the phases exist, but also several flow patterns appear in the packed bed. They range from gas continuous to liquid continuous regimes, depending on the shape and size of particles (and bed) as well as on physical properties and flow velocities of gas and liquid. Because the characteristics of flow and transport phenomenon varies according to the flow pattern, various charts have been proposed to show boundaries between the different regimes.

The investigation on cocurrent packed bed hydrodynamics is basic to evaluate the reactor performance, its optimal shape, the physical and chemical

interactions (holdups, pressure drop, heat and mass transfer) and energetic requirements. The hydrodynamic regimes for downward and upward flows have been examined by various investigators using different procedures, i.e., visual and/or optical observations, electro-conductimetric or thermo-conductimetric tests, and pressure drop measurements.

### **1.3.1 Hydrodynamic Regimes in Cocurrent Downflow**

#### **Operation**

Gas and liquid flowing downwards in cocurrent packed beds compete for the void space. This results in various flow regimes all of which can broadly be divided in two basic categories : low interaction regime ( where liquid holdup and texture are not affected by changes in gas flow rate) and high interaction regime (where changes in gas flow rate affect liquid structure and flow). The low interaction regime, characterized by continuous gas phase and laminar flow of liquid in the form of rivulets and/or films is also called trickle flow. Many different flow patterns are identified in the high interaction regime. For example, in pulsating flow, gas and liquid slugs traverse the column alternately at high gas and liquid flow rates. Another hydrodynamic regime called spray flow is observed at high gas and low liquid flow rates, where the liquid phase flows down the column in the form of droplets entrained by the continuous gas phase. The fourth



regime called the bubble flow appears at high liquid flow rates and low gas flow rates, where the entire bed is filled with the liquid and the gas phase is in the form of slightly elongated bubbles.

### **1.3.2 Hydrodynamic Regimes in Cocurrent Upflow Operation**

The cocurrent upflow operation displays three hydrodynamic regimes. At low gas flow rates, there is bubble flow where the gas phase moves in the continuous liquid phase in the form of bubbles at slightly higher velocities than the liquid. As the gas flow rate is increased, non-homogeneous slug flow is observed, which is characterized by alternate gas-rich and liquid-rich parts passing through the column. With further increase in the gas flow rate, a gas continuous regime termed spray flow is encountered with liquid suspended as a heavy mist in the gas stream.

## **1.4 MASS TRANSFER IN COCURRENT PACKED COLUMNS**

The knowledge of transport characteristics, like gas-liquid mass transfer coefficients and corresponding interfacial areas is crucial to the design and scale-up of cocurrent packed columns. Due to their heterogeneity, the system is

characterized by several mass transfer steps that can seriously affect column behavior and performance.

Figure (1.1a) and (1.1b) illustrate the mass transfer system and show different concentration profiles for solute component when fed to the gas phase and to the liquid phase, respectively. The rates of different mass transfer steps encountered in such type of multiphase contactors, depend on the geometry and size of the column, packing size, void fraction, hydrodynamics, and on the operating conditions.

In downflow cocurrent columns, for regimes characterized by high gas and liquid flow rates (high gas/liquid interaction regimes), gas/liquid mass transfer is promoted by the large interfacial area created so that the mass transfer rate is higher than that found in other multiphase contacting system. The liquid phase mass transfer coefficient  $k_{GL} a_{GL}$ , is affected by both gas and liquid flow rates. At high gas and liquid flow rates, the value of  $k_{GL} a_{GL}$  may exceed  $1 \text{ s}^{-1}$ , a value not achieved in any other type of gas-liquid contactor. The values for upflow cocurrent contactors are upto 100% greater than downflow values in pulsed and spray flow regimes (Specchia et al., 1974) because the gravitational forces lead to higher liquid holdup and pressure drop. In spite of the fact that the data in the literature

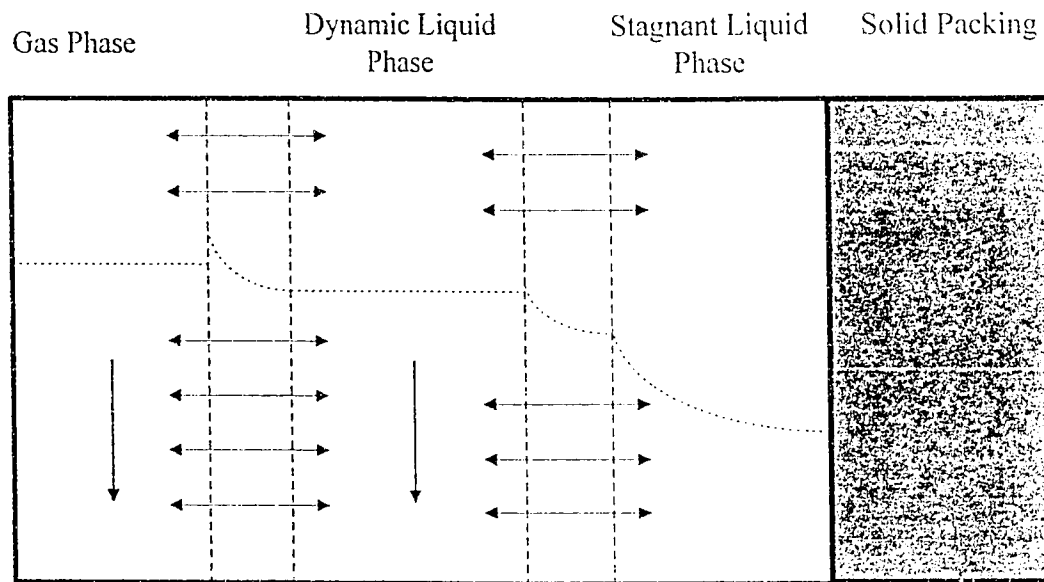


Figure (1.1a) Concentration profile for solute component when fed to the gas phase.

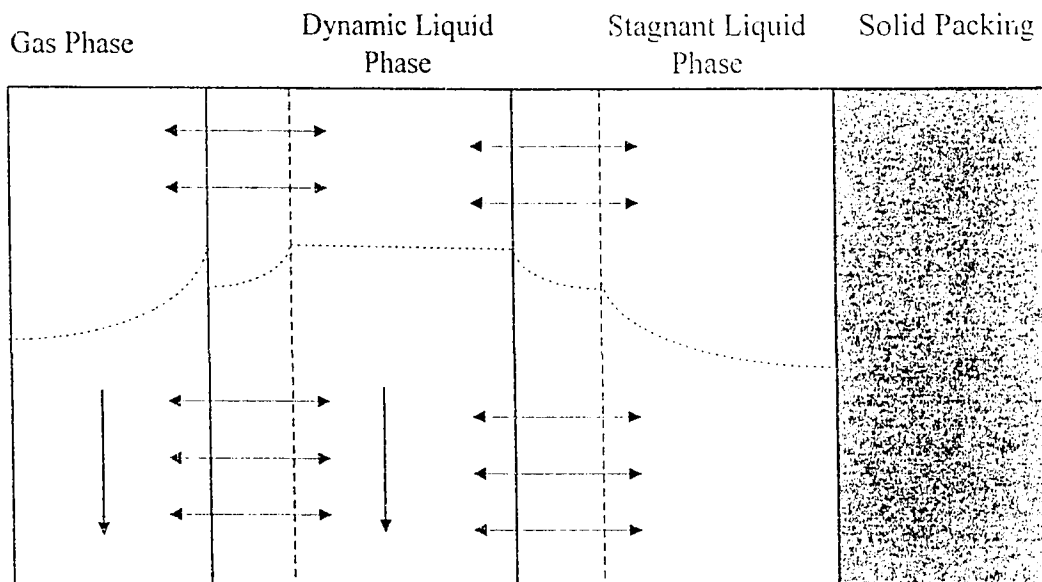


Figure (1.1b) Concentration profile for solute component when fed to the liquid phase.

show a relatively wide scatter, volumetric coefficients appear to be proportional to the specific interfacial area indicating that the liquid side mass transfer coefficient seems to have a constant value between  $3-8 \times 10^{-2}$  ( $\text{cm s}^{-1}$ ). Energy dissipation is mainly used for creation of new gas liquid interface. Values of this interface differ substantially with size and type of packing, and in pulsed and bubble flow regime they can amount to  $10^3$  ( $\text{m}^2/\text{m}^3$ ) at high flow rates of gas and liquid because of the large contribution of small bubbles.

## **1.5 THEORETICAL MODELING OF COCURRENT PACKED COLUMNS**

Although enormous amount of published research work exists for such type of columns, the design of the equipment is still an exercise based on empirical correlations and experimental extrapolations rather than a consequence of a theoretical analysis. The reason being the difficulties involved in scale-up of these devices as the hydrodynamic conditions prevailing inside the column are extremely complex, where parts of the liquid flow over the packing in the form of rivulets, films and droplets. There are zones with varying low renewal rates and semi-stagnant liquid pockets, thus, yielding a very different scenario from that of an ideal piston flow. The liquid-solid contact area displays a wide range of local

situations, depending on the type of operation, liquid and gas flow rates, bed porosity, size and shape of packing, viscosity, density, interfacial tension, reactor dimensions, foaming characteristics of fluids, etc.

As the local scenarios encountered in the cocurrent packed column change from place to place along the column due to the complex interactions of gas and liquid phases, it is imperative, for any meaningful understanding of the various transport processes involved, to develop and define a model which is able to express the local as well as the global behavior of the column. For this purpose, several mathematical models have been proposed in the literature. These are based on the experimental evaluation of the residence time distribution function (RTDF). Attempt is then made to transform the physical picture of the gas and liquid flow in the packed columns into mathematical equations and provide numerical parameters to characterize the hydrodynamics of the flowing phases. These numerical parameters are defined by graphical or numerical comparison of the theoretical and experimental residence time distribution curves in the time domain.

There are two possible approaches to the scale up of cocurrent fixed-bed columns. The first one, the use of pseudo-homogeneous model, considers the system as consisting of a single phase, the liquid. A material balance is written for

only the key component. Dispersion, resistances for inter- and intra-phase mass and heat transfer are ignored and a large stoichiometric excess of gas and also a complete catalyst wetting are assumed.

The second approach, using a heterogeneous model, is more representative of the actual physical system. It leads to a system of differential equations based on material balances for the various species in all the phases. If required, a heat balance is also included. Mass balances must take into account methods of feeding the column, interphase mass transfer, chemical kinetics, longitudinal and/or radial dispersion etc. This is often done through the boundary or the initial conditions. Apart from difficulties in measuring physical and chemical kinetic parameters and establishing adequate boundary conditions, this provides a the more complete and rational approach. Unfortunately, it is frequently difficult to analytically integrate the differential equations making up the model and hence, a numerical solution is usually sought.

## **1.6 IMPORTANT DESIGN PARAMETERS FOR A COCURRENT PACKED COLUMN**

An appropriate design and model for a three phase cocurrent packed column requires the estimation of various transport (momentum, heat and mass), kinetic and mixing parameters. Specifically, the following parameters are needed.

### **1.6.1 Knowledge of Flow Regime and Flow Uniformity**

The mixing characteristics and the transport processes within a packed column depend strongly on the prevailing flow regime. The flow regime largely depends on the flow rates of gas and liquid phases and their relative orientation (cocurrent upwards or cocurrent downwards), the nature, size and status of the packing material, the fluid properties, and the nature of gas and liquid distributors.

The flow regime plays a very important role in column scale up. If the data obtained in the pilot column are to be useful for a larger-scale column, the flow regime in these two columns must be the same. Flow uniformities are also important for the proper reproduction of the data. In large-scale columns, uniform distribution of gas can be difficult. Nonuniformities can cause channeling or

bypassing which can be harmful to the column performance. Flow uniformities can be achieved by adding a calming section before the column.

### **1.6.2 Pressure Drop**

The pressure drop across the column constitutes an important parameter, as throughput as well as mass transfer rates depend on energy dissipation. Various transport variables such as gas-liquid mass transfer coefficient, interfacial area, axial dispersion, etc., can be correlated to the pressure drop using the analogy between mass and momentum transfer processes. Significant pressure drop can also cause large undesired changes in the partial pressure of the reacting gas in the column if a gas-liquid reaction is also taking place.

### **1.6.3 Holdup of Various Phases**

The gas and liquid holdups play an important role in the column performance as they can greatly change the nature of the apparent kinetics of the reaction. The holdup of a phase is usually defined as the volume of the phase per unit column volume. However, for a fixed-bed column the gas and liquid holdups are often defined on the basis of void volume of the column. In a fixed-bed column the liquid holdup is divided into two parts: dynamic holdup, which depends largely



on the gas and liquid flow rates and the properties of the fluids and the packing material, and stagnant holdup, which depends to a large extent on the nature of the packing (e.g., shape, porosity and void fraction) and the fluid properties.

There is a strong relationship between the liquid holdup and the pressure drop in a downflow packed column. Liquid holdup also affects other parameters such as the degree of wetting of packing, the thickness of the liquid film around the particle, the capacity of the column to take up the heat generated in case of exothermic reactions taking place without thermal runaway occurring etc. Moreover, it is important in scaling up from smaller to larger columns to ensure that the hold-up remains at its optimum value.

Liquid holdup has been measured by a number of techniques. Some of which are,

- By weighing the dry column and subtracting this result from the weight of the column when liquid flows through it to obtain the total liquid holdup.
- By simultaneously shutting off the inlet and outlet streams and then draining the reactor to obtain the dynamic holdup. If the column is weighed after draining it one obtains the stagnant holdup as well.

- By tracer techniques, to obtain the total liquid up. The tail of the RTD is due to the stagnant liquid and may be used to derive the stagnant liquid holdup and hence also the dynamic liquid holdup. Alternatively, experiments may be carried out using decreasing step injections of tracer in order to accurately determine the total, dynamic and stagnant liquid holdups.

### **1.6.4 Residence-time Distribution and Axial Mixing**

When the fluid elements pass through the column, the exchange of mass between the fluid elements occurs both on a microscale as well as on a macroscale. The mixing process on a macroscale is characterized by the residence-time distribution of the fluid elements. In a three-phase column, significant axial mixing occurs in both the gas and liquid phases. When the macromixing in both axial and radial direction is incomplete, the macromixing in the axial direction is characterized by 'axial dispersion'. The role of RTD, which is normally measured separately for each flowing phase by tracer techniques, must be taken into account in column performance.

### 1.6.5 Gas-Liquid Mass Transfer

The importance of gas-liquid mass transfer on the column performance depends upon the flow conditions in the column and the nature of the reaction system. Two important parameters characterizing the gas-liquid mass transfer are the gas-liquid mass transfer coefficient and the gas-liquid interfacial area. Both of these parameters depend on the flow conditions and the nature and status of the solid packing. Estimation of the gas-liquid mass transfer rates also requires the knowledge of solubilities of absorbing and/or desorbing species and their variation with temperature (i.e. knowledge of heats of solution).

### 1.6.6 Intrinsic Kinetics

For most reaction systems, the intrinsic kinetic rate can be expressed either by a power-law expression or by the Langmuir-Hinshelwood model. The intrinsic kinetics should include both the detailed mechanism of the reaction and the kinetic expression and heat of reaction associated with each step of the mechanism.

## 1.7 OBJECTIVES

The overall purpose of this research project is to develop a mathematical model to predict the performance of cocurrent packed columns. The specific objectives to be achieved are:

- 1) To develop an efficient model to analyze and simulate the hydrodynamic behavior of cocurrent packed beds with up-flow and down-flow.
- 2) To define and validate the operating parameters required for a realistic analysis.
- 3) To test the model predictions on the available data reported in the literature for such systems.
- 4) To develop a theoretical model to predict the performance of gas absorption and air stripping in cocurrent packed columns.
- 5) To extend the model to gas absorption accompanied by chemical reaction involving variety of reaction kinetics representing systems of industrial importance.
- 6) To test these model predictions with experimental data reported in the literature.

# CHAPTER 2

## LITERATURE REVIEW

---

Three phase fixed bed columns are used in chemical industries in order to provide suitable contact between liquid and gaseous reactants and a solid catalyst if required, with a cocurrent flow of the two phases. For about thirty years now, chemical engineers attention has been addressed to such systems, owing to their suitability for many operations in chemical, oil refining, petrochemical and biochemical processes. Performance prediction and scale up of these columns are rather difficult problems in chemical engineering, as the column's production capacity not only depends on the chemical kinetics and the mean residence time of the reactants, but the complex hydrodynamic phenomena also strongly influence the mass transfer processes occurring in a multiphase system. Despite the appearance of two monographs (Shah, 1979; Ramachandran and Chaudhari, 1983) and extensive research activity in the last three decades, many problems remain to be solved. Data and methodology important for design and reliable prediction of performance are still missing. Scale up of cocurrent fixed bed columns is still far from being a standard routine for chemical engineers.

In view of the extensive applications of these systems in the industry (Shah, 1979; Morsi et al., 1982; Gianetto and Silveston, 1986), enormous amount of public research work exists for such type of columns as reviewed by Saterfield (1975), Charpentier (1976), Hoffman (1978), Shah (1978, 1979), Herskowitz and Smith (1983), Gianetto and Silveston (1986) and Gianetto and Specchia (1992). Several researchers have published a considerable amount of information related to different features of such type of columns. In the following sections, a brief survey of important investigations pertaining to this work are presented.

## **2.1 HYDRODYNAMICS OF COCURRENT PACKED COLUMNS**

Various flow regimes may exist in cocurrent gas liquid packed columns i.e. trickling, pulsing, bubble and spray flows. Due to the vast difference in the hydrodynamic characteristics of these regimes, the respective heat and mass transfer rates, holdup, and pressure drop also differ in a significant way. For this reason, in the design or scale-up of these systems, it is imperative to predict which flow regime to expect for a given system and a specified set of operation conditions.

The present approach relies heavily on empirical flow regime maps that have been developed in the last three decades (Sato et al., 1973, Charpentier and

Favier 1975; Fukushima and Kusaka, 1977). However, because of the large number of variables such as bed porosity, size and shape of particles, viscosity, density, interfacial tension, column dimensions, flow rates etc., that seem to have an important effect on the bed operation, most existing flow maps are valid only with the range of conditions under which the data were obtained.

For the downflow systems, Charpentier and co-workers (1968, 1971, 1975, 1976, 1979) indicated that the flow pattern boundaries depend on the foaming capacity of the liquid phase. They presented separate flow pattern diagrams for foaming and non foaming liquids. Their diagram for the non-foaming liquids, give results similar to the ones obtained by Sato et al. (1973) for an air-water system. Chou et al. (1977) indicated that besides fluid properties, the bed porosity and the wetting characteristics of the particles are also important in determining the flow transitions. Specchia and Baldi (1977) introduced the term "poor interaction regime" for the trickle flow or gas continuous flow regime because of the existence of very little interaction of gas and liquid. Other flow regimes such as pulsed flow, spray flow, etc., in which significant interaction between gas and liquid exists were all together denoted as high interaction regimes. For the non-foaming liquid, the transition conditions from a poor to high interaction regime obtained by these authors agreed well with those reported by Charpentier and Favier (1975). Recently Gianetto and Specchia (1992) presented a much improved

flow map as shown in Figure (2.1a) for downflow systems outlining the transitions from one hydrodynamic regime to another. This flow map takes into account the results of many authors working with different gas-liquid systems (foaming and non-foaming) and packing shape and size (Gianetto et al., 1970; Sato et al., 1973; Charpentier and Favier, 1975; Chou et al., 1977; Specchia and Baldi, 1977; Gianetto et al., 1978; Morsi et al., 1982; Blok et al., 1983; Tosun, 1984; Ng, 1986; Ellman, 1988; Grosser et al., 1988; Wild et al., 1991). Ng (1986) is the only investigator who tried to predict the transition from one hydrodynamic regime to another on theoretical basis.

The upflow systems requiring higher energy consumption are considered less extensively in the literature (Turpin, 1966; Specchia et al., 1974; Charpentier, 1976; Hoffman, 1978; Ross, 1990). Although the presented results are partially in disagreement, the flow map shown in Figure (2.1b), proposed by Turpin and Huntington (1967) seems to represent satisfactorily the more recent data (Gianetto and Specchia, 1992).

## **2.2 MASS TRANSFER STUDIES FOR COCURRENT PACKED COLUMN**

Earliest studies of mass transfer for downflow cocurrent gas absorption are reported by Reiss (1967). For pulse and spray flow regimes, he presented



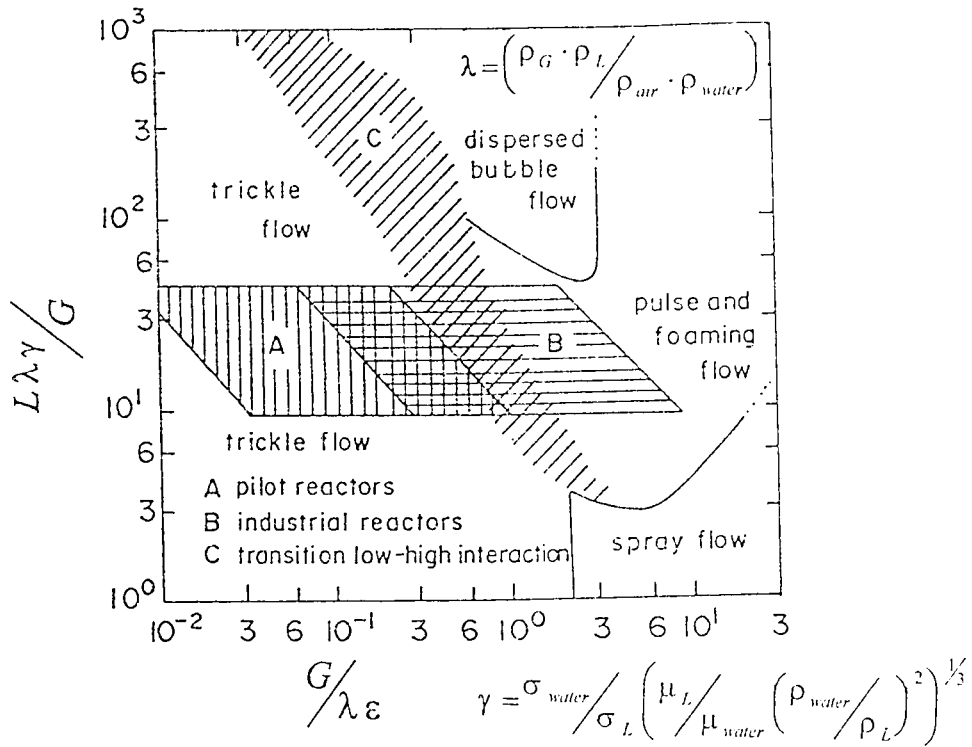


Figure (2.1a) Hydrodynamic flow map for the downflow system (Gianetto and Speechia, 1992)

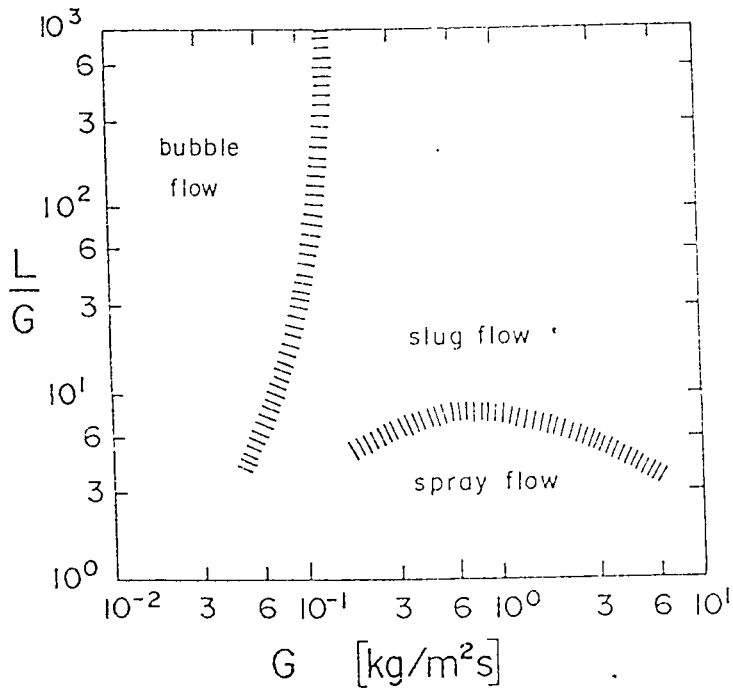


Figure (2.1b) Hydrodynamic flow map for the upflow system (Turpin and Hungtington, 1967)

extensive data for 12.5, 25 and 76 mm polyethylene Raschig rings. Since then, many studies have been reported in the literature.

Some early investigators related  $k_{GL} a_{GL}$  to liquid and gas velocities by either dimensional (Gianetto et al., 1970; Goto and Smith, 1975) or dimensionless (Goto and Smith, 1975) correlations. Goto and Smith (1975) presented a dimensionless correlation relating Sherwood numbers to the liquid phase Reynolds and Schmidt numbers. The dimensional correlations presented by different workers assumed that  $k_{GL} a_{GL}$  is proportional to  $U_L^{\bar{r}} U_G^s$ . Some of the values of  $\bar{r}$  and  $s$  for various type of packings reported in the literature, are summarized in table (2 1).

Several investigators have presented an energy correlation (in which  $k_{GL} a_{GL}$  is related to the two phase pressure drop) for the gas-liquid mass transfer coefficient (Reiss, 1967; Satterfield, 1975; Charpentier, 1976). Charpentier (1976) proposed an improved relation for trickling systems with low gas and liquid flow rates.

Fukushima and Kusaka (1977) reported mass transfer data for relatively large size particles (1.3 and 2.5 cm ceramic spheres and 1.2 cm ceramic Raschig rings) using oxygen absorption into sodium sulphite solution. The data were presented in terms of liquid Reynolds number, liquid holdup, column and particle diameter, and a shape factor.

**Table 2.1** Reported values of coefficients used in correlations for calculating  $k_{GL} a_{GL}$ , for various packings.

Investigator	Year	Packing Type	$\bar{F}$	$s$
Ufford and Perona	1973	1.9-cm Berl saddles	0.82	0.46
		1.3-cm Raschig rings	0.93	0.42
		0.63-cm Raschig rings	1.06	0.75
Sato et al.	1972	Glass spheres; dia. from 2.5 to 12.17 mm	0.80	0.80
Sylvester and Pitayagulsarn	1975	0.32 cm $\times$ 0.32 cm cylinders	1.20	0.30

For packings of much smaller diameter, Seirafi and Smith (1980) measured  $k_{GL} a_{GL}$  by a dynamic method that calculates the mass transfer coefficient from the zero and first moments of the experimental breakthrough curve measured in the liquid effluent. Mass transfer coefficients were measured as a function of the liquid superficial flow rates with a constant gas superficial flow rate.

For small diameter packings, Mahajani and Sharma (1979) measured mass transfer coefficients by a chemical technique employing the absorption of pure  $\text{CO}_2$  into aqueous solutions of NaOH, into n-butanol containing monethanolamine, and into p-xylene containing cyclohexylamine. For measurements in the trickle flow regime,  $k_{GL} a_{GL}$  values for organic systems were higher than those for aqueous solutions. This could be due to the influence of diffusivities which are higher in organic systems.

Morsi (1982) measured  $k_{GL} a_{GL}$  in the trickle flow regime for non-viscous and viscous liquids by a chemical technique absorbing lean  $\text{CO}_2$  in air into ethanol and ethylene glycol solutions of diethanolamine. The studies were carried out for small diameter packings and  $k_{GL} a_{GL}$  obtained with viscous organic solvents were higher than those obtained with a non-viscous one.

Correlation of gas-liquid mass transfer coefficients for organic solutions and small sized packing both with and without chemical reaction was undertaken by Turek and Lange (1981) and Turek et al (1979). They reported that at low liquid flow rates, the gas flow rate increases the  $k_{GL}$ ,  $a_{GL}$  values.

A highly recommended correlation based on a very large amount of data obtained with different gas-liquid systems in a wide range of operating conditions is proposed by Ellman (1988).

Larachi et al. (1990, 1991 and 1992), Wammes et al. (1990,1991) proposed correlations for mass transfer in pressurized upflow and downflow systems. They reported the effect of increased density on the hydrodynamics and overall performance.

A brief summary of experimental studies particularly related to gas absorption with chemical reaction is presented in Table (2.2),

**Table 2.2** Experimental studies of gas absorption with chemical reaction in downflow and upflow cocurrent packed columns.

<b>Downflow Operation</b>		
Investigator	Year	Salient features
Gianetto et al.	1970	<ul style="list-style-type: none"> <li>• Carbonation of sodium hydroxide</li> </ul>
	1973	
Hirose et al.	1974	
Mitchell and Perona	1979	
Shende and Sharma	1974	<ul style="list-style-type: none"> <li>• Oxidation of sodium dithionite</li> <li>• Reported 15-20% higher values of effective interfacial area.</li> </ul>
Fukushima and Kusaka	1977	<ul style="list-style-type: none"> <li>• Carbonation of Sodium Sulphite</li> </ul>
Mahajani and Sharma	1979	<ul style="list-style-type: none"> <li>• Studied absorption of CO<sub>2</sub>/O<sub>2</sub> in different organic solvents</li> </ul>
Morsi	1982	
Morsi et al.	1984	
Mahajani and Sharma	1980	<ul style="list-style-type: none"> <li>• Oxidation of Sodium Dithionite</li> </ul>

<b>Upflow Operation</b>		
Investigator	Year	Salient features
Mashelkar and Sharma	1970	<ul style="list-style-type: none"> <li>• Absorption of CO<sub>2</sub> in a variety of electrolytic and non-electrolytic solutions</li> <li>• Reported increase in overall mass transfer coefficient for cocurrent upflow operation</li> </ul>
Saada	1972	<ul style="list-style-type: none"> <li>• Carbonation of Sodium Hydroxide</li> </ul>
Ohshima et al.	1976	<ul style="list-style-type: none"> <li>• Oxidation of Sodium Sulphite</li> </ul>

## 2.3 THEORETICAL MODELING OF COCURRENT PACKED COLUMNS

The most investigated differential model in the literature is the one parameter axial dispersion model. It characterizes the backmixing by a simple one-dimensional Fick's law type diffusion equation. The constant of proportionality in this equation is known as axial dispersion coefficient. The assumption that all the mixing processes follow a Fick's law type diffusion equation, regardless of the actual mechanism, becomes, of course, increasingly dubious with large degree of backmixing. However, its simplicity made it the most widely used model. The model can be represented by the following partial differential equation,

$$h_t \frac{\partial c}{\partial t} = D_L \frac{\partial^2 c}{\partial z^2} - U \frac{\partial c}{\partial z} \quad (2.1)$$

Michell and Furzer (1972) claimed that the axial dispersion model does not adequately describe the nature of flow in cocurrent packed column. They further claimed that this model gives insufficient tailing.

Deans and Lapidus (1960) and Deans (1963) proposed a two-parameter modified mixing cell model, which assumes that each cell contains stagnant and flowing regions. Due to backmixing mass exchange between the flowing and stagnant regime occurs. When the number of cells is very large, the model reduces

to cross flow model proposed by Hoogendoorn and Lips (1965). The liquid phase is supposed to be in ideal plug flow while the stagnant region is completely mixed.

The model can best be represented by a set of partial differential equations

$$h_d \frac{\partial c_d}{\partial t} = -k_{SD} a_{SD} (c_d - c_s) - U_L \frac{\partial c_d}{\partial z} \quad (2.2)$$

$$h_s \frac{\partial c_s}{\partial t} = k_{SD} a_{SD} (c_d - c_s) \quad (2.3)$$

Hoogendoorn and Lips (1965) fitted this model to counter-current flow data. Hochman and Effron (1969) extended this model to cocurrent flows. The drawbacks in the model are that it does not account for axial dispersion and it predicts concentration wavefronts traveling at infinite speed.

Buffham et al. (1970) and Buffham (1971) proposed a two parameter probabilistic time delay model. This model assumes that the liquid would flow in plug flow except for the fact that fluid elements are randomly delayed in time. However, it was shown that with suitable redefinition of parameters, this model reduces in mathematical terms to the modified mixing cell or cross-flow model.

Van Swaij et al. (1969), and Bennet and Goodridge (1970) independently put forward a three-parameter Piston-Dispersion-Exchange (P-D-E) Model or



Dispersed Crossflow Model. The model is based on the same concept as the crossflow or modified mixing cell model, except that axial dispersion in the dynamic phase is also considered. So the backmixing is due to both axial dispersion and transfer of mass between dynamic and stagnant regions. The partial differential equations describing this model are,

$$h_d \frac{\partial c_d}{\partial t} = D_L \frac{\partial^2 c_d}{\partial z^2} - U_L \frac{\partial c_d}{\partial z} - k_{SD} a_{SD} (c_d - c_s) \quad (2.4)$$

$$h_s \frac{\partial c_s}{\partial t} = k_{SD} a_{SD} (c_d - c_s) \quad (2.5)$$

Matsuura et al. (1976) applied the Dispersed Cross Flow Model to cocurrent flows and assessed the relative importance of two dispersion mechanisms by comparing the Peclet number obtained by using the Axially Dispersed Plug Flow Model with that obtained by using the Dispersed Cross-Flow Model. They concluded that stagnant regions contribute nearly 90% of the total dispersion at moderate liquid flow rates. Other studies on Cross Flow Model are carried out by Hinduja et al. (1977, 1980).

Dispersed Cross Flow Model has been shown to correlate data better than the previous models, but considers the stagnant regions to be completely mixed. Kan and Greenfield (1983) pointed out that the mixing in the stagnant regions is

not necessarily complete, and for a realistic picture, this factor must be taken into account. They modified Matsuura's model by assuming that the mixing in the stagnant region is not necessarily complete and termed it the Ideal Plug Flow Stagnancy Model. They approximated the transport phenomenon by the equations,

$$\frac{\partial c_d}{\partial t} = D_L \frac{\partial^2 c_d}{\partial z^2} - U_L \frac{\partial c_d}{\partial z} - \frac{(1-\phi)}{\phi L_S} D_S \frac{\partial c_S}{\partial y} \Big|_{y=0} \quad (2.6)$$

$$\frac{\partial c_S}{\partial t} = D_S \frac{\partial^2 c_S}{\partial y^2} \quad (2.7)$$

They established that  $D_S$  does not necessarily have to be the diffusivity of the tracer, as its value is quite different and does not vary much with different tracers with varying diffusivities. Although the model proposed by them is quite comprehensive, they made too many simplifying assumptions. They took the axial dispersion coefficient as zero and further assumed that at the stagnant and dynamic liquid interphase the concentrations in both phases are equal, implying a very high value of mass transfer coefficient between phases. Further they did not employ the more realistic Danckwerts boundary conditions for the dynamic phase. With these simplifications, they obtained an analytical solution for an impulse input of a tracer.

Skomorokov and Kirillov (1986) extended the P-D-E model to the cocurrent upflow systems. They made a study of the parameters involved and

concluded that the dynamic characteristics of the liquid phase are affected mainly by the existence of dynamic zones and the exchange rate between these and the flowing liquid.

## 2.4 LIQUID HOLDUP CORRELATIONS

### 2.4.1 Dynamic Liquid holdup

There have been several literature reviews on the liquid holdup (Satterfield, 1975; Schwartz et al., 1976; Weekman, 1976; Hofmann, 1977, 1978; Charpentier, 1979; Gianetto et al., 1978; Herskowitz and Smith, 1983; Ramachandran et al., 1987). Ellman (1988) gave a table of empirical correlations for liquid holdups.

In general, the liquid holdup correlations may be divided into two types:

- 1) Those which relate the total or the dynamic holdup to the Lockhart-Martinelli parameter (1949),  $\chi$ , defined for the high interaction regime as,

$$\chi^2 = \frac{(dp/dz)_L}{(dp/dz)_G} = \left(\frac{L}{G}\right)^2 \left(\frac{\rho_G}{\rho_L}\right)^{1.1} \left(\frac{\mu_L}{\mu_G}\right)^{0.2} \quad (2.8)$$

such as the correlation of Larkins et al. (1961), Charpentier et al. (1971, 1975), Midoux et al. (1976), Morsi et al. (1981) and Rao et al. (1983, 1985).

- 2) Those which correlate the total or dynamic liquid holdup with dimensionless groups characterizing the flow phenomena associated with the liquid as well as the properties of the liquid and the packing, such as the correlations of Turpin and Huntington (1967), Hochman and Effron (1969), Goto et al. (1977) Specchia and Baldi (1977), Matsuura et al. (1979) and Rao et al. (1983, 1985).

Interestingly, several of the correlations of the second group take absolutely no account of the influence of the gas on liquid holdup. On the other hand, the correlations belonging to the first group depend on the single phase gas and liquid pressure drops. However, most of these correlations are not applicable over wide ranges of system conditions. An improved correlation for the liquid holdup derived from fundamental considerations and a wide ranging data base of experimental results was presented by Ellman et al. (1990). It is applicable to industrial systems as it is based on wide variations of all the important variables including measurements at high pressures.

## 2.4.2 Stagnant Liquid holdup

The stagnant holdup results from a balance between surface tension forces and gravitational effects. Dombrowski and Brownell (1954) and Nenninger and Storrow (1958) developed correlations to predict residual holdup considering these effects. Charpentier et al. (1968) related the stagnant holdup to the Eotvos number which represents the ratio of gravitational to surface tension forces.

Relatively few studies have been reported on developing correlations for stagnant holdup. Saez and Carbonell (1985) modified the correlation of Charpentier et al. (1968) to predict stagnant holdup in packed bed based on a physically more realistic characteristic length .

## 2.4 ANALYSIS OF THE PUBLISHED WORK

The following conclusions are drawn from the literature survey,

- i) Very few theoretical studies have been undertaken to predict the performance of cocurrent packed columns.
- ii) Available theoretical models have been solved for simple cases by employing unrealistic assumptions.

- iii) Complex nature of these systems necessitates a comprehensive theoretical model to adequately predict the conditions prevailing in the column.
- iv) Experimental data available in the literature can be used for the development and validation of an improved model.

# CHAPTER 3

## MATHEMATICAL MODEL FORMULATION

---

### 3.1 DEVELOPMENT OF A BASIC MODEL

The mathematical formulation of a given system requires a basic understanding and identification of various phenomena occurring inside it, to deduce the model equations, and some reasonable assumptions to solve them. Keeping these in mind, fluid behavior in an elemental section of a packed column is considered. Though the detailed flow pattern in the bed is quite complicated, it is idealized by assuming that the interstitial region between the packing is partly occupied by the gas and partly by the liquid, which is further subdivided into 'stagnant' and 'dynamic' regions. The packing is assumed to be non-porous, in contact with the stagnant layer, outside which we have dynamic liquid flowing axially along with the gas (see Figure 3.1). It is further assumed that the radial concentration gradients inside the column are negligible and that due to the very small thickness of the stagnant zone, curvature effects of the packing can be neglected, with the result, that the whole bed can be approximated by a flat geometry. Few additional assumptions are, constant temperature of the system,

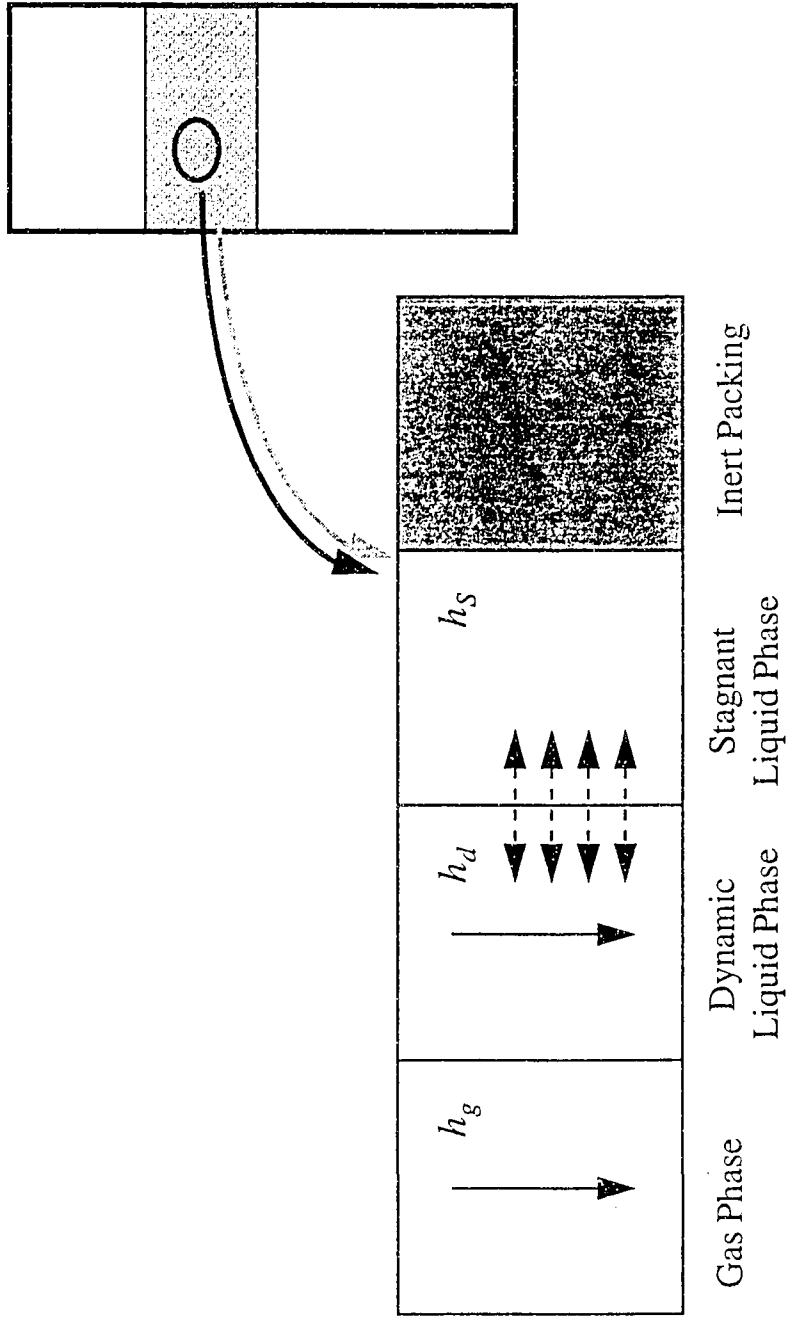


Figure (3.1) Schematic diagram of a representative element of the bed.



constant dispersion coefficient in the stagnant zone, negligible pressure drop across the column and negligible contribution of other mechanical effects.

With these assumptions, it is concluded that for the case of a non-volatile tracer, following phenomenon must be considered before applying the material balance in both the liquid zone.

- i) Accumulation of mass in the stagnant and dynamic zone.
- ii) Transport of mass across the stagnant film which surrounds the stagnant zone (external mass transfer).
- iii) Internal mixing within the stagnant zone defined by a Fickian type of equation.
- iv) Axial dispersion in the dynamic zone.

Based on the material balance in the dynamic liquid phase, one gets the following unsteady state differential equation,

$$h_d \left( \frac{\partial c_d}{\partial t} \right) = D_L h_d \left( \frac{\partial^2 c_d}{\partial z^2} \right) - U_L \left( \frac{\partial c_d}{\partial z} \right) - k_{SD} a_{SD} (c_d - c_s|_{y=0}) \quad (3.1)$$

At the entrance and exit of the column, the boundary conditions for this phase can be written as,

$$\text{At } z=0, t > 0 \quad D_L \left( \frac{\partial c_d}{\partial z} \Big|_{z=0^+} \right) = - U_L (c_d|_{z=0^-} - c_d|_{z=0^+}) \quad (3.2)$$

$$\text{At } z=L_C, t>0 \quad \left. \frac{\partial c_d}{\partial z} \right|_{z=L_C} = 0 \quad (3.3)$$

Similarly, an unsteady state mass balance in the stagnant liquid phase described by a Fickian type equation can be written as,

$$\left( \frac{\partial c_s}{\partial t} \right) = D_s \left( \frac{\partial^2 c_s}{\partial y^2} \right) \quad (3.4)$$

The boundary conditions at the stagnant and dynamic liquid interphase, and at the surface of the solid packing can be written as,

$$\text{At } y=0, t>0 \quad D_s \left( \left. \frac{\partial c_s}{\partial y} \right|_{y=0} \right) = -k_{SD} (c_d - c_s|_{y=0}) \quad (3.5)$$

$$\text{At } y=L_S, t>0 \quad \left. \frac{\partial c_s}{\partial y} \right|_{y=L_S} = 0 \quad (3.6)$$

The corresponding initial conditions for the dynamic and stagnant phase are,

$$\text{At } z \geq 0, t=0 \quad c_d = c_d^o \quad (3.7)$$

$$\text{At } y \geq 0, t=0 \quad c_s = c_s^o \quad (3.8)$$

Equations (3.1) to (3.8) can be reduced to corresponding dimensionless forms by introducing the following dimensionless parameters :

$$\begin{aligned} C_d &= \frac{c_d}{c_{d^o}}, & C_s &= \frac{c_s}{c_{d^o}}, & x &= \frac{z}{L_C}, & \eta &= \frac{y}{L_S}, \\ \phi &= \frac{h_d}{h_t}, & \theta &= \frac{t U_L}{h_t L_C}, & Pe_L &= \frac{U_L L_C}{D_L}, \end{aligned} \quad (3.9)$$

$$K_{SD}^* = \frac{k_{SD} a_{SD} L_C}{U_L}, \quad \beta = \frac{L_C D_S h_t}{U_L L_S^2}, \quad Bi = \frac{k_{SD} L_S}{D_S},$$

For the dynamic liquid phase, the dimensionless equation is,

$$\phi \left( \frac{\partial C_d}{\partial \theta} \right) = \frac{h_d}{Pe_L} \left( \frac{\partial^2 C_d}{\partial x^2} \right) - \left( \frac{\partial C_d}{\partial x} \right) - K_{SD}^* (C_d - C_S|_{\eta=0}) \quad (3.10)$$

With the dimensionless boundary conditions given as :

$$\text{At } x = 0, \theta > 0 \quad \left. \frac{\partial C_d}{\partial x} \right|_{x=0^+} = -Pe_L (C_d|_{x=0^-} - C_d|_{x=0^+}) \quad (3.11)$$

$$\text{At } x = 1, \theta > 0 \quad \left. \frac{\partial C_d}{\partial x} \right|_{x=1} = 0 \quad (3.12)$$

For the stagnant liquid phase the dimensionless form of the unsteady state material balance is,

$$\left( \frac{\partial C_S}{\partial \theta} \right) = \beta \left( \frac{\partial^2 C_S}{\partial \eta^2} \right) \quad (3.13)$$

and the corresponding dimensionless boundary conditions are,

$$\text{At } \eta = 0, \theta > 0 \quad \left. \frac{\partial C_S}{\partial \eta} \right|_{\eta=0} = -Bi (C_d - C_S|_{\eta=0}) \quad (3.14)$$

$$\text{At } \eta = 1, \theta > 0 \quad \left. \frac{\partial C_S}{\partial \eta} \right|_{\eta=1} = 0 \quad (3.15)$$

Similarly, the initial conditions can be rewritten in dimensionless form as,

$$\text{At } x \geq 0, \theta = 0 \quad C_d = C_d^o \quad (3.16)$$

$$\text{At } \eta \geq 0, \theta = 0 \quad C_S = C_S^o \quad (3.17)$$

The resulting non-dimensional model equations are parabolic partial differential equations and the associated boundary conditions are of Neumann type. For this case these are represented by Danckwerts boundary conditions.

### 3.2 MODEL EQUATIONS FOR GAS ABSORPTION

In order to develop a comprehensive model for gas absorption in packed columns an effort was made to keep the model simple and yet, as realistic as possible, employing minimum of assumptions. Keeping in mind the important role played by the gas phase in such operations, a heterogeneous system was considered in the model formulations. For the evaluation of liquid phase residence time distribution, an improved P-D-E model proposed in Section (3.1) is used. The gas phase is defined by a P-D model with mass exchange between gas and liquid phases, which was shown by different investigators (Hochman and Elfron, 1969 ; Dunn et al., 1977), to satisfactorily interpret the gas phase RTD.

For the model development same assumptions and phenomena are considered as discussed in Section (3.1). Some additional phenomena which are also considered to be important are listed as follows.

- Accumulation of mass in the gas phase.
- Transport of mass across the gas and liquid film interface.
- Axial dispersion in the bulk gas.

The resulting unsteady state differential equation for the material balance in the gas phase gives,

$$h_g \left( \frac{\partial c_g}{\partial t} \right) = D_G h_g \left( \frac{\partial^2 c_g}{\partial z^2} \right) - U_G \left( \frac{\partial c_g}{\partial z} \right) - k_{GL} a_{GL} (H c_g - c_d) \quad (3.18)$$

The boundary conditions for this phase at the entrance and exit of the column can be written as,

$$\text{At } z=0, t>0 \quad D_G \left( \frac{\partial c_g}{\partial z} \Big|_{z=0} \right) = - U_G (c_g|_{z=0^-} - c_g|_{z=0^+}) \quad (3.19)$$

$$\text{At } z=L_C, t>0 \quad \frac{\partial c_g}{\partial z} \Big|_{z=L_C} = 0 \quad (3.20)$$

The transient mass balance for the dynamic liquid phase takes the form,

$$h_d \left( \frac{\partial c_d}{\partial t} \right) = D_L h_d \left( \frac{\partial^2 c_d}{\partial z^2} \right) - U_L \left( \frac{\partial c_d}{\partial z} \right) - k_{SD} a_{SD} (c_d - c_s|_{y=0}) + k_{GL} a_{GL} (H c_g - c_d) \quad (3.21)$$

with the boundary conditions,

$$\text{At } z=0, t>0 \quad D_L \left( \frac{\partial c_d}{\partial z} \Big|_{z=0^+} \right) = - U_L (c_d|_{z=0^-} - c_d|_{z=0^+}) \quad (3.22)$$

$$\text{At } z = L_C, t > 0 \quad \left. \frac{\partial c_d}{\partial z} \right|_{z=L_C} = 0 \quad (3.23)$$

Similarly, an unsteady state mass balance in the stagnant liquid phase described by a Fickian type equation can be written as,

$$\left( \frac{\partial c_S}{\partial t} \right) = D_S \left( \frac{\partial^2 c_S}{\partial y^2} \right) \quad (3.24)$$

The corresponding boundary conditions at the stagnant and dynamic liquid interphase, and at the surface of the solid packing can be written as,

$$\text{At } y = 0, t > 0 \quad D_S \left( \left. \frac{\partial c_S}{\partial y} \right|_{y=0} \right) = -k_{SD} (c_d - c_S|_{y=0}) \quad (3.25)$$

$$\text{At } y = L_S, t > 0 \quad \left. \frac{\partial c_S}{\partial y} \right|_{y=L_S} = 0 \quad (3.26)$$

For the system defined above the initial conditions are,

$$\text{At } z \geq 0, t = 0 \quad c_g = c_g^o \quad (3.27)$$

$$\text{At } z \geq 0, t = 0 \quad c_d = c_d^o \quad (3.28)$$

$$\text{At } y \geq 0, t = 0 \quad c_S = c_S^o \quad (3.29)$$

Equations (3.18) to (3.29) are normalized by the introduction of following dimensionless parameters :

$$C_d = \frac{c_d}{Hc_{g_o}}, \quad C_S = \frac{c_S}{Hc_{g_o}}, \quad C_g = \frac{c_g}{c_{g_o}},$$

$$\begin{aligned}
x &= \frac{z}{L_C}, & \eta &= \frac{y}{L_S}, & \phi &= \frac{h_d}{h_t}, \\
\theta &= \frac{t U_L}{h_t L_C}, & Pe_L &= \frac{U_L L_C}{D_L}, & Pe_G &= \frac{U_G L_C}{D_G}, \\
K_{SD}^* &= \frac{k_{SD} a_{SD} L_C}{U_L}, & St &= \frac{k_{GL} a_{GL} L_C}{U_L}, & \xi &= \frac{U_G}{U_L}, \\
\beta &= \frac{L_C D_S h_t}{U_L L_S^2}, & Bi &= \frac{k_{SD} L_S}{D_S}, & \psi &= \frac{h_g}{h_t},
\end{aligned} \tag{3.30}$$

The dimensionless mass balance equation for the gas phase becomes,

$$\frac{\partial C_g}{\partial \theta} = \frac{\xi}{\psi} \left[ \frac{h_g}{Pe_G} \left( \frac{\partial^2 C_g}{\partial x^2} \right) - \left( \frac{\partial C_g}{\partial x} \right) - \frac{St}{\xi} H(C_g - C_d) \right] \tag{3.31}$$

With the corresponding dimensionless boundary conditions given as :

$$\text{At } x=0, \theta > 0 \quad \left. \frac{\partial C_g}{\partial x} \right|_{x=0^+} = -Pe_G (C_g|_{x=0^-} - C_g|_{x=0^+}) \tag{3.32}$$

$$\text{At } x=1, \theta > 0 \quad \left. \frac{\partial C_g}{\partial x} \right|_{x=1} = 0 \tag{3.33}$$

The dimensionless equation for the dynamic liquid phase is,

$$\phi \left( \frac{\partial C_d}{\partial t} \right) = \frac{h_d}{Pe_L} \left( \frac{\partial^2 C_d}{\partial x^2} \right) - \left( \frac{\partial C_d}{\partial x} \right) - K_{SD}^* (C_d - C_S|_{\eta=0}) + St (C_g - C_d) \tag{3.34}$$

With the dimensionless boundary conditions,

$$\text{At } x=0, \theta > 0 \quad \left. \frac{\partial C_d}{\partial x} \right|_{x=0^+} = -Pe_L (C_d|_{x=0^-} - C_d|_{x=0^+}) \tag{3.35}$$

$$\text{At } x=1, \theta > 0 \quad \left. \frac{\partial C_d}{\partial x} \right|_{x=1} = 0 \quad (3.36)$$

The dimensionless unsteady state material balance for the stagnant liquid phase is written as ,

$$\left( \frac{\partial C_s}{\partial \theta} \right) = \beta \left( \frac{\partial^2 C_s}{\partial \eta^2} \right) \quad (3.37)$$

and the corresponding dimensionless boundary conditions are,

$$\text{At } \eta=0, \theta > 0 \quad \left. \frac{\partial C_s}{\partial \eta} \right|_{\eta=0} = -Bi(C_d - C_s|_{\eta=0}) \quad (3.38)$$

$$\text{At } \eta=1, \theta > 0 \quad \left. \frac{\partial C_s}{\partial \eta} \right|_{\eta=1} = 0 \quad (3.39)$$

Similarly, the initial conditions can be rewritten in dimensionless form as,

$$\text{At } x \geq 0, \theta = 0 \quad C_g = C_g^o \quad (3.40)$$

$$\text{At } x \geq 0, \theta = 0 \quad C_d = C_d^o \quad (3.41)$$

$$\text{At } \eta \geq 0, \theta = 0 \quad C_s = C_s^o \quad (3.42)$$

### 3 MODEL EQUATIONS FOR STRIPPING

The basic model Equations (3.18) to (3.29) for the liquid and gas phase defined in Section (3.2) can be applied to the case of stripping. However, for the



convenience of comparing the model predictions to the experimental data, the dimensionless parameters are redefined as follows:

$$\begin{aligned}
C_d &= \frac{c_d}{c_{d_0}}, & C_s &= \frac{c_s}{c_{d_0}}, & C_g &= \frac{H c_g}{c_{d_0}}, \\
x &= \frac{z}{L_C}, & \eta &= \frac{y}{L_S}, & \phi &= \frac{h_d}{h_t}, \\
\theta &= \frac{t U_L}{h_t L_C}, & Pe_L &= \frac{U_L L_C}{D_L}, & Pe_G &= \frac{U_G L_C}{D_G}, \\
K_{SD}^* &= \frac{k_{SD} a_{SD} L_C}{U_L}, & St &= \frac{k_{GL} a_{GL} L_C}{U_L}, & \xi &= \frac{U_G}{U_L}, \\
\beta &= \frac{L_C D_S h_t}{U_L L_S^2}, & Bi &= \frac{K_{SD} L_S}{D_S}, & \psi &= \frac{h_g}{h_t},
\end{aligned} \tag{3.43}$$

The dimensionless mass balance equation for the gas phase becomes,

$$\frac{\partial C_g}{\partial \theta} = \frac{\xi}{\psi} \left[ \frac{h_g}{Pe_g} \left( \frac{\partial^2 C_g}{\partial x^2} \right) - \left( \frac{\partial C_g}{\partial x} \right) - \frac{St}{\xi} H (C_g - C_d) \right] \tag{3.44}$$

With the corresponding dimensionless boundary conditions given as :

$$\text{At } x = 0, \theta > 0 \quad \left. \frac{\partial C_g}{\partial x} \right|_{x=0^+} = -Pe_G \left( C_g \Big|_{x=0^-} - C_g \Big|_{x=0^+} \right) \tag{3.45}$$

$$\text{At } x = 1, \theta > 0 \quad \left. \frac{\partial C_g}{\partial x} \right|_{x=1} = 0 \tag{3.46}$$

For the dynamic liquid phase, the dimensionless equation is,

$$\phi \left( \frac{\partial C_d}{\partial t} \right) = \frac{h_d}{Pe_L} \left( \frac{\partial^2 C_d}{\partial x^2} \right) - \left( \frac{\partial C_d}{\partial x} \right) - K_{SD}^* (C_d - C_S|_{\eta=0}) + St (C_g - C_d) \quad (3.47)$$

With the dimensionless boundary conditions,

$$\text{At } x=0, \theta > 0 \quad \left. \frac{\partial C_d}{\partial x} \right|_{x=0^+} = -Pe_L (C_d|_{x=0^-} - C_d|_{x=0^+}) \quad (3.48)$$

$$\text{At } x=1, \theta > 0 \quad \left. \frac{\partial C_d}{\partial x} \right|_{x=1} = 0 \quad (3.49)$$

The stagnant liquid phase dimensionless unsteady state material balance is written as,

$$\left( \frac{\partial C_S}{\partial \theta} \right) = \beta \left( \frac{\partial^2 C_S}{\partial \eta^2} \right) \quad (3.50)$$

and the corresponding dimensionless boundary conditions are,

$$\text{At } \eta=0, \theta > 0 \quad \left. \frac{\partial C_S}{\partial \eta} \right|_{\eta=0} = -Bi (C_d - C_S|_{\eta=0}) \quad (3.51)$$

$$\text{At } \eta=1, \theta > 0 \quad \left. \frac{\partial C_S}{\partial \eta} \right|_{\eta=1} = 0 \quad (3.52)$$

Similarly, the initial conditions can be rewritten in dimensionless form as,

$$\text{At } x \geq 0, \theta = 0 \quad C_g = C_g^o \quad (3.53)$$

$$\text{At } x \geq 0, \theta = 0 \quad C_d = C_d^o \quad (3.54)$$

$$\text{At } \eta \geq 0, \theta = 0 \quad C_S = C_S^o \quad (3.55)$$

### 3.4 MODEL EQUATIONS FOR GAS ABSORPTION WITH CHEMICAL REACTION

The model equations for gas absorption, developed in Section (3.2), can be used with some modification to incorporate the effect of chemical reaction of the solute gas being absorbed, with some suitable reactant in the liquid phase. For this system, additional mass balances have to be written for the reactant in both the dynamic and stagnant liquid phases. The resulting partial differential equations include an additional term to incorporate the effect of chemical reaction (intrinsic kinetics).

The assumptions and phenomena considered in addition to those described in Section (3.2) are listed as follows,

- Accumulation of reactant in the stagnant liquid phase.
- Transport of both the reactant and the solute gas across the dynamic and stagnant liquid interface.
- Axial dispersion of the reactant in the dynamic liquid.
- Occurrence of reaction only in the liquid phases.

The resulting unsteady state differential equation for the material balance when applied for the solute component 1 in the gas phase gives,

$$h_g \left( \frac{\partial c_{g_1}}{\partial t} \right) = D_G h_g \left( \frac{\partial^2 c_{g_1}}{\partial z^2} \right) - U_G \left( \frac{\partial c_{g_1}}{\partial z} \right) - k_{GL} a_{GL} (H c_{g_1} - c_{d_1}) \quad (3.56)$$

The boundary conditions for this phase, at the entrance and exit of the column can be written as,

$$\text{At } z=0, t>0 \quad D_G \left( \frac{\partial c_{g_1}}{\partial z} \Big|_{z=0^+} \right) = - U_G \left( c_{g_1} \Big|_{z=0^+} - c_{g_1} \Big|_{z=0^+} \right) \quad (3.57)$$

$$\text{At } z=L_C, t>0 \quad \frac{\partial c_{g_1}}{\partial z} \Big|_{z=L_C} = 0 \quad (3.58)$$

The transient mass balance for the solute component 1 in the dynamic liquid phase takes the form,

$$h_d \left( \frac{\partial c_{d_1}}{\partial t} \right) = D_{L_1} h_d \left( \frac{\partial^2 c_{d_1}}{\partial z^2} \right) - U_L \left( \frac{\partial c_{d_1}}{\partial z} \right) - k_{SD_1} a_{SD} \left( c_{d_1} - c_{S_1} \Big|_{y=0} \right) + k_{GL} a_{GL} (H c_{g_1} - c_{d_1}) - \langle r_1 \rangle \quad (3.59)$$

with the boundary conditions,

$$\text{At } z=0, t>0 \quad D_{L_1} \left( \frac{\partial c_{d_1}}{\partial z} \Big|_{z=0^+} \right) = - U_L \left( c_{d_1} \Big|_{z=0^+} - c_{d_1} \Big|_{z=0^+} \right) \quad (3.60)$$

$$\text{At } z=L_C, t>0 \quad \frac{\partial c_{d_1}}{\partial z} \Big|_{z=L_C} = 0 \quad (3.61)$$

The transient mass balance for the reactant 2 in the dynamic liquid phase takes the form,

$$h_d \left( \frac{\partial c_{d_2}}{\partial t} \right) = D_{L_2} h_d \left( \frac{\partial^2 c_{d_2}}{\partial z^2} \right) - U_L \left( \frac{\partial c_{d_2}}{\partial z} \right) - k_{SD_2} a_{SD} \left( c_{d_2} - c_{S_2} \Big|_{y=0} \right) - \langle r_2 \rangle \quad (3.62)$$

with the boundary conditions,

$$\text{At } z=0, t>0 \quad D_L \left( \frac{\partial c_{d_2}}{\partial z} \Big|_{z=0^+} \right) = -U_L (c_{d_2}|_{z=0^-} - c_{d_2}|_{z=0^+}) \quad (3.63)$$

$$\text{At } z=L_C, t>0 \quad \frac{\partial c_{d_2}}{\partial z} \Big|_{z=L_C} = 0 \quad (3.64)$$

Similarly, an unsteady state mass balance for the component  $i$  in the stagnant liquid phase described by a Fickian type equation can be written as,

$$\left( \frac{\partial c_{S_i}}{\partial t} \right) = D_{S_i} \left( \frac{\partial^2 c_{S_i}}{\partial y^2} \right) - \langle r_i \rangle \quad (3.65)$$

where,  $i=1$  for the solute gas and  $i=2$  for reactant in the liquid.

The corresponding boundary conditions at the stagnant and dynamic liquid interphase and at the surface of the solid packing can be written as,

$$\text{At } y=0, t>0 \quad D_{S_i} \left( \frac{\partial c_{S_i}}{\partial y} \Big|_{y=0} \right) = -k_{SD_i} (c_{d_i} - c_{S_i}|_{y=0}) \quad (3.63)$$

$$\text{At } y=L_S, t>0 \quad \frac{\partial c_{S_i}}{\partial y} \Big|_{y=L_S} = 0 \quad (3.64)$$

The initial conditions for the system defined above are,

$$\text{At } z \geq 0, t=0 \quad c_g = c_g^o \quad (3.65)$$

$$\text{At } z \geq 0, t=0 \quad c_{d_i} = c_{d_i}^o \quad (3.66)$$

$$\text{At } y \geq 0, t=0 \quad c_{S_i} = c_{S_i}^o \quad (3.67)$$

Equations (3.56) to (3.67) are normalized by the introduction of following dimensionless parameters :

$$\begin{aligned}
C_{d_i} &= \frac{c_{d_i}}{H c_{g_0}}, & C_{s_i} &= \frac{c_{s_i}}{H c_{g_0}}, & C_g &= \frac{c_g}{c_{g_0}}, \\
x &= \frac{z}{L_C}, & \eta &= \frac{y}{L_S}, & \phi &= \frac{h_d}{h_t}, \\
\theta &= \frac{t U_L}{h_t L_C}, & Pe_{L_i} &= \frac{U_L L_C}{D_{L_i}}, & Pe_G &= \frac{U_G L_C}{D_G}, \\
K_{SD_i}^* &= \frac{k_{SD_i} a_{SD} L_C}{U_L}, & St &= \frac{k_{GL} a_{GL} L_C}{U_L}, & \xi &= \frac{U_G}{U_L}, \\
\beta_i &= \frac{L_C D_{S_i} h_t}{U_L L_S^2}, & Bi_i &= \frac{k_{SD_i} L_S}{D_{S_i}}, & \psi &= \frac{h_g}{h_t},
\end{aligned} \tag{3.68}$$

The dimensionless mass balance equation for the solute component 1 in the gas phase becomes,

$$\frac{\partial C_{g_1}}{\partial \theta} = \frac{\xi}{\psi} \left[ \frac{h_g}{Pe_G} \left( \frac{\partial^2 C_{g_1}}{\partial x^2} \right) - \left( \frac{\partial C_{g_1}}{\partial x} \right) - \frac{St}{\xi} H (C_{g_1} - C_{d_1}) \right] \tag{3.69}$$

With the dimensionless boundary conditions,

$$\text{At } x=0, \theta > 0 \quad \left. \frac{\partial C_{g_1}}{\partial x} \right|_{x=0^+} = -Pe_G \left( C_{g_1}|_{x=0^-} - C_{g_1}|_{x=0^+} \right) \tag{3.70}$$

$$\text{At } x=1, \theta > 0 \quad \left. \frac{\partial C_{g_1}}{\partial x} \right|_{x=1} = 0 \tag{3.71}$$

For the dynamic liquid phase, the dimensionless equation for the solute component 1 is,

$$\phi \left( \frac{\partial C_{d_1}}{\partial t} \right) = \frac{h_d}{Pe_{L_1}} \left( \frac{\partial^2 C_{d_1}}{\partial x^2} \right) - \left( \frac{\partial C_{d_1}}{\partial x} \right) - K_{SD_1}^* (C_{d_1} - C_{S_1}|_{\eta=0}) + St (C_{g_1} - C_{d_1}) - \langle R_1 \rangle \quad (3.72)$$

With the dimensionless boundary conditions,

$$\text{At } x=0, \theta > 0 \quad \left. \frac{\partial C_{d_1}}{\partial x} \right|_{x=0^+} = -Pe_{L_1} (C_{d_1}|_{x=0^-} - C_{d_1}|_{x=0^+}) \quad (3.73)$$

$$\text{At } x=1, \theta > 0 \quad \left. \frac{\partial C_{d_1}}{\partial x} \right|_{x=1} = 0 \quad (3.74)$$

For the dynamic liquid phase, the dimensionless equation for the reactant 2 is,

$$\phi \left( \frac{\partial C_{d_2}}{\partial t} \right) = \frac{h_d}{Pe_{L_2}} \left( \frac{\partial^2 C_{d_2}}{\partial x^2} \right) - \left( \frac{\partial C_{d_2}}{\partial x} \right) - K_{SD_2}^* (C_{d_2} - C_{S_2}|_{\eta=0}) - \langle R_2 \rangle \quad (3.75)$$

With the dimensionless boundary conditions,

$$\text{At } x=0, \theta > 0 \quad \left. \frac{\partial C_{d_2}}{\partial x} \right|_{x=0^+} = -Pe_{L_2} (C_{d_2}|_{x=0^-} - C_{d_2}|_{x=0^+}) \quad (3.76)$$

$$\text{At } x=1, \theta > 0 \quad \left. \frac{\partial C_{d_2}}{\partial x} \right|_{x=1} = 0 \quad (3.77)$$

The dimensionless unsteady state material balance for the component i in the stagnant liquid phase is written as ,

$$\left( \frac{\partial C_{S_i}}{\partial \theta} \right) = \beta_i \left( \frac{\partial^2 C_{S_i}}{\partial \eta^2} \right) - \langle R_i \rangle \quad (3.78)$$

and the corresponding dimensionless boundary conditions are,

$$\text{At } \eta = 0, \theta > 0 \quad \left. \frac{\partial C_{S_i}}{\partial \eta} \right|_{\eta=0} = -Bi_i \left( C_{d_i} - C_{S_i} \Big|_{\eta=0} \right) \quad (3.79)$$

$$\text{At } \eta = 1, \theta > 0 \quad \left. \frac{\partial C_{S_i}}{\partial \eta} \right|_{\eta=1} = 0 \quad (3.80)$$

Similarly, the initial conditions can be rewritten in dimensionless form as,

$$\text{At } x \geq 0, \theta = 0 \quad C_g = C_g^o \quad (3.81)$$

$$\text{At } x \geq 0, \theta = 0 \quad C_{d_i} = C_{d_i}^o \quad (3.82)$$

$$\text{At } \eta \geq 0, \theta = 0 \quad C_{S_i} = C_{S_i}^o \quad (3.83)$$

The reaction scheme considered in this work is first order in both the solute gas and the reactant concentrations implying a second order overall reaction. The stoichiometry and kinetics are discussed in Section (7.3) and the corresponding rate expressions take the form,

$$\langle r_1 \rangle = k_R c_{d_1} c_{d_2} \quad \langle r_2 \rangle = 2 \cdot k_R c_{d_1} c_{d_2} \quad (3.84)$$

$$\langle R_1 \rangle = K_R^* C_{d_1} C_{d_2} \quad \langle R_2 \rangle = 2 \cdot K_R^* C_{d_1} C_{d_2} \quad (3.85)$$

where,

$$K_R^* = \frac{k_R H c_{g_o} L_C}{U_L} \quad (3.86)$$



### 3.5 SOLUTION OF THE MODEL EQUATIONS

In simulation problems related to such type of mathematical formulations, the numerical solution scheme of orthogonal collocation has been found to be quite effective as outlined by Hassan and Beg (1987). The resulting partial differential equations are reduced by orthogonal collocation into ordinary differential equations subjected to the nodal distribution as shown in Figure (3.2). The resulting ordinary differential equations are then solved by using Gears algorithm as provided by DIVPAG subroutine available in the IMSL library.

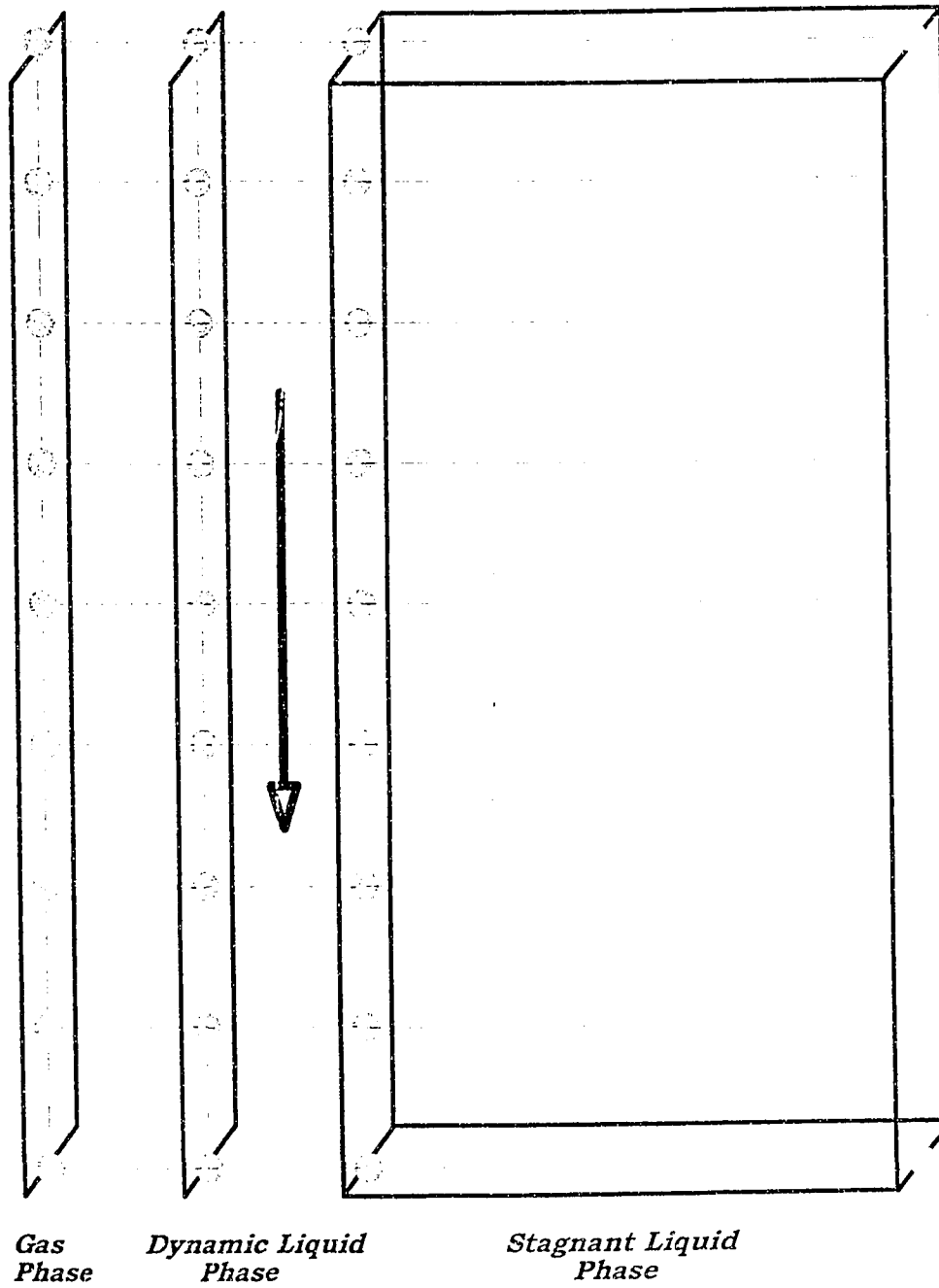


Figure (3.2) Nodal representation of the numerical scheme employed for solving the model equations.

# CHAPTER 4

## HYDRODYNAMIC MODEL: *VALIDATION AND PARAMETRIC STUDY*

---

### 4.1 INTRODUCTION

A quantitative approach to design is more difficult for cocurrent fixed-bed columns than for other multiphase systems because the hydrodynamics is more complicated due to the different flow regimes that occur when the gas and liquid flow rates are varied. This is true with both upflow and downflow systems. With different hydrodynamics, different mass transfer rates arise requiring complicated mathematical models in differential terms. For the proper modeling of performance of such systems, the residence time distributions (RTD's) of various fluid phases are of vital importance. The RTD curve allow the quantitative evaluation of the nature and degree of mixing in each fluid phase, as well as the dynamic holdup of each phase in the column. The RTD for a flowing fluid is normally obtained by the so-called "stimulus-response" technique. This technique involves injection of a tracer at some point within the column and the observation of the corresponding response at the exit or at some other point downstream. Once

the data for the RTD are obtained, the backmixing characteristics for each phase of a multiphase system can be evaluated quantitatively by fitting the appropriate model to this data. This approach implies that a transient analysis of flow model behavior and that of the column is necessary.

Due to crucial role played by the liquid phase in such operations, differential mass balance equations based on the new improved model are developed as shown in Section 3.1. In order to enhance our understanding of the hydrodynamic and mass transfer phenomena inside such column, these equations are then fitted to the experimental data available in the literature, and are further analysed by performing parametric studies.

## **4.2 RESULTS AND DISCUSSION**

The model equations described in Section 3.1 have been solved for a downflow cocurrent packed column subjected to step input in tracer concentration and also for upflow cocurrent column subjected to step decrease in tracer concentration. Parametric studies were carried out for both cases to evaluate the individual effects of parameters of practical significance. Table (4.1) lists the base values of parameters used for the numerical computation. The functional relationships of various model parameters are available in the literature which can be used for

Table 4.1 Base values of parameters used in the numerical model computations for the liquid phase.

Parameters	Downflow Co-Current Column	Upflow Co- Current Column
Superficial liquid velocity, $v_L$ , (m s <sup>-1</sup> )	$1.0 \times 10^{-3}$	$0.786 \times 10^{-3}$
Superficial gas velocity, $v_g$ , (m s <sup>-1</sup> )	0.18	0.20
Column Length, $L$ , (m)	0.725	1.0
Thickness of stagnant region, $L_s$ , (m)	$1.0 \times 10^{-4}$	$9.0 \times 10^{-5}$
Axial dispersion coefficient, $D_L$ , (m <sup>2</sup> s <sup>-1</sup> )	$4.7 \times 10^{-5}$	$9.0 \times 10^{-5}$
Dispersion coefficient in the stagnant region, $D_S$ , (m <sup>2</sup> s <sup>-1</sup> )	$5.0 \times 10^{-11}$	$5.0 \times 10^{-11}$
Mass transfer coefficient between dynamic and stagnant liquid, $k_{SD}$ , (m s <sup>-1</sup> )	$5.5 \times 10^{-8}$	$2.5 \times 10^{-7}$
Interfacial area between dynamic and stagnant liquid, $a_{SD}$ , (m <sup>-1</sup> )	528.16	51.5
Fractional dynamic liquid holdup, $\phi$ , (-)	0.722	0.9756
Total liquid holdup, $h_t$ , (-)	0.19	0.19
Column diameter, $d_C$ , (mm)	25.0	30.0
Packing	0.5 mm glass sphere	3 mm cylinders

model predictions. The relationships used in this particular exercise are discussed below.

#### 4.2.1 Evaluation of Model Parameters

The surface area,  $a_{SD}$ , between stagnant and dynamic phases for interregional mass transfer was calculated by a relationship proposed by Kan and Greenfield (1983), which assumes a simple flat geometry for the stagnant phase. It can be written as,

$$a_{SD} = \frac{(1-\phi)h_t}{L_S} \quad (4.1)$$

where  $L_S$  is the thickness of the stagnant phase,  $h_t$  is total holdup and  $\phi$  is the ratio of dynamic to total liquid holdup. Total liquid holdup,  $h_t$ , can be determined by standard experimental techniques (Yang et al., 1993) or it can be estimated by different correlations available in the literature (Kan and Greenfield, 1979; Ellman et al., 1990; Yang et al., 1993). For the cases being studied experimental values of  $h_t$  reported by the investigators were used. Thickness of the stagnant film,  $L_S$  for the particular geometry of the packing is reported by Kan and Greenfield (1983) to lie in the region of  $10^{-4}$  m. They further reported that the dispersion in the stagnant phase is a mixing process rather than a consequence of molecular diffusion

implying that dispersion coefficient,  $D_S$ , is not a function of molecular diffusivity of the tracer. They reported that the value of  $D_S$  roughly lies in the range of  $10^{-10}$   $\text{m}^2 \text{s}^{-1}$  and does not vary much with different types of tracers. They also presented a relationship for  $D_S$  and  $L_S$  in terms of liquid phase Reynolds number.

The value of  $\phi$  for downflow operations was reported by Kan and Greenfield (1983) to lie between  $(0.73 \pm 0.08)$ . This agrees reasonably well with other studies, as Matsuura et al. (1976) predicts its value to lie between 0.75 to 0.9 and studies of Hochmann and Effron (1969) gives its range to be 0.65 to 0.85. For the upflow cocurrent case, the value of  $\phi$  was reported by Skomorokov and Kirillov (1986) to be around 0.95. Most of the investigators like Kan and Greenfield (1983), Matsuura et al. (1976) and, Skomorokov and Kirillov (1986) report little dependence of  $\phi$  on flow rates. One explanation for this is given by Kan and Greenfield (1983), who point that the stagnant holdup occurs in sheltered regions along the liquid flowpaths, such as crevices between packing particle surfaces, which remain relatively unaffected by the magnitude of flow rates. The axial dispersion coefficient  $D_S$  and mass transfer coefficient between stagnant and dynamic liquid  $k_{SD}$  are estimated from the model fit.

## 4.2.2 Results of Numerical Simulation

The effect of important parameters such as mass transfer coefficient,  $k_{SD}$ , thickness of stagnant liquid film,  $L_S$ , total liquid holdup,  $h_t$ , ratio of dynamic to total liquid holdup,  $\phi$ , Peclet Number,  $Pe_L$ , stagnant phase dispersion coefficient,  $D_S$ , liquid phase Reynolds number,  $Re_L$ , and gas phase Reynolds number,  $Re_G$ , on column dynamics was analyzed. Initially (at  $\theta = 0$ ) the column was considered to be free of any tracer for the down flow operation, i.e.  $C_d = C_s = 0$ , while for the upflow case  $C_d = C_s = 1$  was considered. The inlet condition for the downflow operation was  $C_d|_{x=0^-} = 1$  while for the upflow operation it was

$$C_d|_{x=0^-} = 0.$$

Figure (4.1a) shows the affect of mass transfer coefficient  $k_{SD}$  (between stagnant and dynamic liquid layers) for the down flow condition. It may be observed that the affect of  $k_{SD}$  is insignificant for dimensionless time ( $\theta$ ) less than almost two. However the effect of increase in  $k_{SD}$  lead to decrease in the exit tracer concentration which can be attributed to decrease in the mass transfer resistance



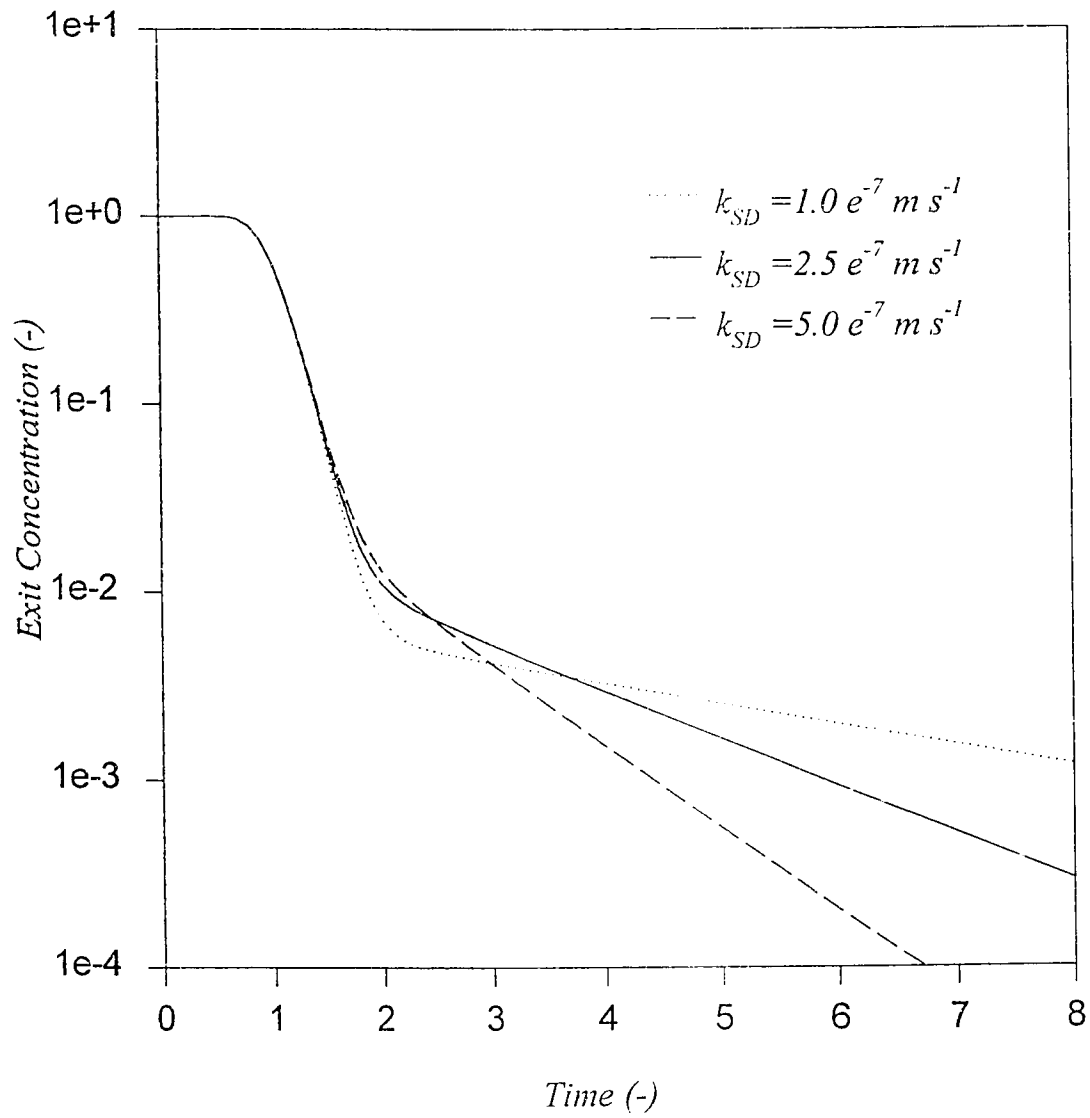


Figure (4.1a) The effect of  $k_{SD}$  on the RTD of co-current upflow packed column for a step decrease in tracer concentration.

between the two liquid layers. For  $\theta < 2$  the concentration driving force between two liquid films is extremely small which leads to poor mass flux and insignificant influence of the mass transfer coefficient  $k_{SD}$ . Once the dynamic phase is eluted a significant driving force is established and it is at this stage that the effect of  $k_{SD}$  becomes appreciable. The corresponding effect of  $k_{SD}$  for the down flow operation is shown in Figure (4.1b). It is evident from this figure that mass transfer effects are represented by tail portion of the breakthrough curve and it takes longer to reach the feed concentration level with smaller value of  $k_{SD}$ .

Figures (4.2a) and (4.2b) show the effect of  $k_{SD}$  on the concentration profile in three dimensions in stagnant phase for the upflow operation. The profiles are much steeper for operation with higher mass transfer coefficient compared to that for lower mass transfer coefficient.

Figures (4.3a) and (4.3b) show the effect of the thickness of stagnant liquid film,  $L_S$ , on the column dynamics for upflow and downflow operations respectively. For upflow conditions the increase in thickness of the stagnant liquid film leads to decrease in the interfacial area and increase of resistance to mixing which results in slowing down the elution rates as highlighted in Figure (4.3a). Similar behavior

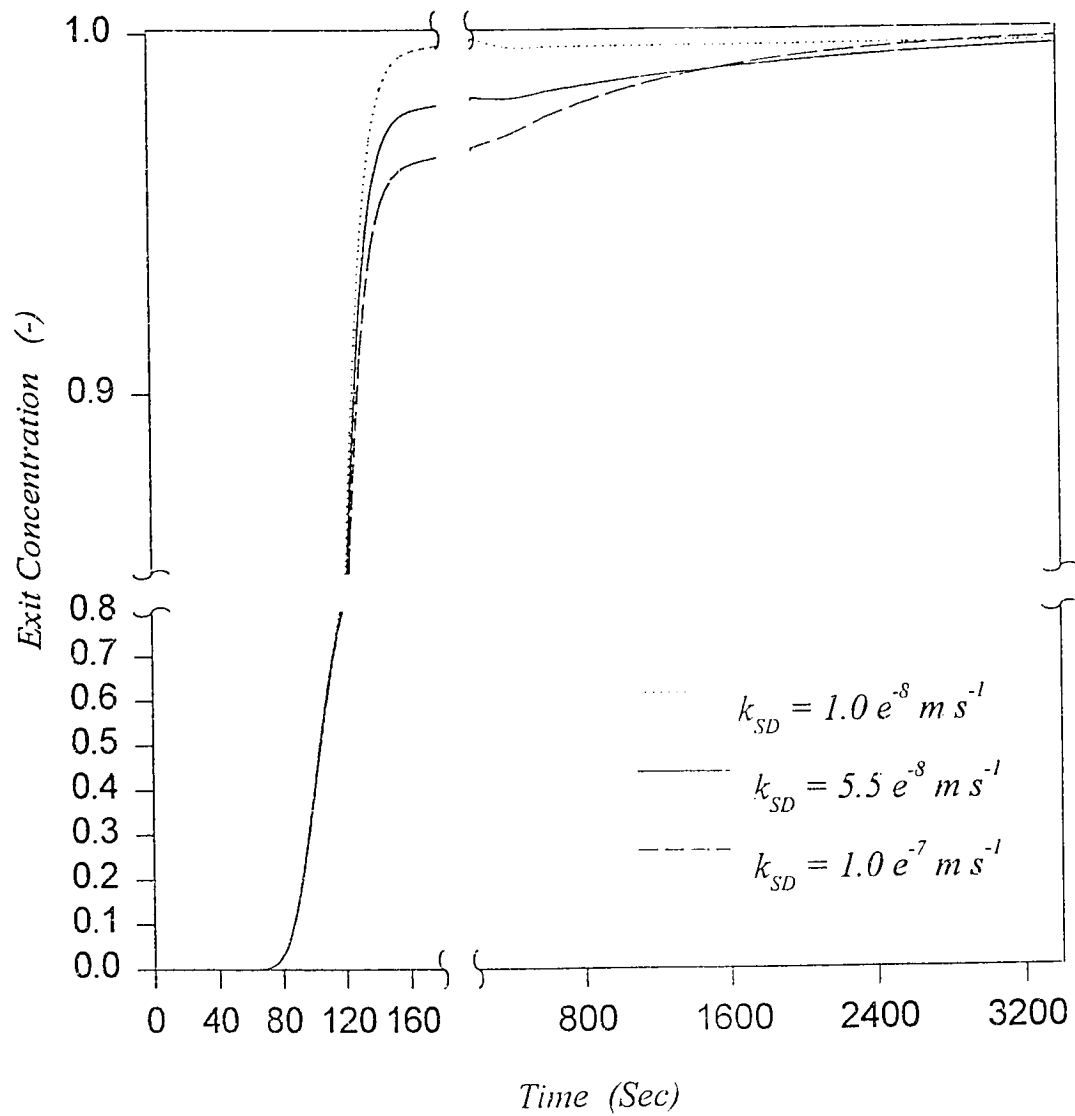


Figure (4.1b) The effect of  $k_{SD}$  on the RTD of co-current downflow packed column for a step input in tracer concentration.

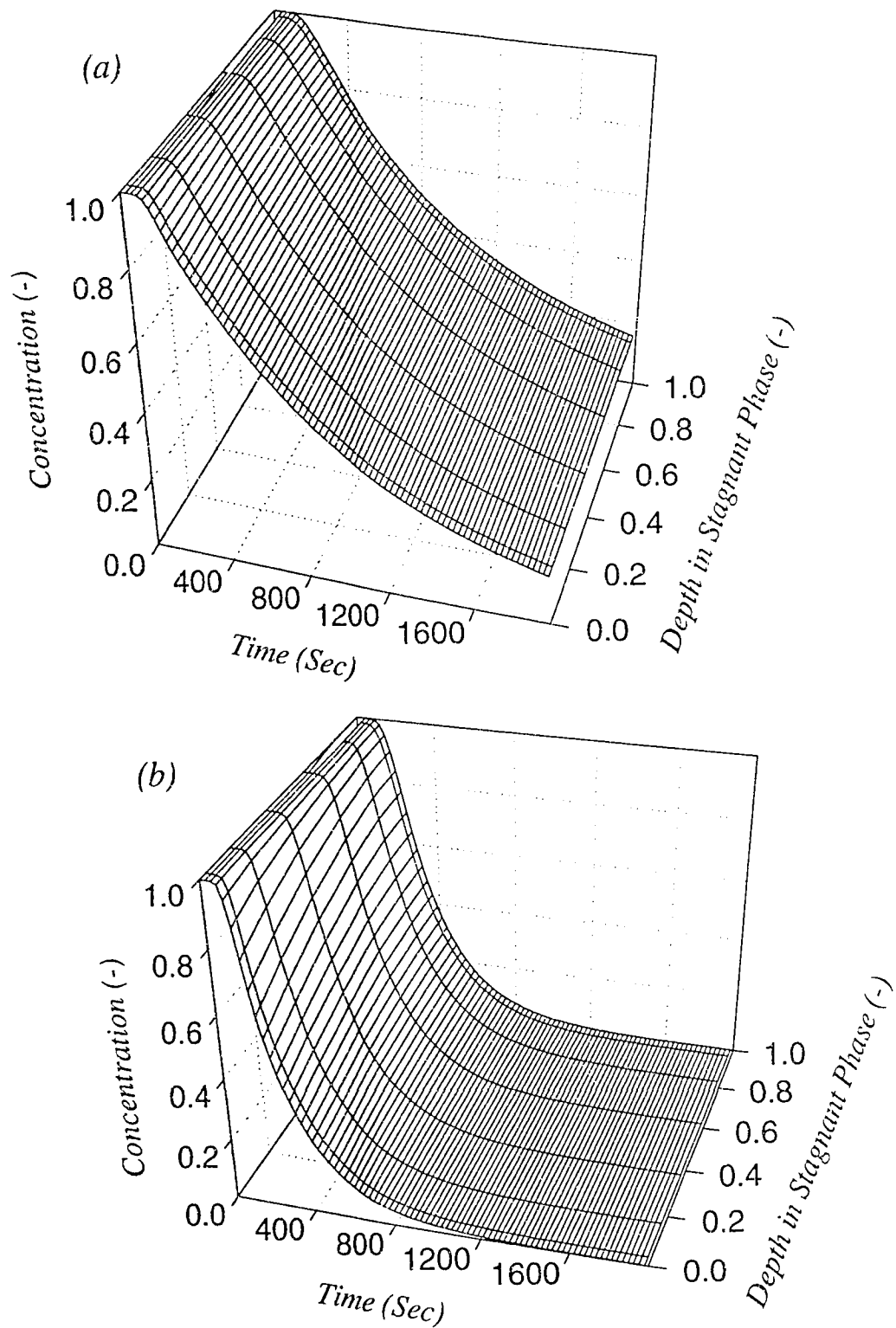


Figure (4.2) Concentration profiles in 3-dimensions for a co-current upflow packed column showing the effect of  $k_{SD}$  when the column is subjected to a step decrease in tracer concentration for : (a)  $k_{SD} = 1.0 \times 10^{-7} \text{ m s}^{-1}$  (b)  $k_{SD} = 5.0 \times 10^{-7} \text{ m s}^{-1}$

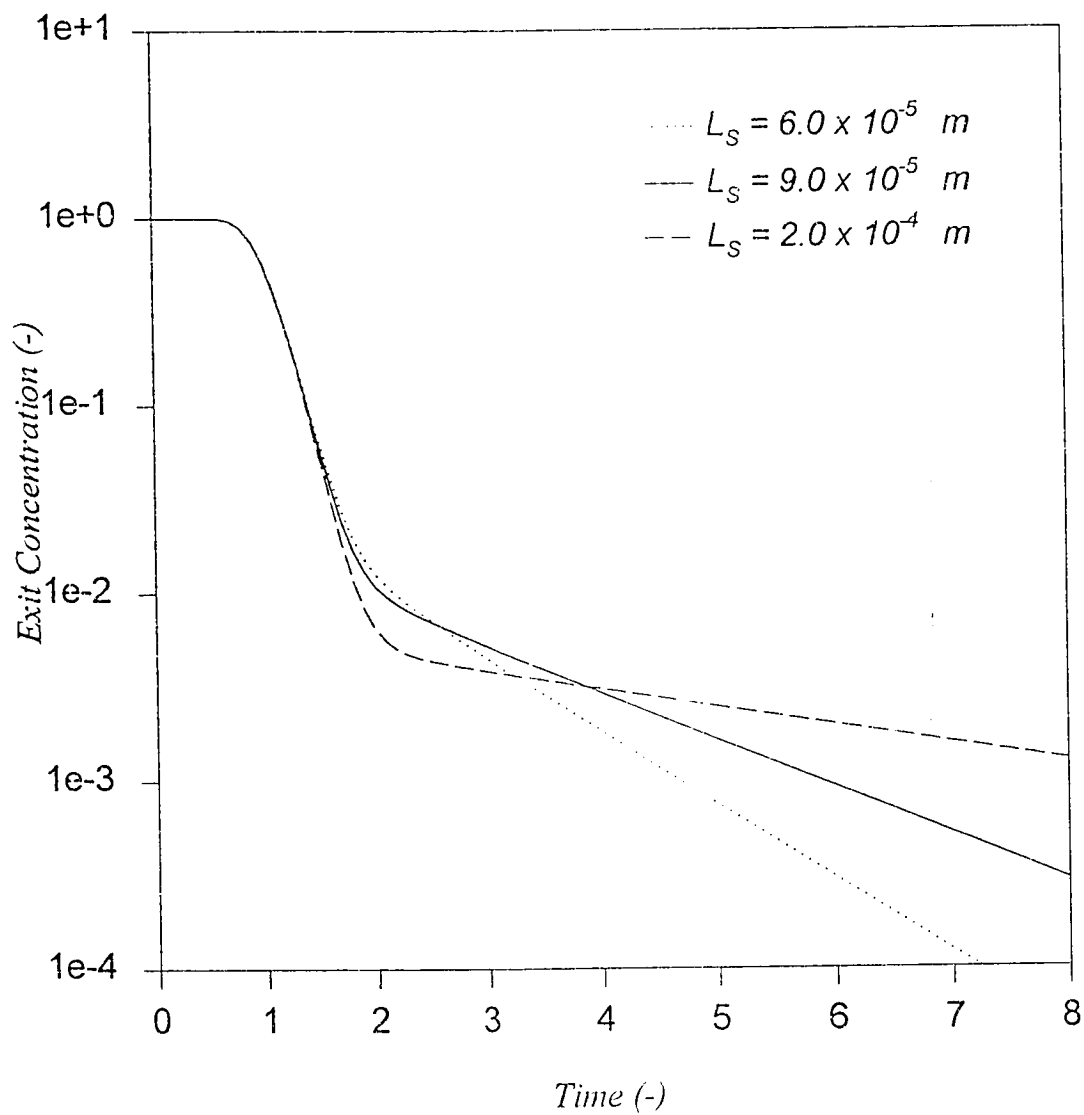


Figure (4.3a) The effect of  $L_S$  on the RTD of co-current upflow packed column for a step decrease in tracer concentration.

is illustrated in Figure (4.3b) for downflow operation. This behavior is more clearly illustrated in Figures (4.4a) and (4.4b) which for the upflow operation describes the concentration history within the stagnant film in a three dimensional plot.

Figure (4.5) shows the effect of dispersion coefficient  $D_S$  in stagnant phase for upflow operation. Large values of  $D_S$  implies better mixing in the stagnant phase which would result in faster elution of the bed compared to higher values of  $D_S$ . Further, a more uniform concentration in the stagnant film is observed for higher values of  $D_S$  (i.e.,  $10^{-10} \text{ m}^2 \text{ s}^{-1}$ ) while a substantial concentration profile is observed for lower value of  $D_S = 10^{-11} \text{ m}^2 \text{ s}^{-1}$  as shown in Figures (4.6a) and (4.6b) respectively. These observations suggest that the effect of backmixing in the stagnant film will only be pronounced at lower values of  $D_S$  of the order of magnitude of  $10^{-11} \text{ m}^2 \text{ s}^{-1}$ .

Figures (4.7a) and (4.7b) show the effect of dynamic liquid holdup  $\phi$ , for the upflow and downflow operations respectively. Higher values of  $\phi$  indicate larger dynamic fraction of the total holdup which results in an initial larger drop in the exit concentration, however, the rate of decrease at larger times remains fairly

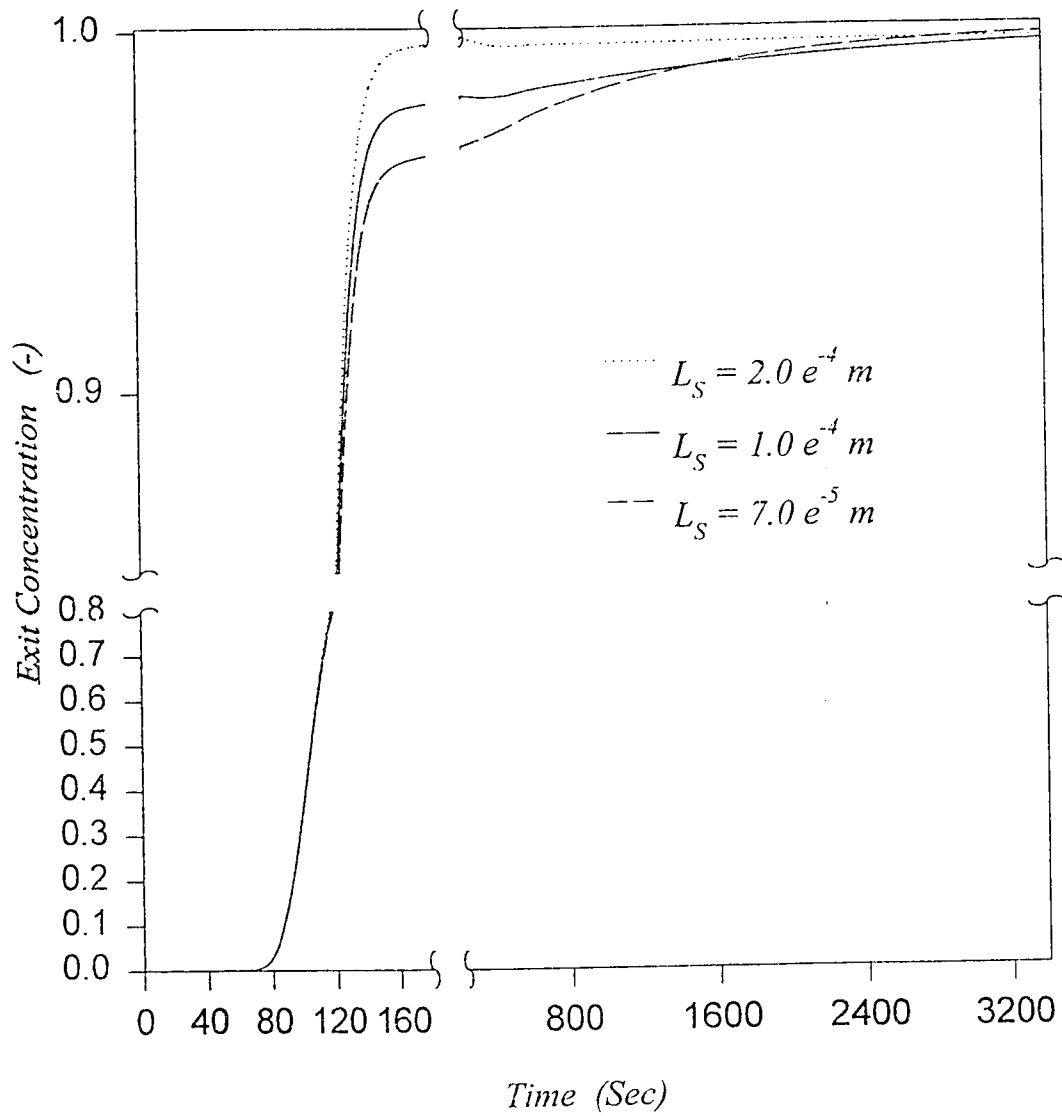


Figure (4.3b) The effect of  $L_S$  on the RTD of co-current downflow packed column for a step input in tracer concentration.

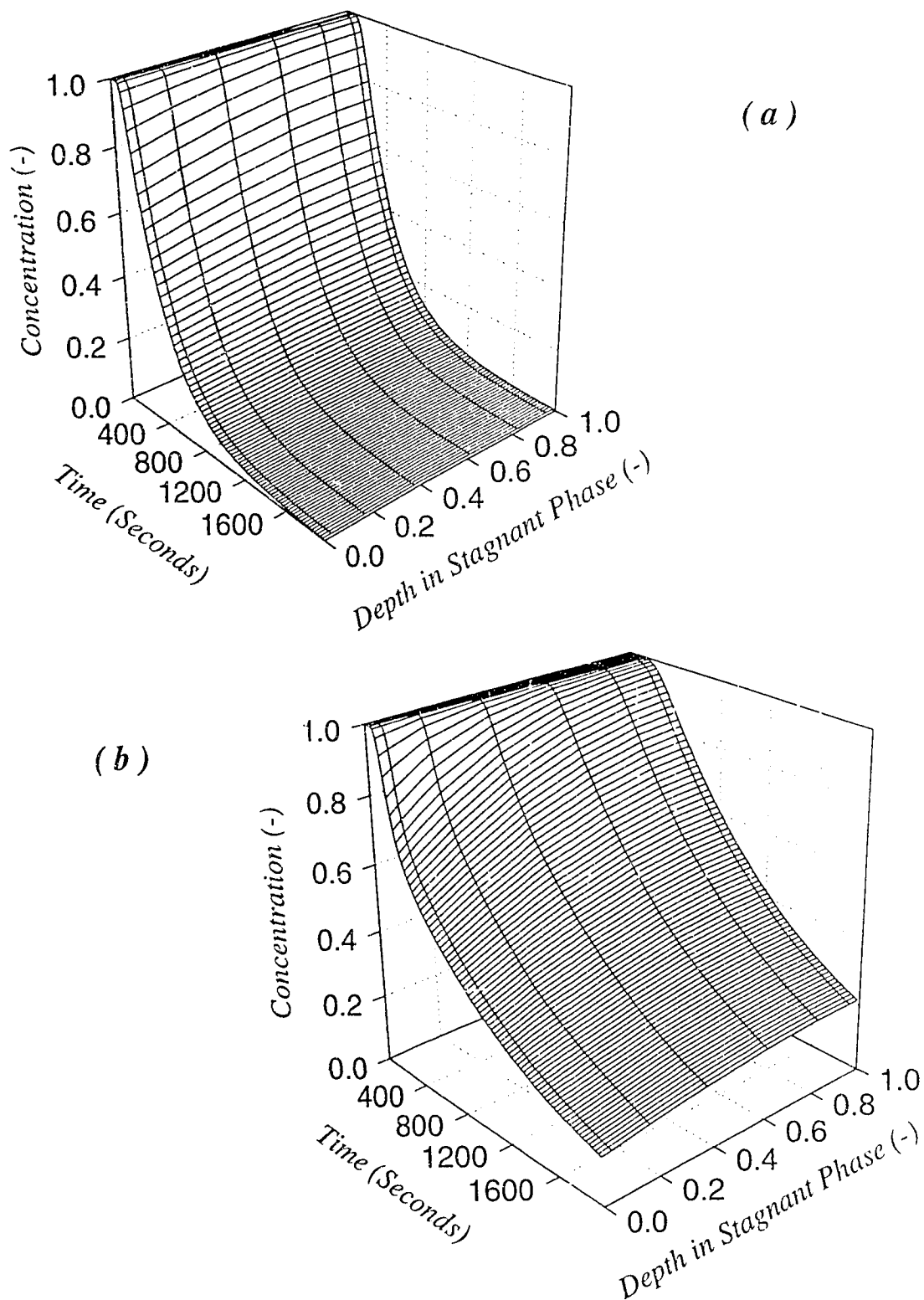


Figure (4.4) Concentration profiles in 3-dimensions for a co-current upflow packed column showing the effect of  $L_S$  when the column is subjected to a step decrease in tracer concentration for: (a)  $L_S = 7.0 e^{-5} \text{ m}$  (b)  $L_S = 2.0 e^{-4} \text{ m}$



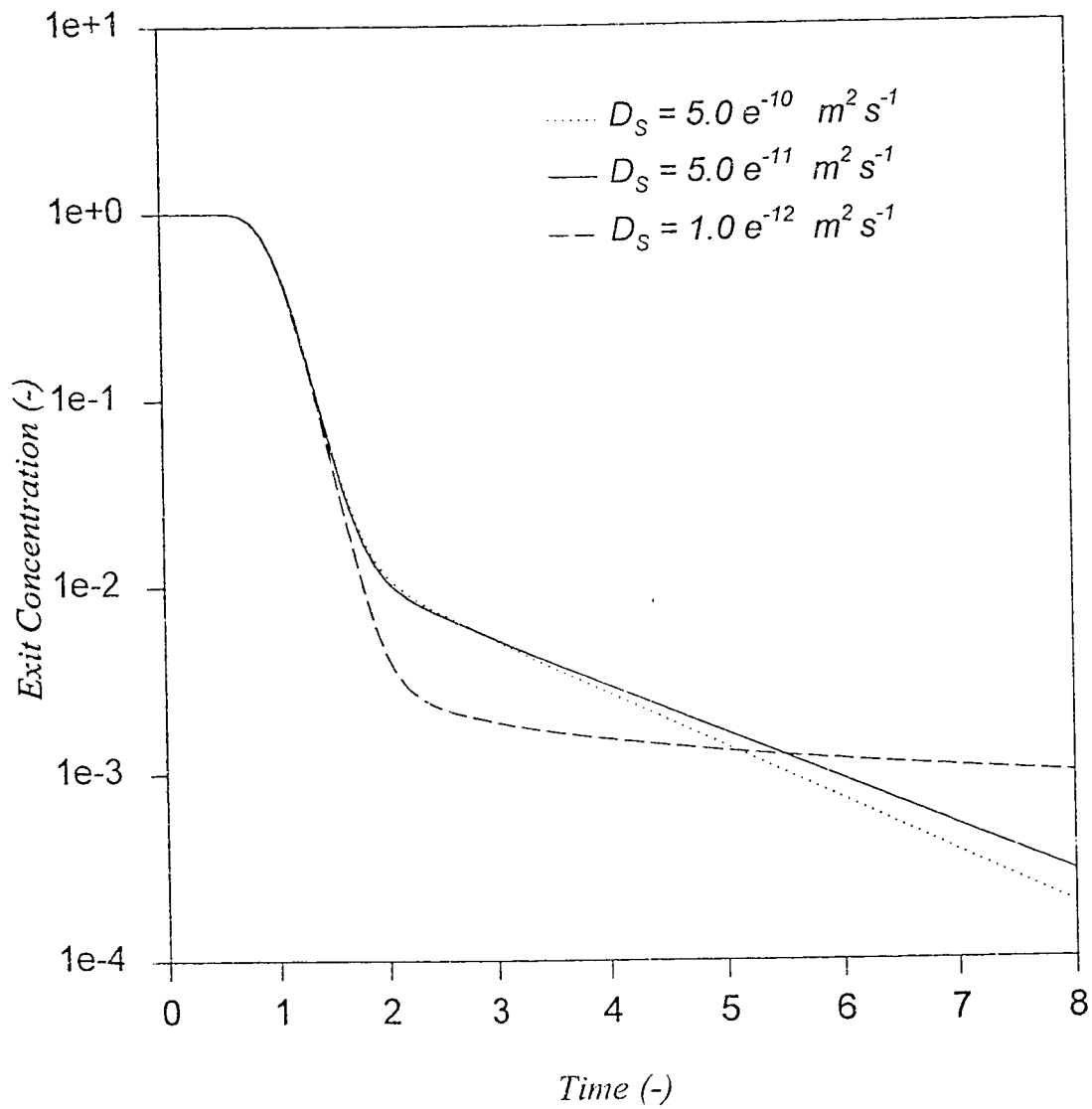


Figure (4.5) The effect of  $D_s$  on the RTD of co-current upflow packed column for a step decrease in tracer concentration.

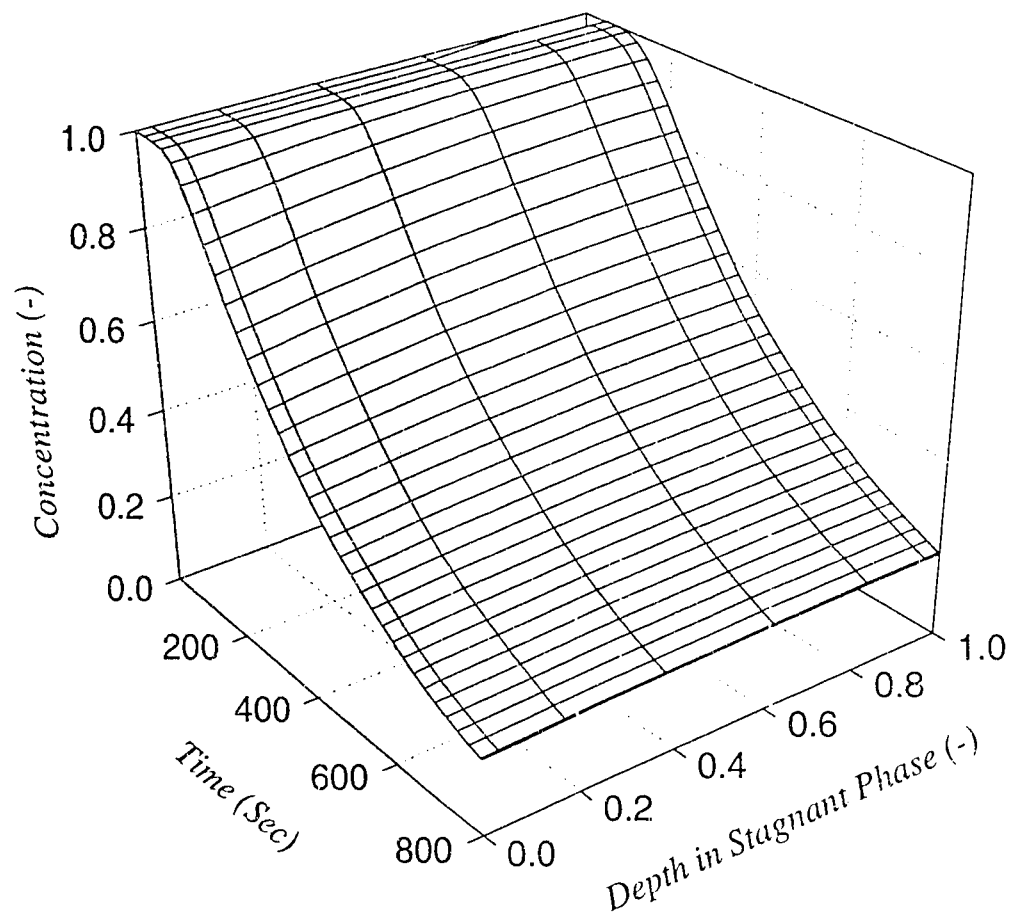


Figure (4.6a) Dynamic concentration profiles in the stagnant phase, for a co-current upflow packed column showing the effect of  $D_s$  when the column is subjected to a step decrease in tracer concentration for,  
 $D_s = 1.0 \times 10^{-10} \text{ m}^2 \text{ s}^{-1}$

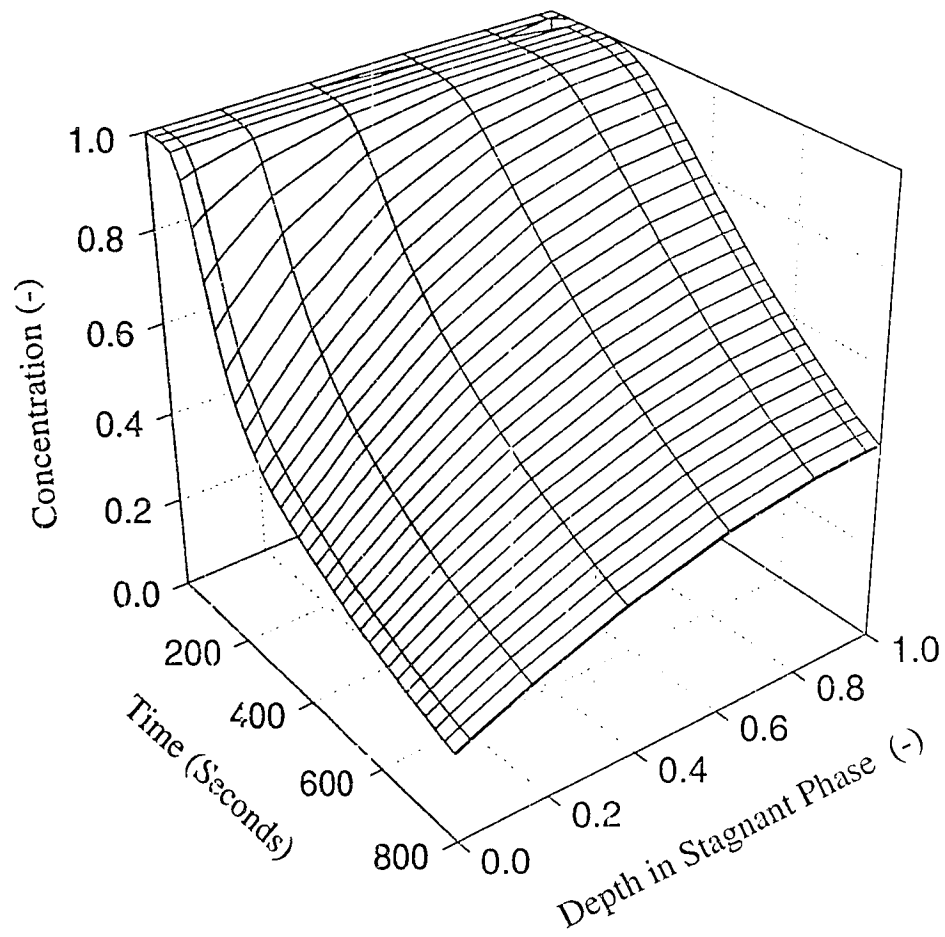


Figure (4.6b) Dynamic concentration profiles in the stagnant phase, for a co-current upflow packed column showing the effect of  $D_S$  when the column is subjected to a step decrease in tracer concentration for,  
 $D_S = 1.0 e^{-11} \text{ m}^2 \text{ s}^{-1}$

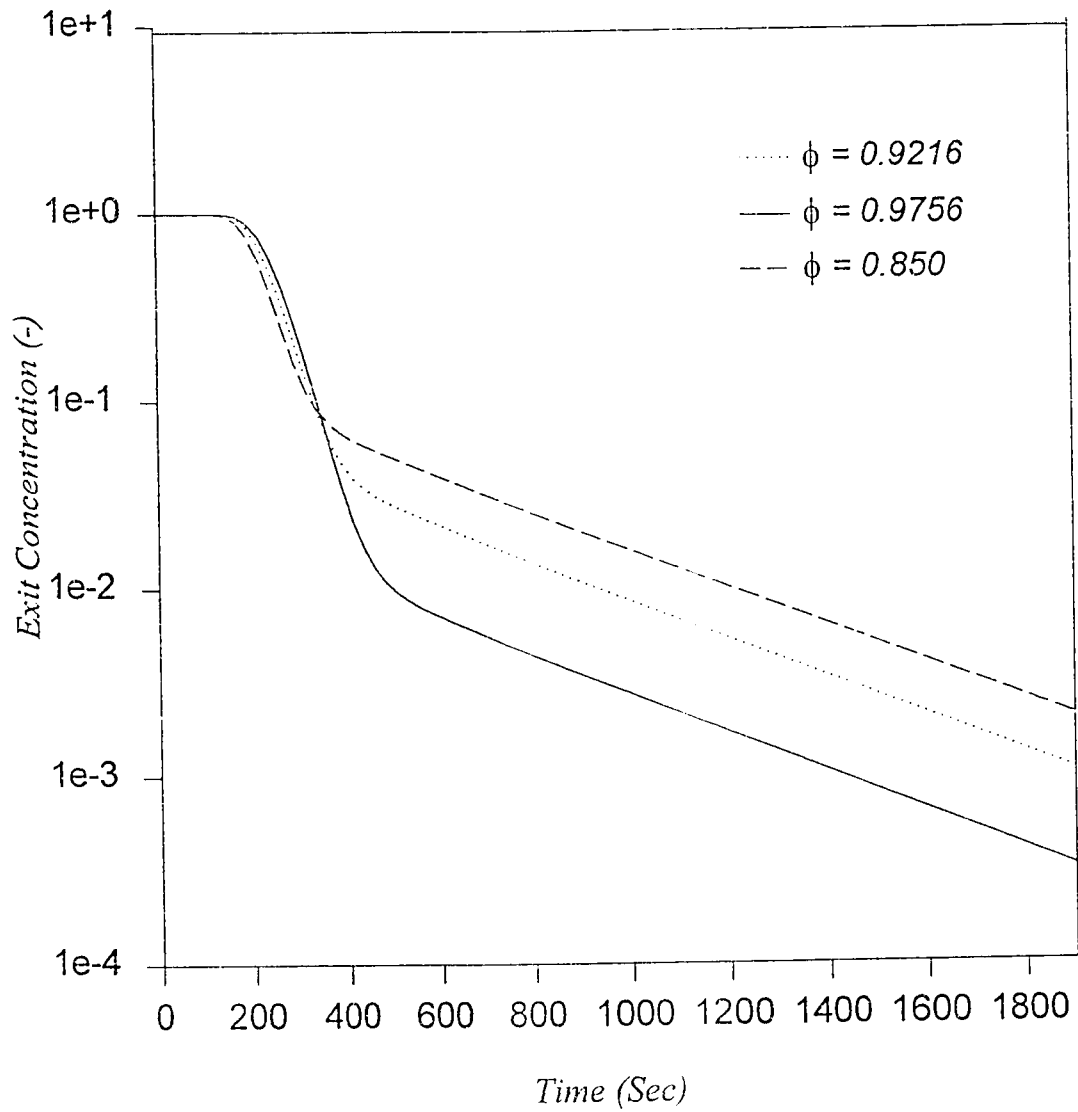


Figure (4.7a) The effect of  $\phi$  on the RTD of co-current upflow packed column for a step decrease in tracer concentration.

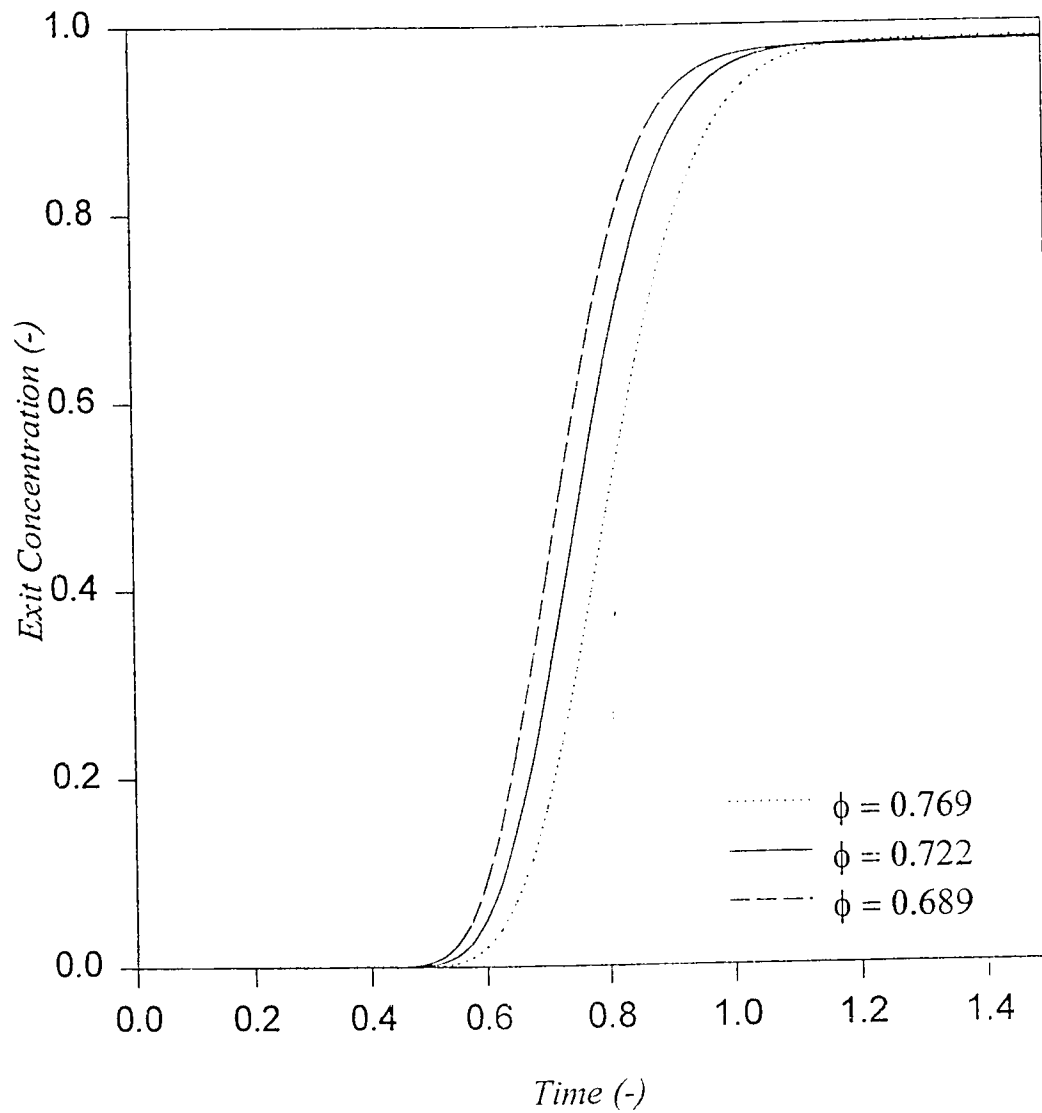


Figure (4.7b) The effect of  $\phi$  on the RTD of co-current downflow packed column for a step input in tracer concentration.

the same for all values of  $\phi$ . Similar behavior is shown for downflow operation. It may further be observed from Figure (4.7b) that an earlier breakthrough is observed for lower values of  $\phi$ . This may be attributed to decrease in values of the effective velocity of the dynamic liquid phase due to the decrease in  $\phi$ .

The effect of total liquid holdup,  $h_t$ , on the column dynamics is shown in Figure (4.8a) and (4.8b) for upflow and downflow operations, respectively. The results show that there is a time lag in the response for larger values of  $h_t$  which would be expected due to longer residence time in the column.

The effect of axial dispersion is shown in Figures (4.9a) and (4.9b) for upflow and downflow operations, respectively. It may be noted that  $Pe_l \rightarrow 0$  corresponds to completely mixed system where tracer is dispersed more uniformly which is observed by the wider spread of the breakthrough curve. However, for  $Pe_l \rightarrow \infty$  the system would move towards plug flow conditions and thereby making the breakthrough curve steeper for both upflow and downflow cases as shown in Figures.

The effect of Reynolds number for the liquid and gas phases for downflow operation is shown in Figures (4.10) and (4.11) respectively. The analysis shows

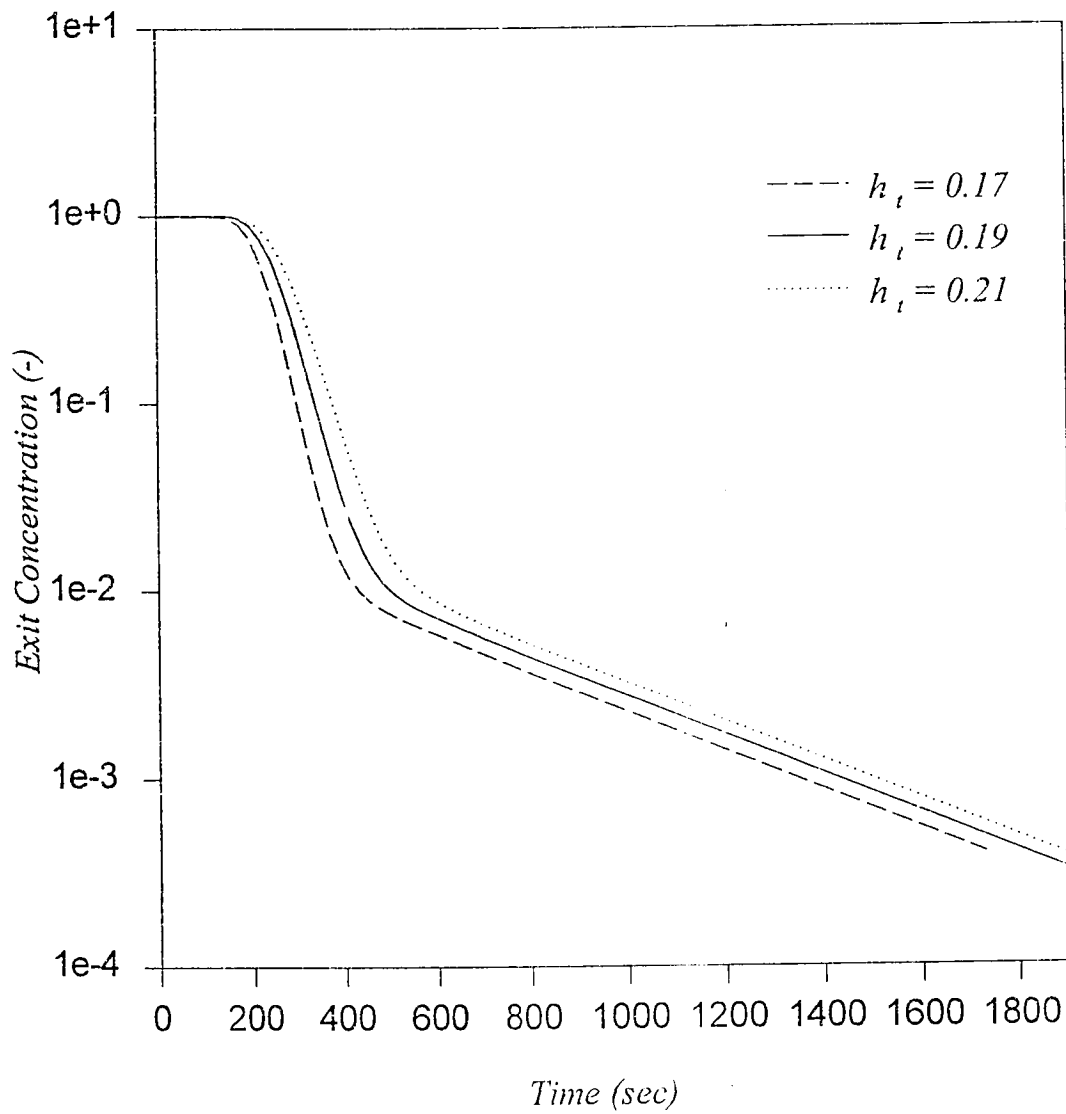


Figure (4.8a) The effect of  $h_t$  on the RTD of co-current upflow packed column for a step decrease in tracer concentration.

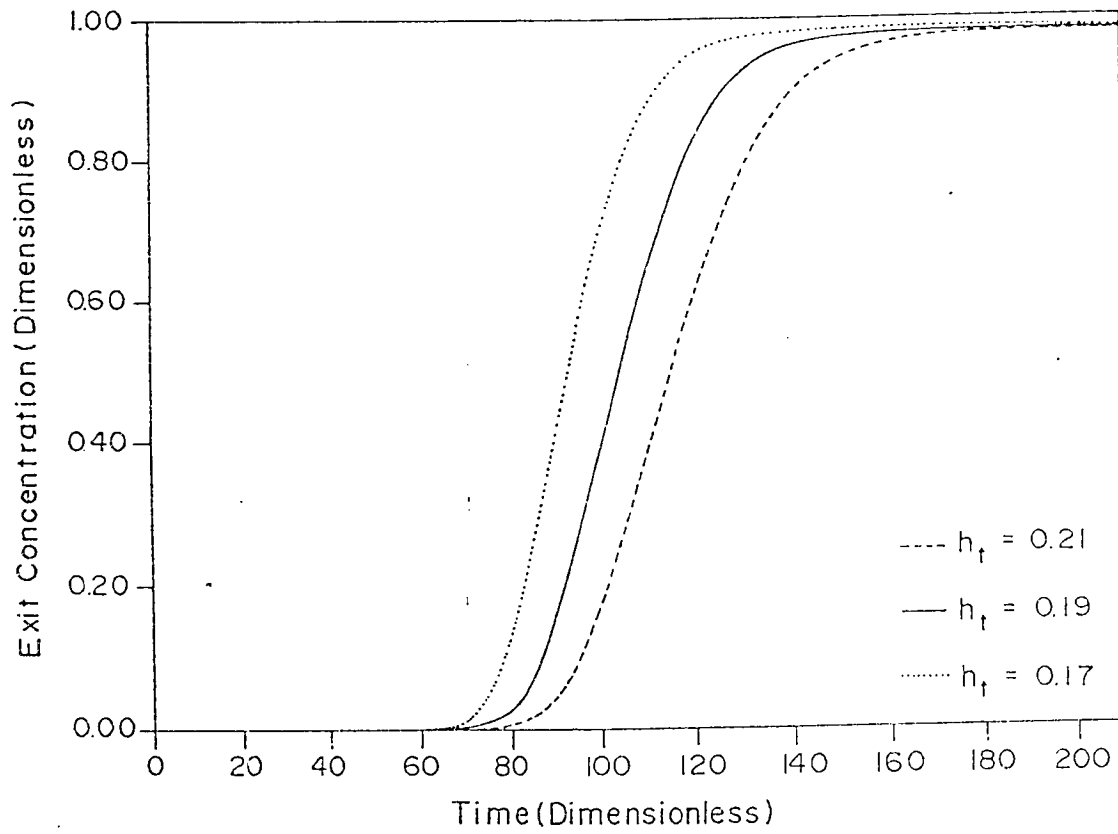


Figure (4.10) Effect of  $h_t$  on the RTD of cocurrent downflow packed column for a step input in tracer concentration.



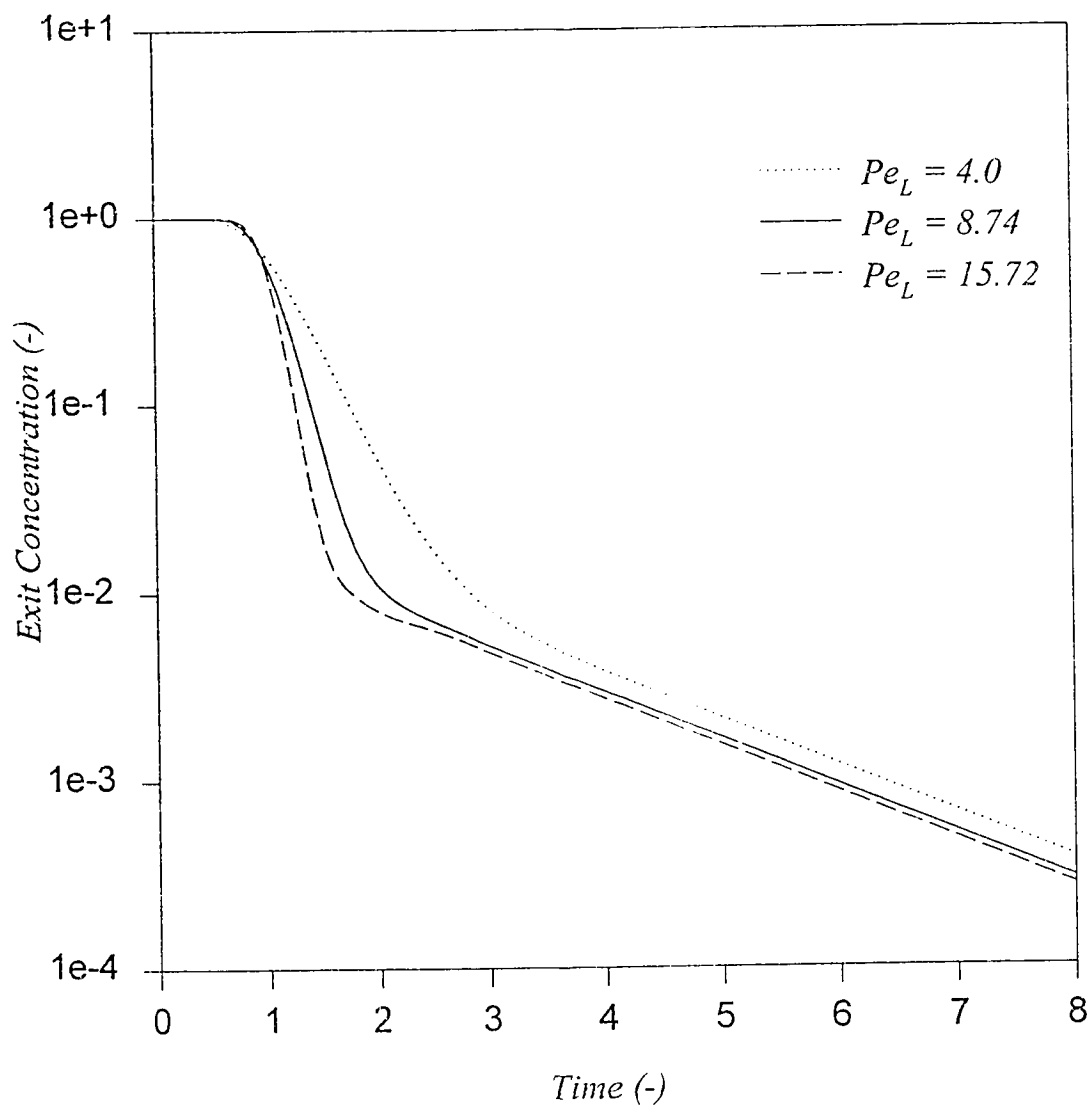


Figure (4.9a) The effect of  $Pe_L$  on the RTD of co-current upflow packed column for a step decrease in tracer concentration.

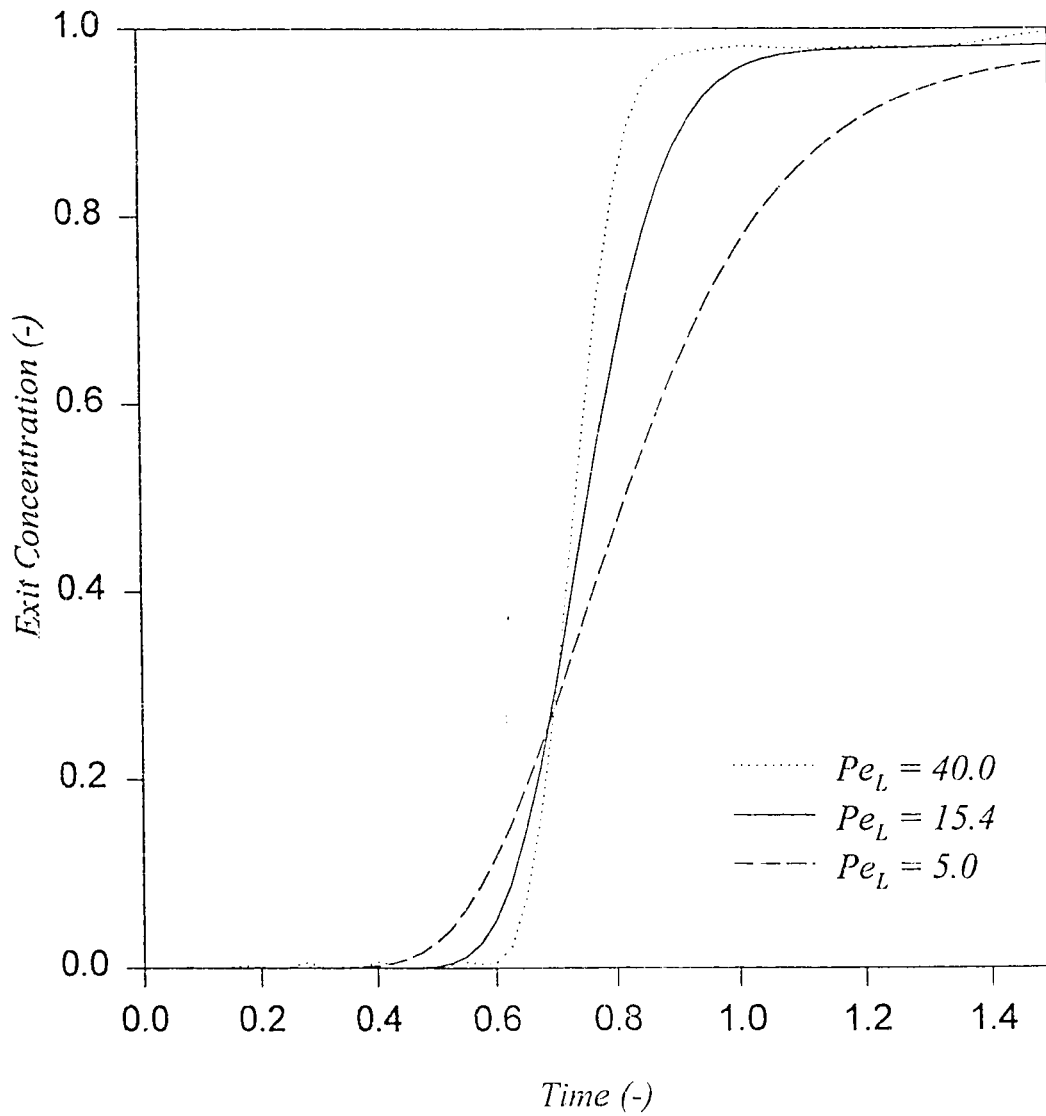


Figure (4.9b) The effect of  $Pe_L$  on the RTD of co-current downflow packed column for a step input in tracer concentration.

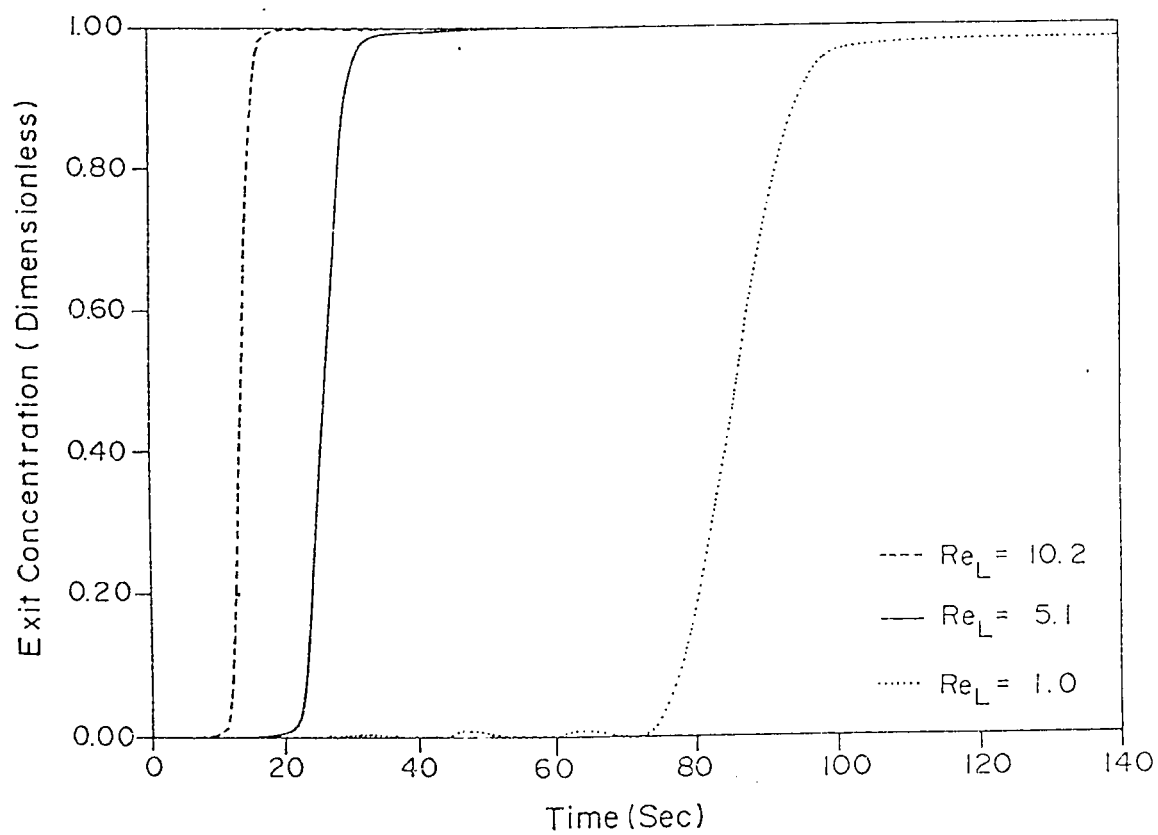


Figure (4.10) Effect of  $Re_L$  on the RTD for  $Re_G = 12.2$ , when a cocurrent downflow packed column is subjected to a step input in tracer concentration.

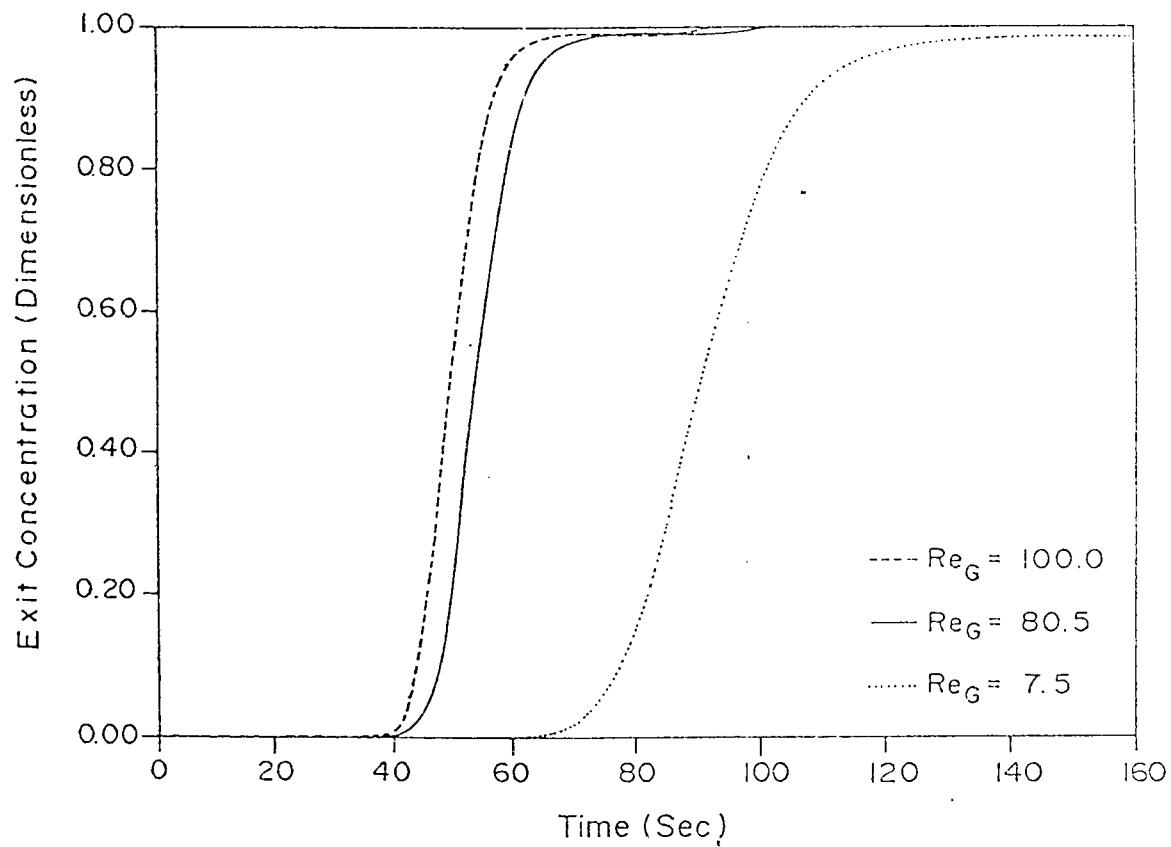


Figure (4.11) Effect of  $Re_G$  on the RTD for  $Re_L = 1.0$ , when a cocurrent downflow packed column is subjected to a step input in tracer concentration.

that the steepness of the response is not significantly affected by either liquid phase or gas phase Reynolds number. The effect of  $Re_L$  and  $Re_G$  is rather on the residence time which shifts the curves to the right, implying a later response of the breakthrough curve.

### **4.2.3 Comparison of Theoretical Predictions with Experimental Data**

The literature review shows that there is a very limiting data available for the experimental measurement of transient response of tracer concentration for studying the column dynamics. Experimental data were reported for the upflow operation by Skomorokov and Kirillov (1986) and down flow operation by Kar and Greenfield (1983). Theoretical predictions using the proposed model were compared with the experimental results obtained by the above investigators, Figures (4.12) and (4.13) and were found to be in close agreement. The parameters used in the analysis are listed in Table (4.1). It may be noted that these realistic parameters if used in the P-D-E model will give relatively poor predictions as shown in Figure (4.12).

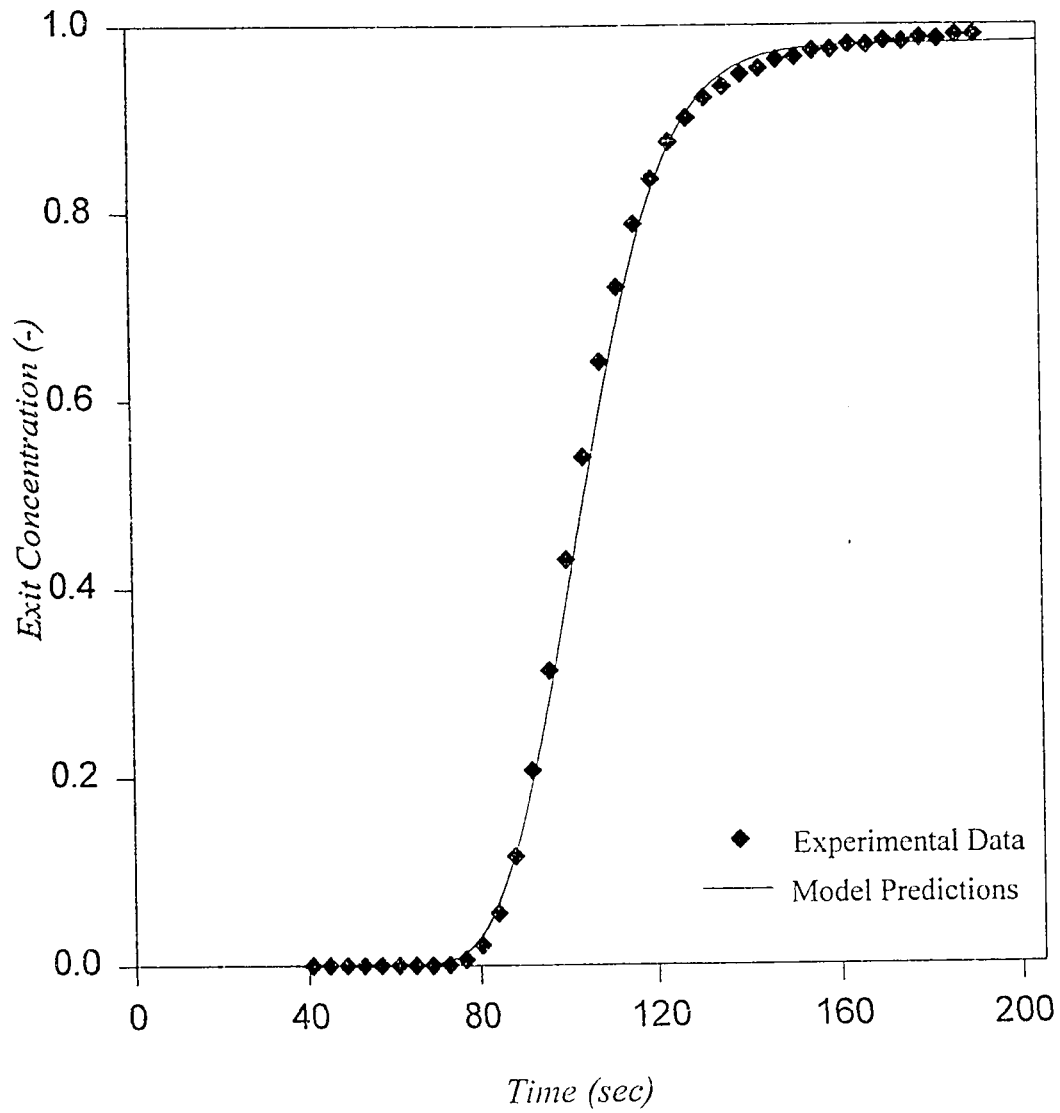


Figure (4.12) Comparison of experimental data and model predictions for a step input in tracer concentration in a co-current downflow packed column.

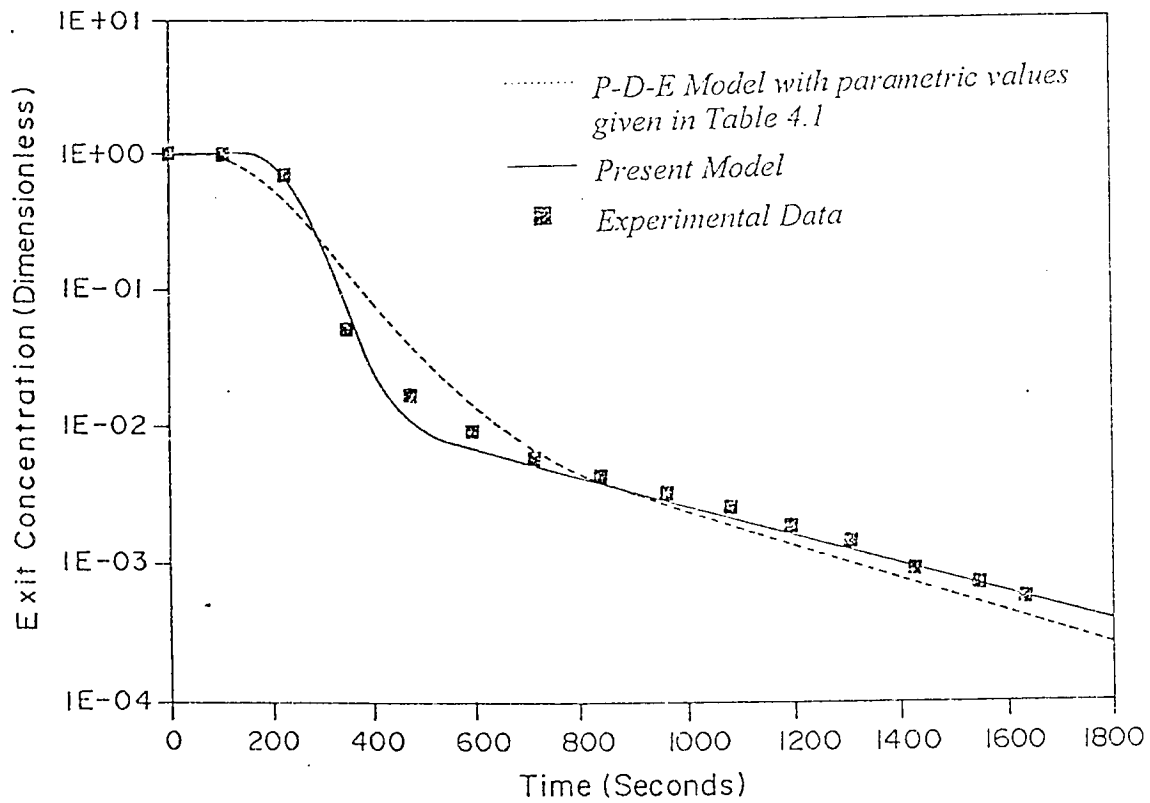


Figure (4.13) Comparison of experimental data with predictions of both the P-D-E and the present model when subjected to base parameters for a step decrease in tracer concentration in a cocurrent upflow packed column (Data of Skomorokov and Kirillov, 1986)

# CHAPTER 5

## MODELING OF GAS ABSORPTION IN COCURRENT PACKED COLUMNS

---

### 5.1 INTRODUCTION

Gas absorption is probably the most important and widely used unit operation in environmental control, chemical, biochemical and petrochemical industries for the selective removal of components from gas mixtures. It involves the transport of a substance from the gaseous phase to the liquid phase, which may then be physically dissolved by the liquid, or may undergo a chemical change. Typical examples of systems involving physical gas absorption can be found in air pollution control, where water, which is readily available at low cost, is used for the treatment of large volumes of low pressure exhaust gas for the prevention of air pollution as solvent losses are difficult to avoid in such installations. Gas phase impurities which are absorbed commercially in water scrubbing operations include ammonia, sulfur dioxide, hydrogen fluoride, silicon tetrafluoride, hydrogen chloride and chlorine. Carbon dioxide, hydrogen sulfide and chlorine are relatively insoluble in water and their absorption rates are determined by the liquid film



resistance, while hydrogen fluoride, silicon tetrafluoride and hydrogen chloride are highly soluble in water, and their absorption is generally found to be gas film controlled. A detailed discussion of such operations has been presented by Kohl and Riensenfeld (1979).

Though various types of equipment can be employed for such operations, packed columns are usually preferred for small installations, for corrosive systems, for liquids with foaming tendencies, for operations requiring very high liquid/gas ratios, and for applications where a low pressure drop is required (Kohl and Riensenfeld, 1979). Packed absorption columns can be operated in a counter-current as well as a cocurrent manner. Cocurrent mode of operation is usually favored when there is no significant difference in the mean concentration driving force, as encountered in the case of absorption of lean pollutants from the gas phase, where the concentration of solute gas absorbed in the liquid is so small so as to result in any appreciable change in the mean concentration driving force.

Due to the complexities outlined earlier, it is imperative for better understanding of such processes, to develop and define a continuum model which is able to express the performance of such columns. It is apparent that for realistic representation a complete model may have to be quite complex, and should take

into account both the heterogeneity of phases, and transport of components between them.

Analysis of the literature survey revealed that most of the models available for cocurrent packed columns consider only the liquid phase and very few theoretical studies have been undertaken which take into account more than one phase. The existing heterogeneous models have been solved for simple cases employing too many simplifying assumptions. Further, there is a scarcity of studies which deal exclusively with the continuum modeling of physical gas absorption in cocurrent packed columns.

## **5.2 RESULTS AND DISCUSSION**

The performance of downflow cocurrent packed column for absorption of various gases with range of properties has been analyzed. The model equations described in Section (3.2.2), have been solved for a wide range of operating parameters using the numerical scheme of orthogonal collocation. The studies were carried out for three different systems, namely absorption of ammonia, hydrogen fluoride, and sulfur dioxide from air into water. The choice of components were made on the basis of the value of Henry's constant as listed in Table (5.1). With Sulfur dioxide which has the lowest Henry's constant that the

absorption process is controlled by the liquid film resistance, while with ammonia having the highest Henry's constant gas film resistance controls. With Hydrogen Fluoride having the intermediate value of Henry's constant both the gas film and the liquid films control the absorption process. Table (5.2) lists the base values of parameters used for the numerical simulation of gas absorption phenomenon for all the three systems of interest.

### 5.2.1 Estimation of Model Parameters

The functional relationships of model parameters are available in the literature which can be used for the model predictions. Estimation of parameters like, thickness of the stagnant liquid phase,  $L_S$ , and dispersion in the stagnant phase,  $D_S$ , are discussed in Section (4.2.1). The surface area,  $a_{SD}$ , between stagnant and dynamic phases for interregional mass transfer was calculated by a relationship proposed by Kan and Greenfield (1986), as outlined in Section (4.2.1).

Additional parameters like, the gas liquid mass transfer coefficient,  $K_{LG}$   $a_{LG}$ , was calculated by a correlation presented by Ellman (1988) and highly recommended by Gianetto and Specchia (1992) as it is based on a very large amount of data obtained with different gas liquid systems in a wide range of operating conditions,

**Table 5.1** Diffusion coefficients and Henry's Law constants for the gas absorption systems.

Component	Henry's Constant*, $H$ $\frac{\text{kmol m}^{-3} \text{ of solution}}{\text{kmol m}^{-3} \text{ of gas}}$	Diffusivity in water, $D_C$ $10^9 \text{ m}^2 \text{ s}^{-1}$
Ammonia	1516.54	2.0
Hydrogen Flouride	234.819	2.54
Sulfer Dioxide	30.33	1.7

\* Values reported by Betterton (1992)

**Table 5.2** Base values of parameters used for the parametric study of the model for gas absorption.

Parameters	Value	Reference
$U_L$ , $\text{m s}^{-1}$	$10^{-3}$	Kan and Greenfield (1983)
$U_G$ , $\text{m s}^{-1}$	0.1	-*
$L_C$ , m	1.0	-*
$d_p$ , m	$10^{-3}$	Kan and Greenfield (1983)
$\varepsilon$	0.4	Kan and Greenfield (1978)
$L_S$ , m	$10^{-4}$	Kan and Greenfield (1983)
$D_S$ , $\text{m}^2 \text{s}^{-1}$	$0.5 \times 10^{-10}$	Kan and Greenfield (1983)
$h_S$	0.0499	Saez and Carbonell (1985)
$h_d$	0.1238	Ellman (1990)
$k_{LG} a_{LG}$ , $\text{sec}^{-1}$	$2.55 \times 10^{-4}$	Ellman (1988)
$k_{SD}$ , $\text{m s}^{-1}$	$5.5 \times 10^{-8}$	Beg et al. (1995)
$Pe_L$	15.425	Beg et al. (1995)
$Pe_G$	39.694	Hochman and Efron (1969)
$\rho_L$ , $\text{kg m}^{-3}$	1000.0	Welty et al. (1976)
$\rho_G$ , $\text{kg m}^{-3}$	1.225	Welty et al. (1976)
$\mu_L$ , Pa sec	$7.44 \times 10^{-4}$	Welty et al. (1976)
$\mu_G$ , Pa sec	$1.8 \times 10^{-5}$	Welty et al. (1976)
$\sigma_L$ , $\text{N m}^{-1}$	$7.15 \times 10^{-2}$	Welty et al. (1976)

\* Chosen arbitrarily.

The calculated parameters used in the analysis,

$h_t$	0.1737
$h_g$	0.2263
$\phi$	0.713
$\psi$	1.303
$\xi$	100.0
$a_{SD}$ , $\text{m}^{-1}$	499.0
$\beta$	0.8686
$K_{SD}^*$	$2.744 \times 10^{-2}$
$St$	0.255
$Bi$	0.11
$Re_L$	1.344
$Re_G$	6.8

$$Sh_{GL}^* = \Omega \cdot \chi_G^A \cdot Re_L^B \cdot We_L^{\bar{C}} \cdot Sc_L^{\bar{D}} \cdot \bar{\theta}^{-E} \quad (5.1)$$

where,

$$\begin{aligned} Sh_{GL}^* &= \frac{k_{GL} \cdot a_{GL} \cdot d_h^2}{D_c} & d_h &= d_p \left\{ \frac{16\varepsilon^3}{9\pi(1-\varepsilon)^2} \right\}^{\frac{1}{3}} \\ \chi_G &= \frac{G}{L} \sqrt{\frac{\rho_L}{\rho_G}} & \bar{\theta} &= \frac{a_p d_h}{(1-\varepsilon)} \\ e_L &= \frac{L^2 d_p}{\rho_L \sigma_L} & Re_L &= \frac{L d_p}{\mu_L} \end{aligned} \quad (5.2)$$

and the values of the coefficient are,

	$\Omega$	$A$	$B$	$\bar{C}$	$\bar{D}$	$E$
For $\chi_G < 0.8$	0.45	0.65	1.04	0.26	0.65	0.325
For $0.8 < \chi_G < 1.2$	0.091	0.95	0.76	0.76	1.14	0.95
For $\chi_G > 1.2$	0.00028	0.85	0.68	0.68	1.70	0.85

Dynamic liquid holdup  $h_d$ , was estimated by a correlation proposed by

Ellman et al. (1990) as given below,

$$h_d = 10^\kappa \cdot \varepsilon \quad (5.3)$$

where,

$$\kappa = 0.001 - \frac{\bar{R}}{\zeta^s} \quad (5.4)$$

and

$$\zeta = \chi_L^{\bar{M}} \cdot Re_L^{\bar{N}} \cdot We_L^{\bar{P}} \left( \frac{a_c \cdot d_h}{(1-\varepsilon)} \right)^{\bar{Q}} \quad \chi_L = \frac{1}{\chi_G} \quad (5.5)$$

and the values of the coefficient are,

	$\bar{R}$	$\bar{S}$	$\bar{M}$	$\bar{N}$	$\bar{P}$	$\bar{Q}$
For $\chi_G < 0.8$	0.16	0.65	0.5	-0.25	0.2	0.25
For $0.8 < \chi_G$	0.42	0.48	0.5	-0.3	0	0.3

Stagnant liquid holdup,  $h_s$ , was calculated by using a correlation presented by Saez and Carbonell (1985),

$$h_s = \frac{1}{20 + 0.9 E\ddot{o}^*} \quad (5.6)$$

where,

$$E\ddot{o}^* = \frac{\rho_L g d_e^2 \varepsilon^2}{\sigma (1-\varepsilon)^2} \quad \text{and} \quad d_e = 6 \frac{V_p}{S_p} \quad (5.7)$$

The estimated ratio of stagnant holdup over dynamic holdup  $\phi$ , agreed reasonably well with studies carried out by Kan and Greenfield (1983), Matsuura et al. (1976), and Hochmann and Effron (1969).

Gas phase Peclet number was obtained from the correlation given by Hochmann and Effron (1969),

$$Pe_G = \left( 1.8 \cdot Re_G'^{-0.7} \cdot 10^{-0.005 Re_L} \right) \frac{L_C h_d}{d_p} \quad (5.8)$$

where,

$$Re'_L = \frac{L d_p}{\mu_L (1 - \varepsilon)} \quad Re'_G = \frac{G d_p}{\mu_G (1 - \varepsilon)} \quad (5.9)$$

Parameters like, liquid phase Peclet number and the mass transfer coefficient between the stagnant and dynamic phases were obtained from the model fit for the experimental data reported by Kan and Greenfield (1986).

## 5.2.2 Results of Numerical Simulation

The effects of important dimensionless parameters, such as, liquid Peclet number,  $Pe_L$ , gas Peclet number,  $Pe_G$ , Stanton number,  $St$ , dimensionless parameter incorporating internal mixing resistance in the stagnant liquid phase,  $\beta$  and dimensionless mass transfer coefficient between stagnant liquid and dynamic liquid,  $K_{SD}^*$ , on the column dynamics were analyzed. Initially (at  $\theta = 0$ ) the column was considered to be free of any absorbate, i.e.,  $C_g = C_d = C_s = 0$ . Then the absorbate was introduced only in the gas phase, which implies that the inlet condition for this phase becomes,  $C_g|_{x=0^-} = 1$ .

Figures (5.1a), (5.1b) and (5.1c) show the dynamics of approach to steady state conditions for ammonia, hydrogen fluoride and sulfur dioxide systems respectively. After the initial abrupt pick up in the gas phase concentration, it



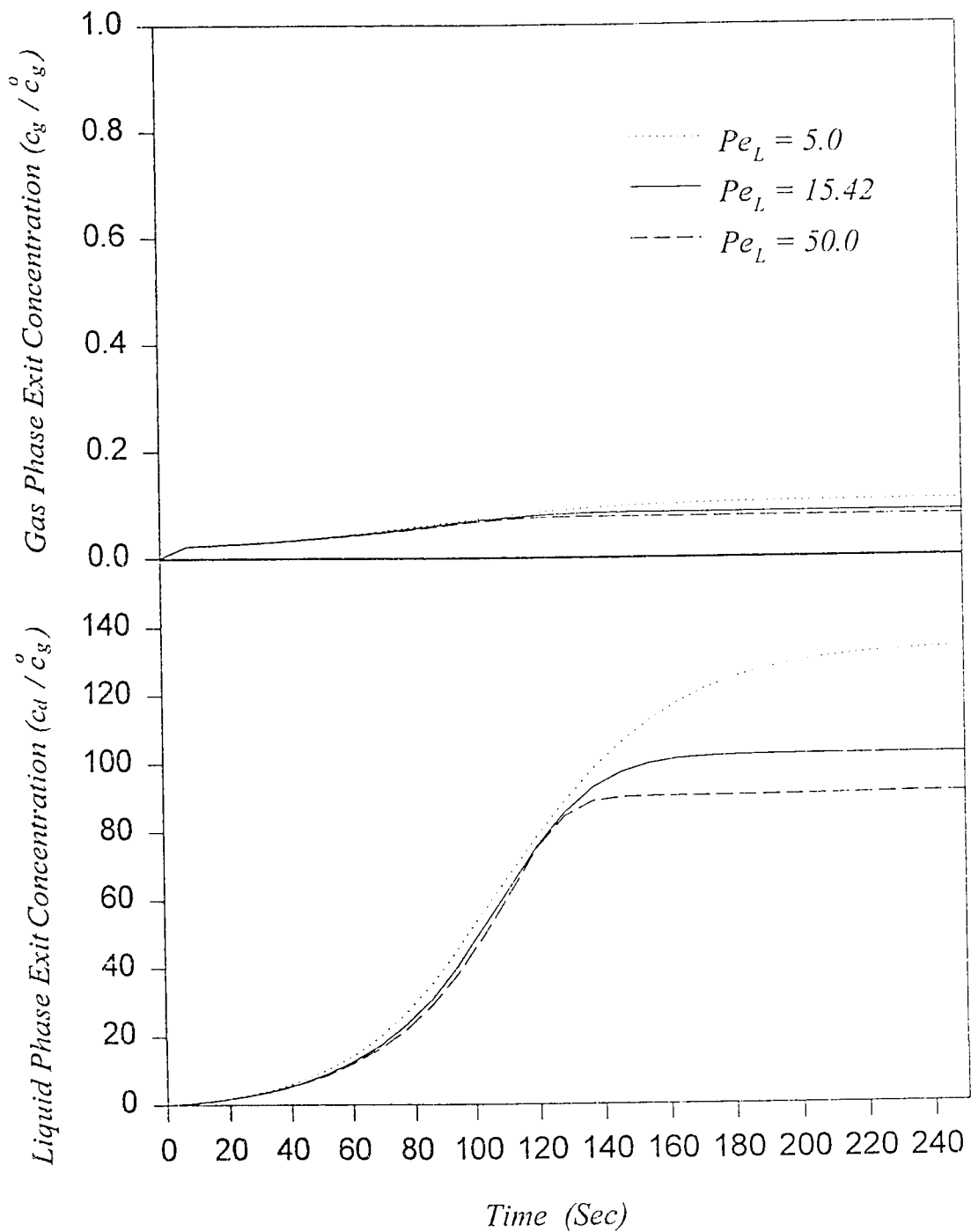


Figure (5.1a) The effect of  $Pe_L$  on the dynamics of gas and liquid phase exit concentrations for absorption of  $\text{NH}_3$ .

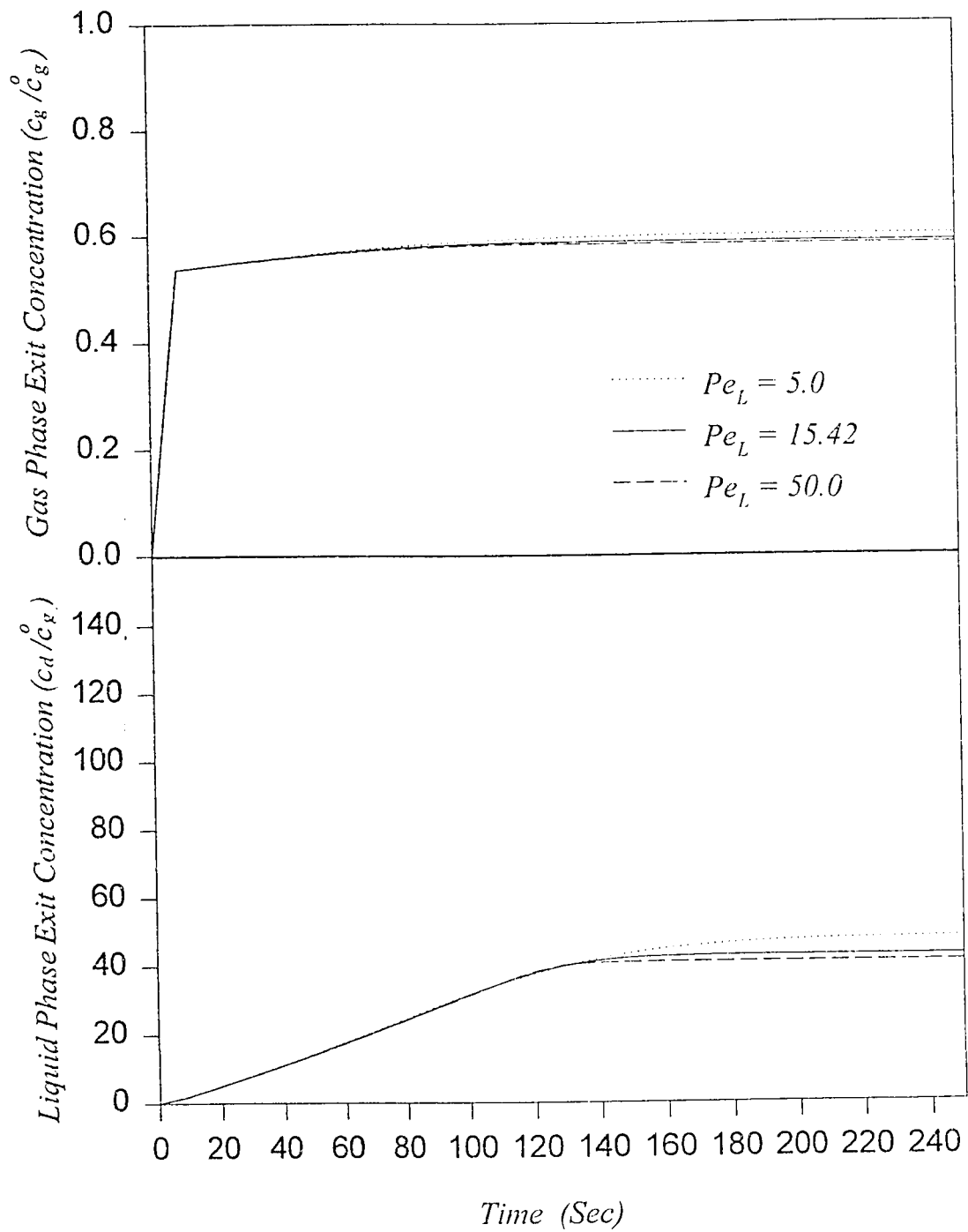


Figure (5.1b) The effect of  $Pe_L$  on the dynamics of gas and liquid phase exit concentrations for absorption of HF .

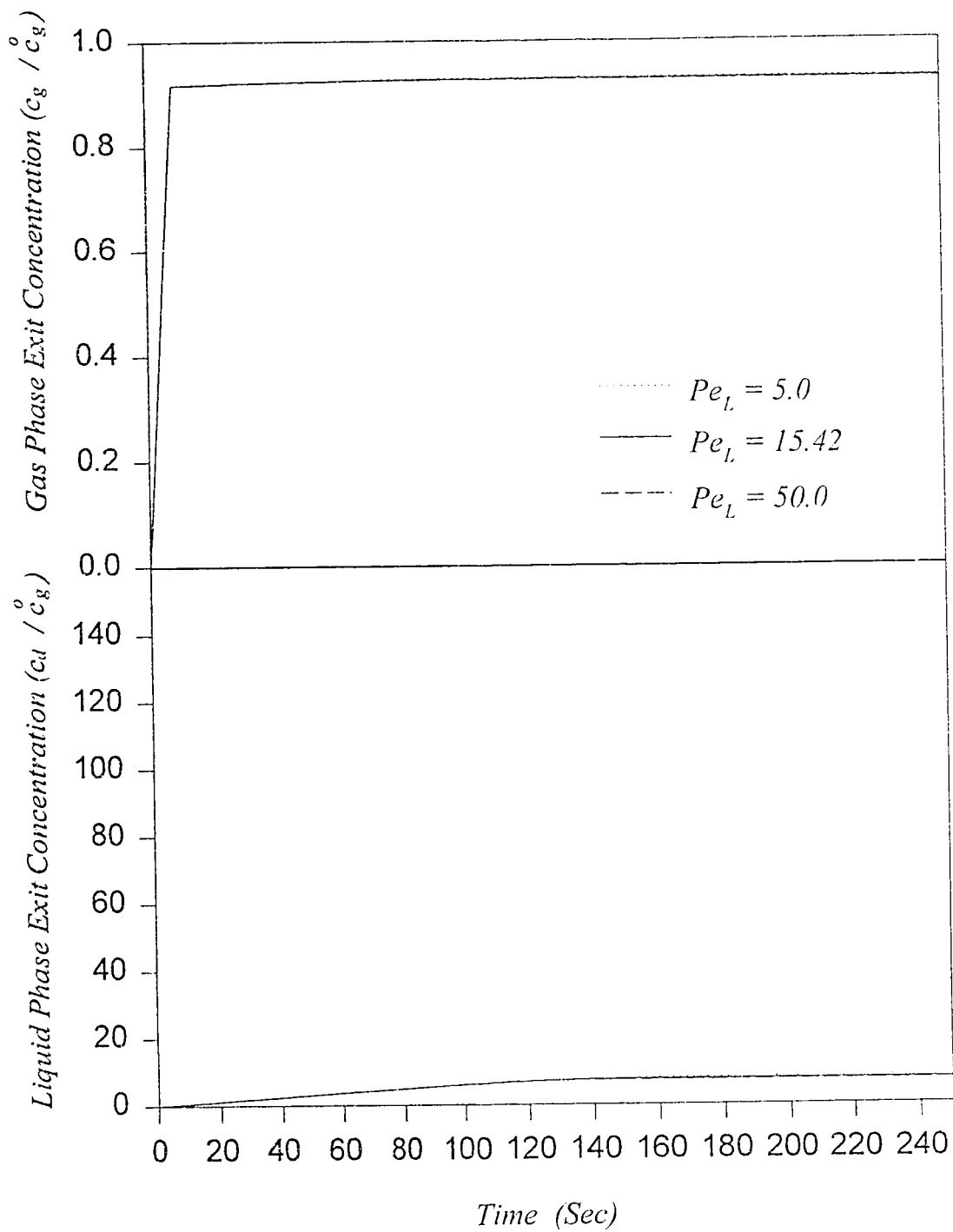


Figure (5.1c) The effect of  $Pe_L$  on the dynamics of gas and liquid phase exit concentrations for absorption of  $SO_2$ .

gradually approaches to a steady state value. This initial rise corresponds to a residence time of about seven seconds. The corresponding liquid phase reaches its steady state value much later. This delay in the response of the liquid phase would be expected due to the absorption of the component in the dynamic and stagnant liquid phases. These figures also show the effect of liquid phase Peclet number,  $Pe_L$ . It may be observed that the effect of  $Pe_L$  is more pronounced in the liquid phase compared to that in the gas phase. Further, the effect is more pronounced for the highly soluble ammonia and least for sulfur dioxide. This may be attributed to high levels of concentration in the liquid phase for the more soluble gas ammonia for which the effect of axial dispersion would be expected to be more significant.

Figures (5.2a), (5.2b) and (5.2c) show the corresponding steady state concentration profiles along the length of the column for the three systems considered. The results show that under identical operating conditions, absorption is maximum for ammonia and minimum for sulfur dioxide. For ammonia, the liquid and gas phase concentrations at the exit of the column approach to equilibrium conditions. In order to achieve similar performance for hydrogen fluoride and sulfur dioxide systems, one has to either increase the length of the absorber or alter the liquid and gas flow rates.

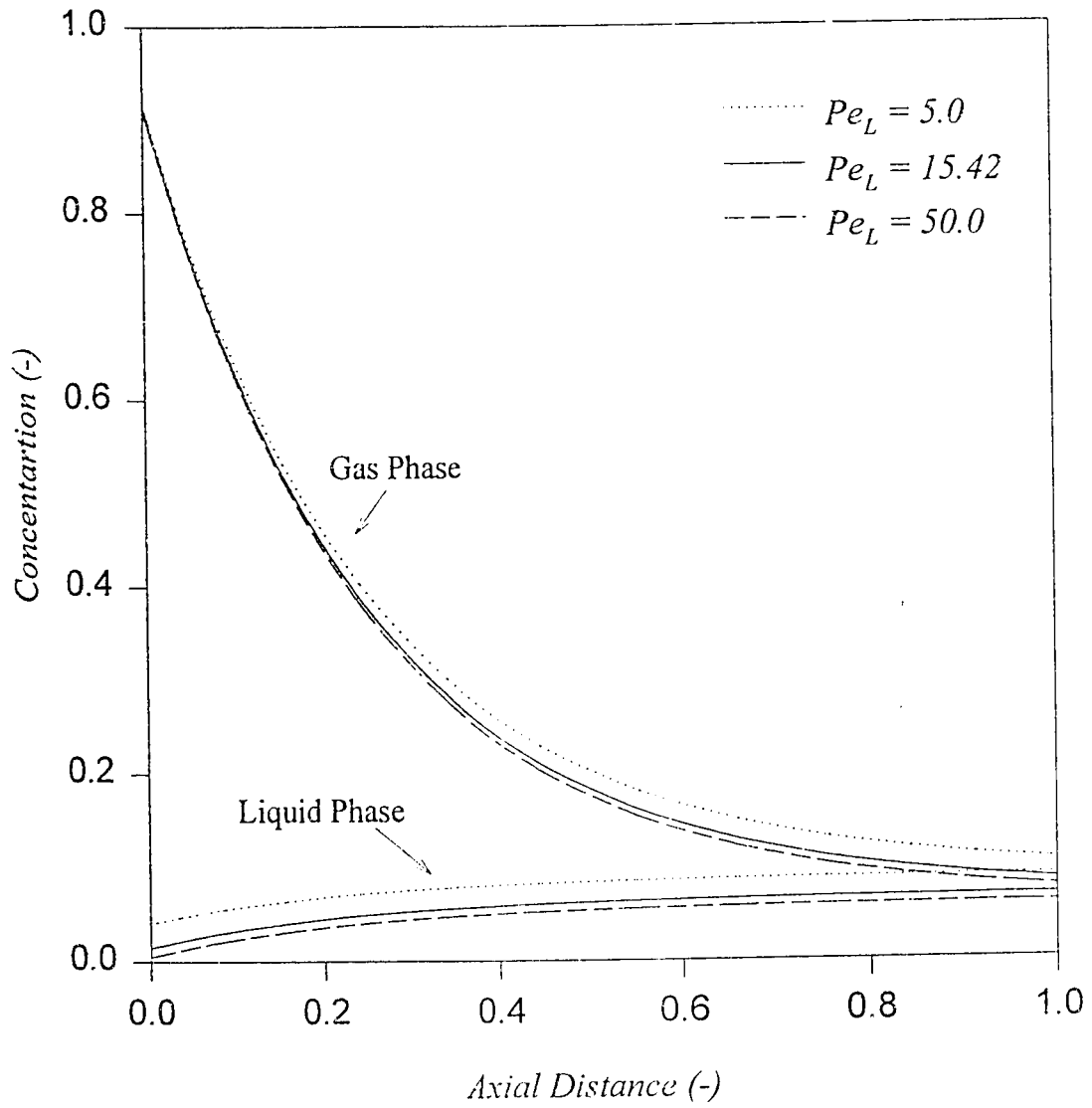


Figure (5.2a) The effect of  $Pe_L$  on steady state gas and liquid phase concentration profiles for absorption of  $\text{NH}_3$ .

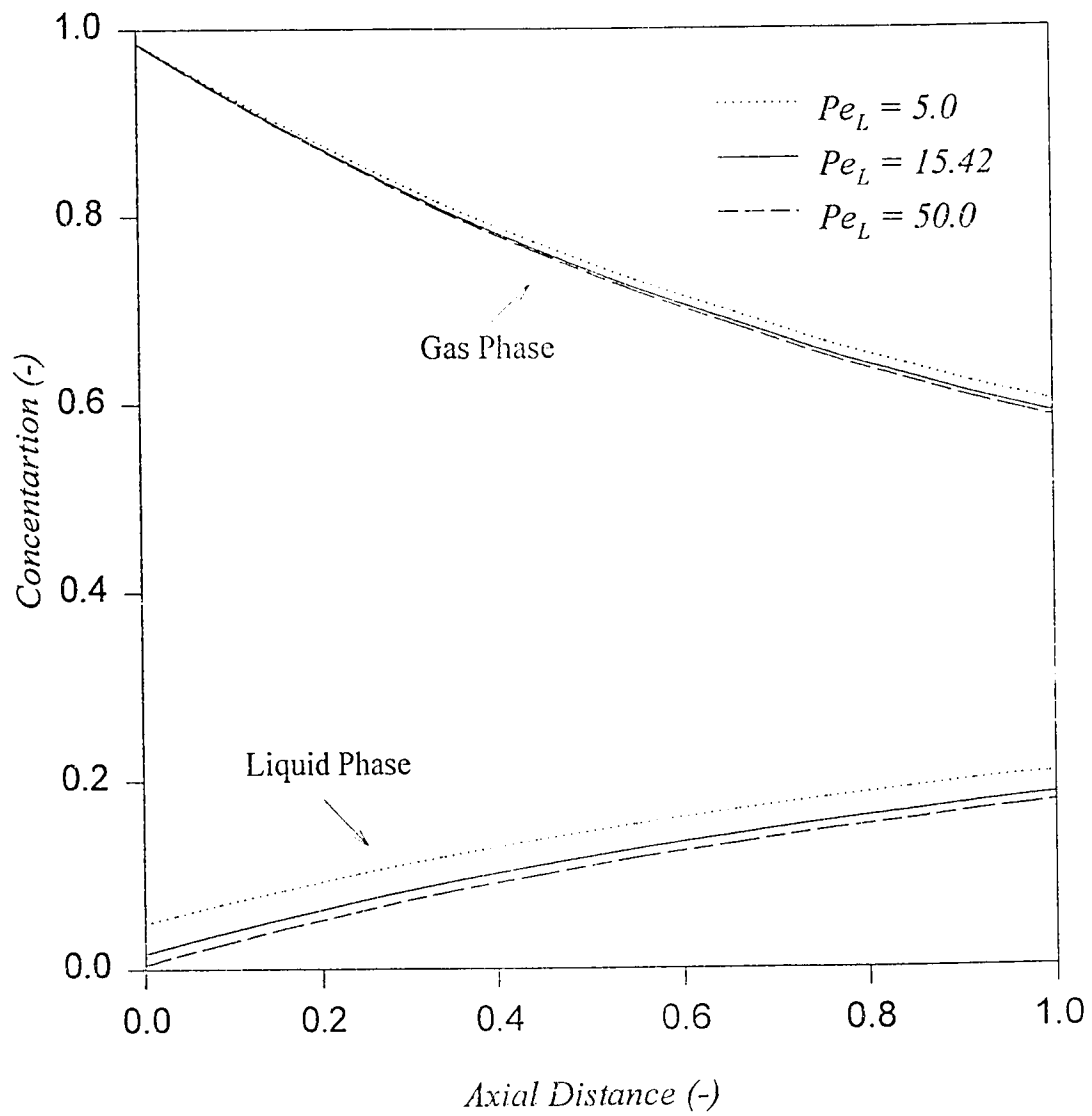


Figure (5.2b) The effect of  $Pe_L$  on steady state gas and liquid phase concentration profiles for absorption of HF.

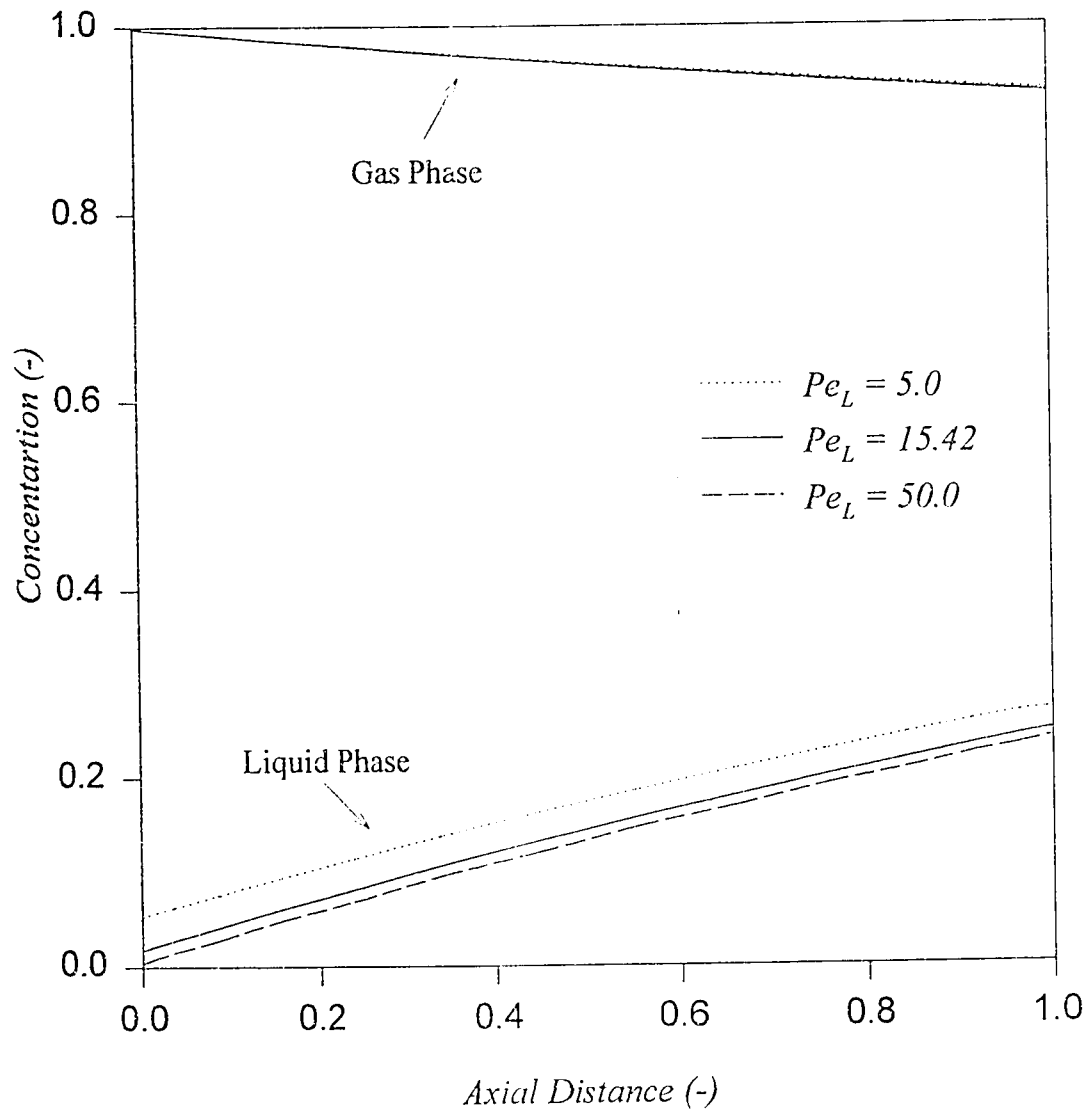


Figure (5.2c) The effect of  $Pe_L$  on steady state gas and liquid phase concentration profiles for absorption of  $SO_2$ .

Figure (5.3a), (5.3b) and (5.3c) show the steady state concentration profiles along the length of the column for ammonia, hydrogen fluoride and sulfur dioxide for various gas phase Peclet numbers,  $Pe_G$ . The effect of axial dispersion is very insignificant for the liquid phase concentration profiles for all the three systems, however, the gas phase concentration profiles are more significantly affected by  $Pe_G$ . The maximum effect is on highly soluble ammonia. A decrease in  $Pe_G$  implies better mixing in the gas phase leading to higher rates of mass transfer and better gradients. These conditions prevail more at the inlet of the column where the concentration levels are maximum. For  $Pe_G > 40$ , the effect is diminished as the column approaches to plug flow conditions.

The effect of Stanton number  $St$ , for the gas phase on the steady state concentration profiles are shown in Figures (5.4a), (5.4b) and (5.4c) for ammonia, hydrogen fluoride and sulfur dioxide respectively. It is apparent in these figures that the effect of the gas phase mass transfer coefficient is most pronounced on the ammonia absorption and the least for the sulfur dioxide absorption. This would be expected in view of the high solubilities of ammonia in water compared to hydrogen fluoride and sulfur dioxide. Further, with the increase of Stanton number, implying lower mass transfer resistance, the liquid and gas phases tend to approach equilibrium more rapidly. The effect of Stanton number on liquid phase



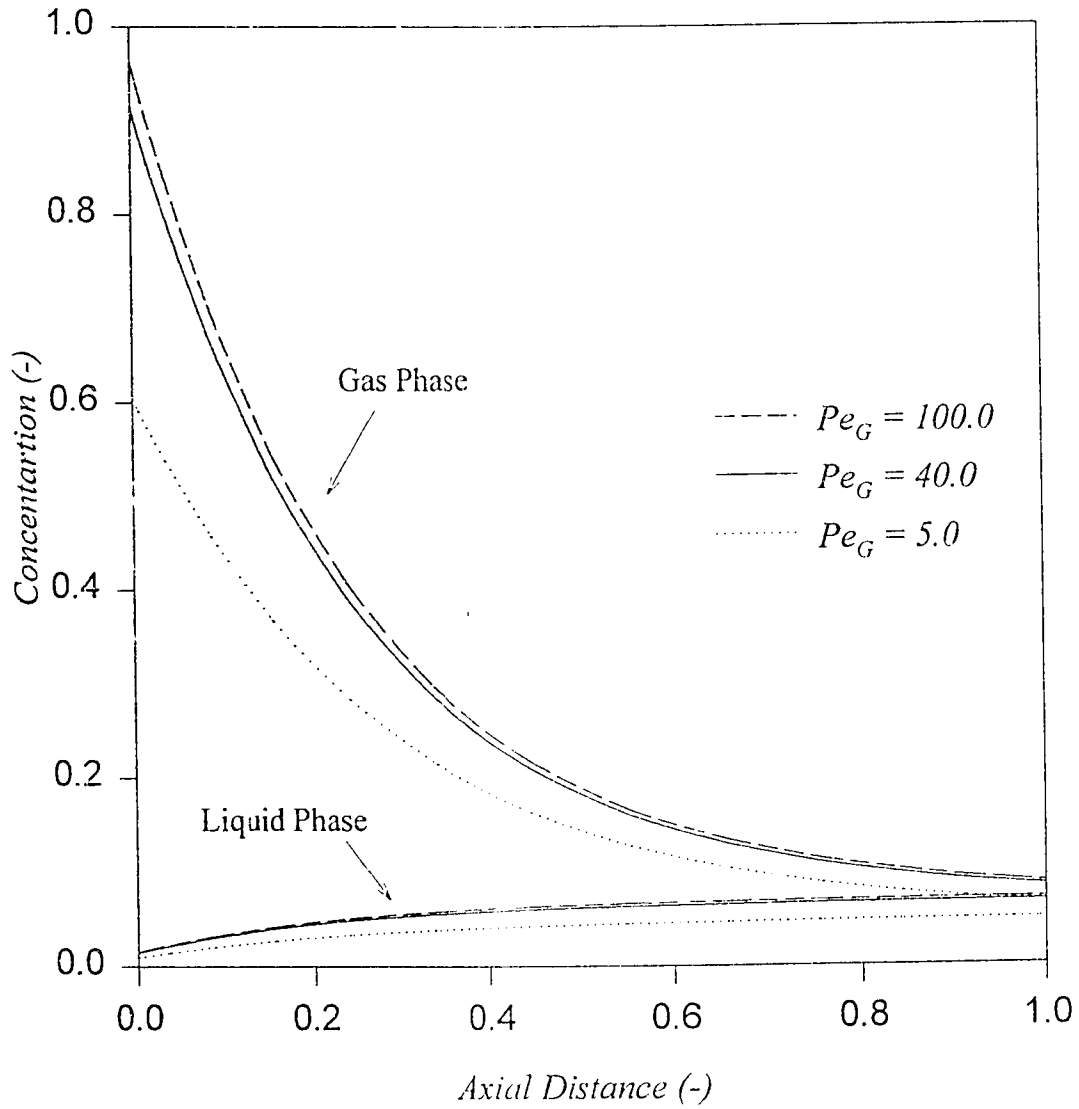


Figure (5.3a) The effect of  $Pe_G$  on steady state gas and liquid phase concentration profiles for absorption of  $\text{NH}_3$ .

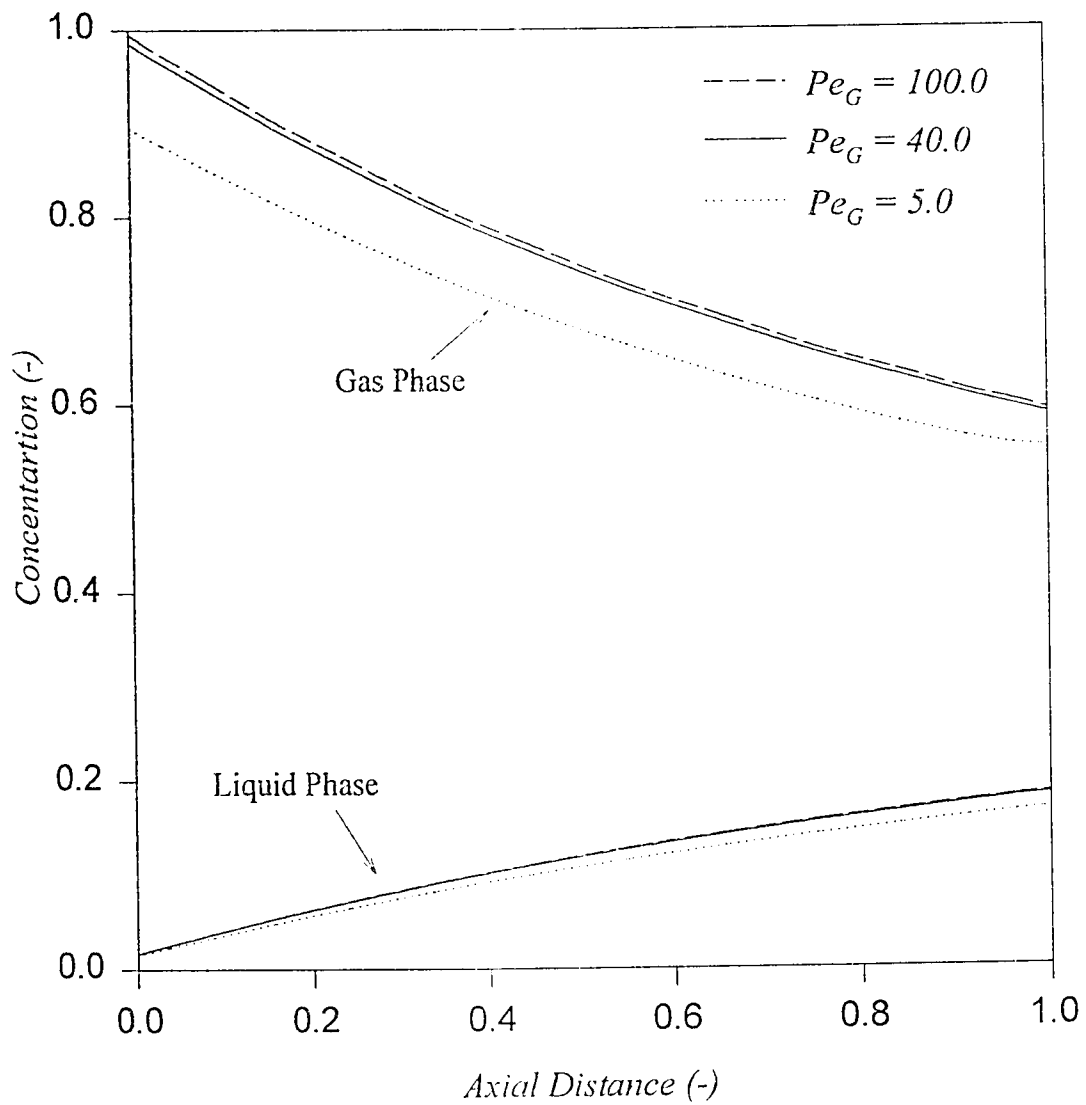


Figure (5.3b) The effect of  $Pe_G$  on steady state gas and liquid phase concentration profiles for absorption of HF.

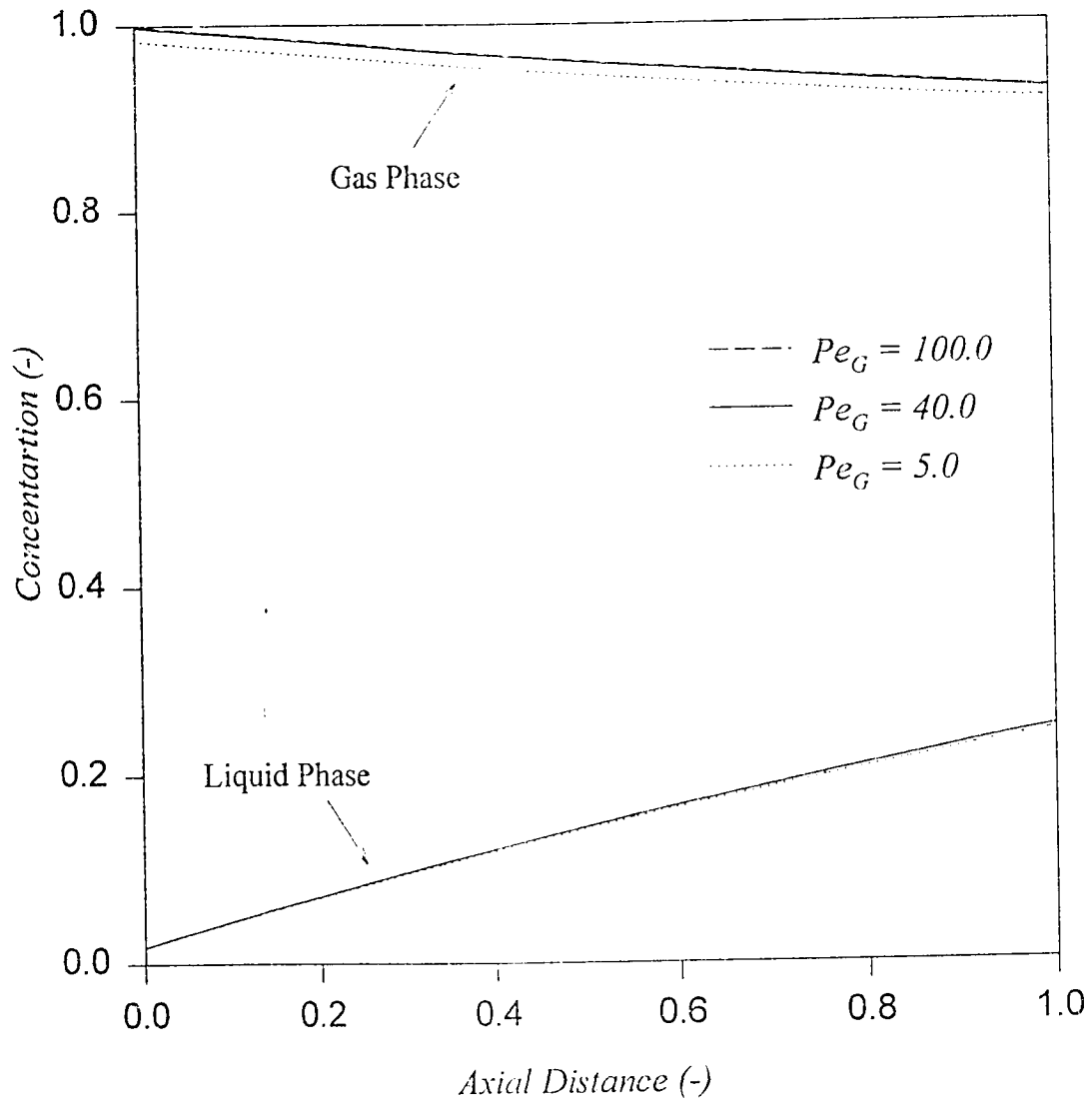


Figure (5.3c) The effect of  $Pe_G$  on steady state gas and liquid phase concentration profiles for absorption of  $SO_2$ .

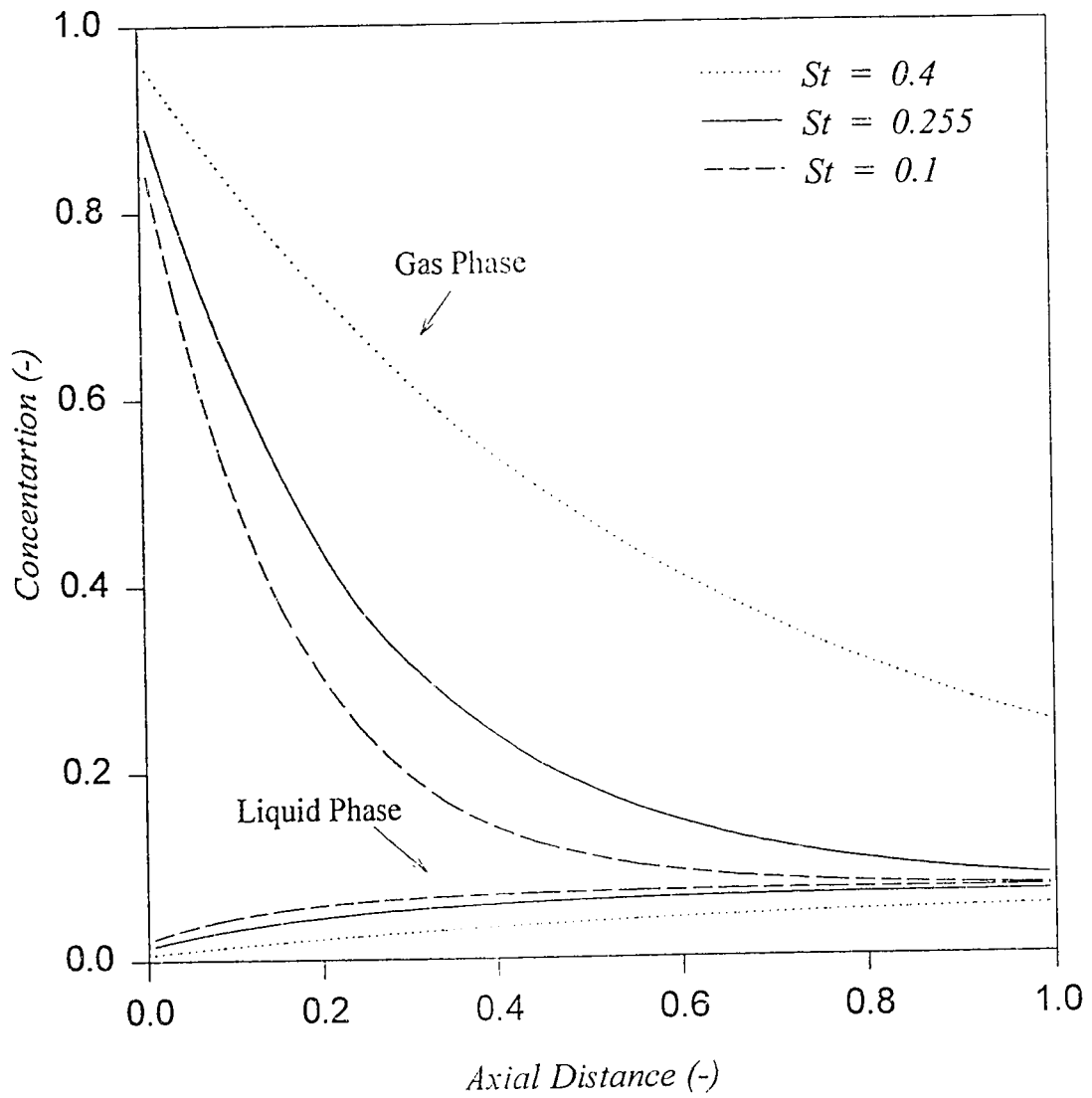


Figure (5.4a) The effect of  $St$  on steady state gas and liquid phase concentration profiles for absorption of  $\text{NH}_3$ .

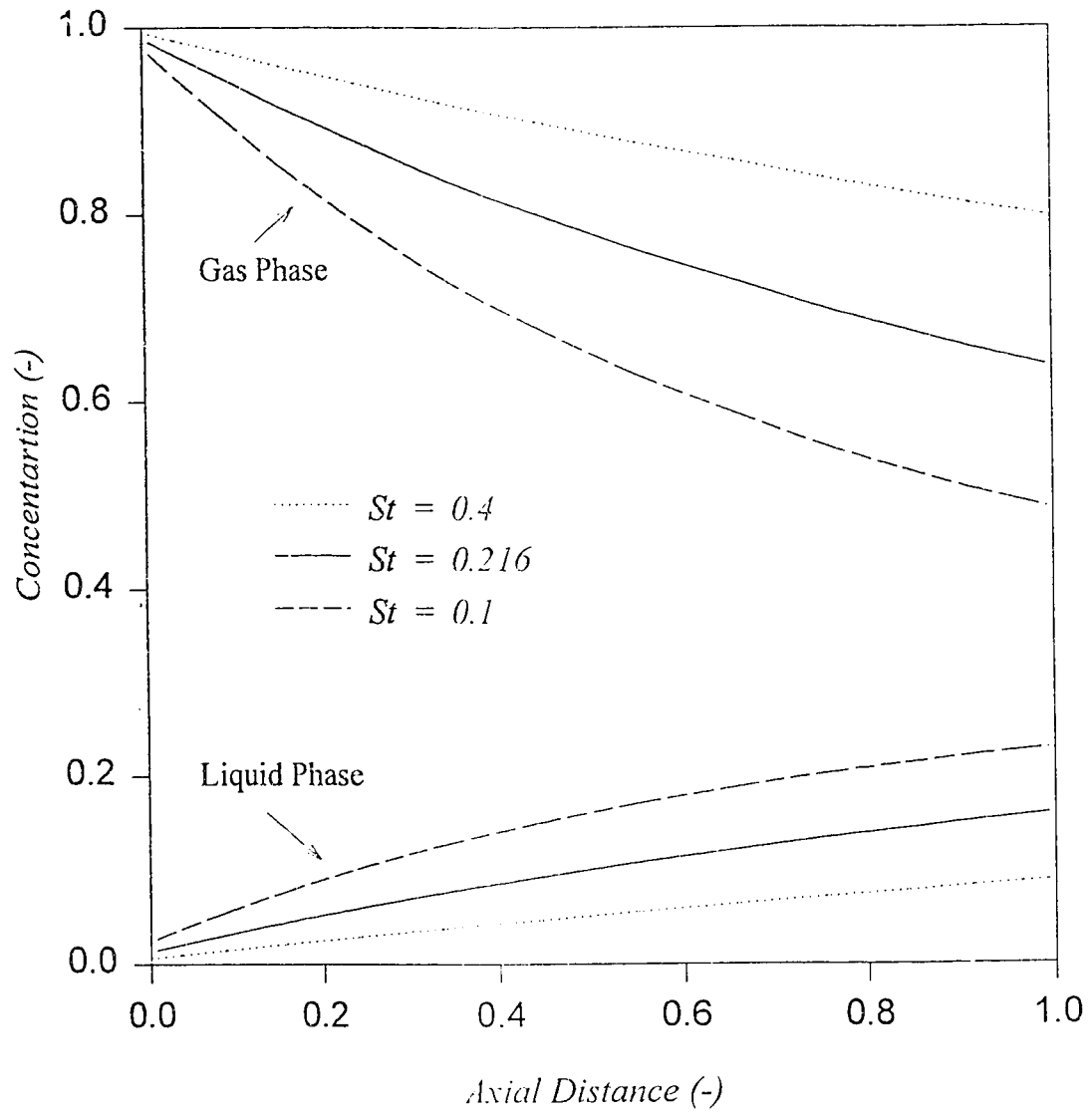


Figure (5.4b) The effect of  $St$  on steady state gas and liquid phase concentration profiles for absorption of HF .

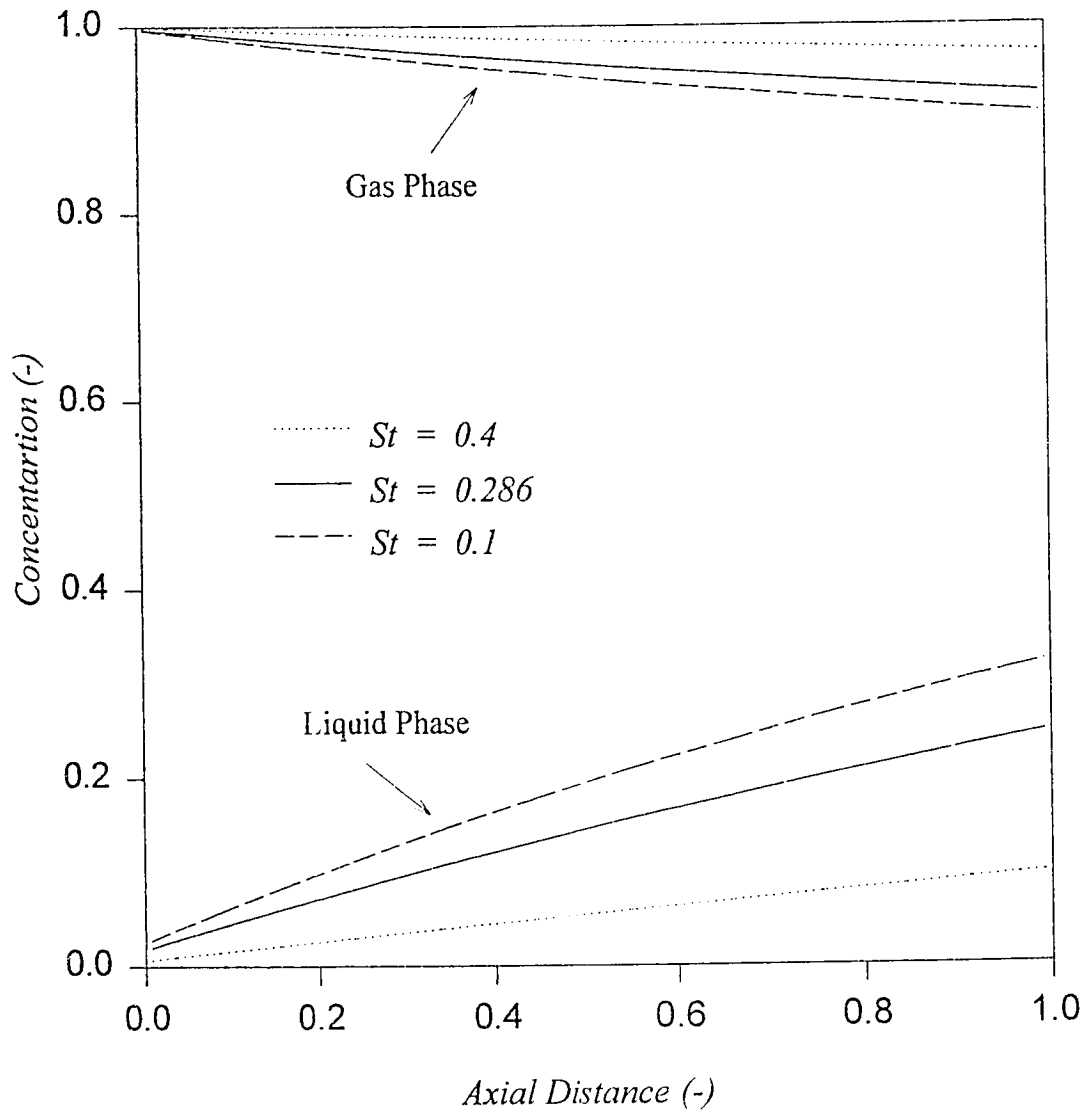


Figure (5.4c) The effect of  $St$  on steady state gas and liquid phase concentration profiles for absorption of  $SO_2$ .

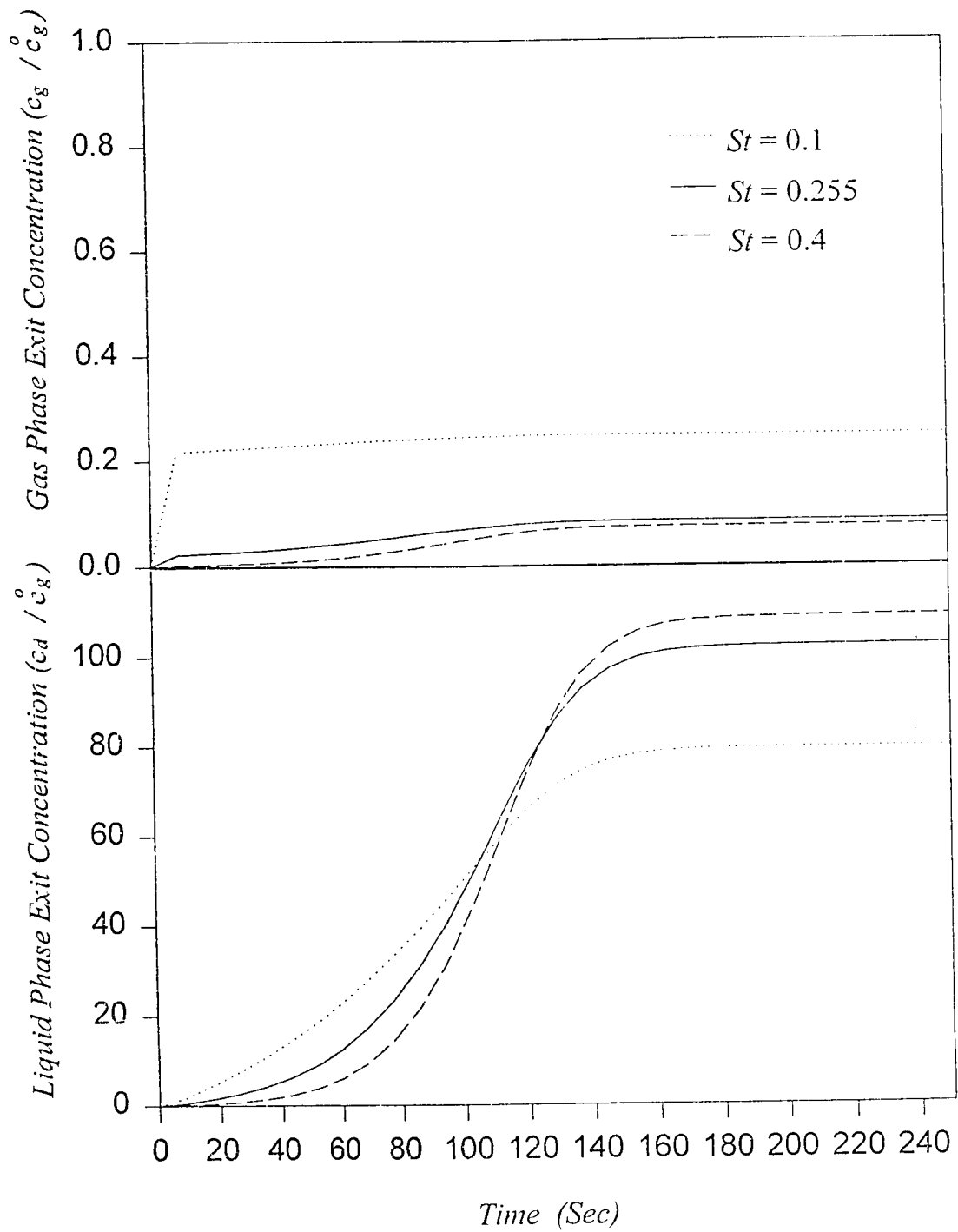
concentration profiles is also pronounced for ammonia which is not so illustrative in Figures (5.4a), (5.4b) and (5.4c) due to the way the dimensionless equilibrium concentrations are defined  $\left( \frac{c_d}{H c_g^o} \right)$ . In order to describe the effect of Stanton

number, the dimensionless exit concentration in the liquid phase was redefined as,

$\left( \frac{c_d}{c_g^o} \right)$ , which is shown in Figures (5.5a), (5.5b) and (5.5c) for ammonia,

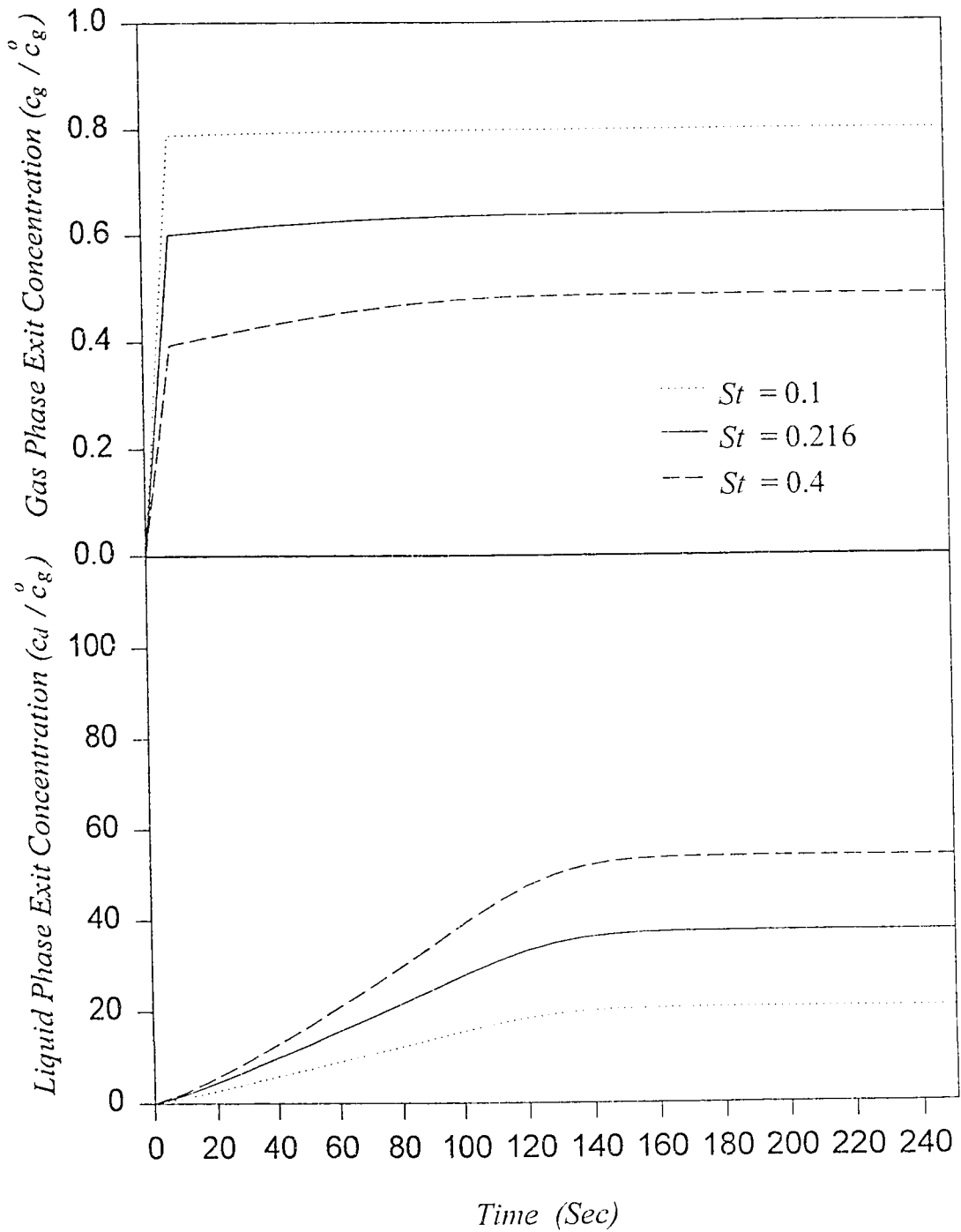
hydrogen fluoride and sulfur dioxide systems respectively.

The effect of parameter  $\beta$ , on the dynamic liquid phase concentration profile is shown in Figure (5.6) for representative case of ammonia absorption. It shows that the effect of  $\beta$  is very small and it appears only in the way, the approach to steady-state is achieved. Small values of  $\beta$ , which implies poor mixing in the stagnant liquid phase, tend to slow down the approach to steady-state. This phenomenon is more explicitly shown in Figures (5.7a) and (5.7b), which displays the concentration profiles in a three dimensional plot. The steady-state is attained very rapidly for higher values of  $\beta = 20$  while it takes much longer time for the case of  $\beta = 0.86$ . Similar trends also observed for parameter,  $K_{SD}^*$ , as shown in Figure (5.8), (5.9a) and (5.9b). Higher values of  $K_{SD}^*$  implies lower mass transfer resistance between the stagnant and dynamic liquid phases.

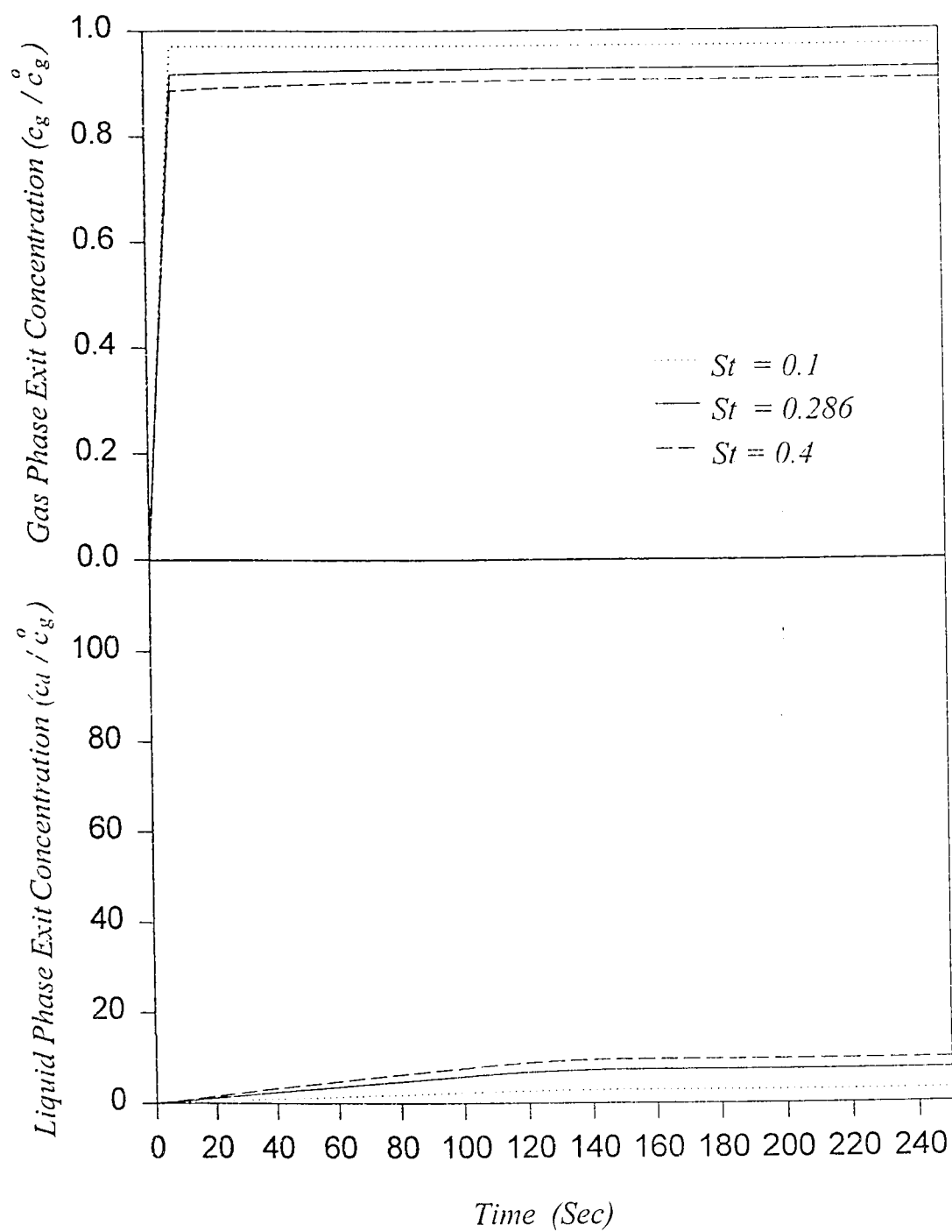


Figure(5.5a) The effect of  $St$  on the dynamics of gas and liquid phase exit concentrations for absorption of  $\text{NH}_3$ .





Figure(5.5b) The effect of  $St$  on the dynamics of gas and liquid phase exit concentrations for absorption of HIF.



Figure(5.5c)

The effect of  $St$  on steady state gas and liquid phase concentrations for absorption of  $SO_2$ .

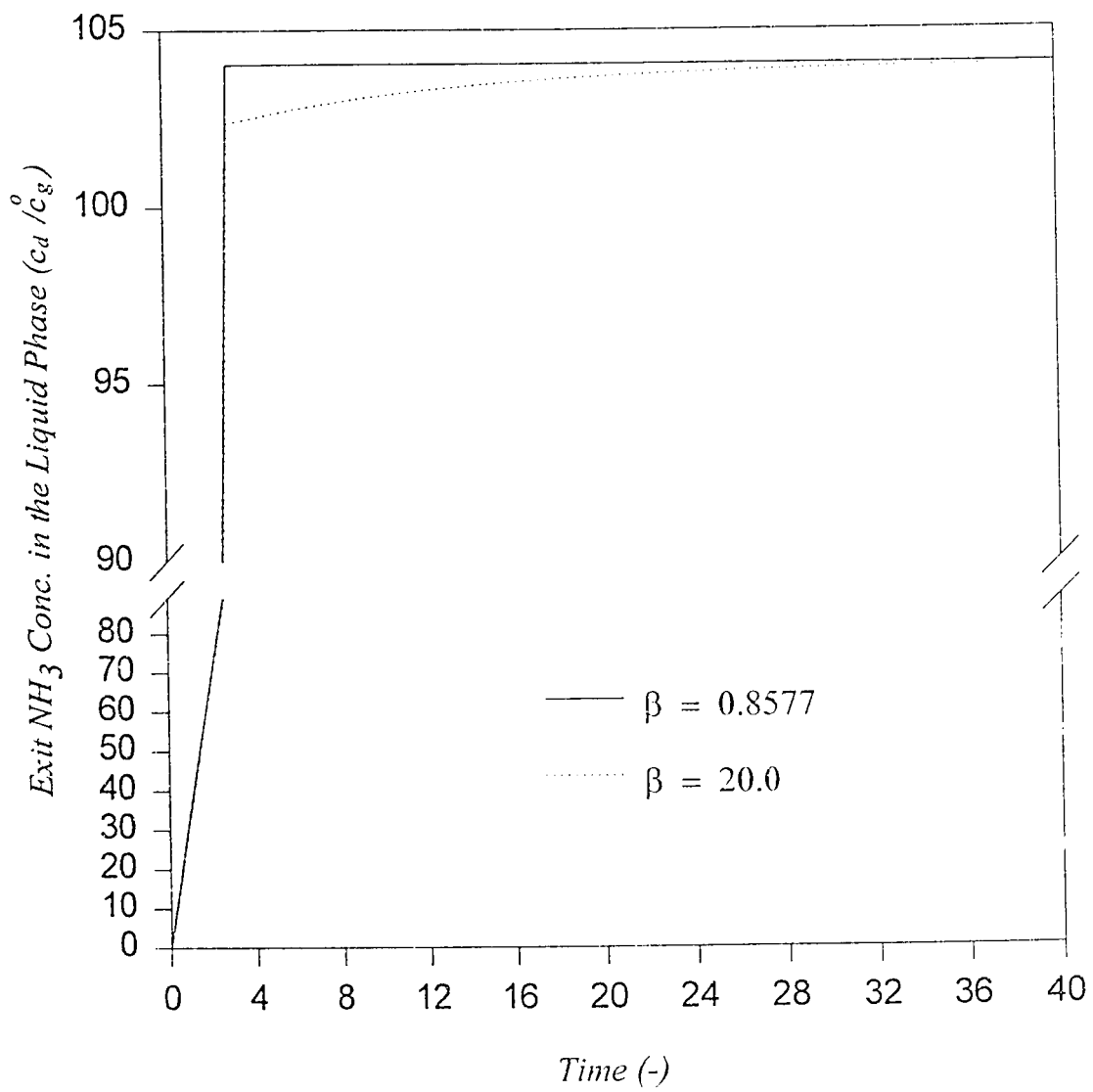


Figure (5.6) The effect of  $\beta$  on the dynamics of liquid phase exit concentrations for absorption of NH<sub>3</sub>.

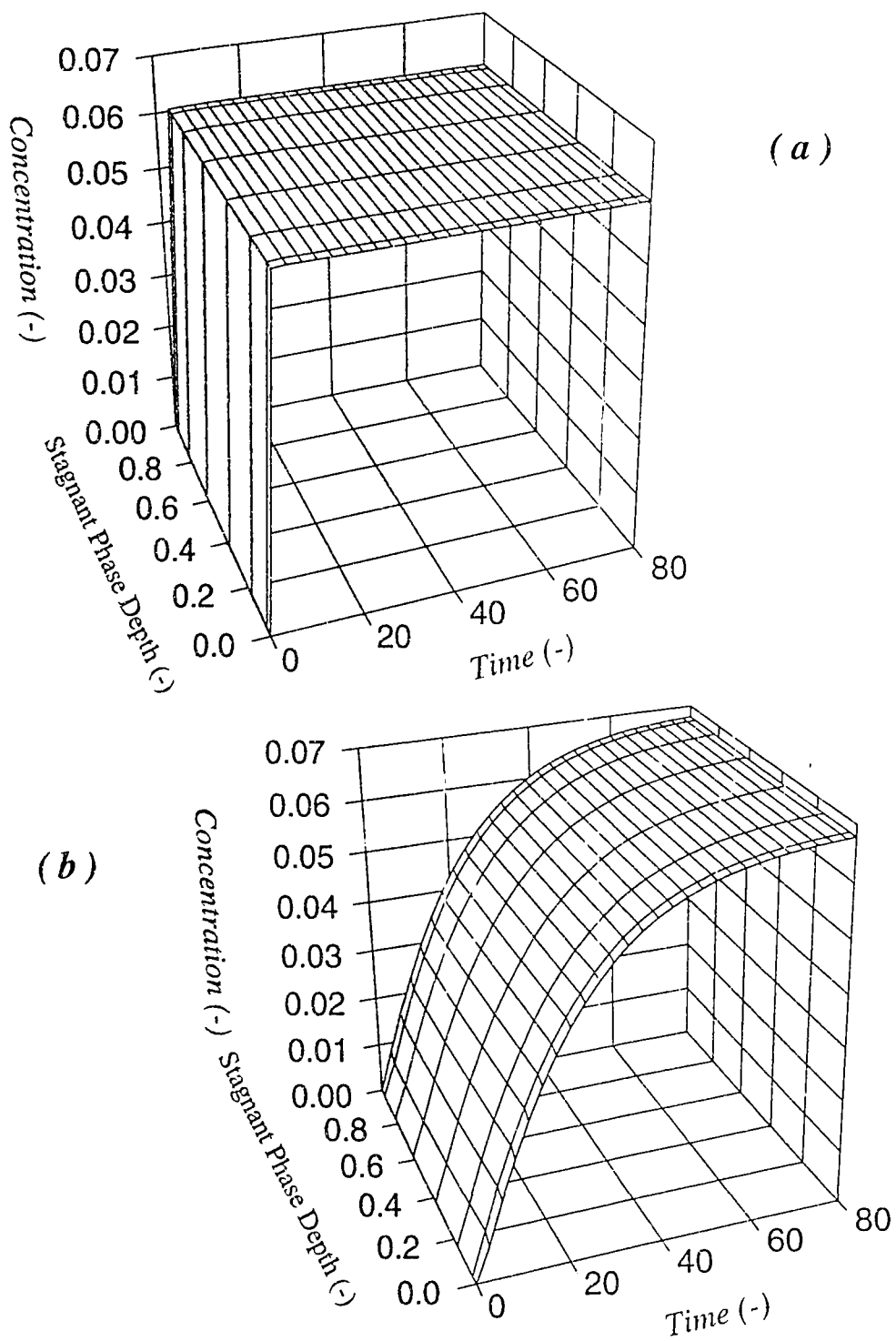


Figure (5.7) Stagnant phase concentration profiles in 3-D for absorption of  $\text{NH}_3$  illustrating the effect of  $\beta$ . (a)  $\beta = 20.0$  (b)  $\beta = 0.8577$

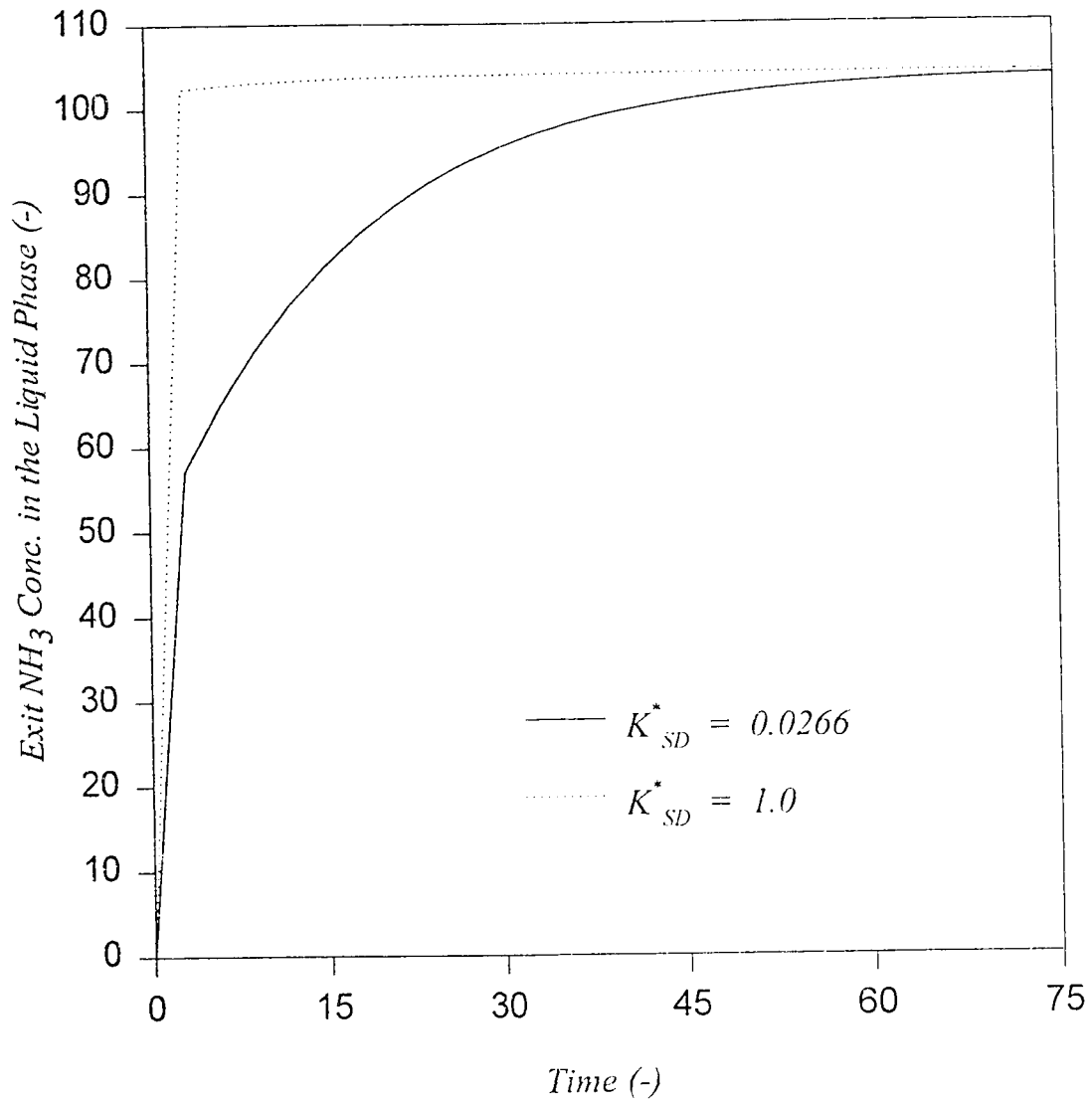


Figure (5.8) The effect of  $K_{SD}^*$  on the dynamics of liquid phase exit concentrations for absorption of NH<sub>3</sub>.

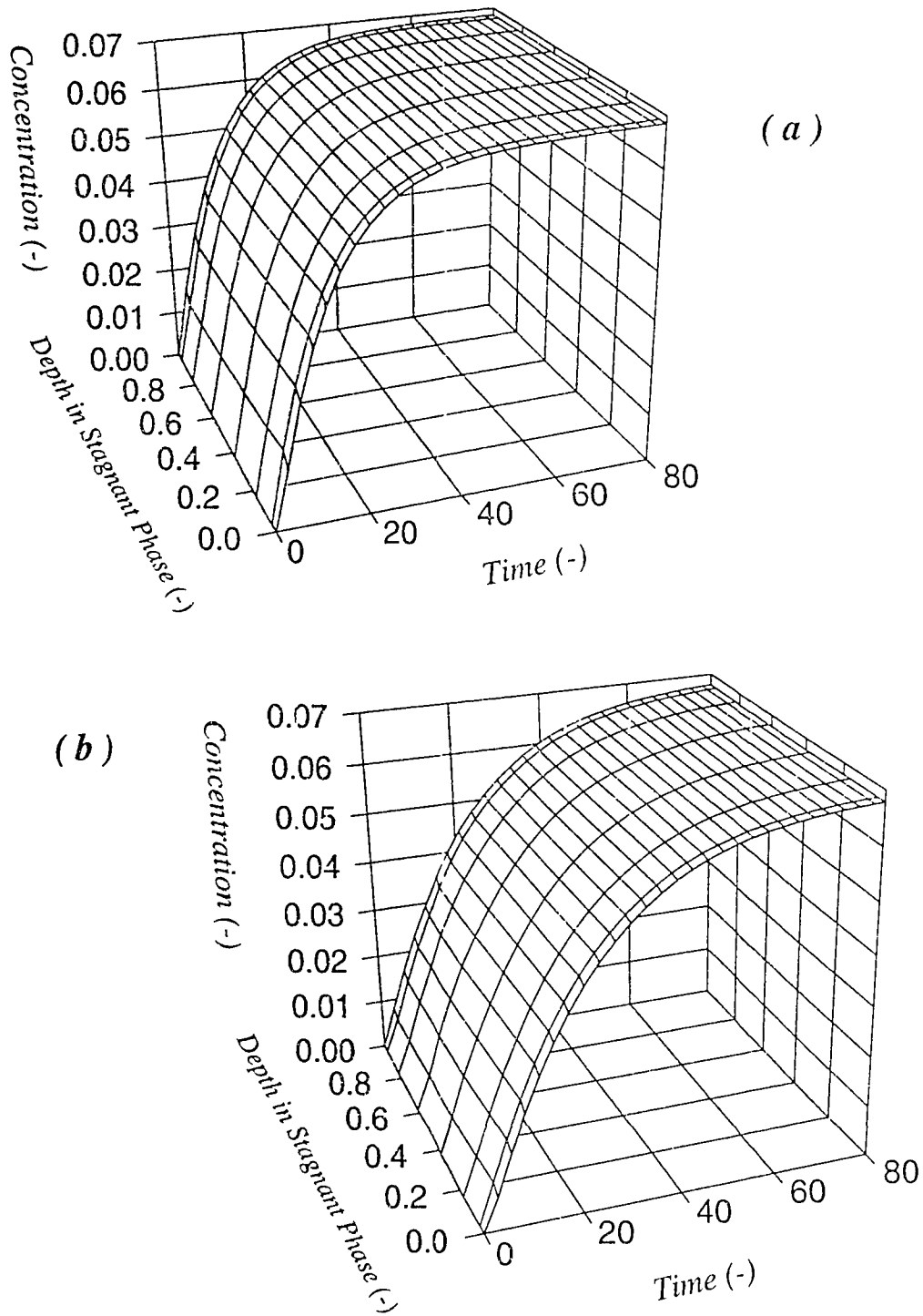


Figure (5.9) Stagnant phase concentration profiles in 3-D for absorption of  $\text{NH}_3$ , illustrating the effect of  $K_{SD}^*$ . (a)  $K_{SD}^* = 1.0$  (b)  $K_{SD}^* = 0.266$

The predictions from the proposed theoretical model are compared with a very limited experimental data (Reiss, 1967) reported in literature for ammonia absorption in water Figure (5.10). The base values reported by the authors were used for model predictions, which are reported in Table (5.3). It is interesting to note that the proposed model shows a close agreement with the experimental data.

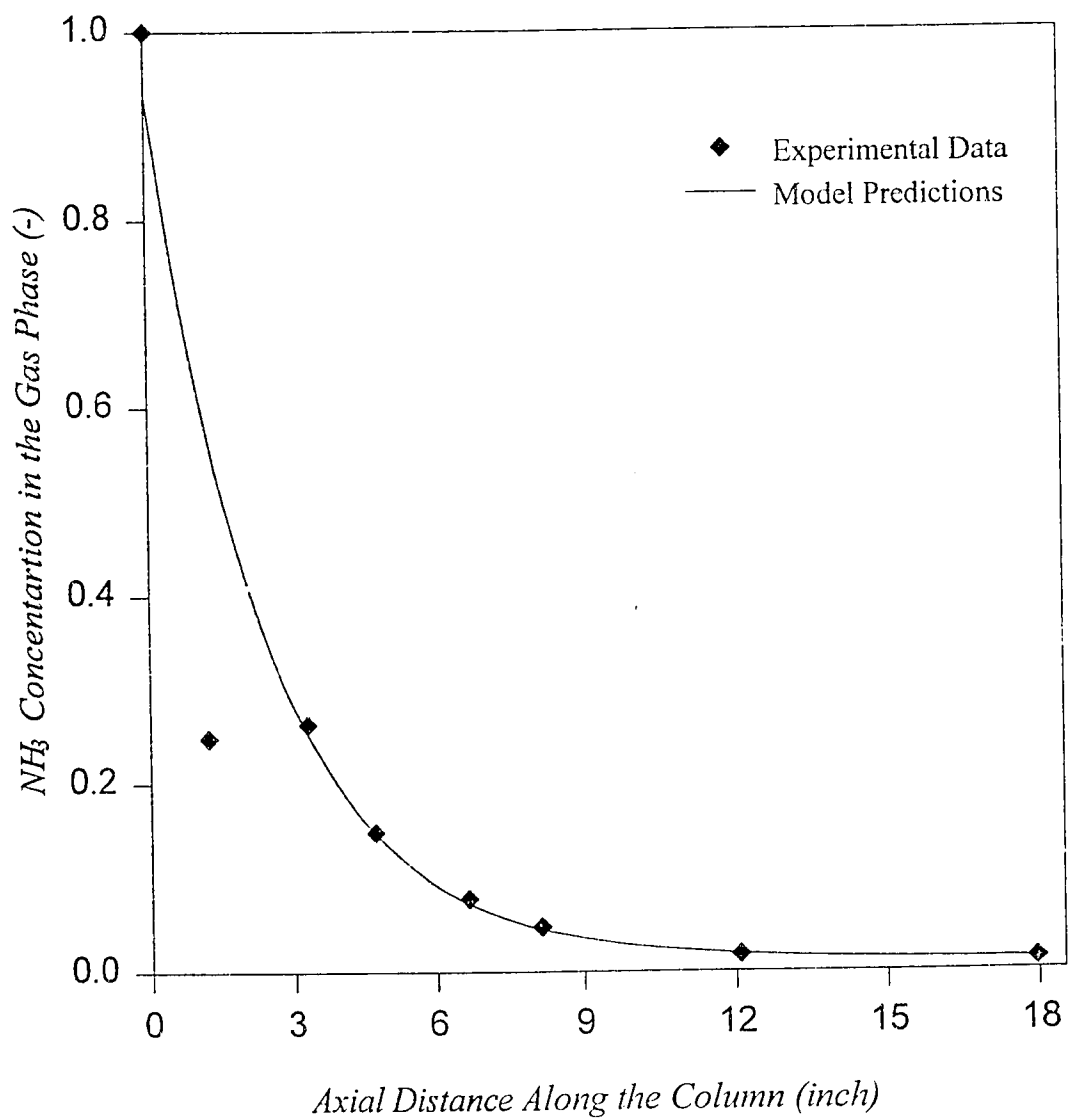


Figure (5.10) Comparison of experimental data with model predictions for absorption for  $\text{NH}_3$  in water (Data of Reiss, 1967).



**Table 5.3** Values of parameters for comparison of theoretical predictions with experimental data for absorption of ammonia in water.

Parameters	Value	Reference
$U_L$ , $\text{m s}^{-1}$	0.043	Reiss (1967)
$U_G$ , $\text{m s}^{-1}$	0.509	Reiss (1967)
$L_C$ , m	0.4572	Reiss (1967)
$d_p$ , m	0.0032	Reiss (1967)
$\varepsilon$	0.726	Reiss (1967)
$L_S$ , m	$10^{-4}$	Kan and Greenfield (1983)
$D_S$ , $\text{m}^2 \text{s}^{-1}$	$0.5 \times 10^{-10}$	Kan and Greenfield (1983)
$h_S$	0.035	Saez and Carbonell (1985)
$h_d$	0.3868	Ellman (1990)
$k_{LG} a_{iG}$ , $\text{sec}^{-1}$	0.0055	Reiss (1967)
$k_{SD}$ , $\text{m s}^{-1}$	$5.5 \times 10^{-8}$	Beg et al. (1995)
$\rho_L$ , $\text{kg m}^{-3}$	1000.0	Welty et al. (1976)
$\rho_G$ , $\text{kg m}^{-3}$	1.225	Welty et al. (1976)
$\mu_L$ , Pa sec	$7.44 \times 10^{-4}$	Welty et al. (1976)
$\mu_G$ , Pa sec	$1.8 \times 10^{-5}$	Welty et al. (1976)
$\sigma_L$ , $\text{N m}^{-1}$	$7.15 \times 10^{-2}$	Welty et al. (1976)

The calculated parameters used in the analysis,

${}^*Pe_L$	100
${}^*Pe_G$	100
$h_t$	0.4218
$h_g$	0.3042
$\phi$	0.917
$\psi$	0.721
$\xi$	11.837
$a_{SD}$ , $\text{m}^{-1}$	350
$\beta$	0.0242
$K_{SD}^*$	$2.025 \times 10^{-4}$
$St$	0.0585
$Bi$	0.11
$Re_L$	184.84
$Re_G$	110.85

\* Assuming plug flow behavior in both the gas and liquid phases.

# CHAPTER 6

## MODELING OF AIR STRIPPING IN COCURRENT PACKED COLUMNS

---

### 6.1 INTRODUCTION

Industrial waste waters from chemical and petrochemical industries often contain high concentrations of some highly toxic materials, and their indiscriminate disposal has become one of the most important environmental issues facing the world today. The United States Environmental Protection Agency (USEPA) has identified more than a hundred toxic organic priority pollutants (Pontius, 1992) which are not only found in industrial waste waters but they also contaminate the ground water aquifers. A high percentage of these pollutants are relatively volatile and their removal may be achieved through aeration. Where feasible, aeration is generally cost effective, particularly when compared with adsorptive processes such as treatment with granular activated carbon (Ball et al., 1984). The Environmental Protection Agency (EPA) has identified air stripping as the least cost, best available technology for the removal of such volatile organic compounds (VOCs) from water. Some of the VOCs commonly found in polluted waters include benzene, toluene, xylene, naphthalene, trihalomethanes and a wide

range of chlorinated hydrocarbons. Contamination occurs from various sources such as gasoline leaks, solvent spills, and process spills and discharges. These VOCs present in polluted waters are generally found to be in trace quantities, and long term exposure to even such low levels of contamination can pose potential health risks, like, carcinogenicity, chronic toxicity, etc. For this reason, Maximum Contamination Levels (MCLs) for some of these have also been established by USEPA (Pontius, 1992).

Different aeration processes employed for the removal of VOCs include diffused aeration, surface aeration, spray aeration, and packed tower aeration. Though comparison studies regarding various alternatives for air stripping treatment processes carried out by Kavanaugh and Trussell (1981) showed that the selection of the equipment depends on the desired removal level and the value of the Henry's constant, packed tower aeration is considered by many researchers (Ball et al., 1984; Umphres et al., 1983; Okoniewski, 1992) to be the most cost effective alternative to meet USEPA regulations. Most of the air stripping studies available in the literature are for a counter-current packed tower, where polluted water is introduced from the top and the air flows counter-currently from the bottom. The main disadvantage of such an operation being that, the column is designed for a very narrow range of air/water flow rates and the gas throughput is limited due to flooding. This phenomenon can be quite crucial for those VOCs,

which are less volatile such as bromoform, dibromochloromethane, etc. Such a limitation is usually overcome by operating the column in a cocurrent manner where both the gas and the liquid flow cocurrently either from top to bottom or vice versa. This mode of operation is quite attractive for the scenario where the concentration of the transferring component in the liquid is low and excess of air is used for stripping so as to shift the equilibrium. Hence, cocurrent packed columns operating at high gas to liquid flow rates present an attractive alternative for air stripping of trace quantities in water.

Although, a large body of published research work exists for the design and operation of air stripping in counter-current packed columns, comparatively very few references exist which deal with air stripping by cocurrent contacting. Most of the existing research work in this regard is experimental and deals exclusively with the desorption of oxygen from water into air in a cocurrent downflow packed column. Mellvold (1965) studied desorption of oxygen in a 2-inch bed packed with 1/4 inch ceramic Raschig rings and 4-6 mm glass beads. The experimental mass transfer coefficients were correlated empirically as a function of gas and liquid flow rates. Reiss (1967) presented a very comprehensive study for the same system employing different column configurations. Correlation for mass transfer coefficients presented were developed in terms of liquid phase energy dissipation. Sato et al. (1972) also presented empirical correlations for gas liquid mass transfer.

for desorption of oxygen from water into a nitrogen gas stream. Another experimental work is presented by Gianetto et al. (1972) who studied desorption of oxygen dissolved in 2N NaOH solution. However studies dealing with a theoretical analysis of air stripping in cocurrent packed columns are scarce. This could be explained by the extremely complex nature of the hydrodynamics conditions prevailing inside such columns.

## 6.2 RESULTS AND DISCUSSION

The performance of downflow cocurrent packed columns for stripping of various organic pollutants from water has been analyzed. The numerical solution of the model equations has been obtained for a wide range of operating parameters. The studies were carried out for air stripping of different VOCs from water i.e. chloroform, dibromochloromethane and bromoform. The choice of VOCs were made on the basis of their Henry's constant as listed in Table (6.1). Chloroform being the most volatile of the three components, has the lowest Henry's constant implying that the stripping process is controlled by the liquid film resistance, while bromoform with highest Henry's constant indicates the control of gas film resistance. Dibromochloromethane having the intermediate value of Henry's constant presents the scenario where both gas and liquid films control the stripping operation.

**Table 6.1** Diffusion coefficients and Henry's Law constants\* for the air stripping systems.

Component	Henry's Constant, $H$ , $\frac{\text{kmol m}^{-3} \text{ of solution}}{\text{kmol m}^{-3} \text{ of gas}}$	Diffusivity in water, $D_c$ , $10^{10} \text{ m}^2 \text{ s}^{-1}$
Chloroform	8.0247	9.86
Dibromochloromethane	30.82	10.0
Bromoform	415.57	9.8

\*Values reported by Velazques and Estevez (1992)

Parametric studies were carried out to evaluate the individual effects of parameters of practical significance. Table (6.2) lists the base values of parameters used for the numerical simulation of air-stripping phenomenon for all the three systems of interest. The functional relationships of model parameters are listed in Section (5.2.1) and (4.2.1) which can be used for model predictions.

The effect of important dimensionless parameters, such as, gas Peclet number,  $Pe_G$ , liquid Peclet number,  $Pe_L$ , liquid Reynolds number,  $Re_L$ , gas phase Reynolds number,  $Re_G$ , and Stanton number,  $St$ , on column dynamics was analyzed. Initially (at  $\theta = 0$ ) the column was considered to be free of any pollutant, i.e.,  $C_g = C_d = C_s = 0$ . Then the pollutant was introduced only in the liquid phase, which implies that the inlet condition for this phase becomes,

$$C_d|_{x=0} = 1.$$

Figures (6.1a), (6.1b) and (6.1c) show the dynamics of approach to steady state conditions for chloroform, dibromochloromethane and bromoform systems respectively. It is evident from these figures that both liquid and gas phases approach the steady state conditions approximately the same time limits, indicating influential control of the liquid hydrodynamics on the stripping operation. These

**Table 6.2** Base values of parameters used for the parametric study of the model for air stripping.

Parameters	Value	Reference
$U_L$ , $\text{m s}^{-1}$	$4.542 \times 10^{-3}$	-*
$U_G$ , $\text{m s}^{-1}$	0.16	-*
$L_C$ , m	1.0	-*
$d_p$ , m	$10^{-3}$	Kan and Greenfield (1983)
$\varepsilon$	0.4	Kan and Greenfield (1978)
$L_S$ , m	$10^{-4}$	Kan and Greenfield (1983)
$D_S$ , $\text{m}^2 \text{s}^{-1}$	$0.5 \times 10^{-10}$	Kan and Greenfield (1983)
$h_S$	0.0499	Sacz and Carbonell (1985)
$h_d$	0.1286	Ellmann et al. (1990)
$k_{LG} a_{LG}$ , $\text{sec}^{-1}$	0.0038	Reiss (1967)
$k_{SD}$ , $\text{m s}^{-1}$	$5.5 \times 10^{-8}$	Beg et al. (1995)
$Pe_L$	15.425	Beg et al. (1995)
$Pe_G$	27.0	Hochmann and Elfron (1969)
$\rho_L$ , $\text{kg m}^{-3}$	1000.0	Welty et al. (1976)
$\rho_G$ , $\text{kg m}^{-3}$	1.225	Welty et al. (1976)
$\mu_L$ , Pa sec	$7.44 \times 10^{-4}$	Welty et al. (1976)
$\mu_G$ , Pa sec	$1.8 \times 10^{-5}$	Welty et al. (1976)
$\sigma_L$ , $\text{N m}^{-1}$	$7.15 \times 10^{-2}$	Welty et al. (1976)

\* Chosen arbitrarily.

The calculated parameters used in the analysis.

$h_t$	0.1785
$h_g$	0.2215
$\phi$	0.72
$\psi$	1.241
$\xi$	35.22
$a_{SD}$ , $\text{m}^{-1}$	499.0
$\beta$	0.1964
$K_{SD}^*$	$6.04 \times 10^{-3}$
$St$	0.832
$Bi$	0.11
$Re_L$	6.1
$Re_G$	10.89



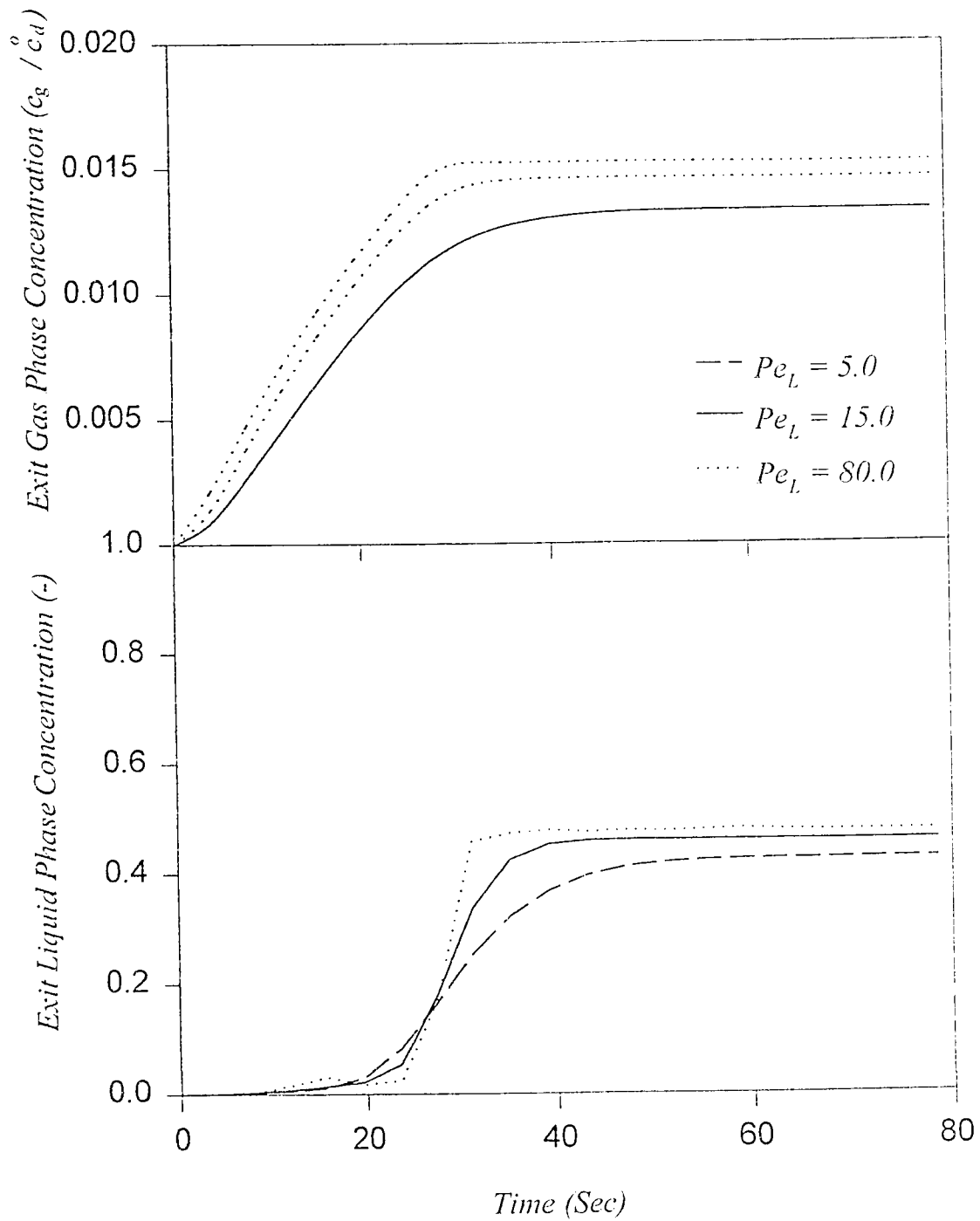


Figure (6.1a) The effect of  $Pe_L$  on the dynamics of gas and liquid phase exit concentrations for stripping of Chloroform .

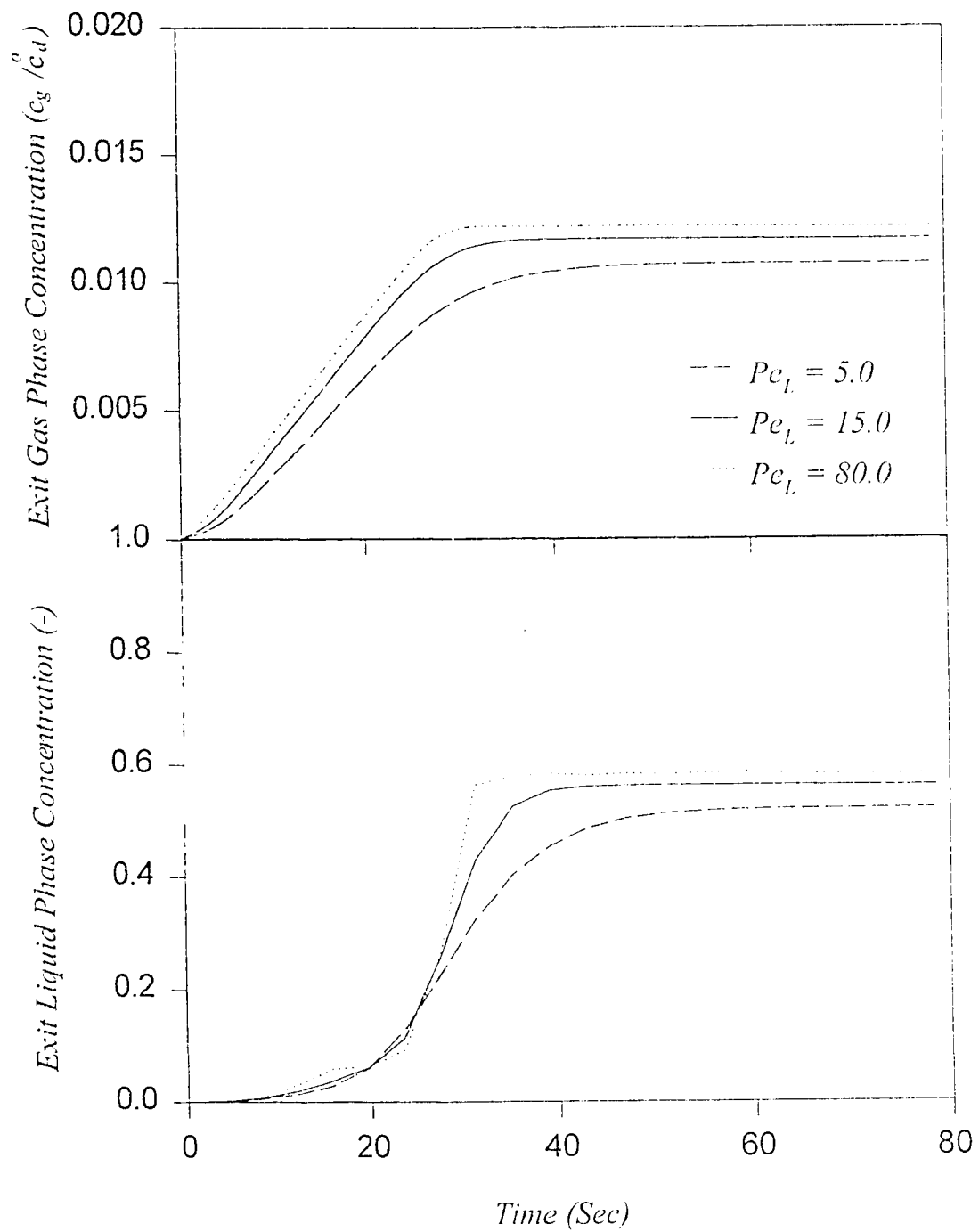


Figure (6.1b) The effect of  $Pe_l$  on the dynamics of gas and liquid phase exit concentrations for stripping of Dibromochloromethane.

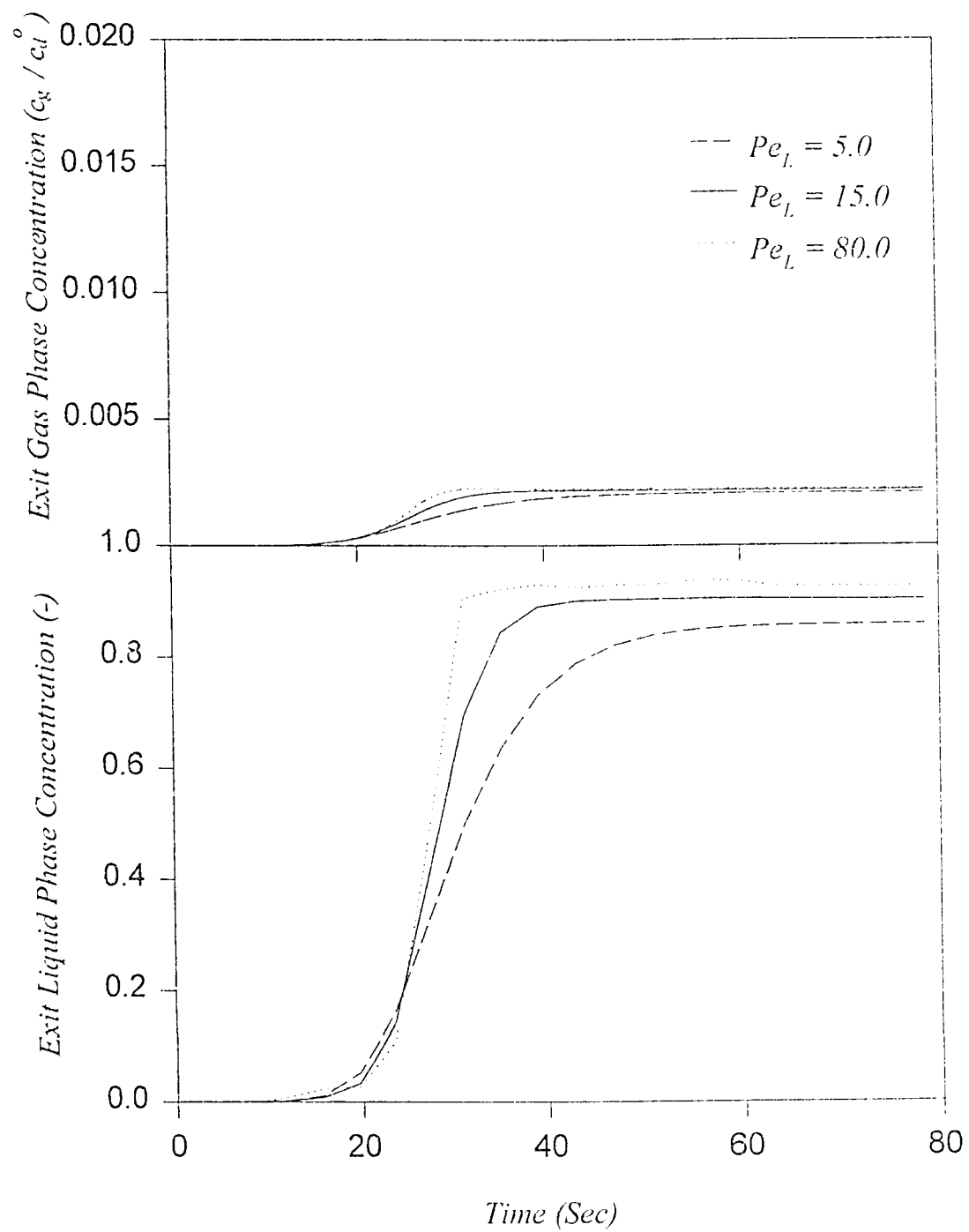


Figure (6.1c) The effect of  $Pe_L$  on the dynamics of gas and liquid phase exit concentrations for stripping of Bromoform.

figures also show the effect of liquid phase Peclet number,  $Pe_L$  on the dynamics of gas and liquid phase exit concentrations. It is evident from these figures that the effect of  $Pe_L$  is insignificant on the dynamics of gas phase concentration, however, for the liquid phase, the concentrations are affected to some extent for the three systems considered. Low values of  $Pe_L$  imply completely mixed flow behavior for which the performance of stripping process is enhanced. The corresponding steady state concentration profiles for these systems are shown in Figures (6.2a), (6.2b) and (6.2c). These figures indicate that equilibrium conditions between gas and liquid phases are not attained for chloroform (Figure 6.2a) and d bromochloromethane (Figure 6.2b) while the equilibrium is established for bromoform almost along the middle of the column under identical operating conditions. This is expected in view of the high value of Henry's constant for this system.

Figures (6.3a), (6.3b) and (6.3c) show the effect of gas phase Peclet number,  $Pe_G$  on the steady state gas and liquid phase concentration profiles. Higher value of  $Pe_G$  improves the stripping performance of the system as reflected by the lower value of liquid phase exit concentrations. Further, equilibrium between the two phases is only attained for the bromoform system as was observed in Figure (6.3c).

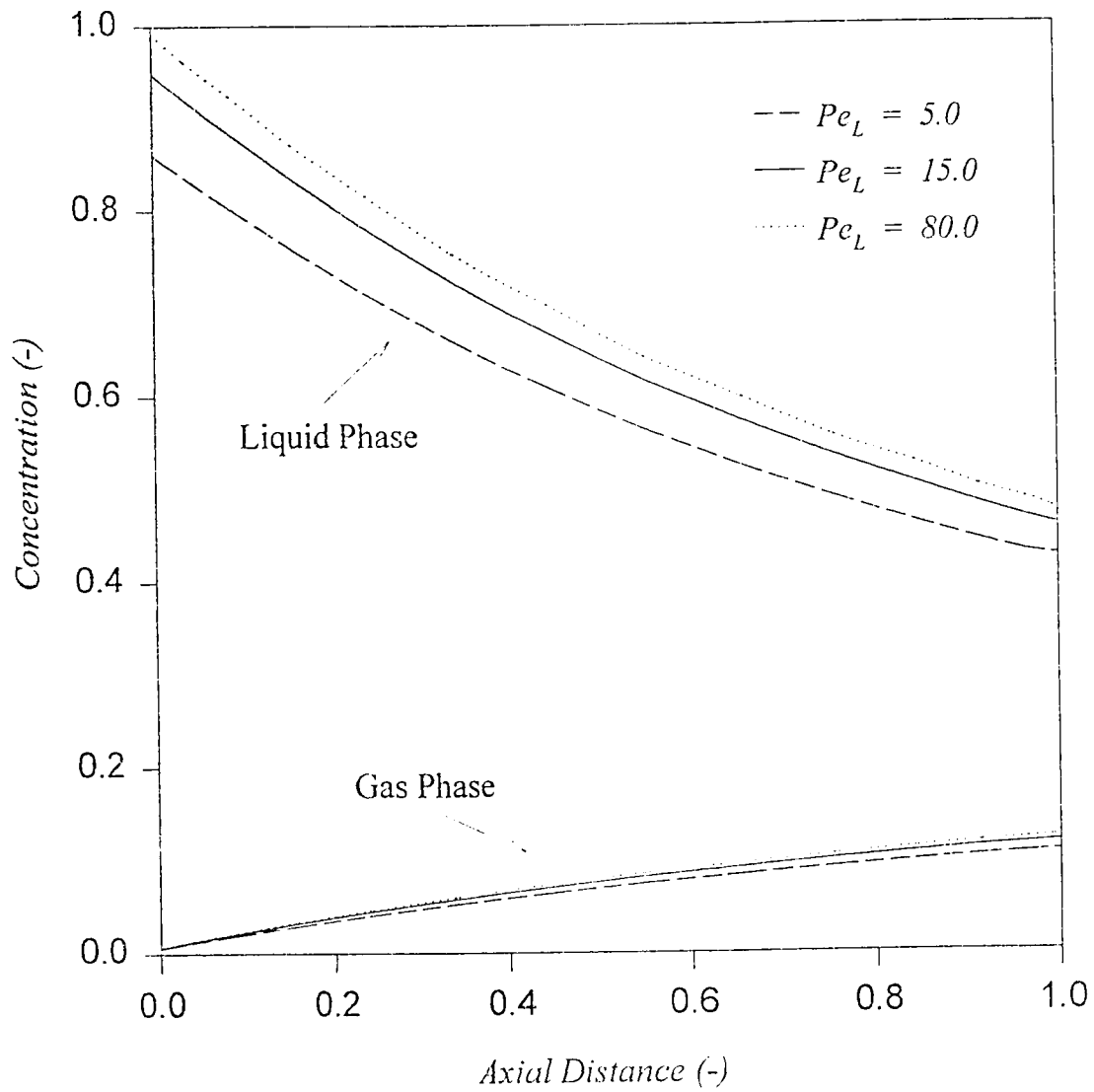


Figure (6.2a) The effect of  $Pe_L$  on steady state gas and liquid phase concentration profiles for stripping of Chloroform .

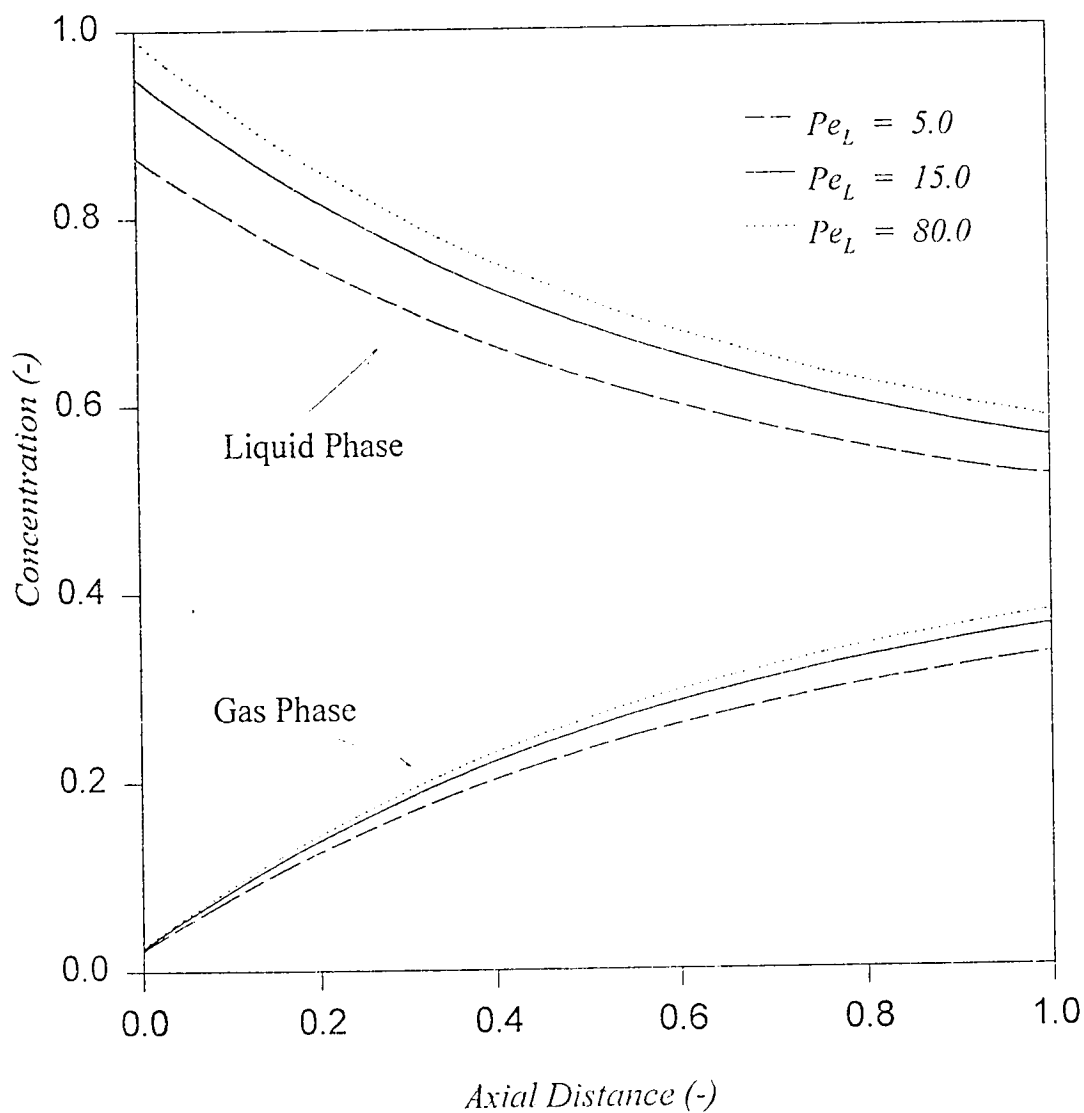


Figure (6.2b) The effect of  $Pe_L$  on steady state gas and liquid phase concentration profiles for stripping of Dibromochloromethane.

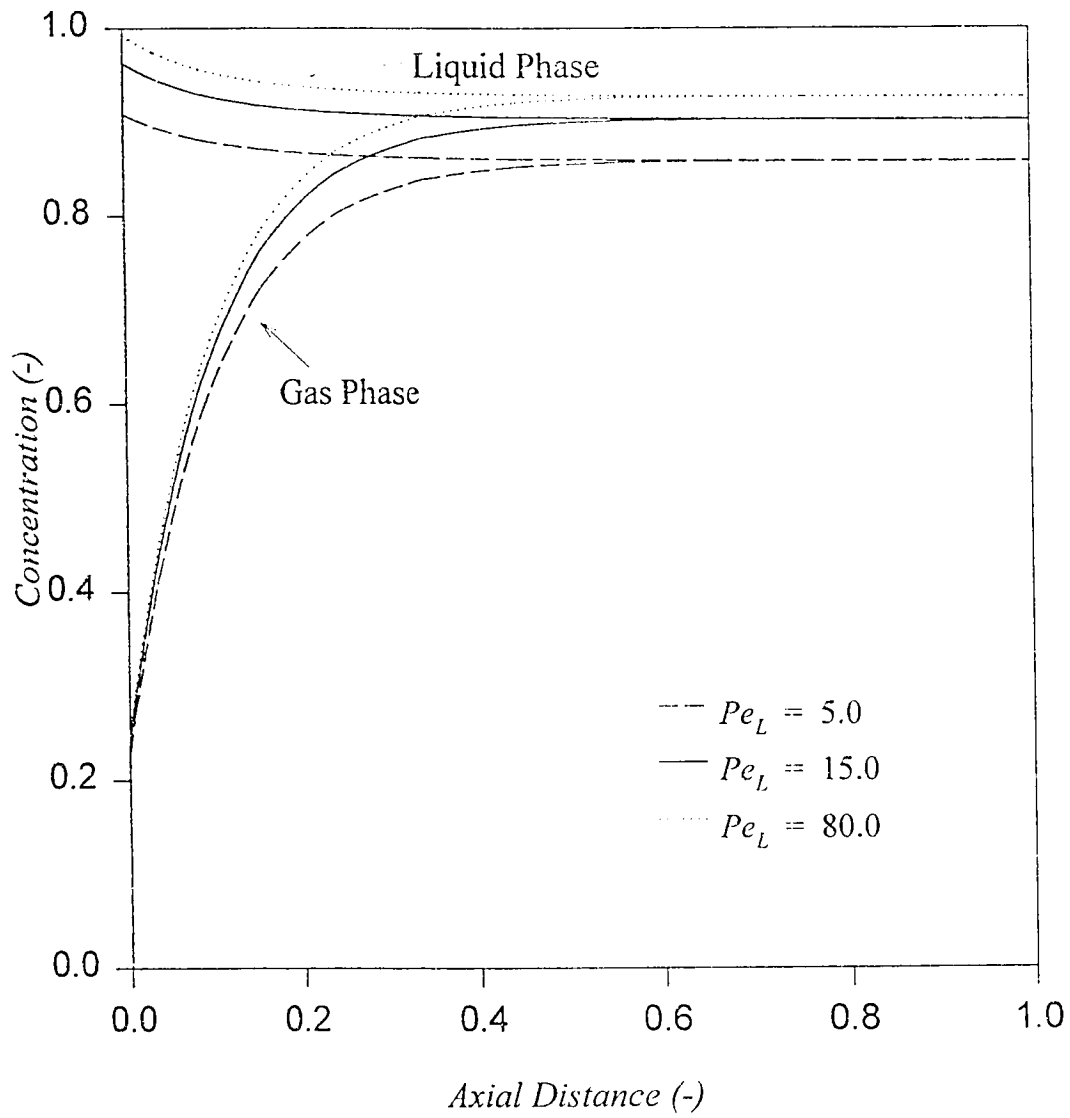


Figure (6.2c) The effect of  $Pe_L$  on steady state gas and liquid phase concentration profiles for stripping of Bromoform.

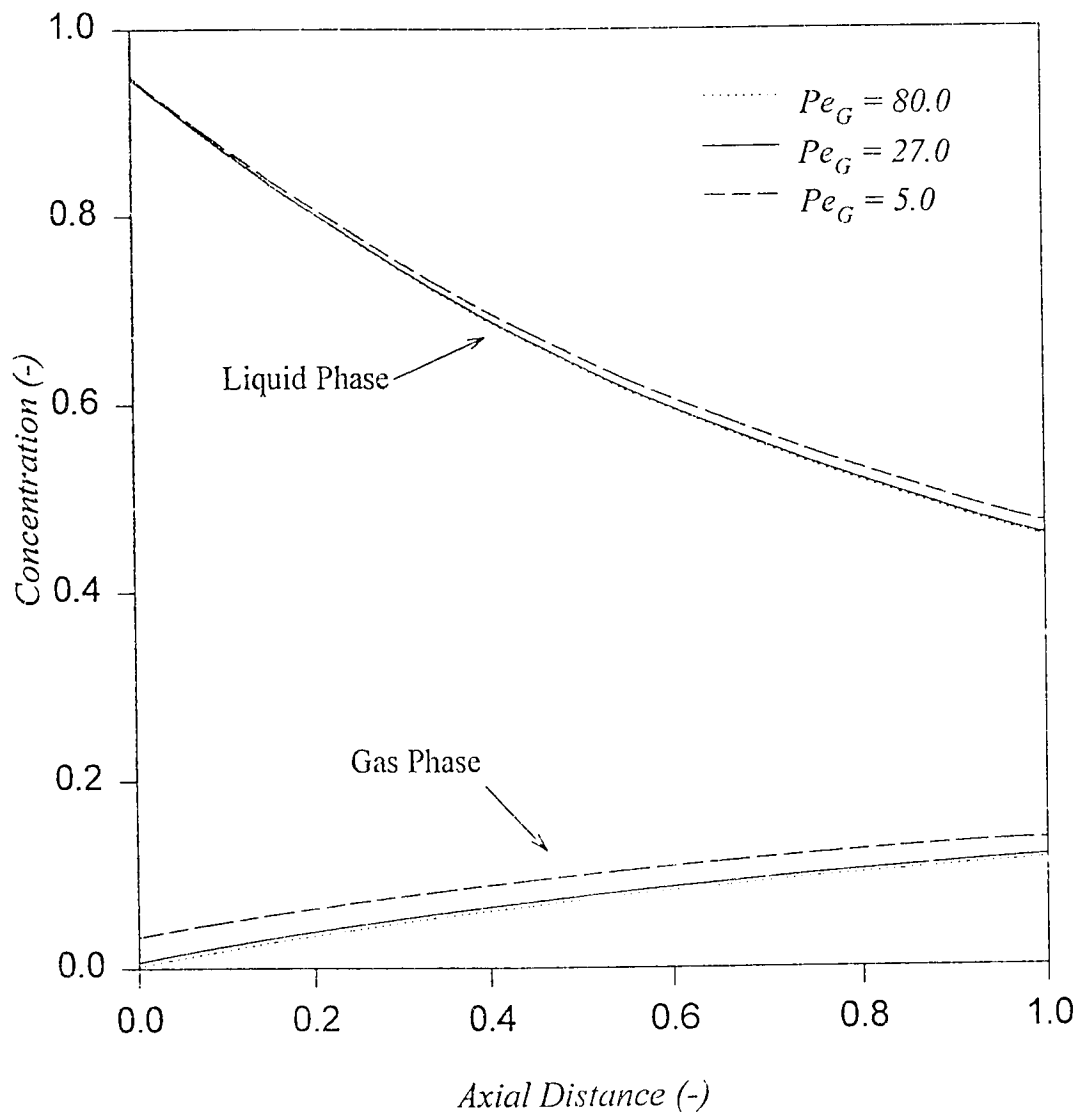


Figure (6.3a) The effect of  $Pe_G$  on steady state gas and liquid phase concentration profiles for stripping of Chloroform .



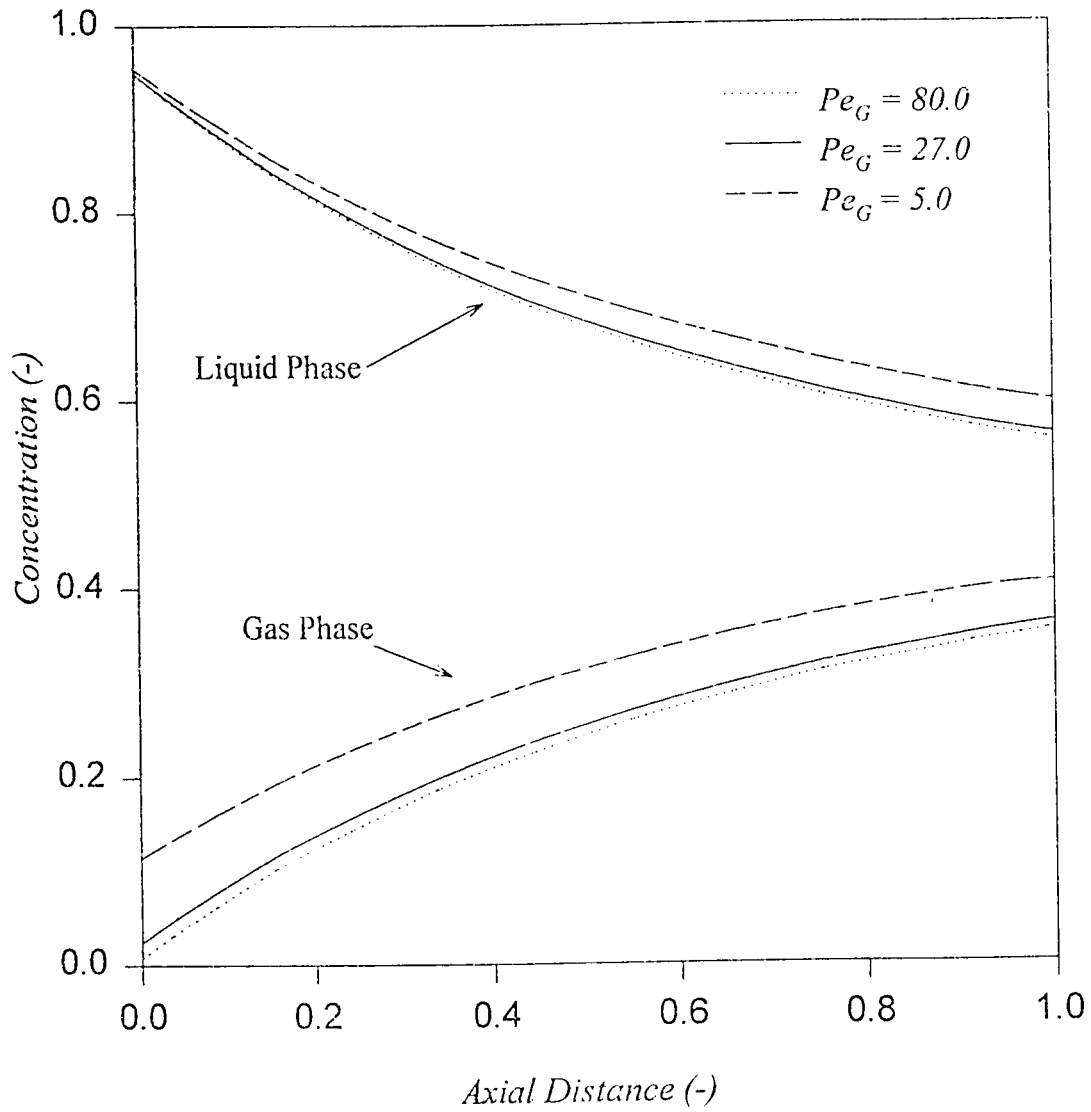


Figure (6.3b) The effect of  $Pe_G$  on steady state gas and liquid phase concentration profiles for stripping of dibromochloromethane.

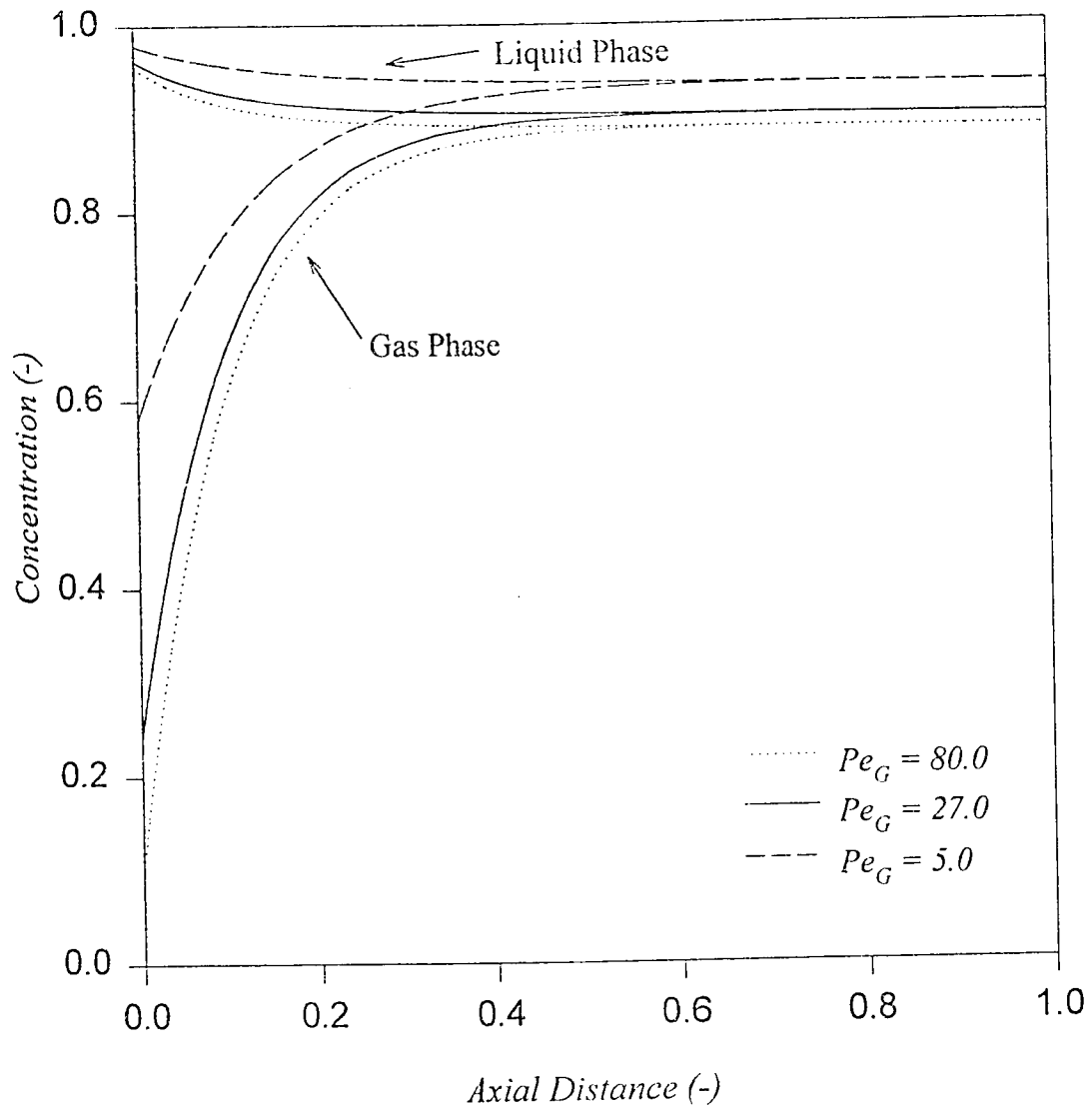


Figure (6.3c) The effect of  $Pe_G$  on steady state gas and liquid phase concentration profiles for stripping of bromoform .

The effect of dimensionless mass transfer coefficient  $St$  on the stripping operation is shown in Figures (6.4a), (6.4b) and (6.4c) for chloroform, dibromochloromethane and bromoform respectively. High values of  $St$  implies low mass transfer resistance so that gas and liquid concentration profiles would approach closer to equilibrium values. On the other hand, for low values of  $St \cong 0.1$ , the gas and liquid phase concentration profiles do not come to equilibrium concentrations even for the highly volatile bromoform. Also, the performance of stripping is better with high value of  $St$  i.e. lower mass transfer resistance. The performance is further illustrated in Figure (6.5a) and (6.5b) which show the dimensionless plot of the dynamic liquid phase concentration profiles of chloroform system at  $St \cong 0.1$  and  $St \cong 2.0$  respectively. For  $St \cong 0.1$ , the concentration fronts are much steeper compared to that for the case of  $St \cong 2.0$  which show a gradual approach to steady state values.

Figures (6.6a), (6.6b) and (6.6c) show the steady state concentration profiles along the length of the column for various values of  $Re_L$  for the three systems considered respectively. The stripping performance of the column increases with the increase in  $Re_L$ . Further, for high values of  $Re_L$  which correspond to low mass transfer resistance, the gas and liquid concentration profiles approach the

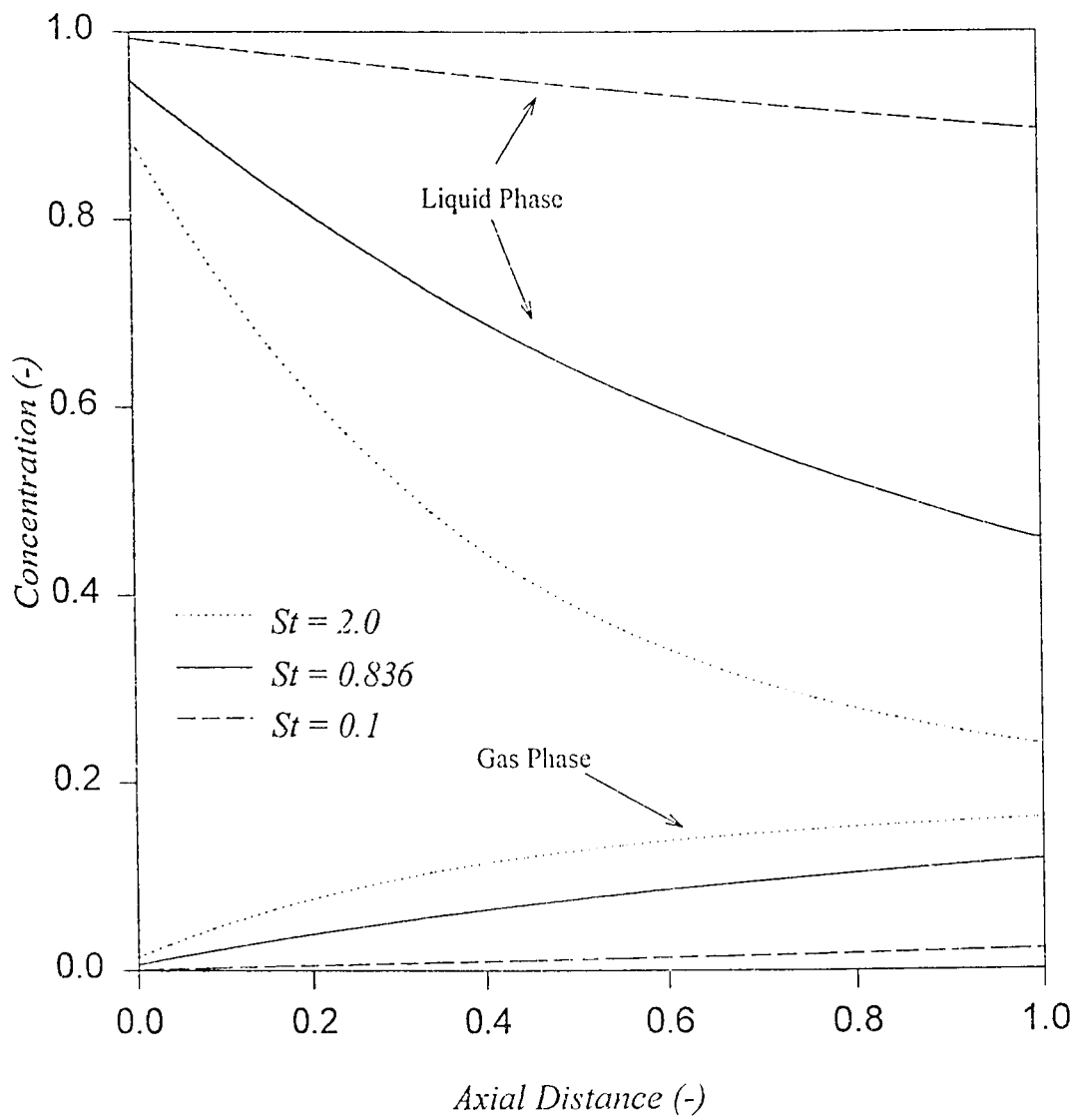


Figure (6.4a) The effect of  $St$  on steady state gas and liquid phase concentration profiles for stripping of Chloroform .

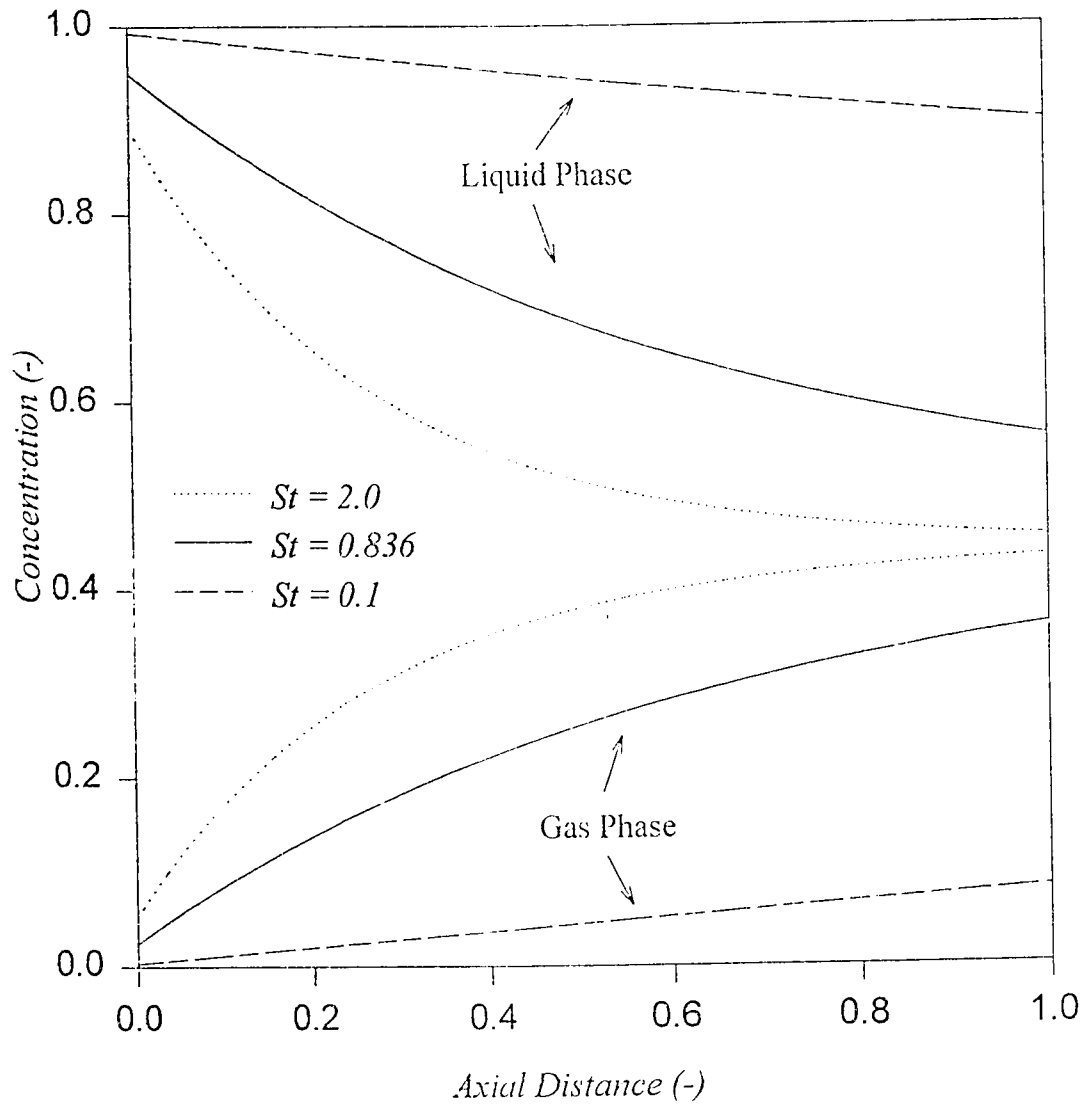


Figure (6.4b) The effect of  $St$  on steady state gas and liquid phase concentration profiles for stripping of Dibromochloromethane.

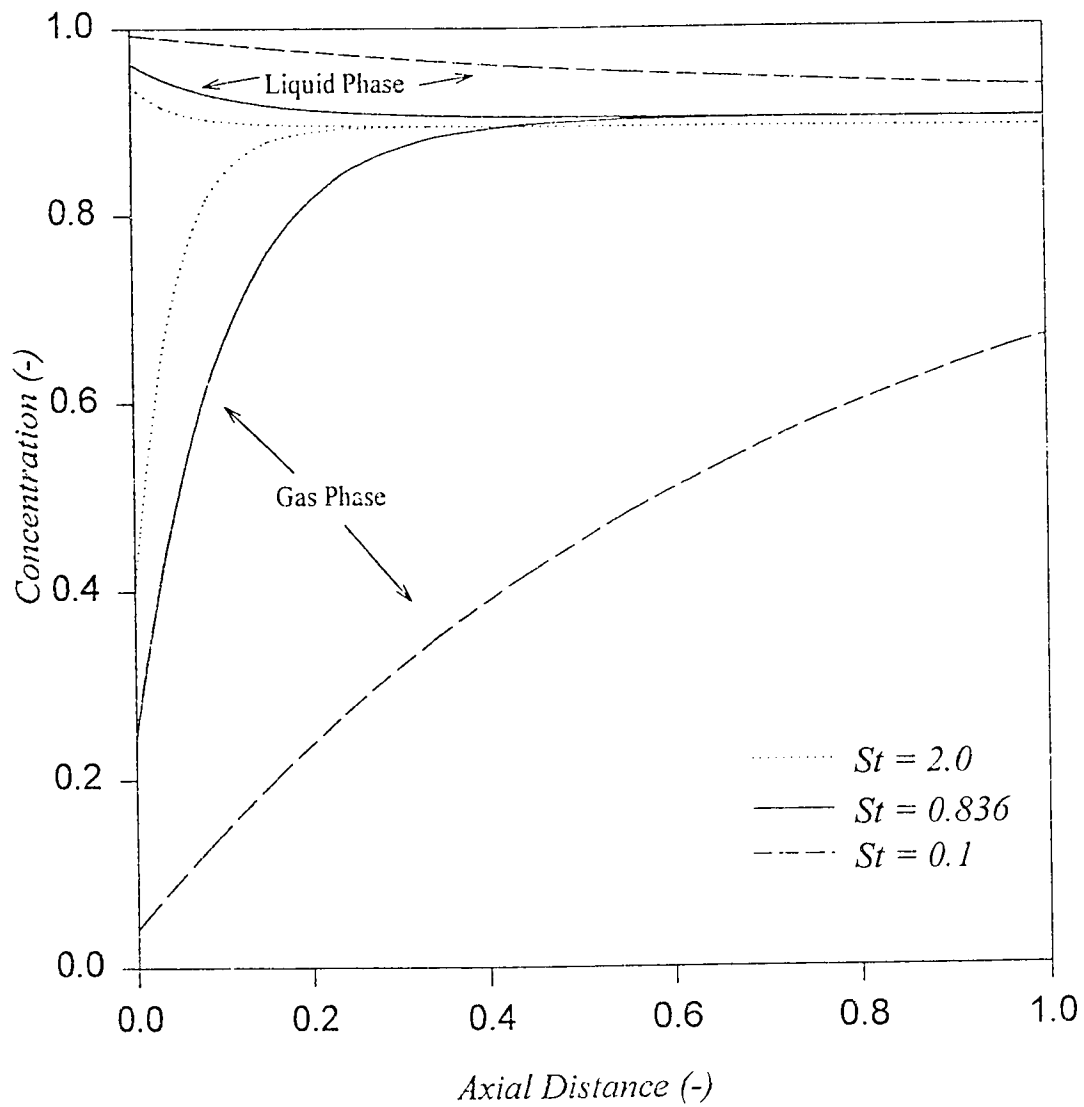


Figure (6.4c) The effect of  $St$  on steady state gas and liquid phase concentration profiles for stripping of Bromoform.

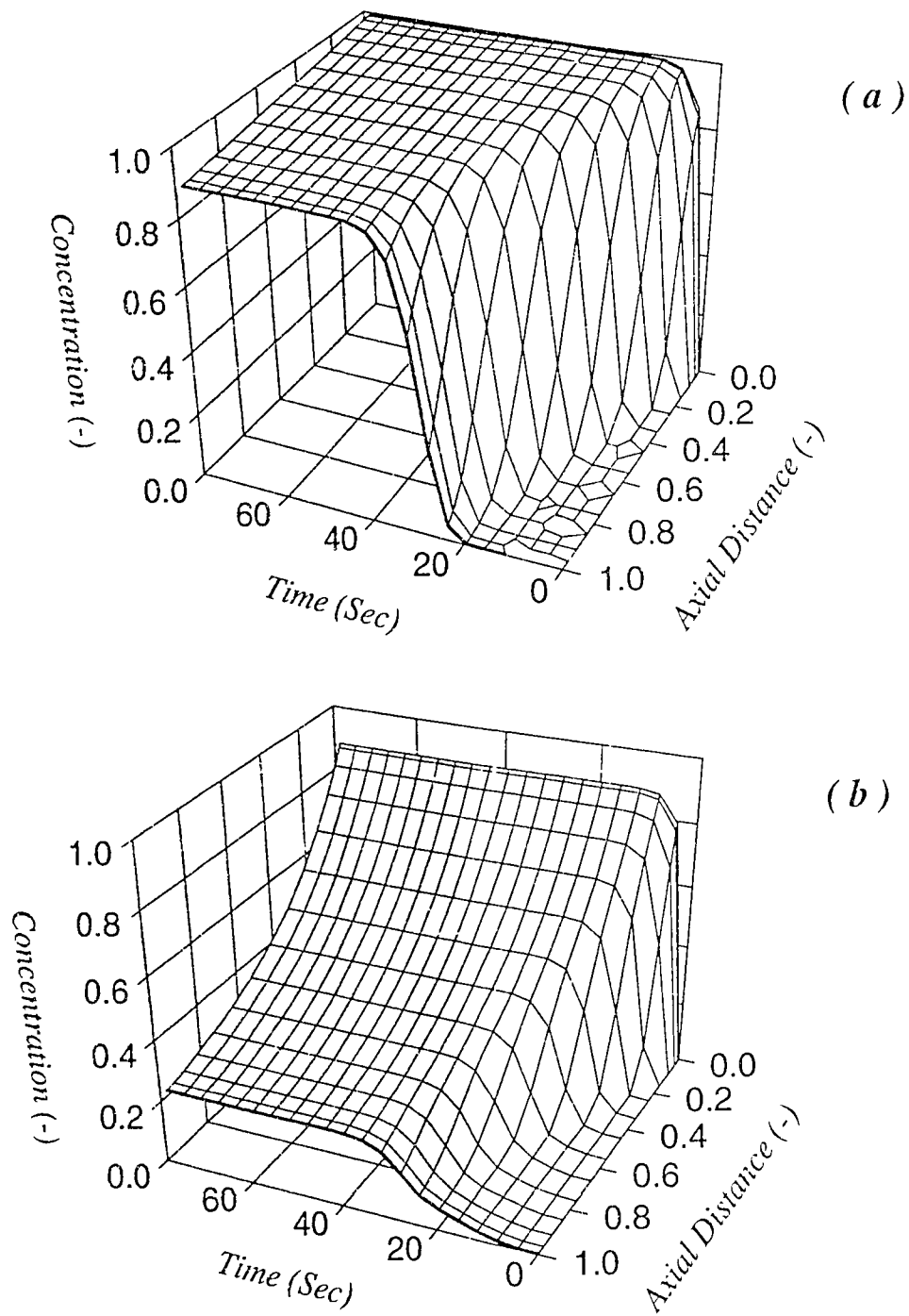


Figure (6.5) Dynamic liquid phase concentration profiles in 3-D for stripping of Chloroform illustrating the effect of  $St$ . (a)  $St = 0.1$  (b)  $St = 2.0$

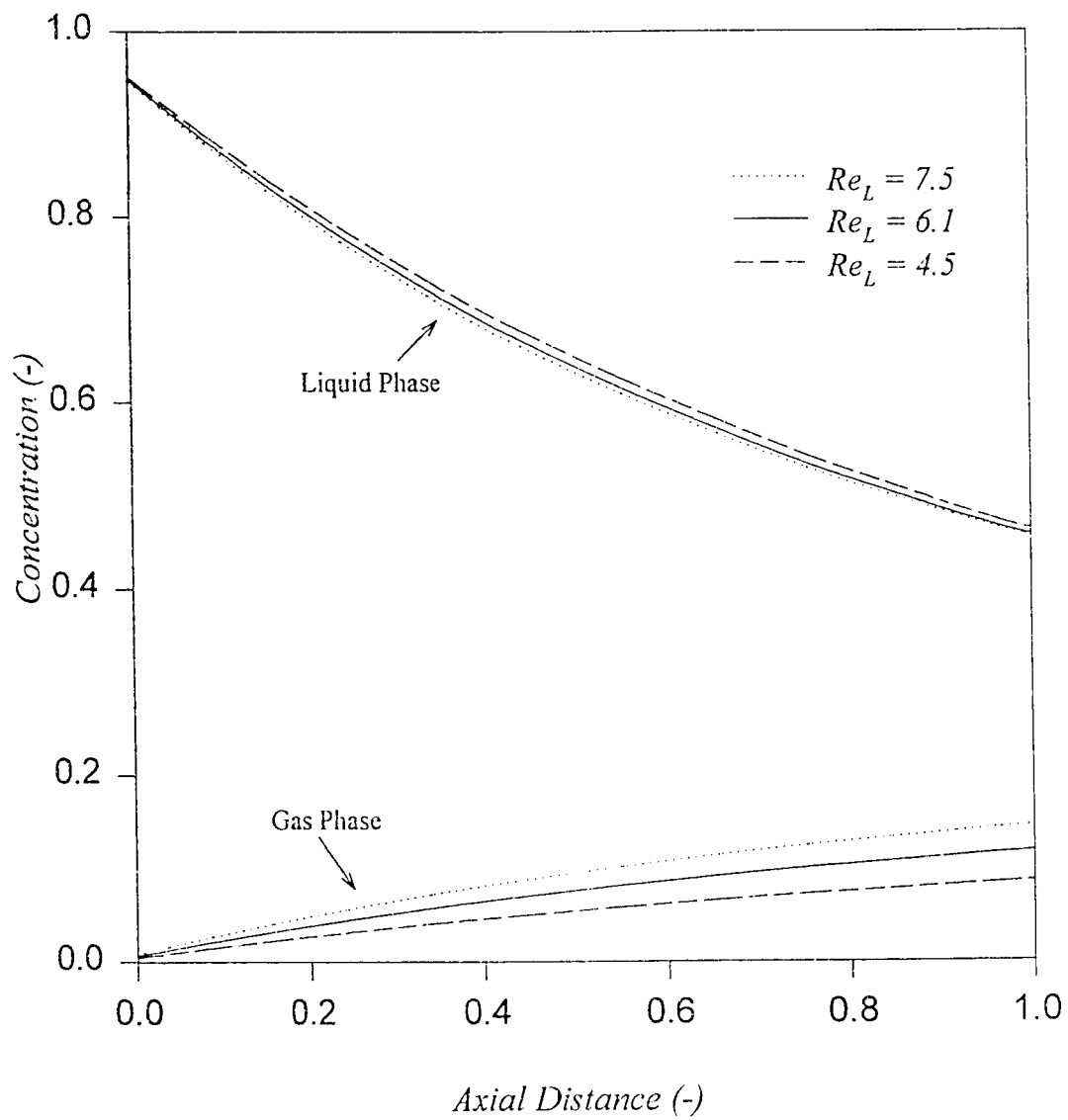


Figure (6.6a) The effect of  $Re_L$  on steady state gas and liquid phase concentration profiles for stripping of Chloroform.



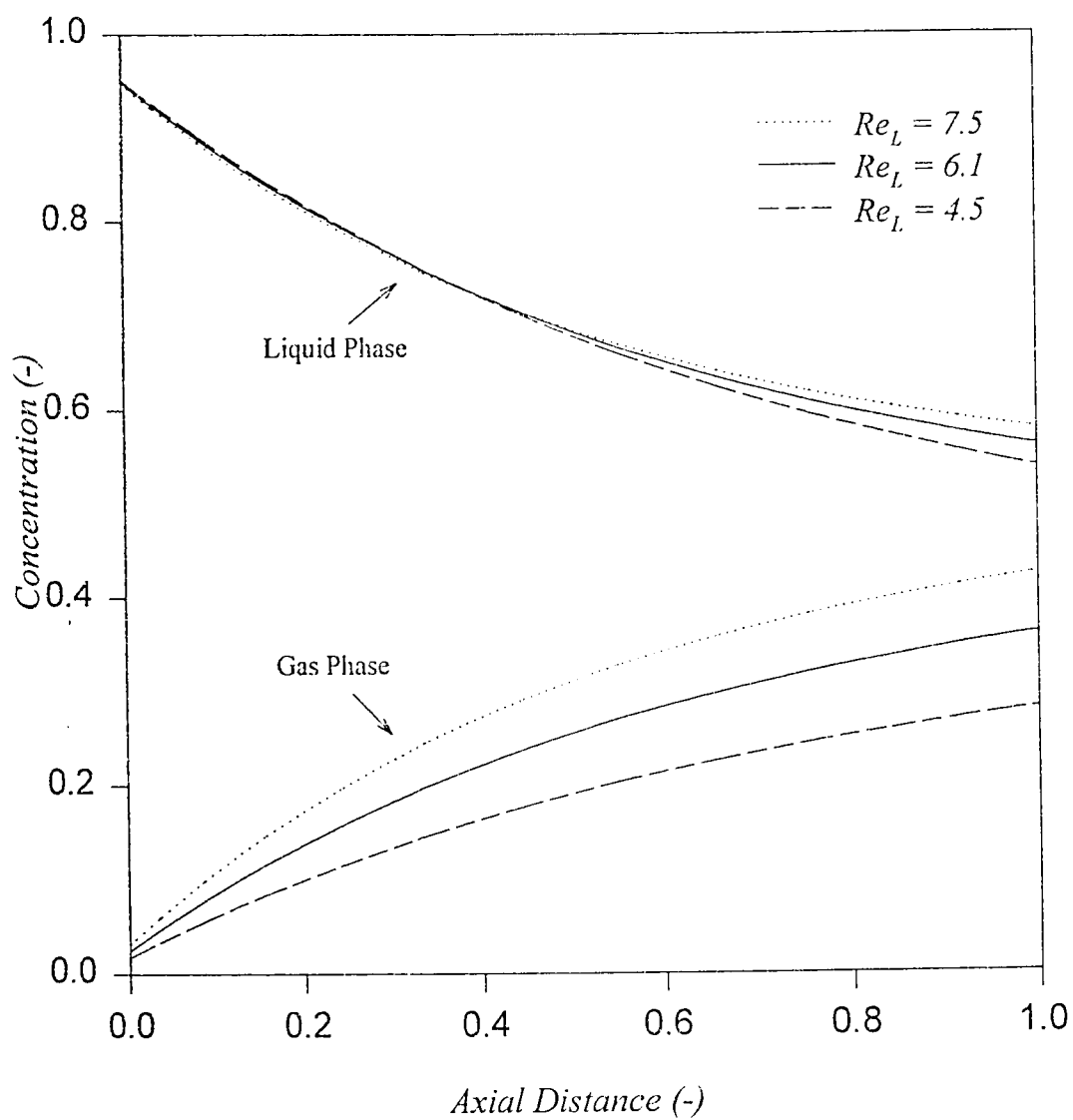


Figure (6.6b) The effect of  $Re_L$  on steady state gas and liquid phase concentration profiles for stripping of Dibromochloromethane.

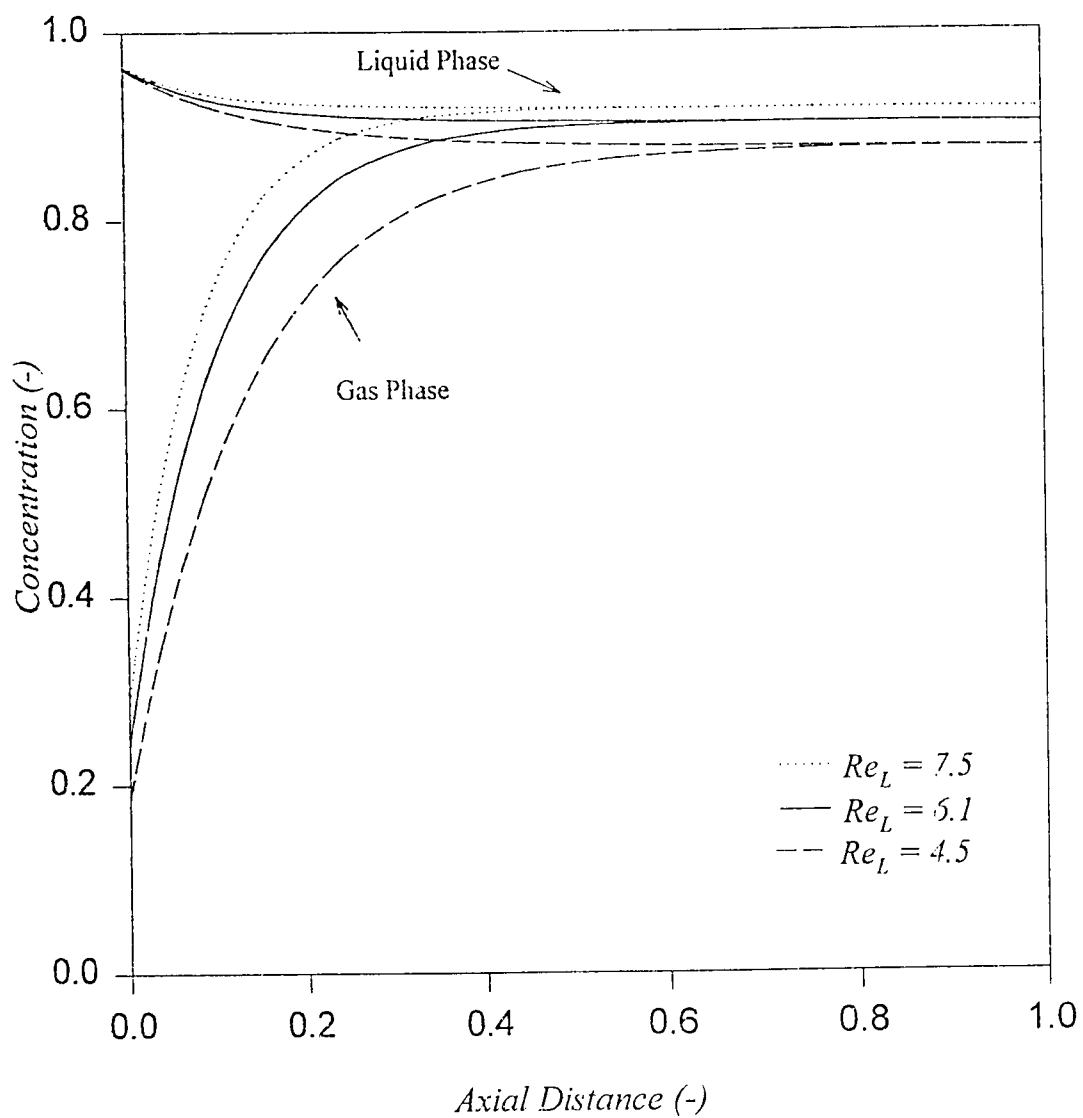


Figure (6.6c) The effect of  $Re_L$  on steady state gas and liquid phase concentration profiles for stripping of Bromoform.

equilibrium within the column. However, the effect of  $Re_L$  is insignificant for the bromoform system for which the equilibrium conditions are attained with the first half of the column. The phenomenon is further illustrated in the three dimensional plot for chloroform liquid phase concentration profiles at various time intervals for  $Re_L = 7.0$  and  $Re_L = 5.0$  as shown in Figures (6.7a) and (6.7b) respectively.

Figures (6.8a), (6.8b) and (6.8c) illustrate the effect of  $Re_G$  on the steady state concentration profiles for the systems considered. The stripping performance of all the systems improve with the increase in  $Re_G$ . This could be explained by the increase in concentration driving force between gas and liquid which results due to faster rate of elution by swiftly flowing gas phase, as evident from the figure.

The predictions from the proposed model are also compared with a very limited experimental data ( Reiss, 1967) reported in literature for oxygen desorption from water, Figure (6.9). The base values reported by the authors were used for model predictions, which are reported in Table (6.3). It can be observed that the steady state concentration profile proposed by the theoretical model is in close agreement with the experimental one.

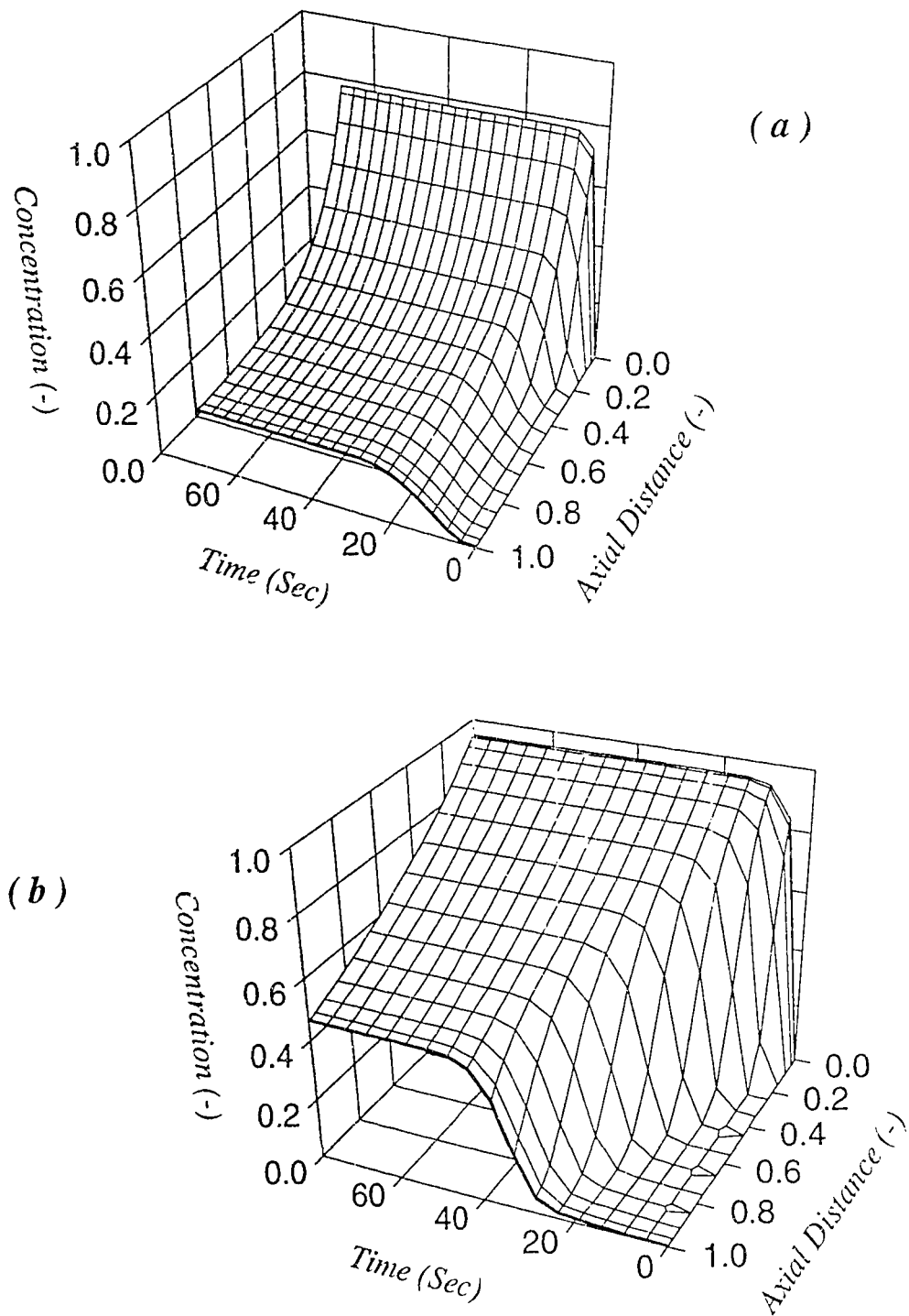


Figure (6.7) Dynamic liquid phase concentration profiles in 3-D for stripping of Chloroform illustrating the effect of  $Re_L$ . (a)  $Re_L = 7.0$  (b)  $Re_L = 5.0$ .

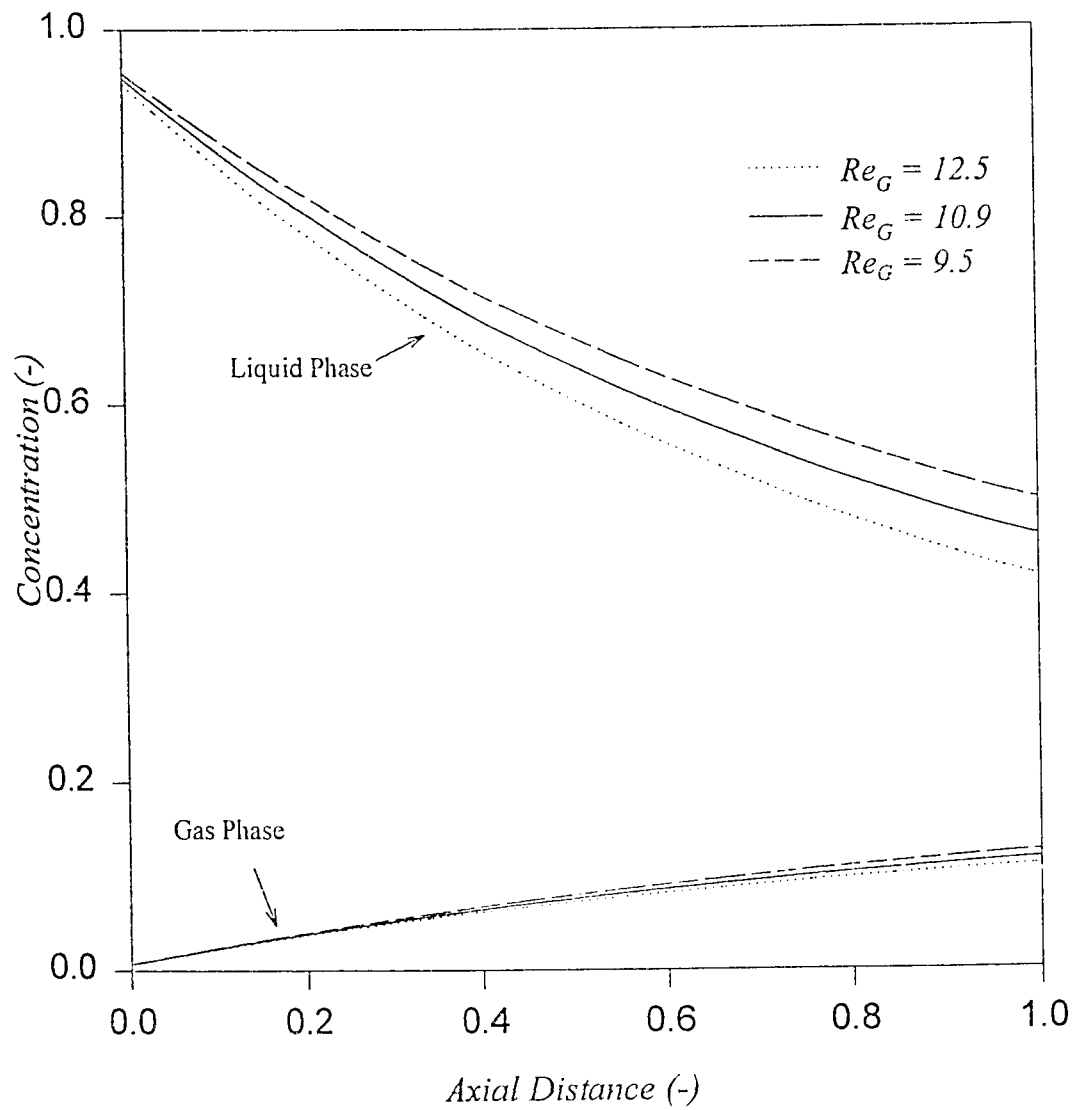


Figure (6.8a) The effect of  $Re_G$  on steady state gas and liquid phase concentration profiles for stripping of Chloroform.

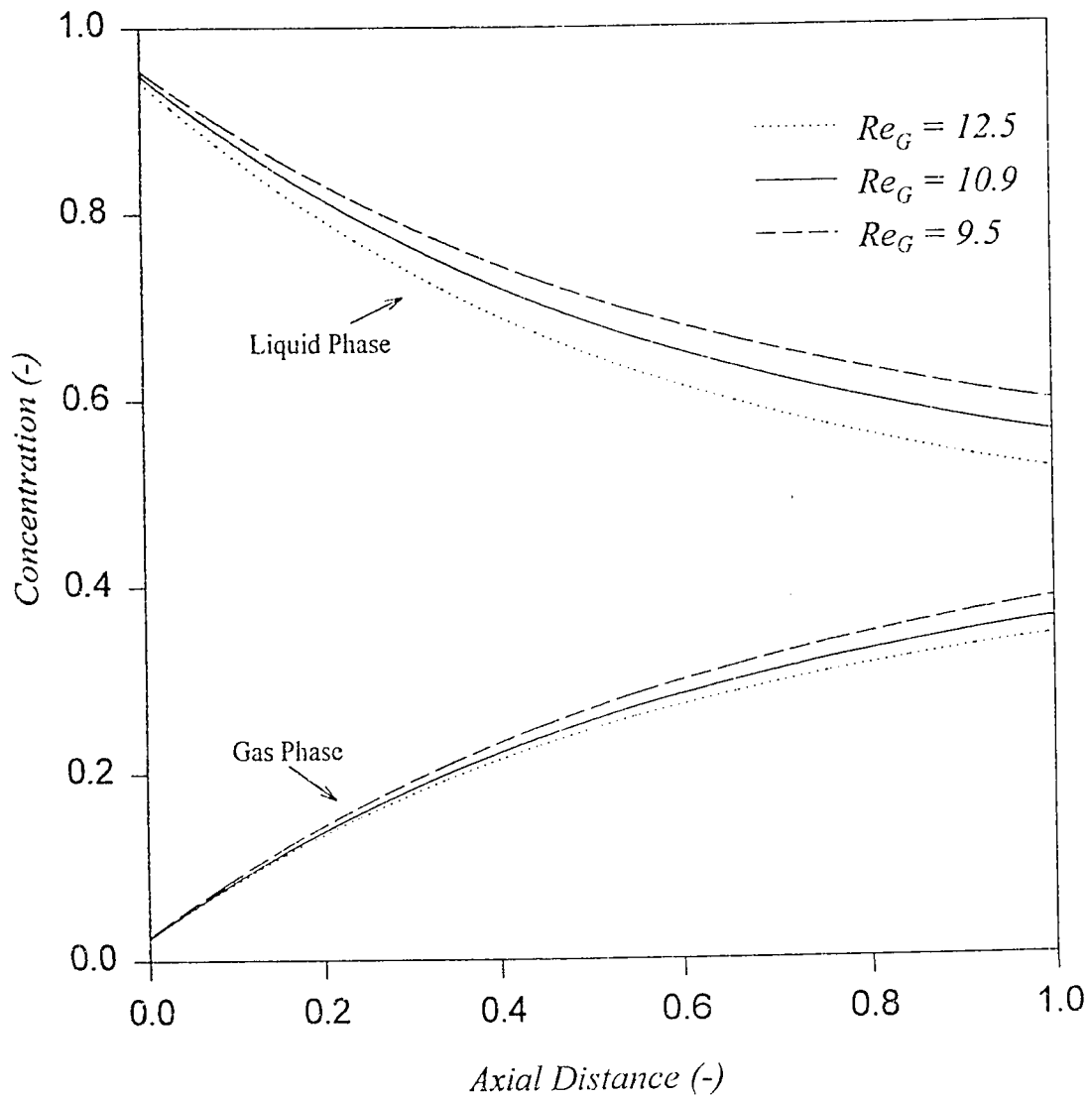


Figure (6.8b) The effect of  $Re_G$  on steady state gas and liquid phase concentration profiles for stripping of dibromochloromethane

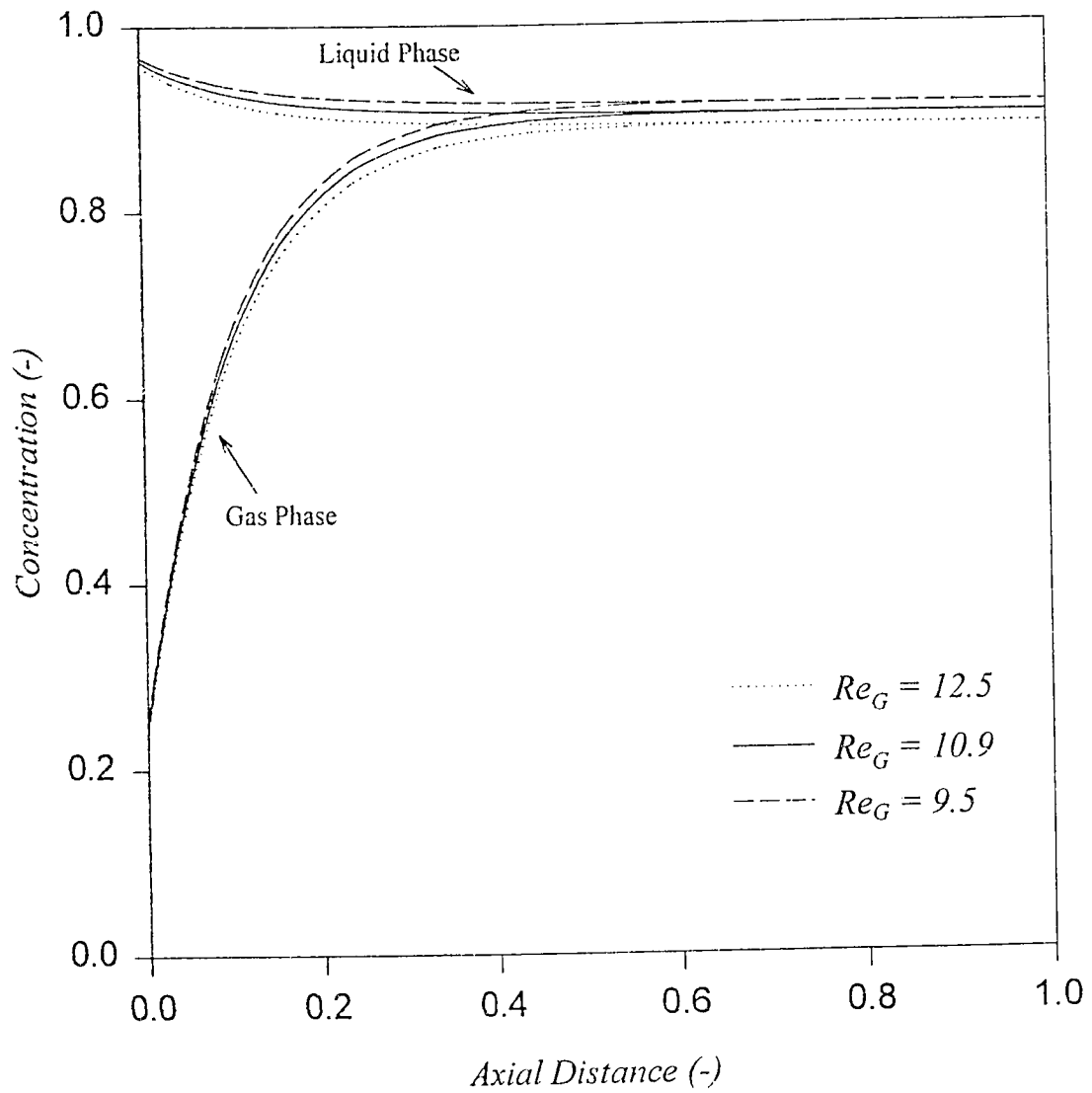


Figure (6.8c) The effect of  $Re_G$  on steady state gas and liquid phase concentration profiles for stripping of Bromoform

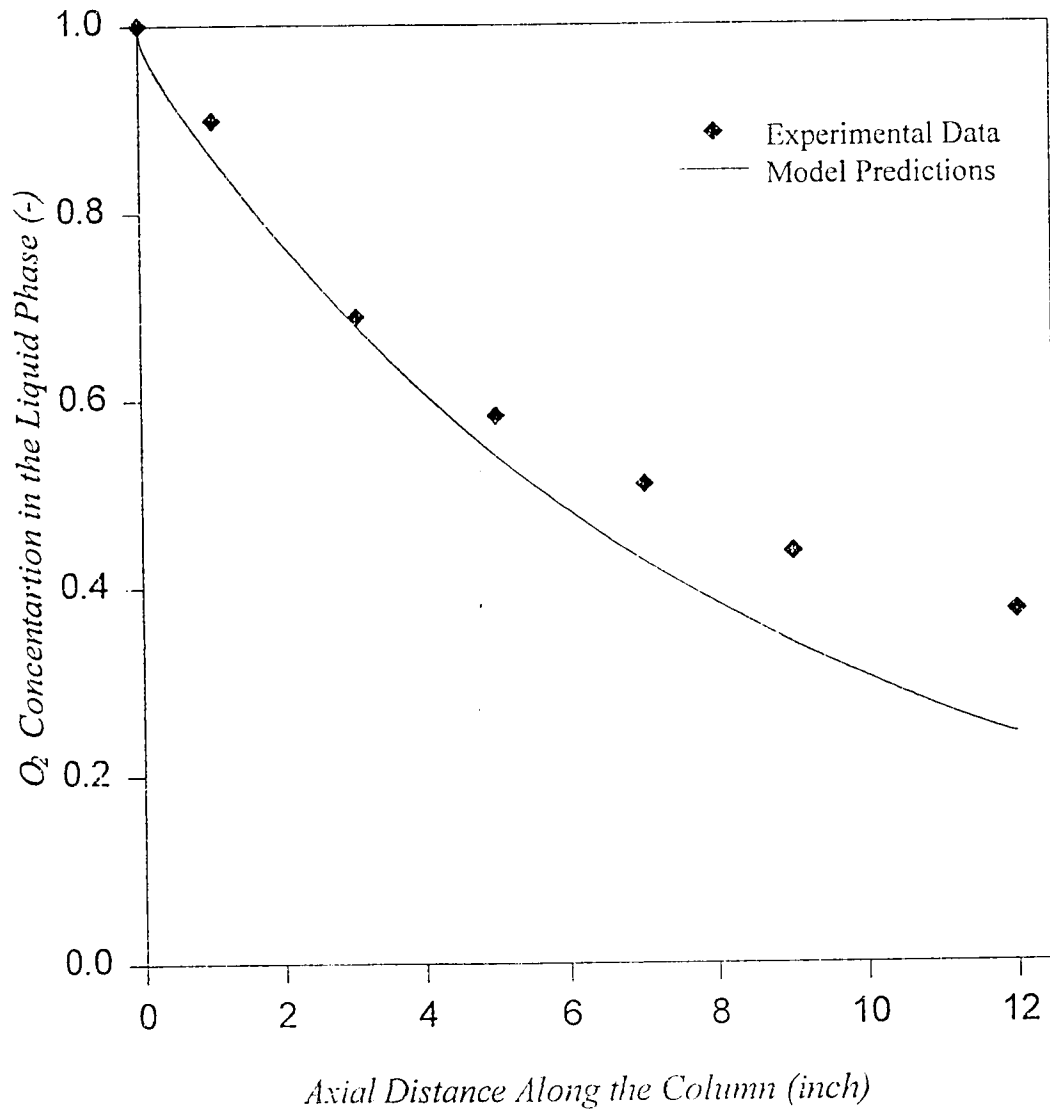


Figure (6.9) Comparison of experimental data with model predictions for desorption of O<sub>2</sub> from water (Data of Reiss, 1967).



**Table 6.3** Values of parameters for comparison of theoretical predictions with experimental data for oxygen desorption from water.

Parameters	Value	Reference
$U_L$ , m s <sup>-1</sup>	0.043	Reiss (1967)
$U_G$ , m s <sup>-1</sup>	0.509	Reiss (1967)
$L_C$ , m	0.3048	Reiss (1967)
$d_p$ , m	0.0032	Reiss (1967)
$\varepsilon$	0.726	Reiss (1967)
$L_S$ , m	$10^{-4}$	Kan and Greenfield (1983)
$D_S$ , m <sup>2</sup> s <sup>-1</sup>	$0.5 \times 10^{-10}$	Kan and Greenfield (1983)
$h_S$	0.035	Saez and Carbonell (1985)
$h_d$	0.3868	Ellman et al. (1990)
$k_{LG} a_{LG}$ , sec <sup>-1</sup>	0.2	Reiss (1967)
$k_{SD}$ , m s <sup>-1</sup>	$5.5 \times 10^{-8}$	Beg et al. (1995)
$\rho_L$ , kg m <sup>-3</sup>	1000.0	Welty et al. (1976)
$\rho_G$ , kg m <sup>-3</sup>	1.225	Welty et al. (1976)
$\mu_L$ , Pa sec	$7.44 \times 10^{-1}$	Welty et al. (1976)
$\mu_G$ , Pa sec	$1.8 \times 10^{-5}$	Welty et al. (1976)
$\sigma_L$ , N m <sup>-1</sup>	$7.15 \times 10^{-2}$	Welty et al. (1976)

**Table 6.3** Continued

The calculated parameters used in the analysis,

$^*Pe_L$	100
$^*Pe_G$	100
$h_l$	0.4218
$h_g$	0.3042
$\phi$	0.917
$\psi$	0.721
$\xi$	11.837
$a_{SD} \cdot m^{-1}$	350
$\beta$	0.01513
$K_{SD}^*$	$1.366 \times 10^{-4}$
$St$	1.434
$Bi$	0.11
$Re_L$	184.84
$Re_G$	110.85

\* Assuming plug flow behavior in both the gas and liquid phases.

# CHAPTER 7

## MODELING OF GAS ABSORPTION WITH CHEMICAL REACTION

---

### 7.1 INTRODUCTION

Gas absorption accompanied by a chemical reaction in the liquid phase is common to a number of chemical process industries. A wide variety of gas-liquid reactions like liquid phase oxidation, chlorination, sulfonation etc., proceed through absorption of the gas followed by chemical reaction in the liquid phase. Absorption with simultaneous chemical reaction is also widely used to remove acid gases such as  $\text{CO}_2$  and  $\text{H}_2\text{S}$  from hydrocarbon and inert mixtures. With regard to air pollution control it presents an attractive alternative for removal of lean pollutants from the gaseous waste stream coming out of industrial installations, by absorbing them in an abundantly available liquid stream like water, where they are readily consumed by a suitable reactant. The chemical reaction can significantly increase the solubility of the gas reducing the required solvent flow rate for a given removal specification. Furthermore, if the chemical reaction is fast enough, it increases the rate of absorption, thus increasing the overall liquid phase mass transfer coefficient and subsequently reducing the size of the required absorption

column. If the solvent is reactive preferably toward one particular gas in a mixture, it can be used for selective removal. An example of this process is the selective removal of H<sub>2</sub>S, when CO<sub>2</sub> and H<sub>2</sub>S mixtures are passed through a column using aqueous methyldiethanolamine which reacts instantaneously with H<sub>2</sub>S and relatively slowly with CO<sub>2</sub> (Astarita et al., 1983).

For the purposes outlined above, different configuration of gas liquid contactors are used in practice depending on the nature of the system, particularly on the mass and heat transfer effects. Co-current packed columns are an attractive option as they offer a mass transfer efficiency that is considerably higher than that of conventional counter current columns. This is the result of their increased interfacial area, which may exceed the geometric area, and increased values of mass transfer coefficient. Such enhancement is particularly apparent when transfer is controlled by resistance in the liquid phase where  $k_{GL}$  increases are 40-fold for approximately 15-fold increase in velocity (Gianetto et al., 1972). The overall rate of the process is controlled by the following steps (Satterfield, 1975).

- a) Mass transfer at the gas side of the interface
- b) Mass transfer at the liquid side of the interface
- c) Chemical reaction

One or several of these steps can be rate determining. Especially the steps (a) and (b) will be highly influenced by the column hydrodynamics. The coefficient  $k_G$  increases slightly with increases in either the liquid or gas rate, while  $k_L$  is affected little by the changes in gas rate and increases considerably with the liquid rate. Mean  $k_L$  values about ten times greater than those obtained with counter current columns under normal conditions (Danckwerts and Sharma, 1966) were observed.

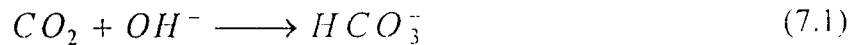
Due to the complex hydrodynamics prevailing inside cocurrent packed columns, theoretical analysis of gas absorption with chemical reaction in such columns is important for the fundamental understanding of the physico-chemical phenomena and also in connection with equipment design and scale-up. Although, numerous empirical studies have been undertaken in this regard as discussed earlier in this thesis, there is a lack of theoretical work carried out in this area, hence necessitating such a study.

## **7.2 CHEMISTRY OF THE PROCESS MODELED**

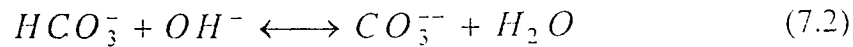
Due to the ease of availability of experimental data, the absorption of  $\text{CO}_2$  from air into aqueous solution of sodium hydroxide was considered as the model system. Also, as we are interested in modeling of absorption of lean pollutants

from exhaust gases. The absorption of  $\text{CO}_2$  in NaOH presents a parallel case as it is industrially used for gases containing very low concentrations of  $\text{CO}_2$  with partial pressure of almost  $10^{-3}$  atmospheres (Astarita et al., 1983). The chemistry of this system has been extensively studied both theoretically and experimentally as documented by Sherwood and Pigford (1952), Astarita (1967) and Astarita et al. (1983).

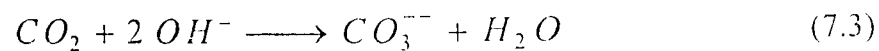
The controlling reaction is,



which is followed by



Reaction (7.2) may be considered to be instantaneous, while reaction (7.1) proceeds at a finite rate. When a substantial amount of free hydroxide is present, reaction (7.2) is completely displaced to the right. Thus, the overall reaction which takes place during absorption of carbon dioxide in hydroxide solution may therefore be assumed, to be the following :



the rate of which can be written as,

$$r_{\text{CO}_2} = k_R [\text{CO}_2][\text{OH}^-] \quad (7.4)$$

The advantage of this type of reaction is that, within certain hydroxyl ion concentration limits, it can be treated as irreversible. In addition, the controlling resistance to the mass transfer is located almost entirely in the liquid phase.

### 7.3 RESULTS AND DISCUSSION

The model equations discussed in Section (3.4) have been solved for CO<sub>2</sub> removal from air by aqueous solution of sodium hydroxide in a cocurrent down flow packed column. The system was studied for a step input in CO<sub>2</sub> concentration in the gas phase, and parametric studies were carried out to evaluate the individual effects of parameters of practical significance. Table (7.1) lists the base values of parameters used for the numerical computation. The various model parameters involved were evaluated by the functional relationships discussed in Section (4.2.1) and (5.2.1). The kinetics, other related physical properties of the system being studied, and column dimensions were taken from the data reported by Morsi et al. (1984).

The effect of important parameters like liquid and gas phase Peclet number  $Pe_L$ ,  $Pe_G$ , Liquid and gas phase Reynolds number  $Re_L$ ,  $Re_G$ , Stanton number  $St$ , and dimensionless reaction rate constant  $K_R^*$ , on column performance were studied. Initially (at  $\theta = 0$ ) the column was considered to be free of any absorbate,

**Table 7.1** Values of parameters for comparison of theoretical predictions with experimental data for absorption of CO<sub>2</sub> in NaOH solution

Parameters	Value	Reference
$\bar{U}_L$ , m s <sup>-1</sup>	0.00399	Morsi et al. (1984)
$U_G$ , m s <sup>-1</sup>	0.0906	Morsi et al. (1984)
$L_C$ , m	0.49	Morsi et al. (1984)
$d_p$ , m	0.00116	Morsi et al. (1984)
$\varepsilon$	0.263	Morsi et al. (1984)
$L_S$ , m	10 <sup>-4</sup>	Kan and Greenfield (1983)
$D_S$ , m <sup>2</sup> s <sup>-1</sup>	0.5 × 10 <sup>-10</sup>	Kan and Greenfield (1983)
$h_S$	0.05	Saez and Carbonell (1985)
$h_d$	0.0827	Ellman et al. (1990)
$k_{LG} a_{LG}$ , s <sup>-1</sup>	0.28	Ellman (1988)
$k_{SD}$ , m s <sup>-1</sup>	5.5 × 10 <sup>-8</sup>	Beg et al. (1995)
$H$ , kmol m <sup>-3</sup> liq./kmol m <sup>-3</sup> gas	0.8	Morsi et al. (1984)
$Pe_L$	15.0	Matsurra et al. (1976)
$Pe_G$	11.95	Hochmann and Effron (1969)
$k_R$ , m <sup>3</sup> kmol <sup>-1</sup> s <sup>-1</sup>	7850.0	Morsi et al. (1984)
$\rho_L$ , kg m <sup>-3</sup>	1003.0	Morsi et al. (1984)
$\rho_G$ , kg m <sup>-3</sup>	1.225	Welty et al. (1976)
$\mu_L$ , Pa s	1.04 × 10 <sup>-3</sup>	Morsi et al. (1984)
$\mu_G$ , Pa s	1.8 × 10 <sup>-5</sup>	Welty et al. (1976)
$\sigma_L$ , N m <sup>-1</sup>	6.28 × 10 <sup>-2</sup>	Morsi et al. (1984)

The calculated parameters used in the analysis,

$h_l$	0.1327
$h_g$	0.1303
$\phi$	0.623
$\psi$	0.982
$\xi$	22.72
$a_{SD}$ , m <sup>-1</sup>	500.0
$\beta$	0.0815
$K_{SD}^*$	3.38 × 10 <sup>-3</sup>
$St$	34.38
$Bi$	0.11
$Re_L$	4.461
$Re_G$	7.152



i.e.,  $C_g = C_{d_1} = C_{S_1} = 0$ , and the entire liquid phase was assumed to contain maximum NaOH concentration, i.e.,  $c_{d_2} = c_{S_2} = 0.2$  or  $C_{d_2} = C_{S_2} = 147.96$ . Then the absorbate was introduced only in the gas phase, which implies that the inlet condition for this phase becomes,  $C_g|_{x=0^-} = 1.0$  .

As shown in Figure (7.1), the gas phase  $\text{CO}_2$  concentration profile along the length of the column is unaffected by the variation of  $Pe_L$ . This may be attributed to zero concentration of solute gas at the gas-liquid interface for all values of  $Pe_L$  considered, because of the reaction being instantaneous. However, the concentration profile for NaOH in the liquid phase shows a marked influence of  $Pe_L$ . This would be expected as low values of  $Pe_L$  correspond to high degree of mixing in the liquid phase, thus lowering the concentration profile of unreacted NaOH in the liquid phase. The dynamics of the system are illustrated in Figure (7.2), which also shows the effect of  $Pe_L$  on the transient exit concentration profiles. It is evident from the figure that the gas phase attains steady state much earlier than the liquid phase. Further, decrease in  $Pe_L$  results in slow approach to steady state.

Figure (7.3) show the effect of gas phase Peclet number,  $Pe_G$  on the steady state concentration profiles of the system. High values of  $Pe_G$  imply plug flow

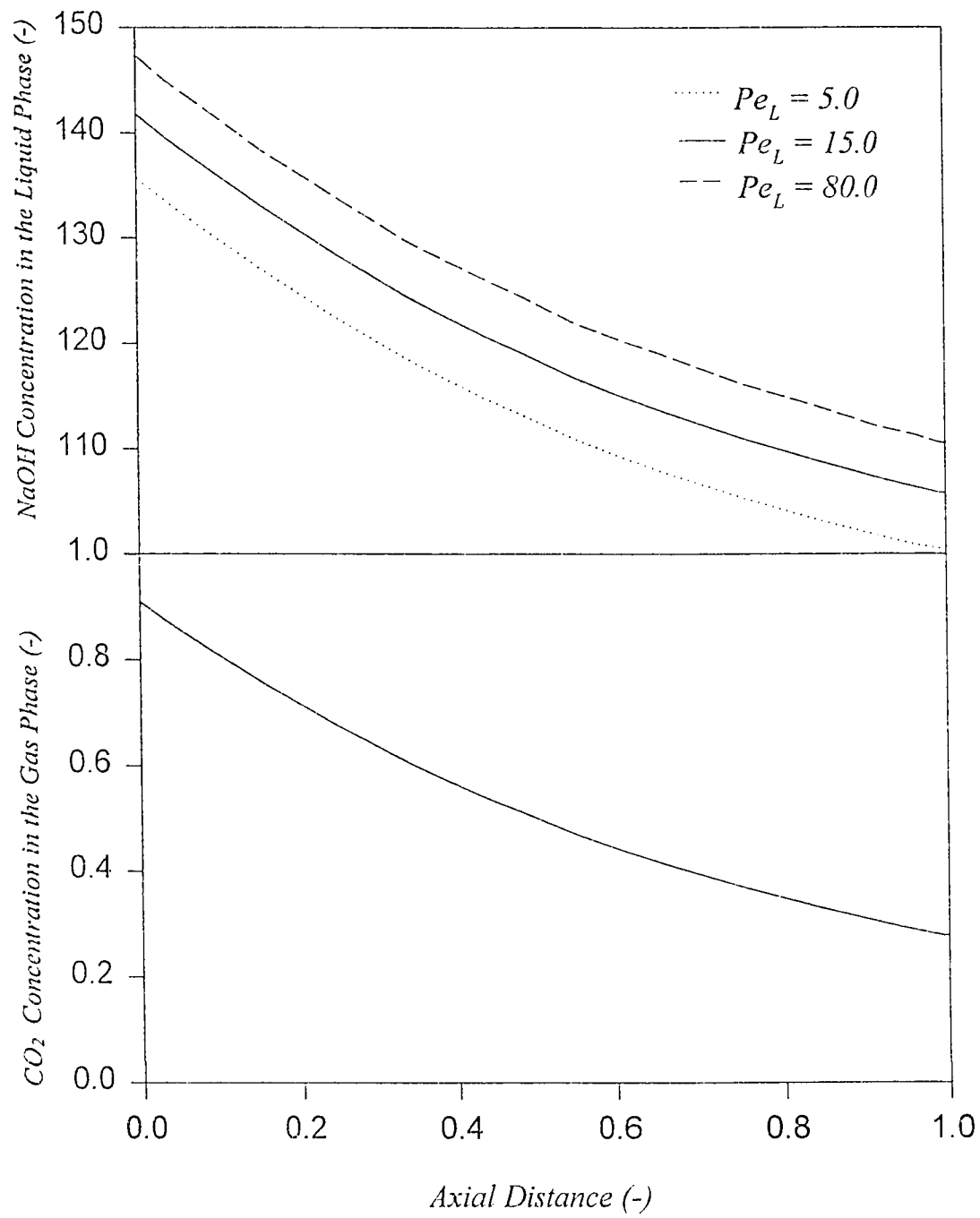


Figure (7.1) Effect of  $Pe_L$  on steady state concentration profiles along the length of the column for  $\text{CO}_2$  in the gas phase and NaOH in the liquid phase.

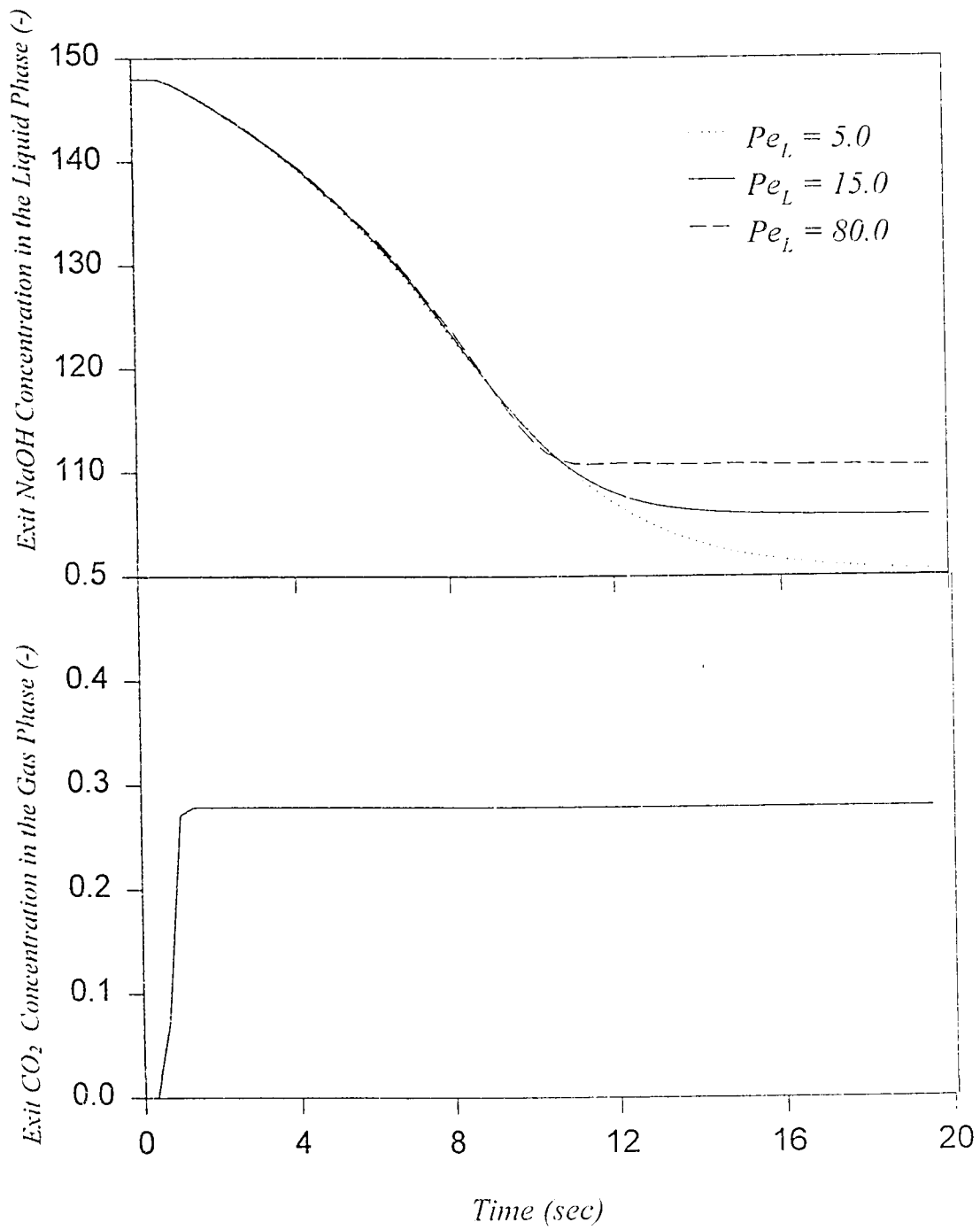


Figure (7.2) Effect of  $Pe_L$  on transient exit concentrations for  $\text{CO}_2$  in the gas phase and NaOH in the liquid phase.

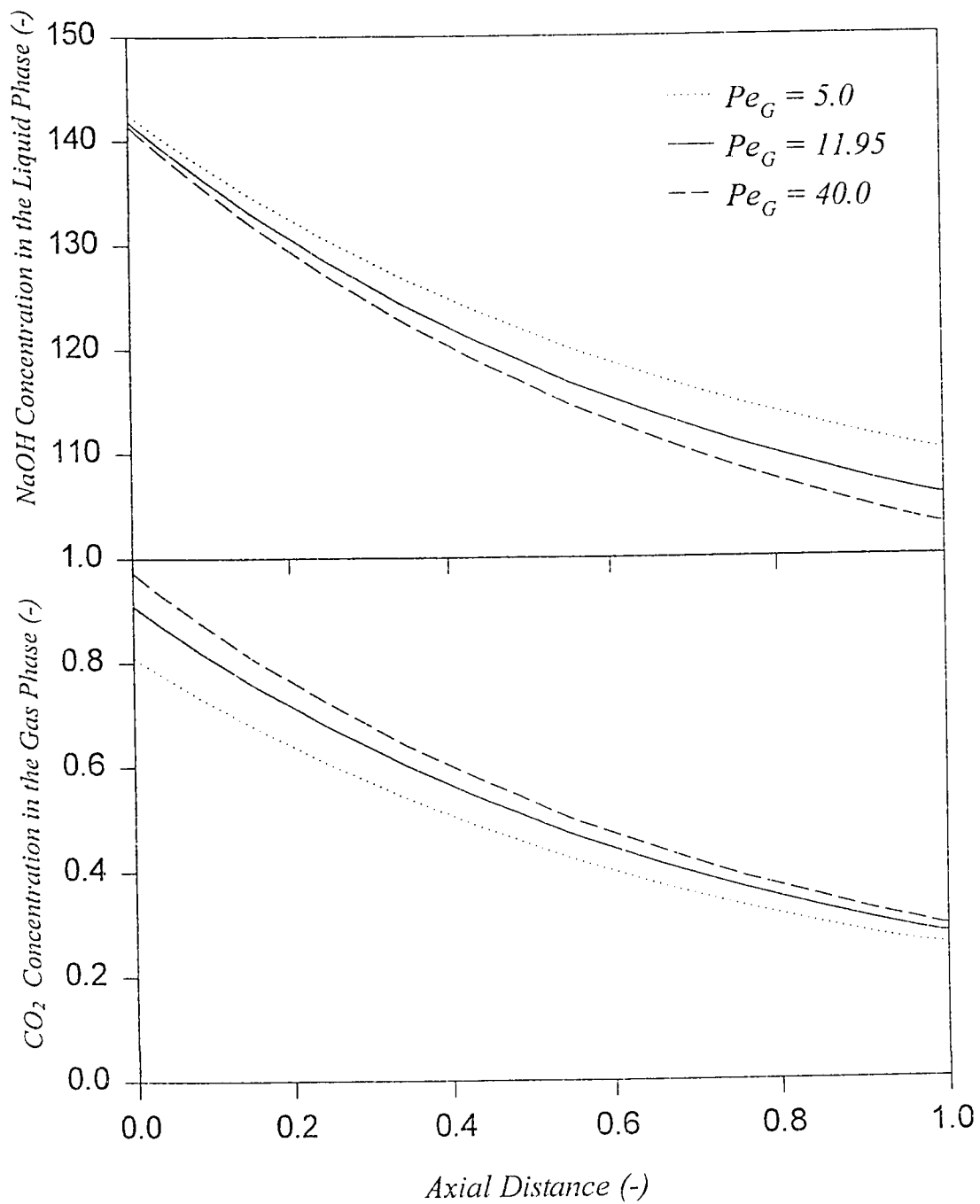


Figure (7.3) Effect of  $Pe_G$  on steady state concentration profiles along the length of the column for  $\text{CO}_2$  in the gas phase and NaOH in the liquid phase.

behavior, which results in larger concentration gradient in the gas phase causing higher mass transfer rates and more consumption of NaOH in the liquid phase.

Effects of variation in liquid phase Reynolds number,  $Re_L$ , on the system are shown in Figure (7.4). Lower values of  $Re_L$  imply larger time of contact between the two phases, resulting in high mass transfer to the liquid phase and therefore decline of NaOH concentration in the liquid phase as shown in the figure. However, the corresponding  $CO_2$  concentration profile in the gas phase shows higher concentrations all along the reactor providing a higher concentration driving force for higher rates of mass transfer of  $CO_2$  to the liquid phase.

Figure (7.5) highlights the effect of gas phase Reynolds number,  $Re_G$ , on the steady state concentration profiles of  $CO_2$  in the gas phase and unreacted NaOH in the liquid phase. As evident from the figure, high values of  $Re_G$  leads to higher concentration gradients in the gas phase. Further it may be noted that high values of  $Re_G$  provide high values of mass transfer coefficient,  $k_{GL} a_{GL}$ , which leads to increased mass transfer rates and hence more consumption of NaOH in the liquid, as also shown in Figure (7.5) by low values of unreacted NaOH concentrations.

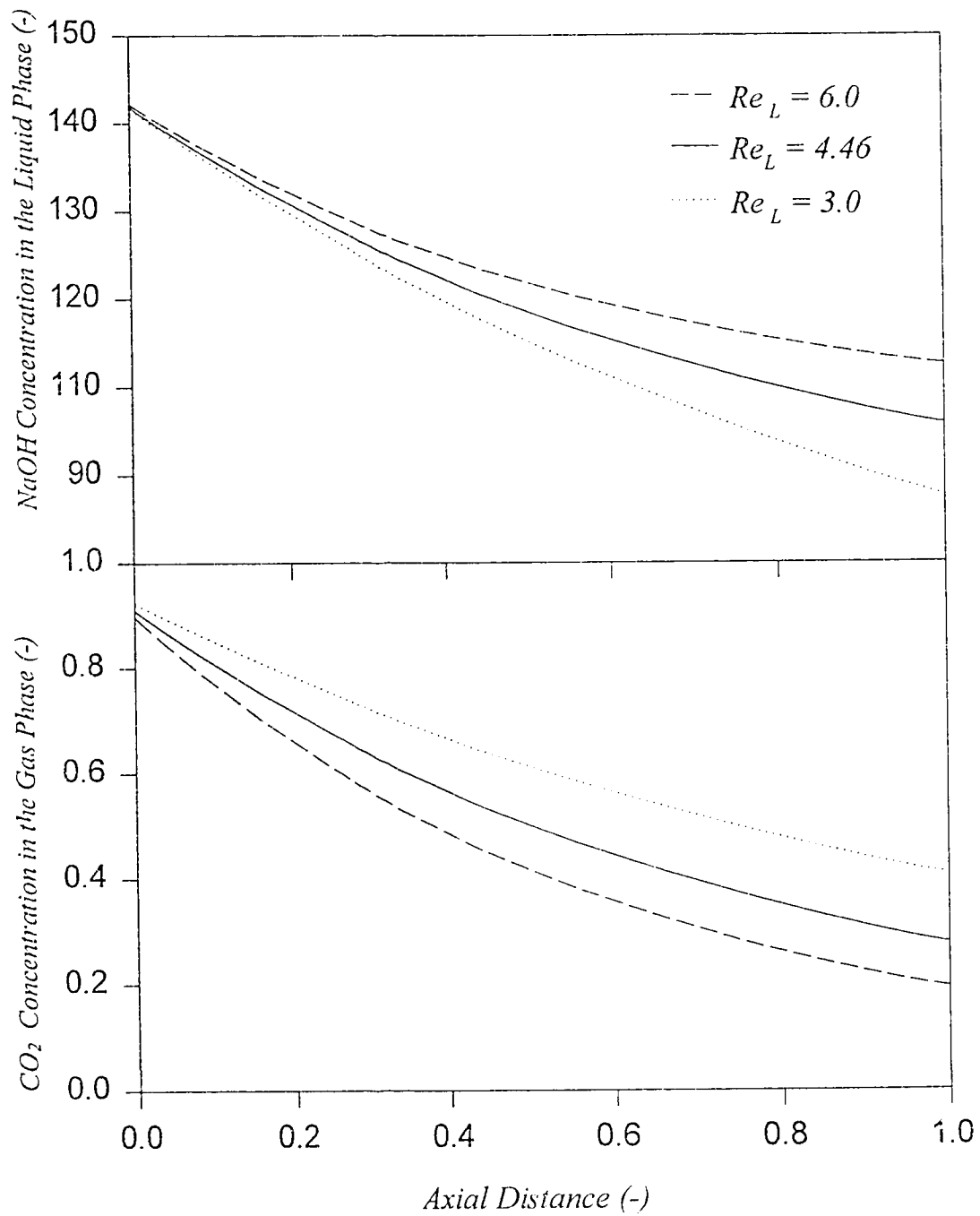


Figure (7.4) Effect of  $Re_L$  on steady state concentration profiles along the length of the column for CO<sub>2</sub> in the gas phase and NaOH in the liquid phase.

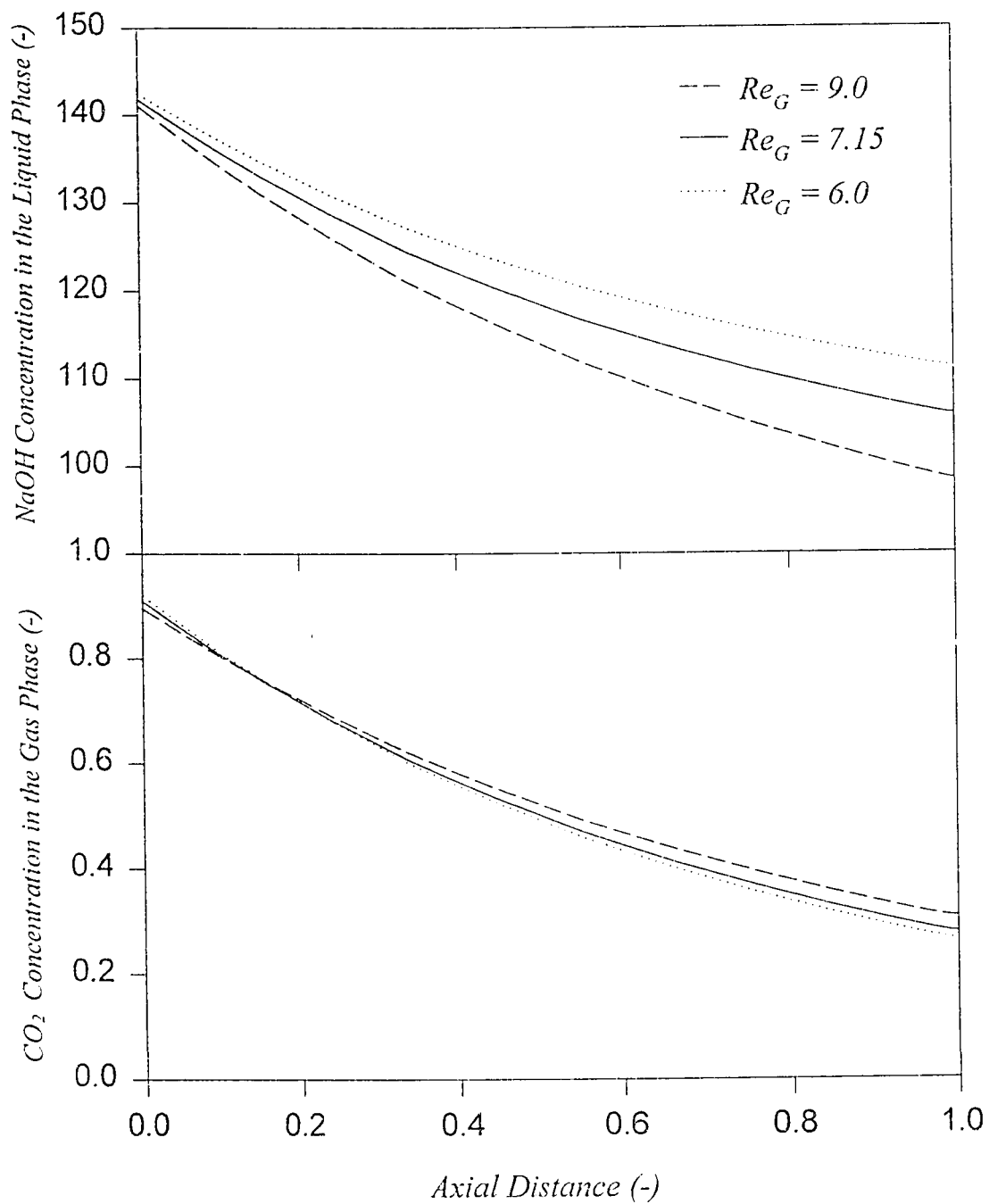


Figure (7.5) Effect of  $Re_G$  on steady state concentration profiles along the length of the column for  $CO_2$  in the gas phase and NaOH in the liquid phase.

Figure (7.6) shows the effect of Stanton number,  $St$  on the steady state concentration profiles of the system. High values of  $St$  imply lower resistance to mass transfer which leads to increased rate of mass transfer from gas to the liquid phase. As a result, more NaOH is consumed causing lower concentrations of NaOH in the liquid phase and  $\text{CO}_2$  in the bulk gas phase.

In order to illustrate the effect of  $K_R^*$  on the performance of the system, three dimensional concentration profiles are shown in Figure (7.7). High values of  $K_R^*$  imply instantaneous reaction which results in complete conversion of  $\text{CO}_2$  at the gas-liquid interface as depicted by zero concentrations of  $\text{CO}_2$  in the bulk liquid all along the length of the reactor as shown in Figure (7.7a). However, for lower value of  $K_R^*$ , signifying a slow reaction,  $\text{CO}_2$  concentration in the bulk liquid is finite as shown in Figure (7.7b). This finite increase in  $\text{CO}_2$  concentration in the liquid phase leads to reduced concentration driving forces hence causing poor diffusional mass transfer from the gas phase and therefore, results in low consumption of NaOH in the liquid phase. This is better illustrated in Figure (7.8) where high concentration of residual NaOH in the liquid phase are observed for low values of  $K_R^*$ .



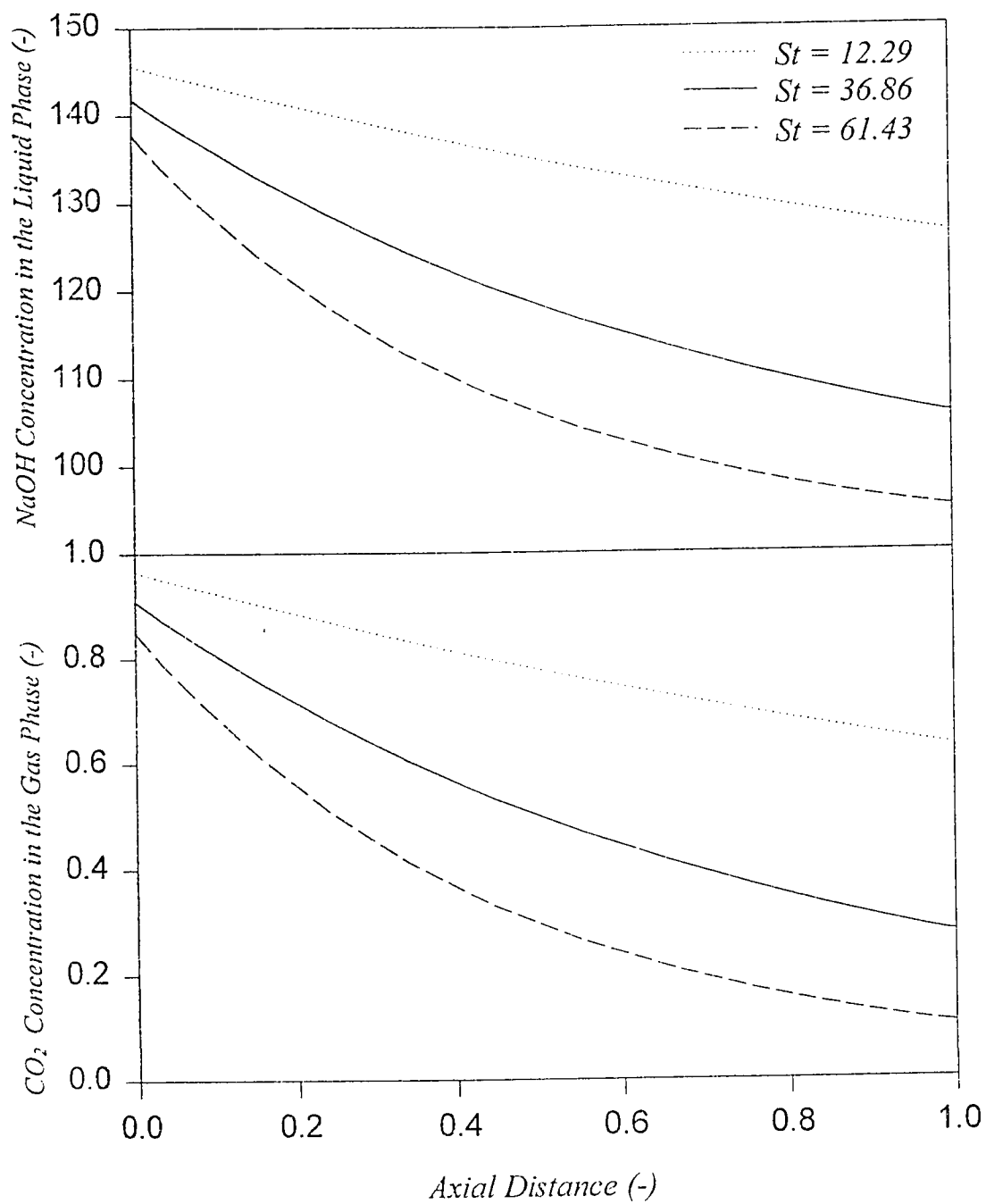


Figure (7.6) Effect of  $St$  on steady state concentration profiles along the length of the column for  $\text{CO}_2$  in the gas phase and  $\text{NaOH}$  in the liquid phase.

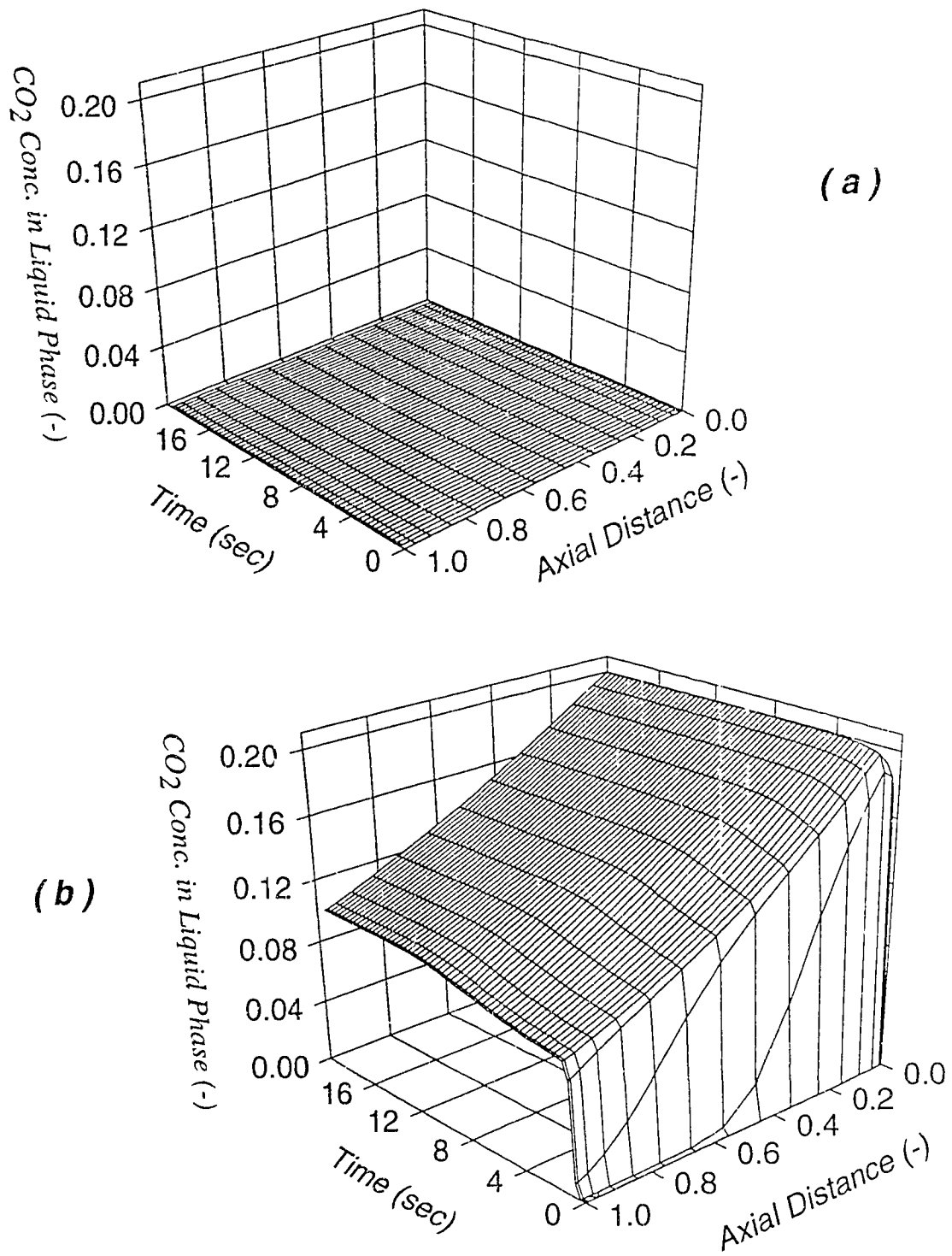


Figure (7.7) 3-D concentration profiles for  $\text{CO}_2$  in the dynamic liquid phase, illustrating the effect of  $K_R^*$ , (a)  $K_R^* = 1303.8$  (b)  $K_R^* = 0.83$

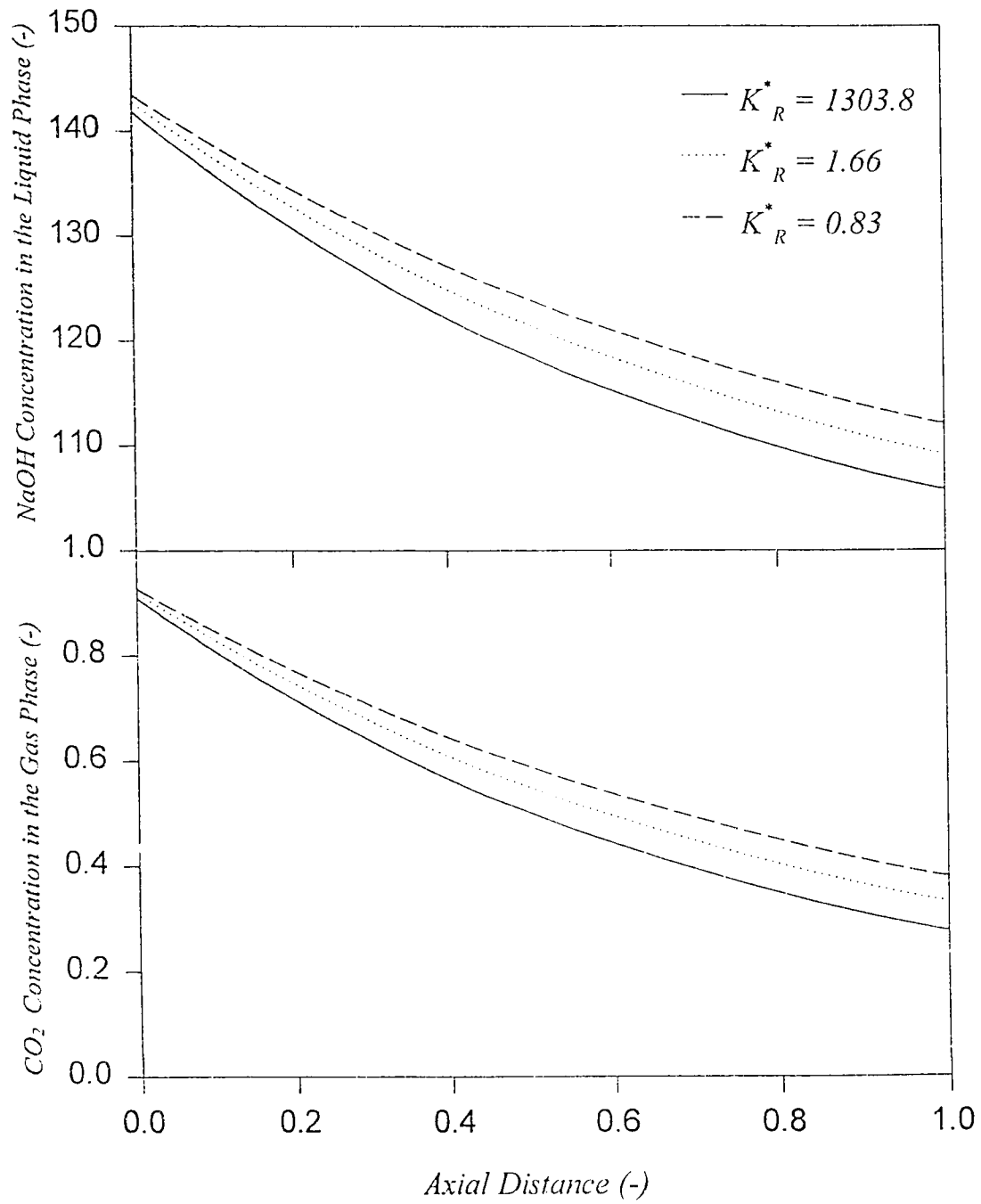


Figure (7.8) Effect of  $K_R^*$  on steady state concentration profiles along the length of the column for CO<sub>2</sub> in the gas phase and NaOH in the liquid phase.

Figure (7.9) shows the comparison of the model predictions with the limited data available in the literature for absorption of  $\text{CO}_2$  in aqueous solution of NaOH at three different gas flow rates. The predictions show a reasonable agreement with the experimental data. The small discrepancies can be attributed to the accuracy of correlations used and the error involved in the experimental measurements. All the relevant parameters used in the predictions were obtained from the available correlations reported earlier as listed in Table (7.1). The overall mass transfer coefficient was found to have the most pronounced effect on the performance of the system. It may be noted that a generalized correlation proposed by Eilman (1990) was used to calculate the overall mass transfer coefficient for the system. More reliable and accurate predictions could have been obtained, if a correlation specifically developed for the proposed system was available.

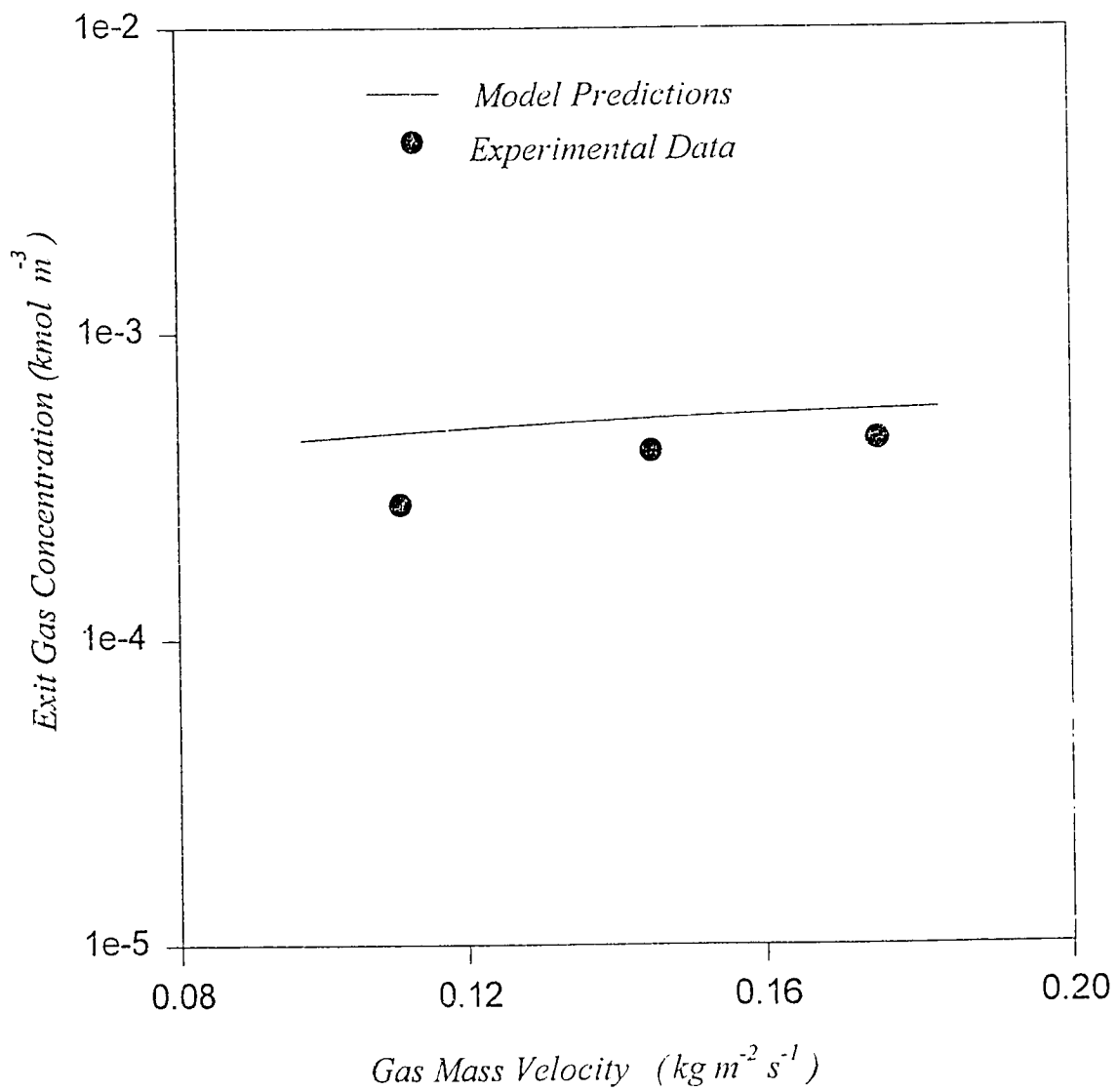


Figure (7.9) Comparison of experimental data with model predictions for absorption of  $\text{CO}_2$  in aqueous solution of  $\text{NaOH}$  (Data of Morsi et al., 1984), for constant liquid mass velocity =  $4.0 \text{ (kg m}^{-2} \text{s}^{-1})$

# CHAPTER 8

## **CONCLUSIONS AND RECOMMENDATIONS**

### 8.1 CONCLUSIONS

A more realistic model has been developed for the study of hydrodynamics and mass transfer in a cocurrent packed column. It proposes that the liquid phase is divided into two regions, an axially dispersed dynamic liquid region and a stagnant region where the mixing phenomena is described by a Fickian type equation, with mass transfer between the two. The model is numerically solved and its validation is carried out by fitting its predictions to the experimental data obtained from tracer analysis for both the upflow and downflow modes of operation. Parametric studies are also carried out to study the effects of different model parameters. Some of the conclusions drawn from this study are given as under,

- The mass transfer coefficient,  $k_{SD}$ , and the thickness of the stagnant film,  $L_S$ , only affect the tail portion of the breakthrough curve. The concentration profiles become steeper with increase in  $k_{SD}$  and decrease in  $L_S$ .

- The effect of dispersion coefficient,  $D_S$ , in the stagnant phase is only pronounced at low values of  $D_S$  around  $10^{-11}$  m s<sup>-1</sup>.
- Higher values of dynamic liquid holdup,  $\phi$ , result in an initial longer drop in concentration followed by a constant falling rate which is independent of  $\phi$ .
- Large Reynolds number ( $Re_L$  &  $Re_G$ ) and low values of total liquid holdup result in a faster response of the breakthrough curve.
- Axial dispersion coefficient,  $D_L$ , only affects the spread of the breakthrough curve.
- The model provides a good representation of the experimental data for both the downflow and upflow modes of operation.

The model is then extended to analyze and simulate the absorption of lean pollutants from gas phase into water. Three absorption systems are explored, namely absorption of ammonia, sulfur dioxide and hydrogen fluoride from air into water. Parametric studies are carried out to study the influence of parameters of practical importance and the model predictions are also compared with the limited experimental data available for absorption of ammonia in water. Following are some of the conclusions,

- Under identical operating conditions, absorption is maximum for ammonia and minimum for sulfur dioxide.
- The effect of  $Pe_L$ ,  $Pe_G$  and  $St$ , is more pronounced for highly soluble ammonia and least for sulfur dioxide.
- The effect of  $Pe_G$  is more pronounced on the gas phase concentration profile and is less significant on the liquid phase concentration profile.
- Plug flow conditions in the gas phase are achieved for  $Pe_G > 40$ .
- Increase in Stanton number results in faster approach to equilibrium.
- Stagnant liquid phase does not have much effect on gas absorption, and plays a very small role in the approach to steady state conditions.
- The predictions from the proposed model are in close agreement with the experimental data for absorption of ammonia.

The model equations are also used to carry out numerical simulations for the stripping of different volatile organic compounds (chloroform, dibromochloromethane and bromoform) from water into air, to study the affect of various parameters. Further the model predictions for desorption of oxygen from water into air are successfully compared with the experimental available in the literature. The resulting conclusions from this study are as under,



- Both the liquid and gas phases approach steady state at approximately the same time.
- For the given column dimensions and flow conditions, equilibrium between gas and liquid phases is only obtained for the least volatile bromoform.
- Decrease in  $Pe_L$  and increase in  $Pe_G$  result in enhanced stripping.
- High values of  $St$  result in better performance and closer approach to equilibrium.
- Increase in  $Re_L$  results in better stripping and faster approach to equilibrium within the column for chloroform and dibromochloromethane systems. However, the effect of  $Re_L$  at given conditions is insignificant for bromoform system.
- Stripping performance of all the systems increase with the increase in  $Re_G$ .
- The predictions from the proposed model are in reasonable agreement with the experimental data for desorption of oxygen.

Finally the model was extended to incorporate the phenomena of gas absorption with chemical reaction in the liquid phase. The system investigated was that of absorption of  $CO_2$  from that of air in to an alkaline solution of NaOH. The effects of various parameters influencing this phenomena were investigated, and

the predictions from the proposed model were compared with experimental data reported in the literature. Following conclusions were drawn from this work:

- There is no significant effect of  $Pe_L$  on the gas phase. Increase in  $Pe_L$  only lowers the entire steady state concentration profile of NaOH in the liquid phase.
- Gas phase attains steady state a lot earlier than the liquid phase.
- Both the gas and liquid phases are affected by  $Pe_G$ . High values of  $Pe_G$  result in steeper concentration profiles and hence enhanced absorption of  $CO_2$ .
- Increase in  $Re_L$  facilitates absorption.
- $Re_G$  does not have a significant effect on gas phase, though the NaOH exit concentration in the liquid phase goes down as the result of increased  $Re_G$ .
- Increase in  $St$  results in enhanced absorption.
- There is no significant effect of  $K_R^*$  on the system for  $K_R^* > 100$ .
- For values of  $K_R^* < 100$ , significant concentration profile of  $CO_2$  is observed in the liquid phase which was previously absent, hence indicating a decrease in absorption efficiency.

- The model predictions are in reasonable agreement with the experimental data.

## **8.2 RECOMMENDATIONS FOR FUTURE STUDIES**

Based on the experiences acquired during the course of this work, following recommendations are suggested to future researchers :

- For the proper applicability of the model equations, experimental RTD data for real commercial reactors is needed.
- Most of the reported data in the literature is obtained by operating the column under trickle flow conditions. To extend the applicability of the model to pulsating and spray flow regime, it must be validated and tested for the experimental data obtained under such conditions.
- As opposed to air water system, experimental data for systems possessing different physical properties must be obtained and the applicability of the model to such systems must be tested.

- In the present work, only the systems with negligible thermal effects were considered. It would be interesting if the current model is extended to incorporate the thermal balance and is then applied to non-isothermal systems.
- Due to great applicability of cocurrent packed columns in catalytic reactions, extension of current model equations to include the effect of catalytic packing with liquid-solid mass transfer would be a significant contribution to this area.
- More comprehensive and general correlations for model parameters must be developed. These should take into account different system properties, reactor configuration, flow conditions and scale-up phenomena.

## BIBLIOGRAPHY

---

- Astarita, G. (1967) *Mass transfer with chemical reaction*. Elsevier Publishing Co., New York.
- Astarita, G., Savage, D.W. and Bisio, A. (1983) *Gas treating with chemical solvents*. John Wiley & sons, New York.
- Ball, W.P., Jones, M.D., and Kavanaugh, M.C. (1984) Mass transfer of volatile organic compounds in packed tower aeration. *J. WPCF.*, 56, 127.
- Beg, S. A., Hassan, M. M. and Naqvi, M. S. M. (1995) Hydrodynamics and mass transfer in a co-current packed column : A theoretical study. *Chem. Eng. J.*, submitted.
- Bennett, A. and Goodridge, F. (1970) Hydrodynamic and mass transfer studies in packed absorption columns - Part I: Axial liquid dispersion. *Trans. Inst. Chem. Eng.*, 48, T232.
- Betterton, E.A. (1992) Henry's law constants of soluble and moderately soluble organic gases: Effects on aqueous phase chemistry. *Gaseous Pollutants: Characterization and Cycling. Advances in Environmental Science and Technology*, (J.O. Nriagu, Ed.); John Wiley & Sons Inc., Vol. 24, 1.
- Blok, J. R., Varkevisser, J. and Drinkenburg A. A. H. (1983) Transient flow, holdup and pressure drop in packed columns with gas-liquid downflow. *Chem. Eng. Sci.*, 38, 687.
- Buffham, B. A., Gibilaro, L. G. and Rathor, M. N. (1970) A probabilistic time delay description of flow in packed beds. *AIChE J.*, 16, 218.
- Buffham, B. A. (1971) The effects of intrasolid resistance and axial mixing on transient exchange in packed beds and the unified time delay model. *Chem. Eng. J.*, 2, 71.
- Charpentier, J. C., Prost, C. Van Swaaij, W. and LeGoff, P. (1968) Etude de la retention de liquide dans une colonne a garnissage a co-courant et a contre-courant de gas-liquide. *Chimie et Ind. Genie Chim.*, 99, 803.

- Charpentier, J. C., Bakos, M. and LeGoff, P. (1971) Hydrodynamics of two-phase concurrent downflow in packed bed reactors. Gas-liquid flow regimes. Liquid axial dispersion and dead zones. *Proc. 2nd Conf. Appl. Phys. Chem.*, Veszprem, Hungary, Vol. 2.
- Charpentier, J. C. and Favier, M., (1975) Some liquid holdup experimental data in trickle bed reactors for foaming and non-foaming hydrocarbons. *AIChE J.*, 21, 1213.
- Charpentier, J. C. (1976) Recent progress in two-phase gas-liquid mass transfer in packed beds. *Chem. Eng. J.*, 11, 161.
- Charpentier, J. C. (1979) Hydrodynamics of two-phase flow through porous media. *Chem. Eng. of Gas-Liquid-Solid Catalyst Reactions*. (Ed. L'Homme, G.A.) Cebedoc, Liege, Belgium.
- Chou, T. S., Worley, Jr. F. L. and Luss, D. (1977) Transition to pulsed flow in mixed-phase cocurrent downflow through a fixed bed. *Ind. Eng. Chem. Process Des. Dev.*, 16, 424.
- Danckwerts, P.V. and Sharma, M.M. (1966) The absorption of carbon dioxide in solutions of alkalis and amines. *The Chem. Eng.*, 44, CE244.
- Deans, H. A. and Lapidus, L. (1960) A computational model for predicting and correlating the behavior of fixed bed reactors. I: Derivation of model for non reactive systems. II: Extension to chemically reactive systems. *AIChE J.*, 6, 656, 663.
- Deans, H. A. (1963) A mathematical model for dispersion in the direction of flow in porous media. *Soc. Petrol. Eng. J.*, 3, 49.
- Dombrowski, H.S. and Brownell, L.E., (1954) Residual equilibrium saturation of porous media. *Ind. Eng. Chem.*, 6, 1207.
- Dunn, W.E., Vermuelen, T., Wilke, C.R. and Word, T.T. (1977) Longitudinal dispersion in packed gas-absorption columns. *Ind. Eng. Chem. Fund.*, 16, 116.
- Ellman, M. J. (1988) Caracteristiques des reactures triphasiques a lit fixe fonctionnat a cocuorant ver le bas. These de Doctorat, INPL: Nancy, France.

- Ellman, M. J., Midoux, N., Laurent, A. and Charpentier, J. C., (1988) A new, improved pressure drop correlation for trickle bed reactors. *Chem. Eng. Sci.*, 43, 2201.
- Ellman, M.J., Midoux, N., Wild, G., Laurent, A. and Charpentier, J.C. (1990) A new, improved liquid hold-up correlation for trickle-bed reactors. *Chem. Eng. Sci.*, 45, 1677.
- Fukushima, S. and Kusaka, K. (1977) Interfacial area and boundary of hydrodynamic flow region in packed column with cocurrent downward flow. *J. Chem. Eng. Japan*, 10, 461.
- Gianetto, A., Baldi, G. and Specchia, V. (1970) Absorption in packed towers with cocurrent downward high-velocity flows I - interfacial areas. *Quad. Ing. Chim. Ital.*, 6, 125.
- Gianetto, A., Specchia, V. and Baldi, G. (1973) Absorption in packed towers with concurrent downward high-velocity flows -II: mass transfer. *AIChE J.*, 19, 916.
- Gianetto, A., Baldi, G., Specchia, V. and Sicardi, S. (1978) Hydrodynamics and solid-liquid contacting effectiveness in trickle bed reactors. *AIChE J.* 24, 1087.
- Gianetto, A. and Silveston, P. L. (1986) *Multiphase Chemical Reactors : Theory, Design & Scale up*, Hemisphere Publishing Corporation, N.Y.
- Gianetto, A. and Specchia, V. (1992) Trickle-bed reactors: State of art and Perspectives. *Chem. Eng. Sci.*, 47, 3197.
- Goto, S. and Smith, J. M. (1975) Trickle bed reactor performance Part I: holdup and mass transfer effects. *AIChE J.*, 21, 706.
- Goto, S., Levec, J. and Smith, J. M. (1977) Trickle bed oxidation reactor. *Catal. Rev. Sci. Eng.*, 15, 187.
- Grosser, K., Carbonell, R. G. and Sundaresen S. (1988) The onset of pulsing in two phase cocurrent downflow through a packed bed. *AIChE J.*, 34, 1850.

- Hassan, M. M. and Beg, S. A. (1987) Theoretical analysis of packed bed biological reactor for various reaction kinetics. *Chem. Eng. J.*, 36, B15.
- Herskowitz, M. and Smith, J. M. (1983) Trickle bed reactors: A review. *AIChE J.*, 29, 1.
- Hinduja, M. J. (1977) A Non-Fickian Model for Dispersion in Packed Beds, Thesis, Rice Univ., USA.
- Hinduja, M. J., Sundaresan, S. and Jackson, R. (1980) A cross-flow model of dispersion in packed bed reactors. *AIChE J.*, 26, 274.
- Hirose, T., Toda, M. and Sato, Y. (1974) Liquid phase mass transfer in packed bed reactor with cocurrent gas-liquid downflow. *J. Chem. Eng. Japan*, 7, 187.
- Hochman, J. M. and Effron, E. (1969) Two phase concurrent downflow in packed beds. *Ind. Eng. Chem. Fundamentals.*, 8, 63.
- Hofmann, H. P. (1977) Hydrodynamics, transport phenomena and mathematical models in trickle bed reactors *Int. Chem. Eng.*, 17, 19.
- Hofmann, H. P. (1978) Multi-phase catalytic packed bed reactors *Catal. Rev. & Sci. Eng.*, 17, 71.
- Hoogendoorn, C. J. and Lips, J. (1965) Axial mixing of liquid in gas-liquid flow through packed beds. *Can. J. Chem. Eng.*, 43, 125.
- Kan, K. M. and Greenfield, P. F. (1978) Multiple hydrodynamic states in cocurrent two-phase downflow through packed beds. *Ind. Eng. Chem., Process Des. Dev.* 17, 482.
- Kan, K. M. and Greenfield, P. F. (1983) A residence-time model for trickle-flow reactors incorporating incomplete mixing in stagnant regions. *AIChE J.*, 29, 123.
- Kavanaugh, M.C. and Trussel, R.R. (1981) Air stripping as a treatment process. *Proc. AWWA Conf., St. Louis, USA.*
- Kohl, A. L. and Riensenfeld, F. C. (1979) *Gas Purification*; Gulf Publishing Book Company: Houston, Texas.



- Krischer, O. and Kast, W. (1978) *Die wissenschaftlichen Grundlagen der Trocknungstechnik*, 3, Auflage, Springer-Verlag, Berlin.
- Larachi, F., Midoux, N. and Laurant, A. (1990) 2nd Int. Sym. on High Pressure Chem. Eng., Paper session I, 24-26 september 1990, Erlangen, F.R.G.
- Larachi, F., Midoux, N., Laurant, A. and Wild, G. (1991) Experimental study of a trickle bed reactor operating at high pressure: Two phase pressure drop and liquid saturation. *Chem. Eng. Sci.*, 46, 1233.
- Larachi, F., Midoux, N., Laurant, A. and Wild, G. (1992) Proc. ISCRE, 12th, Torino, Italy.
- Larkins, R.P., White, R.R. and Jeffrey, D.W. (1961) Two phase concurrent flow in packed bed. *AIChE J.*, 7, 231.
- Lockhart, R.W. and Martinelli, R.C. (1949) Proposed correlation of data for isothermal two-phase two-component flow in pipes. *Chem. Eng. Prog.*, 45, 39.
- Mahajani, V. V. and Sharma, M. M. (1979) Effective interfacial area and liquid side mass transfer coefficient in trickle bed reactors. *Chem. Eng. Sci.*, 34, 1425.
- Mahajani, V. V. and Sharma, M. M. (1980) Mass transfer in packed columns: co-current (downflow) operation: 1 in. and 1.5 in. metal pall rings and ceramic intalox saddles: multifilament gauze packings in 20 cm and 38 cm i.d. columns. *Chem. Eng. Sci.*, 35, 941.
- Mashelkar, R. A. and Sharma, M. M. (1970) Mass transfer in bubble and packed bubble columns. *Trans. Inst. Chem. Eng.*, 48, T162.
- Matsuura, A., Akehata, T. and Shirai, T. (1976) Axial dispersion of liquid in concurrent gas-liquid downflow in packed beds. *J. Chem. Eng. Japan.*, 9, 294.
- Matsuura, A., Akehata, T. and Shirai, T. (1979) Correlation for dynamic holdup in packed beds with cocurrent gas-liquid downflow. *J. Chem. Eng. Japan.*, 12, 263.

- McIlvroid, H.G. (1956) Mass transfer in cocurrent gas-liquid flow through a packed column. Ph.D thesis, Carnegie Institute of Technology.
- Mitchell, M.G. and Perona, J.J. (1979) Gas-liquid interfacial areas for high porosity tower packings in concurrent downward flow. *Ind. Eng. Chem. Process Des. Dev.*, 18, 316.
- Michell, R. W. and Furzer, I. A. (1972) Trickle flow in packed beds. *Trans. Inst. Chem. Eng.*, 50, 334.
- Midoux, N, Favier, M. and Charpentier, J.C. (1976) Flow pattern, pressure loss and liquid holdup data in gas liquid downflow packed beds with foaming and non-foaming hydrocarbons. *J. Chem. Eng. Japan*, 9, 350.
- Morsi, B. I., Midoux, N., Laurent, A., Barthole-Delaunay, G., Storck, A. and Charpentier, J. C. (1981) Hydrodynamics and gas-liquid-solid interfacial parameters of cocurrent downward two phase flow in trickle bed reactors. *Proc. AIChE annual meeting, 1981.*, AIChE, New Orleans, L.A.
- Morsi, B. I., Midoux, N., Laurent, A. and Charpentier, J. C. (1982) Hydrodynamics and interfacial area in downward cocurrent gas-liquid flow through fixed beds. Influence of the nature of the liquid. *Intern. Chem. Eng.*, 22, 142.
- Morsi, B. I., Laurent, A., Midoux, N., Barthole-Delaunay, G., Storck, A. and Charpentier, J. C. (1984) Hydrodynamics and gas-liquid-solid interfacial parameters of cocurrent downward two phase flow in trickle bed reactors. *Chem. Eng. Commun.*, 25, 267-293.
- Nenninger, E. and Storrow, J.A. (1958) Drainage of packed beds in gravitational and centrifugal-force fields. *AIChE J.*, 4, 305.
- Ng, K. M. (1986) A model for flow regime transitions in cocurrent down-flow trickle bed reactors. *AIChE J.*, 32, 115.
- Ohshima, S., Takematsu, T., Kuriki, Y., Shimada, K., Suzuki, M. and Kato, J. (1976) *J. Chem. Eng. Japan*, 9, 29.
- Okoniewski, B.A. (1992) Remove VOCs from wastewater by air stripping. *Chem. Eng. Prog.*, Feb., 89.

- Pontius, F.W. (1990) Complying with the new drinking water quality regulations. *J. AWWA.*, 87, 32.
- Ramachandran, P.A., and Chaudhari, R.V. (1981) *Three-Phase Catalytic Reactors*. Gordon and Breach Science Publishers, London, England.
- Ramachandran, P.A., Dudukovic, M.P. and Mills, P.L. (1987) Recent advances in the analysis and design of trickle bed reactors. *Reactions and Reaction Engineering* .( Ed. Mashelkar, R.A. and Kumar, R.) Indian Academy of Sciences, Bangalore.
- Rao, V.G., Ananth, M.S. and Varma, W.B.G. (1983) Hydrodynamics of two-phase cocurrent downflow through packed beds. *AIChE J.*, 29, 467.
- Rao, V.G. and Drinkenburg, A.A.H. (1985) A model for pressure drop in two-phase gas-liquid downflow through packed columns. *AIChE J.*, 31, 1010.
- Reiss, L. P. (1967) Cocurrent gas-liquid contacting in packed columns. *Ind. & Eng. Chem. Proc. Des. Dev.*, 6, 486.
- Ross, D. (1990) *Memoire Ingegnieur*, CNAM, Nancy, France.
- Saada, M. Y. (1972) Assessment of interfacial area in cocurrent two phase flow in packed beds. *Chem. Ind. Genie Chem.*, 105, 1415.
- Saez, A. E. and Carbonell, R. G. (1985) Hydrodynamic parameters for gas liquid co-current flow in packed beds. *AIChE J.*, 31,52.
- Sato, Y., Hirose, T., Takahashi, F. and Toda, M. (1972) Performance of fixed bed catalytic reactor with cocurrent gas-liquid flow. *PACHEC'72*, section 8, paper 8.3, 187.
- Sato, Y., Hirose, T., Takahashi, F., Toda, M. and Hashiguchi, Y. (1973) Flow pattern and pulsation properties of cocurrent gas-liquid downflow in packed beds. *J. Chem. Eng. Japan*, 8, 315.
- Satterfield, C. N. (1975) Trickle bed reactors. *AIChE J.*, 21, 209.
- Schwartz, J.G., Weger, E. and Dudukovic, M.P. (1976) A new tracer method for determination of solid-liquid contacting efficiency in trickle bed reactors. *AIChE J.*, 22, 894.

- Seirafi, H. and Smith J. M. (1980) Mass transfer and adsorption in liquid full and trickle-beds. *AIChE J.*, 26, 711.
- Shah, Y. T., Stiegel, G. J. and Sharma, M. M. (1978) Backmixing in gas-liquid reactors. *AIChE J.*, 24, 369.
- Shah, Y. T. (1979) *Gas-Liquid-Solid reactor design*; McGraw-Hill Inc. : NewYork.
- Shende, B. W. and Sharma, M. M. (1974) Mass transfer in packed columns : Co-Current operation. *Chem. Eng. Sci.*, 29, 1763.
- Sherwood, T.K. and Pigford, R.L. (1952) *Absorption and Extraction*. McGraw-Hill Book Co. Inc., New York.
- Skomorokov, V. B., Kirillov, V. A. and Baldi, G. (1986) Simulation of liquid hydrodynamics in cocurrent two-phase upward flow through a packed bed *Chem. Eng. J.*, 33, 169.
- Specchia, V., Sicardi, S. and Gianetto, A. (1974) Absorption in packed towers with cocurrent upward flow. *AIChE J.*, 20, 646.
- Specchia, V., and Baldi G. (1977) Pressure drop and liquid holdup for two phase concurrent flow in packed beds. *Chem. Eng. Sci.*, 32, 515.
- Sylvester, N. D. and Pitayagulsarn (1975) *Ind. & Eng. Chem. Proc. Des. Dev.*, 14, 421.
- Tosun, G. (1984) A study of cocurrent down flow of nonfoaming gas-liquid systems in a packed bed. *Ind. Eng. Chem. Proc. Des. Dev.*, 23, 29.
- Turek, F., Lange, R. and Busch, A. (1979) *Chem. Ing. Technik*, 31, 232.
- Turek, F. and Lange, R. (1981) Mass transfer in trickle bed reactors at low Reynolds numbers. *Chem. Eng. Sci.*, 36, 569.
- Turpin, J. L. (1966) Prediction of pressure drop for two-phase, two-component cocurrent flow in packed beds, Ph.D Thesis, Univ. of Oklahoma, Norman, U.S.A.

- Turpin, J. L. and Huntington, R. L. (1967) Prediction of pressure drop for two-phase, two-component concurrent flow in packed beds. *AIChE J.*, 13, 1196.
- Ufford, R. C. and Perona, J. J. (1973) Liquid phase mass transfer with cocurrent flow through packed towers. *AIChE J.*, 19, 1223.
- Umphres, M.D., Tate, C.H. and Kavanaugh, M.C. (1983) Trihalomethane removal by packed tower aeration. *J. AWWA.*, 75, 414.
- Van Swaaij, W. P. M., Charpentier, J. C. and Villermaux, J. (1969) Residence time distribution in the liquid phase of trickle flow in packed columns. *Chem. Eng. Sci.*, 24, 1083.
- Velazques, C. and Estevez, L.A. (1992) Stripping of trihalomethanes from drinking water in a bubble-column aerator. *AIChE J.*, 38, 211.
- Wammes, W. J. A. (1990) Hydrodynamics in a cocurrent gas-liquid trickle bed reactor at elevated pressures, Ph.D Thesis, Univ. of Twente, The Netherlands.
- Wammes, W. J. A., Middlekamp, J., Huisman, W. J., deBaas, C. M. and Westerterp, K.R. (1991) Hydrodynamics in a cocurrent gas-liquid trickle bed at elevated pressures. *AIChE J.*, 37, 1849.
- Weekman, V.W. (1976) Hydroprocessing reaction engineering. *Proc. 4th. Int./6th Eur. Symp. on Chem. React. Eng.*, VDI, Heidelberg, West Germany, 6-8 Apr.
- Welty, J. R., Wicks, C. E. and Wilson, R. E. *Fundamentals of Momentum, Heat, and Mass Transfer*. John Wiley & Sons : New York.
- Wen, C.Y., Brien, W.S.O. and Liang-Fseng, F. (1963) Mass transfer in packed beds operated cocurrently. *J. Chem. Eng. Data.*, 8, 42.
- Wild, G., Larachi, F. and Laurent, A. (1991) *Revue Inst. Francais du Petrole*, 46, 467.
- Yang, X. L., Wild, G. and Euzen, J. P. (1993) Study of liquid retention in fixed-bed reactors with upward flow of gas and liquid. *Int. Chem. Eng.*, 33, 72.

# Appendix A

## THE ORTHOGONAL COLLOCATION FORMULATION OF MODEL EQUATIONS

---

The transient model equations formulated in Chapter 3 have been solved by the method of orthogonal collocation. The system of coupled partial differential equations resulting from transient mass balances, has been reduced by orthogonal collocation to a system of ordinary differential equations, which are then solved by standard numerical techniques available for the solution of ODEs.

In the present study, the concentration profiles in both the gas and liquid phases have been approximated by non-symmetric polynomials of the type,

$$C^*(x, \theta) = (1-x)C^*(0, \theta) + xC^*(1, \theta) + x(1-x) \sum_{i=1}^m a_i^*(\theta) P_{i-1}(x) \quad (\text{A } 0.1)$$

where  $a_i^*$  are the arbitrary coefficients and  $P_i$  are the non symmetric polynomials defined by the condition,

$$\int_0^1 W(x) P_n(x) P_m(x) dx = 0 \quad (\text{A } 0.2)$$

$$n = 0, 1, 2, \dots, m-1 \quad \& \quad n \neq m$$

In the present study  $W(x)=1$  was used, and the  $x_i$  for the unsymmetric Legendre polynomials were generated. These were further used to generate First and Second Derivative. Two different sets of collocation matrices were generated, one for the axial

length of the column represented by (N+2) number of collocation points (i.e.,  $AX$  and  $BX$  matrix) and the other for the depth in the stagnant liquid phase as described by (M+2) number of collocation points (i.e.,  $AY$  and  $BY$  matrix). This could further be made clear by observing figure (3.2).

### A.1 Orthogonal Collocation Form for Basic Model Equations

Basic model Equation (3.10) may be expressed in collocation points as,

$$\frac{d C_{d_I}}{d \theta} = \frac{1}{\phi} \left[ \frac{h_d}{Pe_L} \sum_{K=1}^{N+2} C_{d_K} BX_{I,K} - \sum_{K=1}^{N+2} C_{d_K} AX_{I,K} - K_{SD}^* (C_{d_I} - C_{S_{I,1}}) \right] \quad (\text{A } 1.1)$$

For  $I = 2, 3, \dots, N + 1$

With boundary conditions written in terms of collocation matrix as,

$$\sum_{K=1}^{N+2} C_{d_K} AX_{1,K} = -Pe_L \left( C_d^o \Big|_{x=0^-} - C_{d_1} \right) \quad (\text{A } 1.2)$$

$$\sum_{K=1}^{N+2} C_{d_K} AX_{N+2,K} = 0 \quad (\text{A } 1.3)$$

Equations (A 1.2) and (A 1.3) are simultaneously solved for  $C_{d_1}$  and  $C_{d_{N+2}}$ . The resulting expressions are then substituted in set of equations given by (A 1.1) to replace the unknown  $C_{d_1}$  and  $C_{d_{N+2}}$ .

For the stagnant phase, the representative mass balance as given by partial differential equation (3.13), can be re-expressed by orthogonal collocation as,

$$\frac{dC_{S_{I,J}}}{d\theta} = \beta \sum_{K=1}^{M+2} C_{S_{I,K}} BY_{J,K} \quad (\text{A 1.4})$$

$$\text{For } I=2,3,\dots,N+1 \text{ \& } J=2,3,\dots,M+1$$

and the corresponding boundary conditions are,

$$\sum_{K=1}^{M+2} C_{S_{I,K}} AY_{1,K} = -Bi(C_{d_I} - C_{S_{I,1}}) \quad (\text{A 1.5})$$

$$\sum_{K=1}^{M+2} C_{S_{I,K}} AY_{M+2,K} = 0 \quad (\text{A 1.6})$$

As previous equations (A 1.5) and (A 1.6) are simultaneously solved for  $C_{S_{I,1}}$  and  $C_{S_{I,M+2}}$  (for,  $I=2,3,\dots,N+1$ ) and the resulting expressions are then resubstituted in set of equations described by (A 1.4).

## A.2 Orthogonal Collocation Form of Model Equations for Gas Absorption or Air Stripping

For the simulation of gas absorption or air stripping, dimensionless mass balance for the gas phase given by Equation (3.31) or (3.44) can be expressed in collocation matrices as,

$$\frac{dC_{g_I}}{d\theta} = \frac{\xi}{\psi} \left[ \frac{h_g}{Pe_G} \sum_{K=1}^{N+2} C_{g_K} BX_{I,K} - \sum_{K=1}^{N+2} C_{g_K} AX_{I,K} - \frac{St}{\xi} H(C_{g_I} - C_{d_I}) \right] \quad (\text{A 2.1})$$

$$\text{For } I=2,3,\dots,N+1$$

With boundary conditions written in terms of collocation matrix as,



$$\sum_{K=1}^{N+2} C_{gK} AX_{1,K} = -Pe_G \left( C_g^o \Big|_{x=0^-} - C_{g1} \right) \quad (\text{A } 2.2)$$

$$\sum_{K=1}^{N+2} C_{gK} AX_{N+2,K} = 0 \quad (\text{A } 2.3)$$

Equations (A 2.2) and (A 2.3) are simultaneously solved for  $C_{g1}$  and  $C_{gN+2}$ . The resulting expressions are then substituted in Equation (A 2.1) to replace the unknown  $C_{g1}$  and  $C_{gN+2}$  with known expression.

Model Equations (3.34) or (3.47) for the dynamic liquid phase are rewritten as,

$$\frac{dC_{dI}}{d\theta} = \frac{1}{\phi} \left[ \frac{h_d}{Pe_L} \sum_{K=1}^{N+2} C_{dK} BX_{I,K} - \sum_{K=1}^{N+2} C_{dK} AX_{I,K} - K_{SD}^* (C_{dI} - C_{S1,1}) + St (C_{gI} - C_{dI}) \right] \quad (\text{A } 2.4)$$

For  $I = 2, 3, \dots, N + 1$

The formulation for corresponding boundary conditions remains the same as discussed in appendix A.1.

For the stagnant phase, the representative mass balance as given by partial differential Equation (3.37) or (3.50), and the corresponding boundary conditions are re-expressed by orthogonal collocation in exactly the similar manner as discussed in Appendix A.1.

### **A.3 Orthogonal Collocation Form of Model Equations for Gas Absorption Accompanied by Chemical Reaction**

For the system of dimensionless model equations representative of gas absorption accompanied by chemical reaction, the equation for the gas phase is similar to the one outlined for physical gas absorption or air stripping, hence its expression in orthogonal matrices remains exactly the same as discussed in appendix A.2. For the liquid phase, we now have two sets of equations representing the two reacting species, which are very similar to the ones discussed for physical gas absorption or stripping, the only difference being the inclusion of an additional reaction term and hence can be treated in the same manner as outlined in appendix A.2.

## *Vita*

Name : Mohammad Salman Mahmood Naqvi

### **Education**

B. Sc. (Engg) : University of Engineering & Technology  
in Chemical Engineering Lahore, Pakistan. (August, 1992)

M.S. Chemical Engineering : King Fahd University of Petroleum &  
Minerals Dhahran, Saudi Arabia.  
(November, 1995)